

Table of Contents

0	Introductory Remarks	1
0.1	Literature for this Lecture	6
0.2	Symbols and Terms	8
0.3	Atomic Units	9
1	Introduction	10
1.1	The Many-Body Hamilton Operator	10
1.2	Separation of the Dynamics of Electrons and Ions	13
1.2.1	Adiabatic Approximation or Born-Oppenheimer Approximation	13
1.2.2	Static Approximation	17
1.2.3	Examples	18
1.2.3a	Structure, Lattice Constant, and Elastic Properties of Perfect Crystals	19
1.2.3b	Lattice Waves (Phonons)	20
1.3	The Ewald Method	21
2	The Fermi Method	27
2.1	Statistical Mechanics	27
2.2	Fermi Statistics of the Electrons	28
2.3	Some Definitions (Jellium Model)	29
3	Electron-Electron Interaction	34
3.1	Hartree Approximation	35
3.2	Hartree-Fock Approximation	42
3.3	The Exchange Interaction	47
3.4	Koopmans' Theorem	54
3.5	The X_α Method	55
3.6	Thomas-Fermi Theory and the Concept of Screening	57
3.7	Density Functional Theory	66
4	Lattice Periodicity	91
4.1	Symmetry	91
4.2	The Bloch Theorem	106
4.3	The Reciprocal Lattice	108
5	The Band Structure of the Electrons	115
5.1	Introduction	115
5.1.1	What Can We Learn from a Band Structure?	118

5.2	General Properties of $\epsilon_n(\mathbf{k})$	123
5.2.1	Continuity of $\epsilon_n(\mathbf{k})$ and Meaning of the First and Second Derivatives of $\epsilon_n(\mathbf{k})$	123
5.2.2	Time Reversal Symmetry	125
5.2.3	The Fermi Surface	128
5.3	The LCAO (linear combination of atomic orbitals) Method	129
5.3.1	Band Structure and Analysis of the Contributions to Chemical Bonding	133
5.4	The Density of States	136
5.5	Other Methods for Solving the Kohn-Sham Equations of Periodic Crystals ..	137
5.5.1	The Pseudopotential Method	137
5.5.2	APW and LAPW	138
5.5.3	KKR, LMTO, and ASW	138
5.6	Many-Body Perturbation Theory (beyond DFT)	138

Chapter 0

Introductory Remarks

A solid or, more generally, condensed matter is a complex many-body-problem ($\sim 10^{23}$ electrons and nuclei per cm^3). The most important foundations of its theoretical description are electronic-structure theory and statistical mechanics. Due to the complexity of the many-body problem there is a large variety of phenomena and properties. Their description and understanding is the purpose of this lecture course on “condensed matter”. Keywords are e.g. crystal structure, hardness, magnetism, conductivity, superconductivity, etc.. The name of this lecture (*Theoretical Material Science*) indicates that we intend to go a step further, i.e., “condensed matter” has been replaced by “materials”. This is a small, but nevertheless important generalization. When we talk about materials, then in addition to phenomena and properties we also think of potential applications, i.e., the possible function of materials, like in electronic, magnetic, and optical devices, sensor technology, catalysts, lubrication, and surface coatings (e.g. with respect to protection against corrosion and mechanical scratch-resistance). It is obvious that these functions, which are determined to a large extent by properties on a nanometer scale, play an important role in many technologies on which our lifestyle and also the wealth of our society are based. Also because of this (next to the fascination of the phenomena in fundamental research) today’s material science is playing a truly significant role.

At the base of the function of materials is the electronic structure. The field of electronic-structure theory, applied to problems from material science described above, is in an important, active phase with rapid developments in the underlying theory, new methods, new algorithms, and new computer codes. For several years now a theory is evolving that, taking advantage of high and highest performance computers, allows (starting from the fundamental equations of the interacting many-body problem) an atomistic modelling of complex systems with predictive power. Two central ingredients of such *ab initio* theories are a reliable description of the underlying elementary processes (e.g. breaking and formation of chemical bonds), and a correct treatment of the statistical mechanics of their interactions.

Because of the importance of many-body effects in the description of the interactions in poly-atomic systems up to now a systematic treatment was barely possible. The complexity of the quantum mechanical many-body problem required the introduction of approximations, which often were not obvious. “Only” since 1978 (or 1982)¹ have reliable calculations for solids been carried out and only this allows to check the possibly reasonable (and often necessary) approximations and to give the reasons for their success; or it is demonstrated which approximations have to be abandoned. And even the available predictive theories received a rigorous foundation (density functional theory) only in 1964.

¹V.L. Moruzzi, J.F. Janak, and A.R. Williams, *Calculated Electronic Properties of Metals*, Pergamon Press (1978) ISBN 0-08-022705-8; and M.T. Yin and M.L. Cohen, *Theory of static structural properties, crystal stability, and phase transformations: Application to Si and Ge*, Phys. Rev. B **26**, 5668 (1982).

Today this development has reached a feasible level for many types of problems, but it is not completed yet.

With these “new” developments the approximations, which in existing text books are introduced *ad hoc*, can be inspected. Further it is possible to make quantitative predictions, e.g. for the properties of new materials. But still *theoretical condensed matter physics* or *theoretical material science*, is in an active state of development. Phenomena investigated or understood in a very incomplete way, include phase transitions, disorder, catalysis, defects (meta-, bistabilities), properties of heterostructures and quantum dots, crystal growth, systems containing *f*-electrons, high-temperature-superconductivity, electronic excitation, and transport.

For modern *theoretical material science* there are two main challenges:

1. To explain experimentally found properties and phenomena and to place them in a bigger context and order. This is done by developing models, i.e., by a reduction to the key physical processes, which enables a qualitative or semi-quantitative understanding. As mentioned before, there are examples for which these tasks are not accomplished yet.
2. To predict, independent of experiment, properties of systems that have not been investigated experimentally so far – or situations that cannot be investigated by experiments directly. The latter include conditions of very high pressures or conditions that are chemically or radioactively harsh.

The latter point shall be illustrated by the following example:

Only today one starts to understand fundamental questions of condensed matter. Until recently it was not possible to show theoretically why diamond (carbon) is harder than Si. Further, properties can be calculated under conditions which are inaccessible by experiment, e.g. the viscosity and the melting temperature of iron at pressures that exist at the earth core. These theoretical investigations have become possible only since 1978 (the example concerning the properties of iron can be investigated only since about 1999²).

The element carbon exists in three solid phases: *i*) as amorphous solid and in crystalline form *ii*) as graphite and *iii*) as diamond^{3,4}. Graphite is the most stable phase, i.e., the one with the lowest internal energy. Diamond is only a metastable state, but with a rather long lifetime. Usually when carbon atoms are brought together graphite or an amorphous phase is formed. Only under certain conditions (pressure, temperature) in the inner earth

²D. Alfe, M.J. Gillan, and G.D. Price, *Nature* **401**, 462 (1999).

³Diamond is the hardest known material, i.e., it has the highest bulk modulus. Diamonds without defects are most transparent to light. At room temperature their thermal conductivity is better than that of any other material.

⁴This statement is slightly simplified. More precisely (up to now) two types of graphite and two types of diamond are known. Additionally since 1968 and 1972, respectively, chaoit and carbon (VI), since 1985 fullerenes (e.g. C₆₀) and since 1991 carbon nanotubes are known. From the latter “soft matter” can be formed, and they can also be used directly as nano-materials (for example as nanotube transistors). These systems will be discussed in more detail later.

were diamonds formed. Therefore, in a certain sense, diamonds are known only accidentally. It cannot be excluded that also other elements (Si, Ge, Ag, Au) can exist in other yet unknown modifications. Examples for new, artificially created materials are semiconductor quantum dot or quantum wire systems, or epitaxial magnetic layers⁵. Once the interactions between atoms are understood, possibly materials with completely new physical properties could be predicted theoretically. As an example, by the theoretical investigation of semiconductor heterostructures or of metal heterostructures it is actually attempted to predict new materials for light emitting diodes (LEDs) or new magnetic memory devices. By the theoretical investigation of alloys and surface alloys (for which no bulk-analogue exists) of new compositions the hope is to find new catalysts. This sounds like being very close to practical application. However, it should be noted that applications of such theoretical predictions cannot be expected in the too near future, because in industry many practical details (concerning the technical processes, cost optimization, etc.) are crucial for the decision if a physical effect will be used in real devices.

A theory is particularly useful, if it has predictive power. In these days there is a change in condensed matter theory. While previously the main focus was on the reproduction of experimental results and on the transfer to similar systems, nowadays theory is applied more and more independent of experiment, e.g. to predict new properties of solids and to stimulate new experiments.

In recent years, two aspects have had a big impact on materials science and condensed matter physics: First, the potential technological importance of semiconductor physics, magnetism, surface physics (computer, communication and information technology, catalysis, lubrication, new materials). Second, since 1980 30 Nobel prizes have been awarded for work in the field of or related to materials science. Just a short list is given here (see also: <http://www.nobel.se/>):

1981 Physics: Nicolaas Bloembergen and Arthur L. Schawlow “for their contribution to the development of laser spectroscopy” and Kai M. Siegbahn “for his contribution to the development of high-resolution electron spectroscopy”.

1981 Chemistry: Kenichi Fukui and Roald Hoffmann “for their theories, developed independently, concerning the course of chemical reactions”.

1982 Physics: Kenneth G. Wilson “for his theory for critical phenomena in connection with phase transitions”.

1982 Chemistry: Aaron Klug “for his development of crystallographic electron microscopy

⁵In 1988, Albert Fert and Peter Grünberg independently discovered that an increased magnetoresistive effect (hence dubbed “giant magnetoresistance” or GMR) can be obtained in magnetic multilayers. These systems essentially consist of an alternate stack of ferromagnetic (e.g., Fe, Co, Ni, and their alloys) and non-ferromagnetic (e.g., Cr, Cu, Ru, etc.) metallic layers. It is unusual that a basic effect like GMR leads in less than a decade after discovery to commercial applications: Magnetic field sensors based on GMR were already introduced into the market as early as 1996, and by now e.g. all read heads for hard discs are built that way. In 2007 Albert Fert and Peter Grünberg were awarded the Nobel Prize in physics.

- and his structural elucidation of biologically important nuclei acid-protein complexes”.
- 1983 Chemistry: Henry Taube “for his work on the mechanisms of electron transfer reactions, especially in metal complexes”.
- 1984 Chemistry: Robert Bruce Merrifield “for his development of methodology for chemical synthesis on a solid matrix”.
- 1985 Physics: Klaus von Klitzing “for the discovery of the quantized Hall effect” (von Klitzing, Dorda, Pepper, *Phys. Rev. Lett.* **45**, 494 (1980); *Physics Today* **38**, 17 (1985)).
- 1985 Chemistry: Herbert A. Hauptman and Jerome Karle “for their outstanding achievements in the development of direct methods for the determination of crystal structures”.
- 1986 Physics: Ernst Ruska “for his fundamental work in electron optics and for the design of the first electron microscope” and Gerd Binnig and Heinrich Rohrer “for their design of the scanning tunneling microscope” (*Physics Today*, Jan. 1987, p. 17) and (Binnig, Rohrer, Gerber, Werbel, *Phys. Rev. Lett.* **49**, 57 (1982)).
- 1986 Chemistry: Dudley R. Herschbach, Yuan T. Lee, and John C. Polanyi “for their contributions concerning the dynamics of chemical elementary processes”.
- 1987 Physics: J. Georg Bednorz and K. Alexander Müller “for their important breakthrough in the discovery of superconductivity in ceramic materials”.
- 1987 Chemistry: Donald J. Cram, Jean-Marie Lejn, and Charles J. Pedersen “for their development and use of molecules with structure-specific interactions of high selectivity”.
- 1988 Chemistry: Johann Deisenhofer, Robert Huber, and Hartmut Michel, “for the determination of the three-dimensional structure of a photosynthetic reaction centre”.
- 1991 Physics: Pierre-Gilles de Gennes “for discovering that methods developed for studying order phenomena in simple systems can be generalized to more complex forms of matter, in particular to liquid crystals and polymers”.
- 1991 Chemistry: Richard R. Ernst “for his contributions to the development of the methodology of high resolution nuclear magnetic resonance (NMR) spectroscopy”.
- 1992 Chemistry: Rudolph A. Marcus “for his contributions to the theory of electron transfer reactions in chemical systems”.
- 1994 Physics: Bertram N. Brockhouse “for the development of neutron spectroscopy” and Clifford G. Shull “for the development of the neutron diffraction technique”.
- 1996 Physics: David M. Lee, Douglas D. Osheroff, and Robert C. Richardson “for their discovery of superfluidity in helium-3”.

- 1996 Chemistry: Robert F. Curl Jr., Sir Harold W. Kroto, and Richard E. Smalley “for their discovery of fullerenes”.
- 1997 Physics: Steven Chu, Claude Cohen-Tannoudji, and William D. Phillips “for development of methods to cool and trap atoms with laser light”.
- 1998 Physics: Robert B. Laughlin, Horst L. Störmer, and Daniel C. Tsui “for their discovery of a new form of quantum fluid with fractionally charged excitations”.
- 1998 Chemistry: Walter Kohn “for his development of the density-functional theory” and John A. Pople “for his development of computational methods in quantum chemistry”.
- 1999 Chemistry: Ahmed H. Zewail “for his studies of the transition states of chemical reactions using femtosecond spectroscopy”.
- 2000 Physics: Zhores I. Alferov and Herbert Kroemer “for developing semiconductor heterostructures used in high-speed- and opto-electronics” and Jack S. Kilby “for his part in the invention of the integrated circuit”.
- 2000 Chemistry: Alan J. Heeger, Alan G. MacDiarmid, and Hideki Shirakawa, “for the discovery and development of conductive polymers”.
- 2001 Physics: Eric A. Cornell, Wolfgang Ketterle, and Carl E. Wieman “for the achievement of Bose-Einstein condensation in dilute gases of alkali atoms, and for early fundamental studies of the properties of the condensates”.
- 2003 Physics: Alexei A. Abrikosov, Vitaly L. Ginzburg, and Anthony J. Leggett “for pioneering contributions to the theory of superconductors and superfluids”.
- 2005 Physics: Roy J. Glauber “for his contribution to the quantum theory of optical coherence” and John L. Hall and Theodor Hänsch for “their contributions to the development of laser-based precision spectroscopy, including the optical comb technique”.
- 2007 Physics: Albert Fert and Peter Grünberg “for their discovery of Giant Magnetoresistance”.
- 2007 Chemistry: Gerhard Ertl “for his studies of chemical processes on solid surfaces”.

In the above list I ignored work on biophysics, though some developments in this area are now becoming also part of condensed matter physics.

The quantum-Hall-effect (Nobel prize 1985) is roughly understood these days, which is true only in a limited way for its “variant” the “fractional quantum-Hall-effect” (Nobel prize 1998). The latter is based on the strong correlation of the electrons and even these days unexpected results are found.

The theory of high- T_c superconductivity is still unclear (Nobel prize 1987). Here, the coupling seems to have a different symmetry than in conventional BCS-superconductors. While high- T_c superconductors have a complex atomic structure and consist of at least 4 elements (z.B. La, Ba, Cu, O), recently a relatively simple material was found (MgB_2), which also has a high critical temperature ($T_c = 39$ K, this corresponds to the temperature of the first high- T_c superconductors; these days high- T_c superconductors with critical temperatures close to 100 K are known).

In this lecture:

1. Equations will not fall down from heaven, but we will derive them from first principles;
2. we will not only give the mathematical derivation, but also, and in particular, we will develop a physical feeling, i.e., we will spend a noticeable amount of time in interpreting equations;
3. we will give the reasons for approximations and clarify their physical meaning and the range of validity (as much as this is possible).

In contrast to most text books we will start with the “adiabatic principle” and subsequently discuss the quantum mechanical nature of the electron-electron interaction. In most text books both are introduced only in the middle or at the end.

In the first part of the lecture we will restrict ourselves – unless stated otherwise – to $T \approx 0$ K. Sometimes an extrapolation to $T \neq 0$ K is unproblematic. Still, one should keep in mind that for $T \neq 0$ K important changes and new effects can occur (e.g. due to the entropy).

0.1 Literature for this lecture:

Author: Ashcroft, Neil W. and Mermin, N. David
Title: Solid state physics
Place: Philadelphia, PA
Year: 1981
Publisher: Saunders College Publishing
ISBN: 0-03-083993-9 = 0-03-049346-3

Author: Kittel, Charles
Title: Quantum theory of solids
Place: Hoboken, NJ
Year: 1963
Publisher: John Wiley & Sons, Inc

Author: Ziman, John M.
Title: Principles of the theory of solids
Place: Cambridge
Year: 1964
Publisher: Cambridge University Press

Author: Ziman, John M.
Title: Models of disorder: the theoretical physics of homogeneously disordered systems
Place: Cambridge
Year: 1979
Publisher: Cambridge University Press
ISBN: 0-521-21784-9 = 0-521-29280-8

Author: Ibach, Harald and Lüth, Hans
Title: Solid-state physics: an introduction to principles of materials science
Edition: 2. Ed.
Place: Berlin
Year: 1995
Publisher: Springer
ISBN: 3-540-58573-7 = 0-387-58573-7

Author: Madelung, Otfried
Title: Festkörpertheorie, 3 Bände
Place: Berlin
Year: 1972
Publisher: Springer

Author: Scherz, Udo
Title: Quantenmechanik
Place: Stuttgart
Year: 1999
Publisher: Teubner
ISBN: 3519032465

Author: Dreizler, Reiner M. and Gross, Eberhard K. U.
Title: Density functional theory: an approach to the quantum many-body problem
Place: Berlin
Year: 1990
Publisher: Springer
ISBN: 3-540-51993-9 = 0-387-51993-9

Author: Parr, Robert G. and Yang, Weitao
Title: Density-functional theory of atoms and molecules
Place: Oxford
Year: 1994
Publisher: Oxford University Press
ISBN: 0-19-509276-7

Author: Anderson, Philip W.
Title: Basic notions of condensed matter physics
Place: London
Year: 1984
Publisher: Benjamin/Cummings
ISBN: 0-8053-0220-4 = 0-8053-0219-0

Author: Marder, Michael P.
Title: Condensed matter physics
Place: New York
Year: 2000
Publisher: John Wiley & Sons, Inc.
ISBN: 0-471-17779-2

Author: Martin, Richard M.
Title: Electronic Structure
Place: Cambridge
Year: 2004
Publisher: Cambridge University Press

0.2 The following symbols and terms are used:

$-e$ charge of the electron
 $+e$ charge of the proton
 m mass of the electron
 \mathbf{r}_k position of electron k
 σ_k spin of electron k
 Z_K nuclear charge of atom K
 Z_{v_K} valence of atom K
 M_K mass of nucleus K
 \mathbf{R}_K position of nucleus K
 ϕ electric field

- Ψ many-body wave function of the electrons and nuclei
- Λ nuclear wave function
- Φ many-body wave function of the electrons
- φ single-particle wave function of the electrons
- χ spin wave function
- $\{\mathbf{R}_I\} \equiv \{\mathbf{R}_1, \dots, \mathbf{R}_M\}$ atomic positions
- $\{\mathbf{r}_i \sigma_i\} \equiv \{\mathbf{r}_1 \sigma_1, \dots, \mathbf{r}_N \sigma_N\}$ electron coordinates (position + spin)
- ϵ_0 dielectric constant of the vacuum
- ϵ_i single particle energy of electron i
- V_g volume of the base region
- Ω volume of a primitive cell
- $v_K^{\text{Ion}}(\mathbf{r})$ potential of ion K at position \mathbf{r}

0.3 Atomic Units

At least at the beginning of the lecture I will use SI-units (**S**ystème **I**nternational d'Unités).

However, in order to simplify the notation in quantum mechanics often the so-called atomic units (a.u.) are introduced. For historic reasons, there are two, slightly different conventions: Rydberg and Hartree atomic units. For both we have

$$\text{length} : \frac{4\pi\epsilon_0\hbar^2}{me^2} = 1 \text{ bohr} = 0.529177 \text{ \AA} = 0.0529177 \text{ nm} \quad , \quad (0.1)$$

and further we have:

	$\frac{e^2}{4\pi\epsilon_0}$	\hbar	m	energy: $\frac{\hbar^2}{2ma_B^2}$	$\frac{\hbar^2}{2m}$	Hamilton operator of hydrogen atom
Rydberg a.u.	2	1	0.5	1 Ry = 13.606 (eV)	1	$-\nabla^2 + \frac{2}{r}$
Hartree a.u.	1	1	1	$\frac{1}{2}$ Ha; 1 Ha = 27.212 (eV)	0.5	$-\frac{1}{2}\nabla^2 + \frac{1}{r}$

Chapter 1

Introduction

1.1 The Many-Body Hamilton Operator

The starting point of a quantitative theoretical investigation of the properties of solids is the many-body Schrödinger equation

$$H\Psi = E\Psi \quad , \text{ with } \Psi = \Psi(\{\mathbf{R}_I\}, \{\mathbf{r}_k, \sigma_k\}) \quad .$$

Here, the many-body wave function depends on the coordinates of all the atoms, \mathbf{R}_I , and on the coordinates and spin coordinates of all electrons. In general, this wave function will not separate into \mathbf{R}_I and (\mathbf{r}_k, σ_k) dependent components. This should be kept in mind when below, and in most parts of this lecture, we will introduce such separation. Of course, we will also discuss the range of its validity. The properties of matter are determined by the electrons and nuclei and in particular by their interaction (10^{23} particles per cm^3). For many quantum mechanical investigations it is useful to start with an approximation, which is called the “frozen-core approximation”. This is a reasonable approximation although *a priori* it is not clear why it is simplifying the theoretical treatment. Later, however, we will realize that the frozen-core approximation in general provides a higher accuracy and reliability to quantitative calculations. This approximation is often helpful or convenient, but not necessarily required, i.e., the many-body problem can also be solved without introducing this approximation.

We will assume that when condensed matter is formed from free atoms, only the valence electrons contribute (significantly) to the interaction between atoms. The electrons close to the nuclei (core electrons), which are in closed shells, in general will only have a small influence on the properties of solids. Exceptions are experiments, which more or less directly measure the core electrons or the region close to the nuclei [e.g. X-ray photo emission (XPS), electron spin resonance (ESR)]. Therefore it is reasonable to introduce the following separation already in the atom, before turning to solids: Nucleus and core electrons shall be regarded as a unit, i.e., the neutral atom consists of a positive, spherically symmetric ion of charge $Z_v e$ and of Z_v valence electrons.

This ion acts on each valence electron with a potential that looks like that shown in Fig. 1.1. The symbols have the following meaning:

Z : nuclear charge of the atom

R_c : radial extension of the core electrons

Z_v : number of valence electrons of the neutral atom

Then the number of core electrons is $Z - Z_v$. The solid is composed of these ions (lattice components) and the valence electrons. As mentioned before, this approximation is not

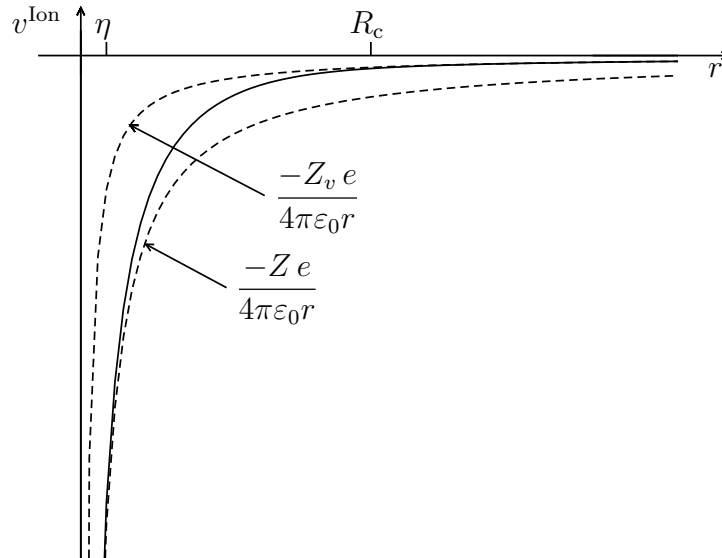


Figure 1.1: Potential of a positive ion (full line), where all electrons, except those in closed shells, have been removed. The dashed curves show the asymptotic behavior for small and large distances.

required in a strict sense. We also did not achieve a lot, because in spite of the frozen-core approximation the quantum mechanical problem still contains 10^{23} particles.

Still the approximation is reasonable and conceptionally appropriate, because it corresponds to the nature of the interaction. In Table 1.1 I give the electronic configuration and the ionic potentials for four examples. Here (and in Fig. 1.1) η is a small number roughly of the order of $R_c/(100 Z)$. The question marks in the range $\eta \leq r \leq R_c$ indicate that in this range no analytic form of the potential can be given. We note that the particular form of $v^{\text{Ion}}(\mathbf{r})$ and the number of valence electrons Z_v have no influence on the form of the equations that will be discussed later in this lecture.

Table 1.1: Electronic configuration and ionic (frozen core) potentials for different atoms.

atom	electronic configuration	Z	Z_v	R_c (bohr)	$v^{\text{Ion}}(r)$ (Ry)
H	$1s^1$	1	1	0	$-2/r$
He	$1s^2$	2	2	0	$-4/r$
C	$[1s^2]2s^2 2p^2$	6	4	0.7	$r \geq R_c : -8/r$ $\eta \leq r \leq R_c : ?$ $r < \eta : -12/r$
Si	$[1s^2 2s^2 2p^6] 3s^2 3p^2$	14	4	1.7	$r \geq R_c : -8/r$ $\eta \leq r \leq R_c : ?$ $r < \eta : -28/r$

For the construction of the Hamilton operator of the many-body Schrödinger equation of a solid, we first start with the classical Hamilton function and subsequently replace the

momentum \mathbf{p} by $(\hbar/i)\nabla$.

The many-body Hamilton operator of the solid has the following contributions:

- 1) The kinetic energy of the electrons

$$T^e = \sum_{k=1}^N \frac{\mathbf{p}_k^2}{2m} \quad . \quad (1.1)$$

- 2) The kinetic energy of the ions (i.e. of the nuclei plus core electrons)

$$T^{\text{Ion}} = \sum_{I=1}^M \frac{\mathbf{P}_I^2}{2M_I} \quad . \quad (1.2)$$

If the solid contains only one type of atom, then $N = Z_v M$.

- 3) The electron-electron interaction

$$V^{e-e}(\{\mathbf{r}_k \sigma_k\}) \approx \frac{1}{2} \frac{1}{4\pi\epsilon_0} \sum_{\substack{k,k' \\ k \neq k'}}^{N,N} \frac{e^2}{|\mathbf{r}_k - \mathbf{r}_{k'}|} \quad . \quad (1.3)$$

We use $\{\mathbf{r}_k \sigma_k\}$ as a short hand notation for all position and spin coordinates of the electrons: $\mathbf{r}_1, \sigma_1, \mathbf{r}_2, \sigma_2, \mathbf{r}_3, \sigma_3, \dots, \mathbf{r}_N, \sigma_N$. Here we have considered only the electrostatic interaction. In general, also the spin of the electrons and the magnetic interaction should and could be taken into account. Spin and magnetism in general require to solve the Dirac equation. Often, however, a scalar-relativistic treatment is sufficient. We will get back to this in Chapter ??.

- 4) The interaction of the ions

$$V^{\text{Ion-Ion}}(\{\mathbf{R}_I\}) \approx \frac{1}{2} \frac{1}{4\pi\epsilon_0} \sum_{\substack{I,J \\ I \neq J}}^{M,M} \frac{e^2}{|\mathbf{R}_I - \mathbf{R}_J|} Z_{v_I} Z_{v_J} \quad . \quad (1.4)$$

Also here (even better justified than for the electrons) we did not consider the spin of the particles. Further we have assumed that the ions cannot get too close to each other, i.e., their interaction potentials can be described by $(Z_v e^2/d) \frac{1}{4\pi\epsilon_0}$. Thus, we also assumed that the distance of two ions d is larger than or equal to $2R_c$, in order to avoid an overlap of the charge densities of the core electrons. If the condition $d \geq 2R_c$ is not valid, the frozen-core approximation cannot be applied. Then $v^{\text{Ion}} \rightarrow v^{\text{Nuc.}} = \frac{1}{4\pi\epsilon_0} \frac{e^2 Z}{r}$ has to be used.

5) The electron-ion-interaction (without nuclear spin)

$$V^{e-\text{Ion}}(\{\mathbf{r}_k\sigma_k\}; \{\mathbf{R}_I\}) = \sum_{I=1}^M \sum_{k=1}^N v^{\text{Ion}}(|\mathbf{R}_I - \mathbf{r}_k|) \quad , \quad (1.5)$$

which is often summarized as:

$$\sum_{I=1}^M v^{\text{Ion}}(|\mathbf{R}_I - \mathbf{r}_k|) = v(\mathbf{r}_k) \quad . \quad (1.6)$$

Here, $v(\mathbf{r}_k)$ is the potential due to all the ions (nuclei + core electrons).

Consequently, the many-body Hamilton operator of the solid reads

$$H = T^e + T^{\text{Ion}} + V^{e-e} + V^{e-\text{Ion}} + V^{\text{Ion-Ion}} \quad . \quad (1.7)$$

1.2 Separation of the Dynamics of Electrons and Ions

1.2.1 Adiabatic Approximation or Born-Oppenheimer Approximation

The dynamics is described by the time-dependent Schrödinger equation

$$i\hbar \frac{\partial \Psi(t)}{\partial t} = H \Psi(t) \quad ,$$

where H is defined in Section 1.1 above (Eq. 1.7). Thus

$$\Psi(t) = e^{-iH \cdot (t-t_0)/\hbar} \Psi(t_0) \quad .$$

Obviously this is the equation we like to solve, but in order to do so, we have to bring it into a more tractable form. How can we split things up? How can we divide the problem into smaller and tractable pieces in order to conquer the whole?

Before we start the mathematical discussion, let me give an initial remark to make the idea plausible: The electrons can react to an external perturbation much faster than the nuclei. This is reflected in the ratio of the (inert) masses of the nuclei and the electrons. Some examples are:

$$\begin{aligned} M_{\text{H}}/m &= 1,840 \quad , \\ M_{\text{Si}}/m &= 25,760 \quad , \\ M_{\text{Ag}}/m &= 86,480 \quad . \end{aligned}$$

Thus it seems to be reasonable to assume that the electrons adjust without noticeable delay to the current lattice geometry $\{\mathbf{R}_I\}$. Then for each lattice geometry, the electrons move independently of the motion of the nuclei (adiabatic principle). Formulated more precisely it can be said that electrons in general react to a perturbation on a time scale of

femtoseconds (10^{-15} s), while nuclei require times of the order of picoseconds (10^{-12} s). We assume that from the electrons point of view the ions do not move (or move sufficiently slow).

To justify this decoupling of the motion of the electrons and the nuclei we now give an (initially) exact discussion.

We define an operator H^e , in order to use its eigenfunctions as basis:

$$H^e(\{\mathbf{R}_I\})\Phi_\nu(\{\mathbf{R}_I\}, \{\mathbf{r}_k\sigma_k\}) = E_\nu^e\Phi_\nu \quad , \quad (1.8)$$

with

$$H^e = T^e + V^{e-\text{Ion}} + V^{e-e} \quad . \quad (1.9)$$

If the kinetic energy of the lattice components would be zero (or $M_I/m \rightarrow \infty$), the electrons could be described by this equation. But strictly speaking the meaning of the functions Φ_ν defined by Eq. (1.8) is only that of basis functions. The arguments $\{\mathbf{R}_I\}$ in the electronic wave function cannot be interpreted as a common variable of the wave function, but as parameters which classify the Hamilton operator H^e (similar to the nuclear charge Z).

The following statement is exact: The solutions of H (defined by Eq. (1.1) - (1.5)) can be expanded in terms of the functions Φ_ν (the eigenfunctions of Eq. (1.8))

$$\Psi = \sum_{\nu} \Lambda_\nu(\{\mathbf{R}_I\})\Phi_\nu(\{\mathbf{R}_I\}, \{\mathbf{r}_k\sigma_k\}) \quad . \quad (1.10)$$

The meaning of Eq. (1.8) and (1.10) can also be expressed as: The eigenfunctions of H^e for each atomic configuration $\{\mathbf{R}_I\}$ form a complete set of functions. Strictly speaking, the eigenfunctions of *one* atomic configuration $\{\mathbf{R}_I\}$ are complete (with respect to the electronic coordinates), i.e., the Hilbert spaces of different atomic configurations $\{\mathbf{R}_I\}$ are the same. Still it is reasonable (here) to consider the functions $\Phi_\nu(\{\mathbf{R}_I\}, \{\mathbf{r}_k\sigma_k\})$ as being dependent of \mathbf{R}_I . Mathematically it would also be correct to take the $H^e(\mathbf{R}_I)$ and the $\Phi_\nu(\{\mathbf{R}_I\}, \{\mathbf{r}_k\sigma_k\})$ of a certain configuration \mathbf{R}_I^0 and to consider the dependence on \mathbf{R}_I only by the coefficients $\Lambda_\nu(\{\mathbf{R}_I\})$. This will be discussed in 1.2.2. Now, we investigate the equation $H\Psi = E\Psi$, representing Ψ by Eq. (1.10).

Obviously, for the operator H^e we have

$$H^e\Lambda_\nu\Phi_\nu = \Lambda_\nu H^e\Phi_\nu = \Lambda_\nu E_\nu^e\Phi_\nu \quad .$$

Also $V^{\text{Ion}-\text{Ion}}$ can be interchanged with Λ_ν , but not T^{Ion} . Applying the chain rule we obtain

$$\nabla_{\mathbf{R}_I}^2(\Lambda_\nu\Phi_\nu) = \Lambda_\nu(\nabla_{\mathbf{R}_I}^2\Phi_\nu) + 2(\nabla_{\mathbf{R}_I}\Lambda_\nu)(\nabla_{\mathbf{R}_I}\Phi_\nu) + (\nabla_{\mathbf{R}_I}^2\Lambda_\nu)\Phi_\nu \quad . \quad (1.11)$$

Now Eq. (1.7) for the state (E, Ψ) is multiplied from the left by Φ_μ^* and integrated over the electronic coordinates. Using Eq. (1.8), the equation used to determine the “wave function of the electrons”, i.e., Φ_μ , we obtain

$$\langle \Phi_\mu | H | \Psi \rangle = E \Lambda_\mu = (E_\mu^e + T^{\text{Ion}} + V^{\text{Ion-Ion}}) \Lambda_\mu + \sum_\nu \sum_{I=1}^M -\frac{\hbar^2}{2M_I} \{ \langle \Phi_\mu | \nabla_{\mathbf{R}_I}^2 | \Phi_\nu \rangle \Lambda_\nu + 2 \langle \Phi_\mu | \nabla_{\mathbf{R}_I} | \Phi_\nu \rangle \nabla_{\mathbf{R}_I} \Lambda_\nu \} . \quad (1.12)$$

For each electronic state (E_μ^e, Φ_μ) there is one such equation. The difficult part in solving Eq. (1.12) are the terms coupling Φ_μ and Φ_ν .

This coupling of different electronic states is caused by the dynamics of the lattice atoms. It is called electron-phonon coupling.

The electron-phonon coupling can be calculated. Then one often finds that for many properties of solids it is not very important and can be neglected. However, for the “standard superconductivity” (BCS-theory) it is essential. Initially, for the new superconductors it was believed that the electron-phonon interaction is not the main origin of superconductivity. Nowadays this is not generally accepted anymore. Actually, it is not clear which is the determining mechanism. For some solids the influence of the electron-phonon coupling on the spectrum of the lattice vibrations can be measured, and for some low-dimensional systems the electron-phonon coupling is even responsible for structural instabilities. The keywords are “Kohn-anomaly”, “Jahn-Teller-effect” and “Peierls instability”. These mechanisms are activated by some properties of the electronic structure. They will be discussed later, when we discuss defects and surfaces.

Up to this point our derivation is exact and general statements concerning the importance of the electron-phonon coupling are usually NOT possible. Still, we now introduce two approximations:

- 1) We assume that the electrons at each time, i.e., for each lattice geometry $\{\mathbf{R}_I\}$, are in an eigenstate of H^e (the motion of the lattice shall not induce transitions from Φ_μ to Φ_ν). The reason is that the electrons react fast and in fact follow instantaneously the nuclear motion. Therefore, the electrons do not feel the nuclear motion and are always in the electronic ground state. The matrix elements $\langle \Phi_\mu | \nabla_{\mathbf{R}_I}^2 | \Phi_\nu \rangle$ and $\langle \Phi_\mu | \nabla_{\mathbf{R}_I} | \Phi_\nu \rangle$ in (1.12) then are zero for $\mu \neq \nu$.

This is called the adiabatic principle or Born-Oppenheimer-approximation. Its validity, i.e., the importance of the off-diagonal elements, in general is hard to evaluate.

- 2) Further we want to estimate the diagonal elements of the electron-phonon interaction:
 - a) The term $\langle \Phi_\mu | \nabla_{\mathbf{R}_I} | \Phi_\mu \rangle = \frac{1}{2} \nabla_{\mathbf{R}_I} \langle \Phi_\mu | \Phi_\mu \rangle$ vanishes exactly, because $\langle \Phi_\mu | \Phi_\mu \rangle = 1$, i.e., it is constant. The derivative of a constant is zero.

b) For the term

$$-\frac{\hbar^2}{2M_I} \langle \Phi_\mu | \nabla_{\mathbf{R}_I}^2 | \Phi_\mu \rangle$$

we find that the electronic wave functions Φ_μ do not depend directly on the nuclear positions \mathbf{R}_I . The strongest imaginable dependence would exist, if the electrons would follow the atoms without any delay and distortion. If we, for example, had a system containing only one valence electron per atom and each electron follows “its” atom without delay (i.e., the valence electrons instantaneously follow the nucleus. This means

$$|\langle \Phi_\mu | \nabla_{\mathbf{R}_I}^2 | \Phi_\mu \rangle| \lesssim |\langle \Phi_\mu | \nabla_{\mathbf{r}_k}^2 | \Phi_\mu \rangle|$$

and further

$$\begin{aligned} \left| \frac{\hbar^2}{2M_I} \langle \Phi_\mu | \nabla_{\mathbf{R}_I}^2 | \Phi_\mu \rangle \right| &\lesssim \left| \frac{m}{M_I} \left\langle \Phi_\mu \left| -\frac{\hbar^2}{2m} \nabla_{\mathbf{r}_k}^2 \right| \Phi_\mu \right\rangle \right| \\ &\approx 10^{-4} \times \text{kinetic energy of an electron.} \end{aligned} \quad (1.13)$$

Thus, for the diagonal elements $\mu = \nu$, but unfortunately only for these, a rough estimation is possible.

From Eq. (1.13) and the adiabatic approximation we obtain the Schrödinger equation for the wave functions of the ions:

$$(T^{\text{Ion}} + V^{\text{Ion-Ion}} + E_\mu^e) \Lambda_\mu = E \Lambda_\mu \quad . \quad (1.14)$$

For the energetically lowest state we will often write

$$V^{\text{Ion-Ion}} + E_{\mu=0}^e = V^{\text{BO}} \quad , \quad (1.15)$$

and V^{BO} is called “potential energy surface” (PES) or “Born-Oppenheimer energy surface”. The PES is the energy surface the nuclei are moving on, according to Eq. (1.14).

When neglecting the coupling terms $\langle \Phi_\mu | \dots | \Phi_\nu \rangle$ in Eq. (1.13), the eigenfunction of the ground state of H has the form:

$$\Psi \rightarrow \Psi^{\text{BO}} = \Lambda_0(\{\mathbf{R}_I\}) \Phi_0(\{\mathbf{R}_I\}, \{\mathbf{r}_k, \sigma_k\}) \quad ,$$

where Φ_0 is determined by Eq. (1.8) and Λ_0 by Eq. (1.14). Equation (1.8) and Eq. (1.14) can be calculated reliably using modern computational methods.

Strictly, the motion of the ions would have to be described quantum mechanically. When Eq. (1.14) is solved, one finds that almost always it can be replaced by the classical (Newton) equations of motion. Quantum mechanical effects like zero point vibrations and tunneling only rarely play an important role. Hydrogen, as the lightest element, is an exception, but already for deuterium a classical treatment is sufficient in most cases.

In general, at stable geometries the functions Λ_0 are narrowly peaked and centered at the atomic sites $\{\mathbf{R}_I\}$. Consequently, for the ground state of Eq. (1.15) we have:

$$E_0 = E_0^e(\{\mathbf{R}_I^0\}) + \frac{1}{4\pi\epsilon_0} \frac{1}{2} \sum_{\substack{I,J \\ I \neq J}}^{M,M} \frac{e^2}{|\mathbf{R}_I^0 - \mathbf{R}_J^0|} Z_{v_I} Z_{v_J} + \langle \Lambda_0 | T^{\text{Ion}} + V^{\text{BO}}(\{\mathbf{R}_I^0 - \mathbf{R}_I\}) | \Lambda_0 \rangle \quad (1.16)$$

The last term describes the quantum mechanical corrections, i.e. zero-point vibrations. Equation (1.17) forms the basis of the *ab initio* calculation of the electronic, structural, elastic and vibrational properties of solids. E_0 is often called total energy (or structural energy). We have recommended (but it is not necessary) to use the frozen-core approximation for $V^{e-\text{Ion}}$ and we have applied the adiabatic approximation.

The Born-Oppenheimer potential, $V^{\text{BO}}(\{\mathbf{R}_I\})$ refers to the *actual* position of the ions (which typically change with time), and it assumes that the functions $\Phi_\mu(\{\mathbf{R}_I\}, \{\mathbf{r}_k, \sigma_k\})$ refer to exactly these positions. A hard proof of the validity of the Born-Oppenheimer approximation is not possible and in fact depends on the actual problem, because there might be situations, in which the electrons react slower than assumed above, and then they will not be able to follow the motion of the nuclei exactly, but with some delay and distortion.

The derivation in this paragraph was reasonable in order to show the form of the matrix elements of the electron-phonon interaction. Further, we wanted to estimate the order of magnitude of the matrix elements. In principle, for each calculation the validity of the Born-Oppenheimer-approximation should be checked by a explicit calculation of the matrix elements in Eq. (1.13) or at least by an estimation.

1.2.2 Static Approximation

We now briefly give an alternative derivation, which is often called the “static approximation”. The nuclei are always in motion, but in many cases will just vibrate around a position that represents a minimum of the Born-Oppenheimer potential energy, $\{\mathbf{R}_I^0\}$, and we now investigate the Hamilton operator $H^e(\{\mathbf{R}_I^0\})$, which yields the wave functions of the electrons $\Phi_\nu(\{\mathbf{R}_I^0\}, \{\mathbf{r}_k, \sigma_k\})$ (cf. Eq. (1.8)). Also the Hamiltonian $H^e(\{\mathbf{R}_I^0\})$ defines (by its eigenvectors) a complete set of functions, which we can use as a basis set for the general problem. Though this basis now refers to a fixed (static) geometry the treatment is as general as that of Section 1.2.2. However, the equation will look different. Nevertheless, they describe the same physics.

In the present treatment the wave function of the solid is

$$\Psi(\{\mathbf{R}_I\}, \{\mathbf{r}_k, \sigma_k\}) = \sum_{\nu} \hat{\Lambda}_{\nu}(\{\mathbf{R}_I\}) \Phi_{\nu}(\{\mathbf{R}_I^0\}, \{\mathbf{r}_k, \sigma_k\}) \quad . \quad (1.17)$$

This equation is (so far) exact, too. But the expansion coefficients are different; therefore the “hat” above the Λ . The components of the Hamilton operator containing the ion-ion

and the electron-ion interaction (cf. Eq. (1.4) and (1.5)), (using $\Delta\mathbf{R}_I = \mathbf{R}_I - \mathbf{R}_I^0$) we write as :

$$V^{\text{Ion-Ion}}(\{\mathbf{R}_I\}) = V^{\text{Ion-Ion}}(\{\mathbf{R}_I^0\}) + V^{\text{ph}}(\{\Delta\mathbf{R}_I\}) \quad , \quad (1.18)$$

$$V^{e\text{-Ion}}(\{\mathbf{R}_I\}, \{\mathbf{r}_k\sigma_k\}) = V^{e\text{-Ion}}(\{\mathbf{R}_I^0\}, \{\mathbf{r}_k\sigma_k\}) + V^{e\text{-ph}}(\{\Delta\mathbf{R}_I\}) \quad . \quad (1.19)$$

From this we obtain the equation for the determination of the coefficients of the expansion and the energy eigenvalues of the solid

$$E_\mu^e \hat{\Lambda}_\mu + T^{\text{Ion}} \hat{\Lambda}_\mu + V^{\text{Ion-Ion}}(\{\mathbf{R}_I^0\}) \hat{\Lambda}_\mu + \sum_\nu \langle \Phi_\mu(\{\mathbf{R}_I^0\}, \{\mathbf{r}_k\sigma_k\}) | V^{e\text{-ph}} + V^{\text{ph}} | \Phi_\nu(\{\mathbf{R}_I^0\}, \{\mathbf{r}_k\sigma_k\}) \rangle \hat{\Lambda}_\nu = E_\mu \hat{\Lambda}_\mu \quad . \quad (1.20)$$

The difference to Eq. (1.12) is that in the second line now there is no differential operator, and E_μ^e is no more a function of $\{\mathbf{R}_I\}$, but is evaluated at point $\{\mathbf{R}_I^0\}$.

Typically the Born-Oppenheimer potential-energy surface has many minima. These correspond to stable or metastable geometries. V^{BO} now is only one point of the Born-Oppenheimer-surface, a minimum. At low temperature this minimum defines the equilibrium geometry.

If we neglect the coupling terms $\langle \Phi_\mu | \dots | \Phi_\nu \rangle$ in Eq. (1.20), for the general wave function of the ground state we have

$$\Psi \rightarrow \Psi^{\text{static}} = \hat{\Lambda}_0 \Phi_0 \quad .$$

Here Φ_0 is the solution of $H^e(\{\mathbf{R}_I^0\})$ and $\hat{\Lambda}_0$ is the solution of $[T^{\text{Ion}} + E_0^e(\{\mathbf{R}_I^0\}) + V^{\text{Ion-Ion}}(\{\mathbf{R}_I^0\})] \hat{\Lambda}_0 = E_0 \hat{\Lambda}_0$. The error which is introduced by this ansatz and by the neglect of the coupling constants of Φ_μ and Φ_ν in Eq. (1.20), respectively, will be discussed in the exercises by a perturbation approach (the result is that in first order the error is zero).

1.2.3 Examples

What can we learn from V^{BO} and the equation

$$E_0 = E_0^e(\{\mathbf{R}_I^0\}) + \frac{1}{4\pi\epsilon_0} \frac{1}{2} \sum_{\substack{I,J \\ I \neq J}}^{M,M} \frac{e^2}{|\mathbf{R}_I^0 - \mathbf{R}_J^0|} Z_{v_I} Z_{v_J} + \text{quantum mechanical corrections for lattice vibrations} \quad ? \quad (1.21)$$

The difficulty in the evaluation of Eq. (1.23) or Eq. (1.8) is the calculation of E_0^e , i.e., the solution of the Schrödinger equation of the electrons. This will be done later (in part 3), and there it will be discussed in greater detail. Now we assume that $E_0^e(\{\mathbf{R}_I\})$ is known, in order to show for two examples, what we can learn using Eq. (1.23).

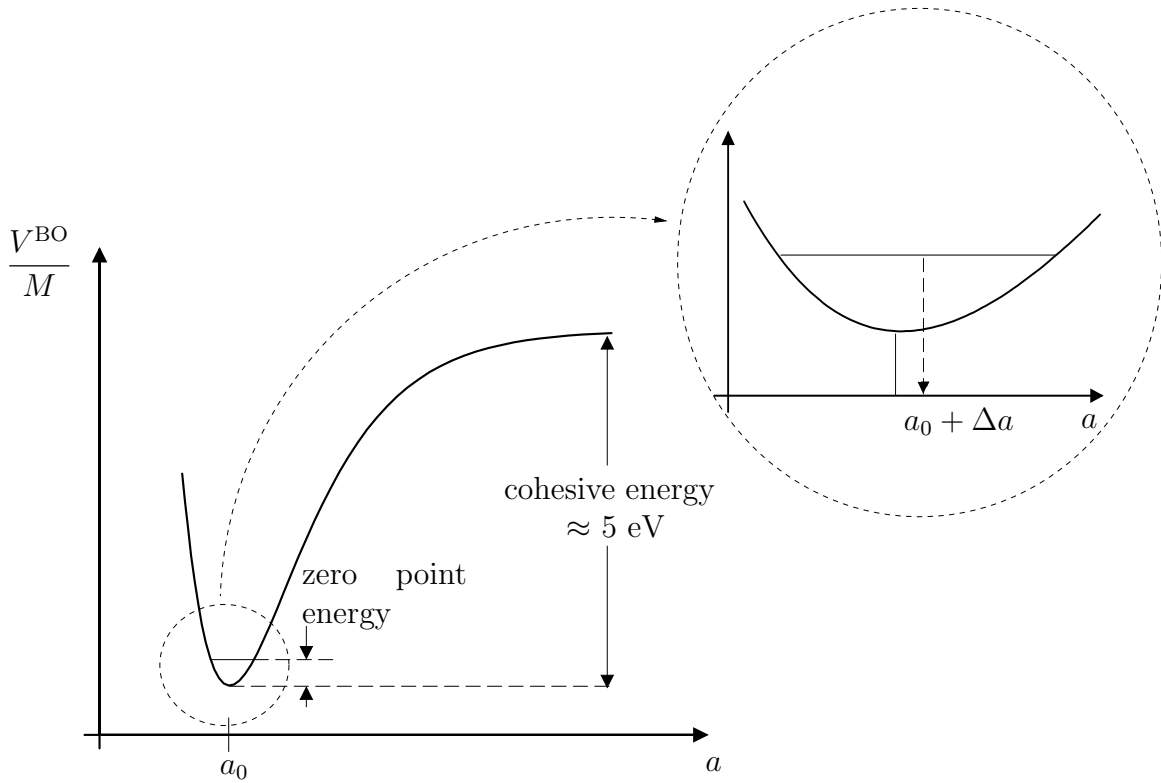


Figure 1.2: The total energy per atom (without zero point vibrations) as a function of the interatomic distance. The minimum of the curve determines the stable equilibrium geometry. The lattice constant, as measured, is not exactly at the minimum of the curve, but it is the average over the zero point vibrations: $a_0 + \Delta a$.

1.2.3a Structure, Lattice Constant, and Elastic Properties of Perfect Crystals

For a cubic crystal, due to the periodicity, the dependence of the total energy E_0 in Eq. (1.23) on the $\{\mathbf{R}_I\}$ is reduced to a single variable a , which determines the interatomic distance in a crystal. In Fig. 1.2 the total energy per atom is shown schematically: The cohesive energy is the energy, which is gained by the formation of the crystal from the individual atoms.

The minimum of the total energy determines the equilibrium position and therefore the lattice constant a_0 of the crystal. The “bulk modulus” B_0 , which describes the dependence of the equilibrium geometry on the external pressure, can be determined from the energy curve $E(a)$. It is defined as the product of the second derivative (curvature) of the energy times the volume V (at the equilibrium distance a_0):

$$B_0 = \frac{1}{K} = V \left. \frac{\partial^2 E(V)}{\partial V^2} \right|_{a=a_0}, \quad (1.22)$$

where V is the volume per atom (for a cubic crystal $V = a^3$), and K is the compressibility.

Figure 1.2 shows the typical course of the binding energy of polyatomic systems as a function of the interatomic distance, and this form is often called “equation of state”. Typically

V^{BO} is calculated for about 10 geometries and the curve is represented by an analytical fit.

The minimum of the “equation of state” is close to, but not exactly the lattice constant of the solid, because the “equation of state” shows a clear asymmetry.

The order of magnitude of the zero point vibrations can be estimated from the uncertainty relation:

$$\Delta P \Delta X \geq \hbar/2 \quad .$$

If $\Delta X = 0.1$ bohr (a typical interatomic distance is 5 bohr ≈ 2.5 Å), for silicon it follows

$$\frac{P^2}{2M} \approx 0.02 \text{eV/atom} \quad .$$

In comparison to the binding energy of the solid (cohesive energy) this is a small number ($\approx \frac{1}{200} E^{\text{coh}}$), but still the zero point vibrations do have a measureable effect (e.g. $\approx 0.1 - 0.5\%$ increase of the lattice constant compared to a neglect of $\langle \Lambda_0 | T^{\text{ion}} + V^{\text{BO}}(\{\Delta \mathbf{R}_I\}) | \Lambda_0 \rangle$).

In Chapter 6 (cohesion) we will e.g. return to the “equation of state” and there we will compare different crystal structures.

Obviously, when higher-energy vibrations are excited (by higher temperatures) the lattice constant increases. This is due to the non-harmonic behavior of V^{BO} around its minimum: For a value smaller than a_0 the potential energy increases strongly due to Pauli repulsion. All solids with one atom per unit cell show such thermal expansion.

1.2.3b Lattice Waves (Phonons)

When intending to calculate the energy of lattice waves (phonons), E_0 has to be investigated as function of the wave length λ and the direction of the lattice wave. Figure 1.3 shows the example of a “frozen phonon”. The magnitude of η “tells”, how many phonons of wave length λ are excited. The energy of this lattice wave follows from the energy difference $E_0(\{\mathbf{R}_I\}) - E_0(\{\mathbf{R}_I^0\})$, where $\{\mathbf{R}_I^0\}$ gives the equilibrium geometry of the lattice and $\{\mathbf{R}_I\}$ the periodically distorted geometry.

From the energy of the lattice wave we can for example obtain quantitative results for the specific heat of the lattice (cf. Ashcroft and Mermin, p. 452-454) and the thermal expansion.

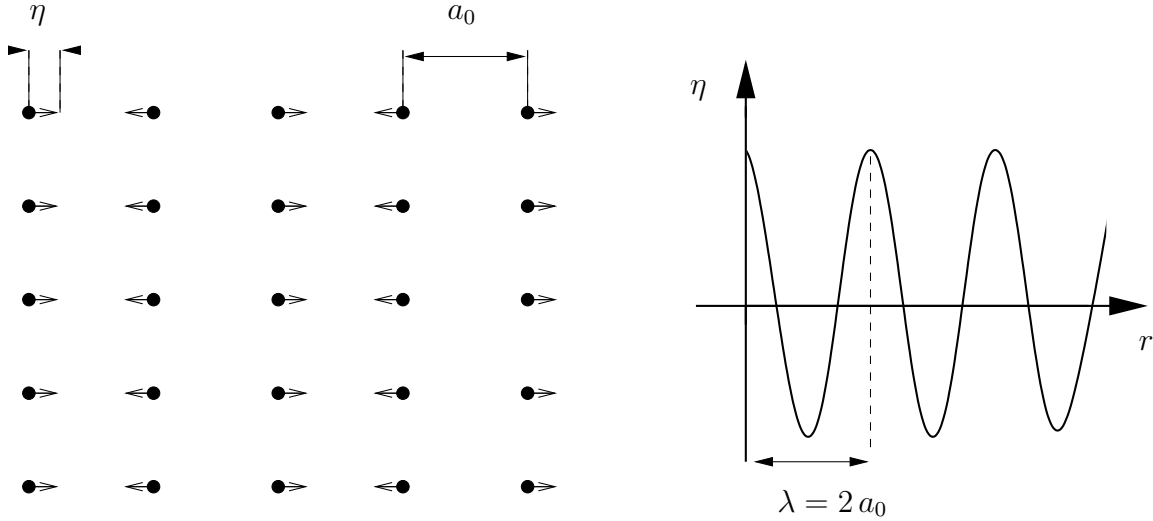


Figure 1.3: Schematic picture of a snapshot of a lattice wave (frozen phonon). The arrows give the direction of the distortion of the atoms. The wave length is $\lambda = 2a_0$, and a_0 is the equilibrium distance of the atoms. The amplitude of the distortion is η .

1.3 The Ewald Method

(References: J.C. Slater, *Insulators, Semiconductors and Metals, Quantum Theory of Molecules and Solids*, Vol. 3, McGraw Hill, 1967, S. 215-220)

The sum appearing in Eq. (1.16)

$$\frac{\langle \Lambda_0 | V^{\text{Ion-Ion}} | \Lambda_0 \rangle}{M} = \frac{E^{\text{Ion-Ion}}}{M} = \frac{1}{M} \frac{1}{4\pi\epsilon_0} \frac{1}{2} \sum_{\substack{I,J \\ I \neq J}}^{M,M} \frac{e^2}{|\mathbf{R}_I^0 - \mathbf{R}_J^0|} Z_{v_I} Z_{v_J} \quad , \quad (1.23)$$

gives the electrostatic interaction energy of the ions and is an important contribution to the total energy. For ionic crystals (e.g. if one considers NaCl as being composed of Na^+ and Cl^- ions) it is even the dominating part of the total energy. Strictly speaking, only the combined electrostatic energy of the ions and the electrons (see Chapter 3), i.e. of the charge neutral solid, is a mathematically well-defined quantity. While the physical meaning of the sum of Eq. (1.23) is clear, summing up the interactions of the point-like charges of the ions is a non-trivial problem. This is because the sum *converges very slowly or not at all*, i.e., even for a very large number of atoms M the result depends on the order of summation, or on the shape of the surface which includes the part already summed up. The reason is the long range of the Coulomb interaction.

In the following we discuss a simple reformulation of the problem which provides a well-behaved expression for the ionic interaction energy. The main idea is to rewrite the interaction energy by (i) adding charge clouds that compensate (or screen) the point-like ions and thereby result in a rapidly convergent sum over charge neutral units, and (ii) subtracting the electrostatic interaction energy of these fictitious charge clouds which is readily obtained from the Poisson equation in Fourier (or reciprocal) space.

The methodical treatment of Eq. (1.23) is important for actual calculations, but it is also interesting, because it clarifies a methodical approach that in a similar way is also helpful for other problems. In general the procedure can be described as follows: If there is an apparently unsolvable problem, first a similar (and possibly uninteresting) problem is solved and then the *difference* of the two systems is investigated.

The problem in the calculation of the sum in Eq. (1.23), i.e., the poor convergence, originates from the fact that the number of atoms of the same distance is growing with separation. We discuss the example of a periodic solid with only one atom per unit cell¹ (and therefore only one atom type). It follows

$$\frac{E^{\text{Ion-Ion}}}{M} = \frac{1}{4\pi\epsilon_0} \frac{1}{2} \sum_{I=2}^M \frac{Z_v^2 e^2}{|\mathbf{R}_I - \mathbf{R}_1|} = \frac{1}{2} Z_v e \phi(\mathbf{R}_1) \quad . \quad (1.24)$$

$\phi(\mathbf{R}_1)$ is the electrostatic potential generated by the ions $I = 2, 3, \dots, M$ at position \mathbf{R}_1 , and because of the periodicity we have $\phi(\mathbf{R}_1) = \phi(\mathbf{R}_2) = \phi(\mathbf{R}_3)$, etc.. The electrostatic potential can be calculated from the Poisson-Equation. If $e n^+(\mathbf{r})$ is the charge density of the nuclei and the core electrons, then we have (Poisson-equation)

$$\nabla^2 \tilde{\phi}(\mathbf{r}) = -\frac{e}{\epsilon_0} n^+(\mathbf{r}) \quad . \quad (1.25)$$

In these equations initially we take into account *all* atoms including ($I = 1$). Later we will remove the contribution of ($I = 1$), which does not appear in Eq. (1.24). We have:

$$\phi(\mathbf{R}_1) = \tilde{\phi}(\mathbf{R}_1) - \text{contribution of the charge density of the ion \#1} \quad . \quad (1.26)$$

First, the reason for the difficulties in evaluating Eq. (1.26) will be pointed out. Because in a periodic crystal $n^+(\mathbf{r})$ is periodic, we have

$$n^+(\mathbf{r}) = \sum_{\mathbf{G}_n} n^+(\mathbf{G}_n) e^{i\mathbf{G}_n \mathbf{r}} \quad (1.27)$$

with

$$n^+(\mathbf{G}_n) = \frac{1}{\Omega} \int_{\Omega} n^+(\mathbf{r}) e^{-i\mathbf{G}_n \mathbf{r}} d^3\mathbf{r} \quad (1.28)$$

and $\mathbf{R}_n \mathbf{G}_n = 2\pi\Gamma$, where Γ is an integer number. Ω is the volume of the unit cell¹ (cf. Chapter 4). We have

$$n^+(\mathbf{G}_n = 0) = \frac{1}{\Omega} Z_v \quad ; \quad (1.29)$$

and because of the Poisson-equation (1.28) it follows for the electrostatic potential $\tilde{\phi}$

$$\nabla^2 \tilde{\phi}(\mathbf{r}) = -\frac{e}{\epsilon_0} \sum_{\mathbf{G}_n} n^+(\mathbf{G}_n) e^{i\mathbf{G}_n \mathbf{r}} \quad (1.30)$$

¹The unit cell is the smallest unit which can be used to construct a periodic solid.

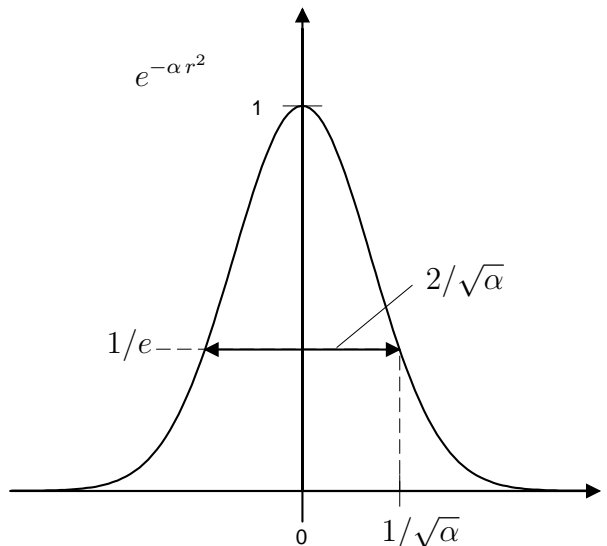


Figure 1.4: Gaussian function $e^{-\alpha r^2}$. The width (at value $e^{-\alpha r^2} = 1/e = 0.368$) is $2/\sqrt{\alpha}$.

and therefore

$$\tilde{\phi}(\mathbf{r}) = \frac{e}{\varepsilon_0} \sum_{\mathbf{G}_n} \frac{n^+(\mathbf{G}_n) e^{i\mathbf{G}_n \mathbf{r}}}{|\mathbf{G}_n|^2} + C \quad , \quad (1.31)$$

which is easily verified by evaluating $\nabla^2 \tilde{\phi}(\mathbf{r})$. We point out that the singularity of Eq. (1.33) for $\mathbf{G}_n = 0$ does not play a role. It is cancelled by a corresponding singularity in the other contributions to the total energy, which appear in V^{e-e} and $V^{e-\text{Ion}}$. This is reasonable, because for a neutral system the term $\mathbf{G}_n = 0$ has to disappear after all. The singularity for $\mathbf{G}_n = 0$ in Eq. (1.33) will therefore be ignored.

If $e n^+(\mathbf{r})$ would only contain the nuclear charges, i.e., δ -functions, then for all terms we have $n^+(\mathbf{G}_n) = \frac{Z_v}{\Omega}$. We note for Eq. (1.24) and (1.31) that *the potential of δ -shaped charge densities converges poorly in real space and in Fourier space.*

On the other hand in Eq. (1.33) one recognizes that the convergence of the series would be better if we had a charge density $n^+(\mathbf{r})$, for which $n^+(\mathbf{G}_n)$ decreases with increasing $|\mathbf{G}_n|^2$. An exponential decay would be best. It follows that a sum of Gaussian functions has to converge nicely. Thus we first investigate such Gaussian-shaped charge densities, although this does not directly correspond to what we are interested in:

$$n_{\text{Gauss}}^+(\mathbf{r}) = Z_v \sum_{I=1}^M \left(\frac{\alpha}{\pi}\right)^{3/2} e^{-\alpha|\mathbf{r}-\mathbf{R}_I|^2} \quad . \quad (1.32)$$

We have normalized the individual Gaussian functions, i.e., we have

$$\int \left(\frac{\alpha}{\pi}\right)^{3/2} e^{-\alpha|\mathbf{r}-\mathbf{R}_I|^2} d\mathbf{r} = 1 \quad , \quad (1.33)$$

and $2/\sqrt{\alpha}$ is the width of the individual Gaussians (cf. Fig. 1.4). The Fourier representa-

tion of $n_{\text{Gauss}}^+(\mathbf{r})$ has the form:

$$n_{\text{Gauss}}^+(\mathbf{G}_n) = \frac{Z_v}{\Omega} \sum_{I=1}^M \int_{\Omega} \left(\frac{\alpha}{\pi}\right)^{3/2} e^{-\alpha|\mathbf{r}-\mathbf{R}_I|^2} e^{-i\mathbf{G}_n\mathbf{r}} d^3\mathbf{r} = \frac{Z_v}{\Omega} e^{-\left(\frac{\mathbf{G}_n^2}{4\alpha}\right)} \quad , \quad (1.34)$$

and for the corresponding electrostatic potential we obtain from the Poisson equation

$$\tilde{\phi}_{\text{Gauss}}(\mathbf{r}) = \frac{Z_v}{\Omega} \frac{e}{\varepsilon_0} \sum_{\mathbf{G}_n} \frac{e^{-\left(\frac{\mathbf{G}_n^2}{4\alpha}\right)} e^{i\mathbf{G}_n\mathbf{r}}}{|\mathbf{G}_n|^2} + C \quad (1.35)$$

$$= \frac{Z_v e}{4\pi\varepsilon_0} \sum_{I=1}^M \frac{\text{erf}(\sqrt{\alpha}|\mathbf{r}-\mathbf{R}_I|)}{|\mathbf{r}-\mathbf{R}_I|} + C \quad . \quad (1.36)$$

Here erf is the error function

$$\text{erf}(x) = \frac{2}{\sqrt{\pi}} \int_0^x e^{-x'^2} dx' \quad . \quad (1.37)$$

This means,

$$\frac{Z_v e}{4\pi\varepsilon_0} \times \frac{\text{erf}(\sqrt{\alpha}|\mathbf{r}-\mathbf{R}_I|)}{|\mathbf{r}-\mathbf{R}_I|} \quad (1.38)$$

is the electrostatic potential, which is created by a Gaussian charge density cloud being centered at position \mathbf{R}_I (cf. Fig. 1.5).

In contrast to $\tilde{\phi}(\mathbf{r})$ in (1.31) this sum (Eq. (1.34) and (1.36)) converges excellently. This is because of the factor $\exp(-\mathbf{G}_n^2/4\alpha)$. The smaller α , the wider are the Gaussians and the smoother is $\phi_{\text{Gauss}}(\mathbf{r})$ and the better is the convergence with respect to \mathbf{G}_n .

Because we are not interested in Gaussian clouds, we write for the density of interest

$$n^+(\mathbf{r}) = \{n^+(\mathbf{r}) - n_{\text{Gauss}}^+(\mathbf{r})\} + n_{\text{Gauss}}^+(\mathbf{r}) \quad . \quad (1.39)$$

Together, the first two components describe a neutral charge, i.e., δ -shaped point charges, which are surrounded by oppositely charged Gaussian clouds and therefore are screened. It is therefore obvious that the sum over such neutral objects converges rapidly in real space. The charge distribution is shown in Fig. 1.6. The last term in Eq. (1.39) converges, as discussed above, very nicely in Fourier space.

We recognize that the contributions being centered at different positions now do not interact (or interact only weakly). The electrostatic field of these two components is:

$$\phi_{1,2}(\mathbf{r}) = \frac{Z_v e}{4\pi\varepsilon_0} \sum_{I=1}^M \left\{ \frac{1 - \text{erf}(\sqrt{\alpha}|\mathbf{r}-\mathbf{R}_I|)}{|\mathbf{r}-\mathbf{R}_I|} \right\} + C \quad . \quad (1.40)$$

The term in the curly brackets of Eq. (1.41) vanishes with increasing distance to the nucleus at position \mathbf{R}_I . Consequently, the sum converges rapidly. Only a few atomic

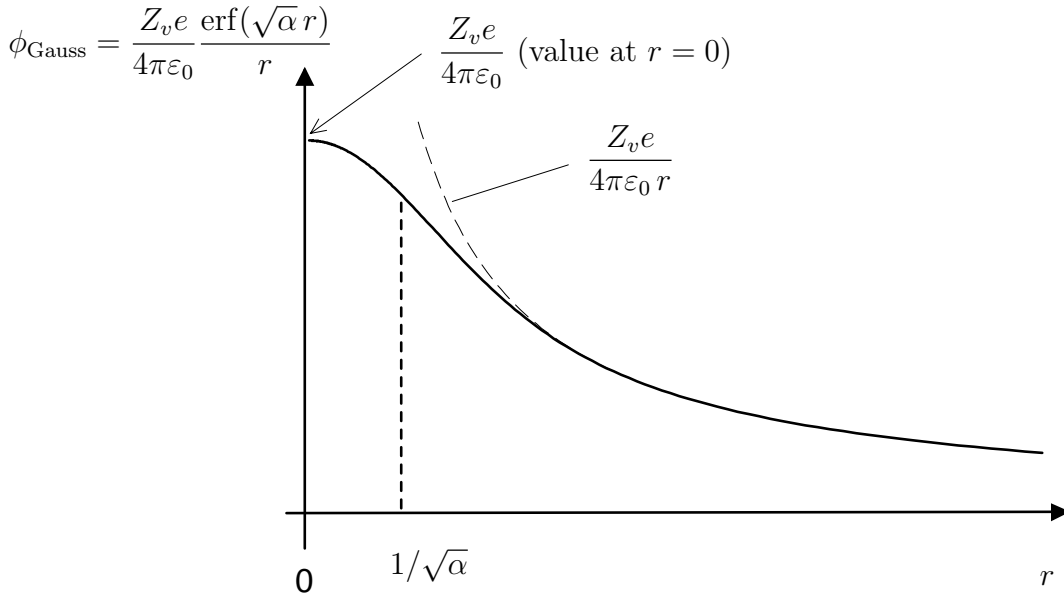


Figure 1.5: The electrostatic potential of a Gaussian shaped charge density of charge $e Z_v$. For large ($r > 1/\sqrt{\alpha}$) the function become identical to $\frac{Z_v e}{4\pi\epsilon_0 r}$.

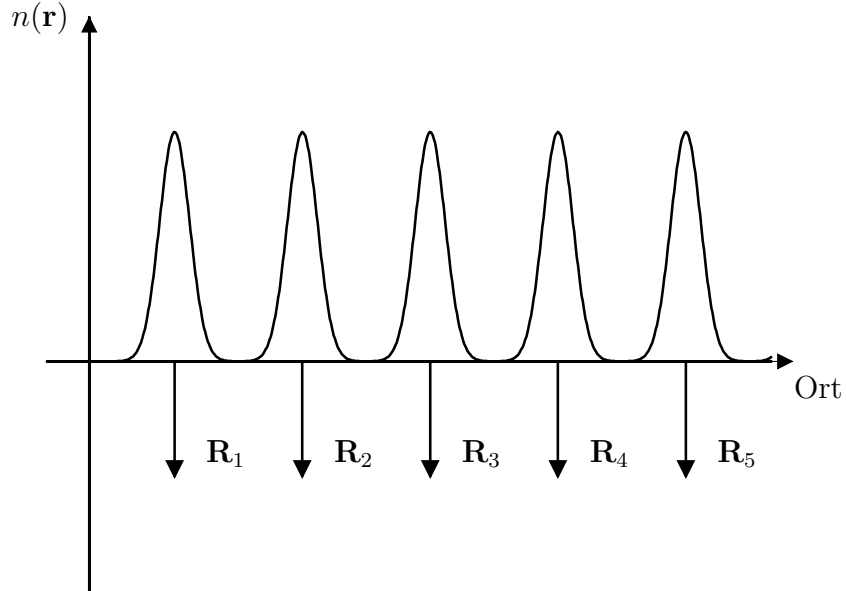


Figure 1.6: Charge distribution of point charges and surrounding Gaussian charge densities. Delta-functions are represented by arrows.

positions in the neighborhood of \mathbf{r} have to be taken into account. The third contribution in Eq. (1.40) of $n^+(\mathbf{r})$, the Gaussian clouds, we describe in the representation (Eq. (1.31)). For the potential that we want to calculate, we obtain

$$\begin{aligned}
 \phi(\mathbf{r}) = & + \frac{Z_v e}{4\pi\epsilon_0} \sum_{I=1}^M \frac{1 - \text{erf}(\sqrt{\alpha}|\mathbf{r} - \mathbf{R}_I|)}{|\mathbf{r} - \mathbf{R}_I|} \\
 & + \frac{Z_v e}{\Omega \epsilon_0} \sum_{\mathbf{G}_n} \frac{e^{-\frac{\mathbf{G}_n^2}{4\alpha}} e^{i\mathbf{G}_n \mathbf{r}}}{|\mathbf{G}_n|^2} - \frac{Z_v e}{4\pi\epsilon_0} \frac{1}{|\mathbf{r} - \mathbf{R}_1|} + C \quad . \quad (1.41)
 \end{aligned}$$

Here we have now removed also the $\mathbf{R}_I = \mathbf{R}_1$ contribution (cf. Eq. (1.26)).

Finally, I will briefly discuss the integration constant C . The electrostatic potential $\phi(\mathbf{r})$, as written down in Eq. (1.42), depends on α . Of course this is unphysical and unwanted. The reason for this dependence is that we have not yet determined the integration constant C , which appeared in the solution of the Poisson-equation for $\phi_{\text{Gauss}}(\mathbf{r})$.

From the condition that ϕ should not depend on α we obtain the integration constant C . It has to be fulfilled:

$$\frac{d\phi(\mathbf{r})}{d\alpha} = 0 \quad . \quad (1.42)$$

The calculation yields:

$$C = -\frac{\pi Z_v e}{\Omega \alpha} \times \frac{1}{4\pi \epsilon_0} \quad . \quad (1.43)$$

Chapter 2

The Fermi Method

2.1 Statistical Mechanics

At finite temperatures there are thermal excitations of the electronic system, i.e., in thermodynamic equilibrium not only the ground state ($E_0^e, \Phi_0(\{\mathbf{r}_{k\sigma}\})$) of H^e is present, but also excited states. Thus, due to thermal fluctuations all states (E_ν^e, Φ_ν) are realized with a certain probability. Assuming that the number of particles and the temperature are determined by external conditions, we have a *canonical ensemble* and the probability $P(E_\nu^e, T)$ for the occupation of state (E_ν^e, Φ_ν) is proportional to $\exp(-E_\nu^e/k_B T)$. Here k_B is the Boltzmann constant. The ensemble is described by the density operator

$$\rho = \sum_\nu P(E_\nu^e, T) |\Phi_\nu\rangle \langle \Phi_\nu| \quad . \quad (2.1)$$

Of course the ensemble of all states has to be normalized to 1 and therefore we have

$$\sum_\nu P(E_\nu^e, T) = 1 = \frac{1}{Z^e} \sum_\nu \exp(-E_\nu^e/k_B T) \quad . \quad (2.2)$$

One obtains

$$Z^e = \sum_\nu \exp(-E_\nu^e/k_B T) = \text{Tr}(\exp(-H^e/k_B T)) \quad . \quad (2.3)$$

Z^e is the partition function of the electrons and is related to the Helmholtz free energy:

$$-k_B T \ln Z^e = F^e = U^e - TS^e \quad , \quad (2.4)$$

where U^e and S^e are the internal energy and the entropy of the electronic systems, i.e. of the electron-hole excitations. Below at Eq. (2.6) we will come back to this point. Consequently, the probability of a thermal occupation of a certain state (E_ν, Φ_ν) is

$$P(E_\nu^e, T) = \frac{1}{Z^e} \exp(-E_\nu^e/k_B T) = \exp[-(E_\nu^e - F^e)/k_B T] \quad . \quad (2.5)$$

At finite temperature we therefore need the full energy spectrum of the many-body Hamilton operator. Then we can calculate the partition function (Eq. (2.3)) and the free energy (Eq. (2.4)). Let us now discuss briefly, how the internal energy and the entropy can be determined separately¹: The internal energy is what up to now we have called total energy at finite temperature:

$$U^e(T) = \sum_\nu E_\nu^e(T) P(E_\nu^e, T) \quad . \quad (2.6)$$

In the general case, i.e., when also atomic vibrations are excited, we have $U = U^e + U^{\text{vib}}$, not just U^e .

¹cf. e.g. N.D. Mermin, Phys. Rev. **137**, A 1441 (1969); M. Weinert and J.W. Davenport, Phys. Rev. B **45**, 13709 (1992); M.G. Gillan, J. Phys. Condens. Matter **1** 689 (1989); J. Neugebauer and M. Scheffler, Phys. Rev. B **46**, 16067 (1992); F. Wagner, T. Laloyaux, and M. Scheffler, Phys. Rev. B **57**, 2102 (1998).

From the laws of thermodynamics $[(\partial u/\partial T)_V = T(\partial s/\partial T)_V]$ and from the third law of thermodynamics ($s \rightarrow 0$ if $T \rightarrow 0$) we obtain

$$s^e = \frac{S^e}{V} = -k_B \sum_i \left[f(\epsilon_i, T) \ln f(\epsilon_i, T) + (1 - f(\epsilon_i, T)) \ln (1 - f(\epsilon_i, T)) \right] . \quad (2.7)$$

Here we used the energy and entropy per unit volume ($u = U/V, s = S/V$), and $f(\epsilon_i, T)$ is the Fermi function (see below). The derivation is particularly simple, if one assumes that we are dealing with independent particles (Eq. (2.11), (2.12), below).

From Eq. (2.4) or (2.7) we obtain the specific heat

$$c_v = \frac{1}{V} \left(\frac{\partial U}{\partial T} \right)_V \quad (2.8)$$

$$= \frac{T}{V} \left(\frac{\partial S}{\partial T} \right)_V . \quad (2.9)$$

Here we removed the superscript e and in fact mean $U = U^e + U^{\text{vib}}$ and $S = S^e + S^{\text{vib}}$. The calculation of c_v of metals is an important example of the importance of Fermi-Dirac statistics of the electrons (cf. Ashcroft-Mermin p. 43, 47, 54).

2.2 Fermi Statistics of the Electrons

Let us assume that the N electrons of our many-body problem occupy single particle levels. Then we also know that due to the Pauli principle each single particle level can be occupied with two electrons at most (one electron with spin up and one electron with spin down). With this assumption it follows (for $T = 0$ K) that the N lowest energy levels ϵ_i are occupied:

$$E^e(T = 0K) = E_0^e = \sum_{i=1}^N \epsilon_i + \Delta , \quad (2.10)$$

where Δ is a correction describing the electron-electron interaction. For independent particles Δ is zero, but for the many-body problem it is very important (see Chapter 3).

The ϵ_i then are eigenvalues of an *effective* single-particle Hamiltonian

$$h = \frac{-\hbar^2}{2m} \nabla^2 + V^{\text{eff}}(\mathbf{r}) .$$

Employing the above description in terms of the density matrix (cf. Marder, Chapter 6.4 and Landau-Lifshitz, Vol. IV) to a situation of independent particles gives for finite temperature the lowest energy that is compatible with the Pauli principle as

$$E^e(T) = \sum_{i=1}^{\infty} \epsilon_i f(\epsilon_i, T) + \Delta . \quad (2.11)$$

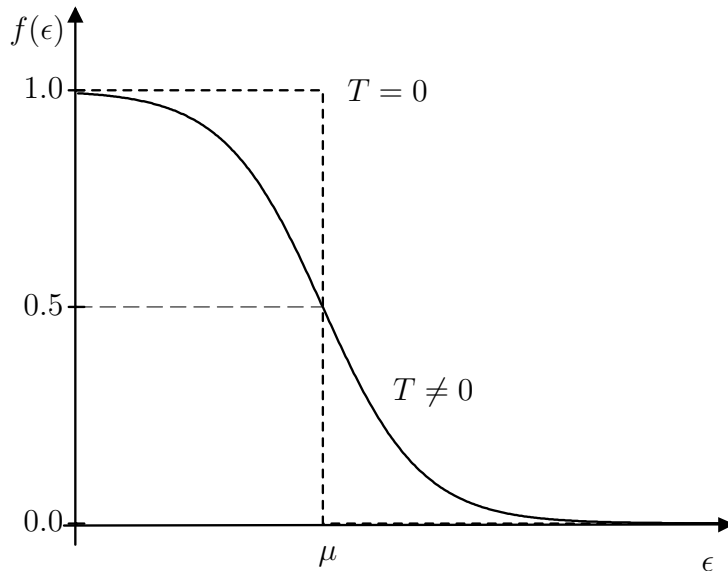


Figure 2.1: The Fermi distribution function [Equation (2.12)].

The index i is running over all single particle states.

The occupation probability (cf. e.g. Ashcroft-Mermin, Eq. (2.41) - (2.49) or Marder, Chapter 6.4) of the i th single particle level ϵ_i is given by the Fermi function:

$$f(\epsilon, T) = \frac{1}{\exp[(\epsilon - \mu)/k_B T] + 1} \quad . \quad (2.12)$$

Here k_B is the Boltzmann constant and μ is the chemical potential of the electrons, i.e., the lowest energy, which is required to remove a particle from the system:

$$-\mu = E^e(N - 1) - E^e(N) \quad . \quad (2.13)$$

How are μ and its temperature dependence determined? The number of electrons is N , and it is independent of the temperature. Therefore, we have

$$N = \sum_{i=1}^{\infty} f(\epsilon_i, T; \mu) \quad . \quad (2.14)$$

For a given temperature this equation contains only one unknown quantity, the chemical potential μ . If all ϵ_i are known, $\mu(T)$ can be calculated.

2.3 Some Definitions

We will now introduce some definitions and constrain ourselves to a so-called “jellium” system. The most simple way (i.e., the crudest approximation to the atomic structure) to investigate the Schrödinger equation of the Hamilton operator

$$H^e = T^e + V^{e-\text{Ion}} + V^{e-e} \quad (2.15)$$

is obtained when setting $V^{e-\text{Ion}} + V^{e-e}$ as a constant function of the electron coordinates. We note that this crude approximation provides reasonable and helpful results for some problems. A system with $V^{e-\text{Ion}} = \text{constant}$ is called “jellium”, and if $V^{e-\text{Ion}}$ as a function of the electronic coordinates is constant, then it can easily be shown that also V^{e-e} is constant² We like to consider here a system without spin-orbit interaction. Thus spin and position coordinates can be separated.

$$\Phi(\{\mathbf{r}_k \sigma_k\}) = \Phi(\{\mathbf{r}_k\})\chi(\{\sigma_k\}) \quad . \quad (2.16)$$

Without introducing a new approximation the zero point of the energy is chosen in a way that the constant potential $V^{e-\text{Ion}} + V^{e-e}$ vanishes. Then the Hamilton operator of the electrons has the simple form

$$H^e = T^e = \sum_{k=1}^N -\frac{\hbar^2}{2m} \nabla_{\mathbf{r}_k}^2 \quad , \quad (2.17)$$

and the many-body Schrödinger equation decomposes into a number of N single particle equations

$$-\frac{\hbar^2}{2m} \nabla^2 \varphi_j(\mathbf{r}) = \epsilon_j \varphi_j(\mathbf{r}) \quad . \quad (2.18)$$

The solutions of Eq. (2.17) are plane waves

$$\varphi_{\mathbf{k}}(\mathbf{r}) = e^{i\mathbf{k}\mathbf{r}} \quad , \quad (2.19)$$

and the energy eigenvalues are

$$\epsilon(\mathbf{k}) = \frac{\hbar^2 \mathbf{k}^2}{2m} \quad , \quad (2.20)$$

where the vectors \mathbf{k} and the components k_x, k_y, k_z have to be interpreted as quantum numbers, up to now noted as index j in (ϵ_j, φ_j) : the state of an electron of the Hamilton operator (2.17) is labeled by the quantum number \mathbf{k} and the spin s . The wave length

$$\lambda = 2\pi/k \quad (2.21)$$

is called de Broglie wave length.

The wave functions in Eq. (2.19) are not normalized (or they are normalized with respect to δ functions). In order to obtain a simpler mathematical discussion often it is useful, or helpful, to constrain the electrons to a finite volume. This volume is called the *base region*, V_g , and it shall be large enough to obtain results independent of its size.³ The base region V_g shall contain N electrons and M atoms. The shape of the base region in principle is meaningless. For simplicity here we chose a box of the dimensions L_x, L_y, L_z (cf. Ashcroft,

²For systems with very low densities, however, electrons will localize themselves at $T = 0\text{K}$ due to the Coulomb repulsion. This is called Wigner crystallization and was predicted in 1930.

³For external magnetic fields the introduction of a base region can give rise to difficulties, because then physical effects often depend significantly on the border.

Mermin: Exercise for more complex shapes). For the wave function we could chose an almost arbitrary constraint (because V_g shall be large enough). It is advantageous to use periodic boundary conditions

$$\varphi(\mathbf{r}) = \varphi(\mathbf{r} + L_x \mathbf{e}_x) = \varphi(\mathbf{r} + L_y \mathbf{e}_y) = \varphi(\mathbf{r} + L_z \mathbf{e}_z) \quad . \quad (2.22)$$

Here \mathbf{e}_x , \mathbf{e}_y , \mathbf{e}_z are the unit vectors in the three Cartesian directions. This is also called the Born-von Karman boundary condition.

As long as V_g , or $L_x \times L_y \times L_z$ is large enough, all physical results do not depend on this treatment. Sometimes also anti-cyclic boundary conditions are chosen in order to check the independence of the results of the choice of the base region.

Using Eq. (2.22) and the normalization condition

$$\int_{V_g} \varphi_{\mathbf{k}}^*(\mathbf{r}) \varphi_{\mathbf{k}'}(\mathbf{r}) d^3 \mathbf{r} = \delta_{\mathbf{k}, \mathbf{k}'} \quad (2.23)$$

we obtain

$$\varphi_{\mathbf{k}}(\mathbf{r}) = \frac{1}{\sqrt{V_g}} e^{i\mathbf{k}\mathbf{r}} \quad . \quad (2.24)$$

Because of Eq. (2.22), i.e., because of the periodicity, only discrete values are allowed for the quantum numbers \mathbf{k} , i.e., $\mathbf{k} \cdot L_i \mathbf{e}_i = 2\pi n_i$ and therefore

$$\mathbf{k} = \left(\frac{2\pi n_x}{L_x}, \frac{2\pi n_y}{L_y}, \frac{2\pi n_z}{L_z} \right) \quad , \quad (2.25)$$

with n_i being arbitrary integer numbers. Thus, the number of vectors \mathbf{k} is countable and finite. Each \mathbf{k} point therefore has the volume

$$\frac{(2\pi)^3}{V_g} \quad (2.26)$$

in k -space.

Each state $\varphi_{\mathbf{k}}(\mathbf{r})$ can be occupied by two electrons. In the ground state at $T = 0$ K the $N/2$ \mathbf{k} points of lowest energy are occupied by two electrons each. Because ϵ depends only on the absolute value of \mathbf{k} , these points fill (for non-interacting electrons) a sphere in \mathbf{k} -space of radius k_F (the ‘‘Fermi sphere’’). We have

$$N = 2 \frac{4}{3} \pi k_F^3 \frac{V_g}{(2\pi)^3} = \frac{1}{3\pi^2} k_F^3 V_g \quad . \quad (2.27)$$

Here the spin of the electron (factor 2) has been taken into account, and $V_g/(2\pi)^3$ is the density of the \mathbf{k} -points (cf. Eq. (2.26)). The particle density of the electrons in jellium is constant:

$$n(\mathbf{r}) = n = \frac{N}{V_g} = \frac{1}{3\pi^2} k_F^3 \quad , \quad (2.28)$$

and the charge density of the electrons is $-en$, and $k_F = \sqrt[3]{3\pi^2 n}$.

For the single particle of the highest energy (in the ground state at $T = 0$ K) we get

$$\epsilon_F = \frac{\hbar^2}{2m} k_F^2 = \frac{\hbar^2}{2m} (3\pi^2 n)^{2/3} \quad . \quad (2.29)$$

Often for jellium-like systems the electron density is given by the *density parameter* r_s . This is defined by a sphere $\frac{4\pi}{3} r_s^3$, which contains exactly one electron. One obtains

$$\frac{4\pi}{3} r_s^3 = V_g/N = 1/n \quad . \quad (2.30)$$

The density parameter r_s is typically given in bohr units.

For metals r_s is typically around 2 bohr (remember: this only refers to the valence electrons), and therefore k_F is approximately 1 bohr $^{-1}$, or 2 Å $^{-1}$, respectively.

Later, we will often apply Eq. (2.29) and (2.30) because some formulas can be presented and interpreted more easily, if ϵ_F , k_F and $n(\mathbf{r})$ are expressed in this way.

Now we introduce the (electronic) density of states:

$$N(\epsilon)d\epsilon = \text{number of states in the energy interval } [\epsilon, \epsilon + d\epsilon] \quad .$$

For the total number of electrons in the base region we have:

$$N = \int_{-\infty}^{+\infty} N(\epsilon) f(\epsilon, T) d\epsilon \quad . \quad (2.31)$$

For free electrons (jellium) we have for the density of states:

$$\begin{aligned} N(\epsilon) &= 2 \frac{V_g}{(2\pi)^3} \int d^3\mathbf{k} \delta(\epsilon - \epsilon_{\mathbf{k}}) \\ &= \frac{2V_g 4\pi}{(2\pi)^3} \int k^2 dk \delta(\epsilon - \epsilon_{\mathbf{k}}) \\ &= \frac{V_g}{\pi^2} \int \frac{d\epsilon_{\mathbf{k}}}{|\nabla_{\mathbf{k}} \epsilon_{\mathbf{k}}|} \frac{2m\epsilon_{\mathbf{k}}}{\hbar^2} \delta(\epsilon - \epsilon_{\mathbf{k}}) \\ &= \frac{V_g}{\pi^2} \int d\epsilon_{\mathbf{k}} \frac{\sqrt{m}}{\hbar\sqrt{2\epsilon_{\mathbf{k}}}} \frac{2m\epsilon_{\mathbf{k}}}{\hbar^2} \delta(\epsilon - \epsilon_{\mathbf{k}}) \\ &= \frac{mV_g}{\pi^2 \hbar^3} \sqrt{2m\epsilon} \quad . \end{aligned} \quad (2.32)$$

For $\epsilon < 0$ we have $N(\epsilon) = 0$. The density of states for two- and one dimensional systems is discussed in the exercises (cf. also Marder).

Figure 2.2 shows the density of states and the occupation at $T = 0$ K and at finite temperature. The density of states at the Fermi level is

$$\frac{N(\epsilon_F)}{V_g} = \frac{3}{2} \frac{N}{V_g} \frac{1}{\epsilon_F} = \frac{m}{\hbar^2 \pi^2} k_F \quad (2.33)$$

The figure shows that at finite temperature holes below μ and electrons above μ are generated.

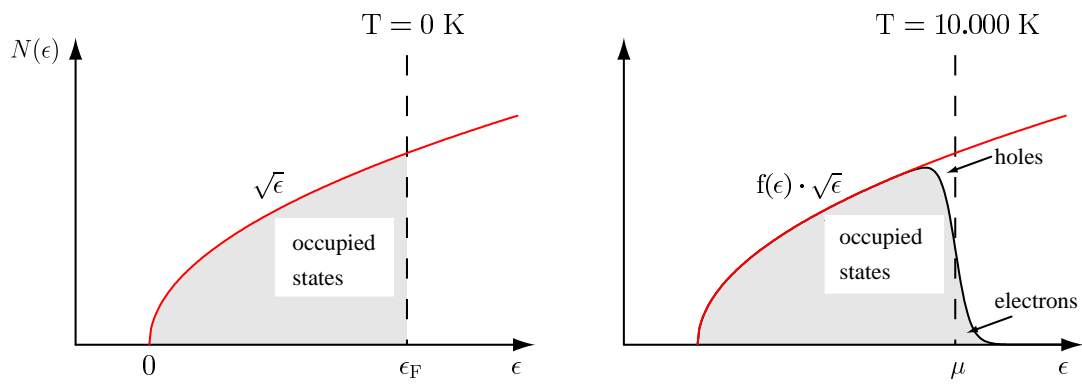


Figure 2.2: Density of states of free electrons $\sqrt{\epsilon}f(\epsilon, T)$ and the separation in occupied and unoccupied states for two temperatures.

Chapter 3

Electron-Electron Interaction

In the adiabatic approximation the motion of the electrons and the nuclei are decoupled. Still, equations (1.9) and (1.13) describe systems containing 10^{23} particles. In the following, we will discuss methods that enable us to deal with a many-body Schrödinger equation like Eq. (1.9). The wave function $\Phi_\nu(\{\mathbf{r}_i\sigma_i\})$ and its energy E_ν^e are determined by the equations (1.9) and (1.10). We write down Eq. (1.10) once more

$$H^e = \sum_{k=1}^N -\frac{\hbar^2}{2m} \nabla_{\mathbf{r}_k}^2 + \sum_{k=1}^N v(\mathbf{r}_k) + \frac{1}{2} \frac{1}{4\pi\epsilon_0} \sum_{\substack{k,k' \\ k \neq k'}}^{N,N} \frac{e^2}{|\mathbf{r}_k - \mathbf{r}_{k'}|} \quad . \quad (3.1)$$

$v(\mathbf{r}_k)$ is the potential of the lattice components (ions or nuclei) of the solid. Often it is called “external potential”.

At this point we briefly recall the meaning of the many-body wave function. It depends on $3N$ spatial coordinates and N spin coordinates. Because the spatial coordinates are all coupled by the operator V^{e-e} , generally they cannot be dealt with separately. In a certain sense this is analogous to the single-particle problem. Here, the wave function $\varphi(x, y, z)$ depends on three spatial coordinates (the spin will be neglected here), and the motion in x -direction is generally not independent of the y -direction. The same is true for x and z , and for y and z . This means, $\varphi(x, y, z)$ does not describe 3 independent one-dimensional particles, but 1 particle with 3 spatial coordinates. In the same way the N -particle Schrödinger equation has to be treated as a many-body equation with $3N$ spatial coordinates. One can say that the total of all the electrons is like a glue, or a mush and not like $3N$ independent particles.

If the electron-electron interaction would be negligible or if it could be described as

$$V^{e-e} \stackrel{?}{=} \sum_{k=1}^N v^{e-e}(\mathbf{r}_k) \quad , \quad (3.2)$$

i.e., the potential at position \mathbf{r}_k does not explicitly depend on the positions of the other electrons, then it would not be a major problem to solve the many-body Schrödinger equation. Unfortunately, such a neglect cannot be justified: The electron-electron interaction is Coulombic; it has an infinite range and for small separations it becomes very strong. Learning about this electron-electron interaction is the most interesting part of solid-state theory. Thus, now we will describe methods, that enable us to take into account the electron-electron interaction in an appropriate manner. There are four methods (or concepts) that can be used:

1. Method of the “effective single-particle theory”: Here we will emphasize in particular the importance of density-functional theory (DFT)¹. Primarily, DFT refers to the

¹1998 Walter Kohn was awarded the Nobel prize in chemistry for the development of density-functional theory.

ground state, E_0^e . In principle it can be used also to calculate excited states. In this chapter we will discuss DFT (and its precursors) with respect to the ground state, and in part II of this lecture we will describe the calculation of excited states and time-dependent DFT (TD-DFT).

2. The Green-function self-energy theory: This method is very general, but not applicable in most cases. One constructs a series expansion in interactions and necessarily many terms have to be neglected, which are believed to be unimportant (cf. e.g. the book by Inkson and the book by Mahan). We will come back to this method in part II of this lecture, because it allows for the calculation of excited states. The first term of such series expansion of Feynman-diagrams is called the *GW*-approximation. Here G is the operator of the Green-function, which e.g. belongs to the *effective* single-particle problem of the Hartree theory or of the density-functional theory, and W is the screened Coulomb interaction of the electrons.
3. Many-body wavefunction approaches (quantum chemistry): Here the basic variable is the many-body wavefunction. There are different methods which seek to obtain increasingly accurate (sophisticated) approximations to the many-body wavefunction. The starting point or lowest level is Hartree-Fock theory, where the wavefunction is described by a single Slater-determinant (as discussed in 3.2, Hartree-Fock theory reduces the to an effective single-particle method). Higher-level methods seek to improve the wavefunction within many-body perturbation theory (here, 2nd and higher-order Møller-Plesset approaches [MPx] are widely used) or non-perturbatively (such as Coupled Cluster [CC] and configuration interaction [CI] approaches). Though these approaches are very successful for molecules, they become computationally too expensive to deal with systems that contain more than ≈ 100 electrons (≈ 1000 if one tries very hard). For solids, these approaches are in general not (yet) feasible.
4. The quantum Monte Carlo method: Here the expectation value of the many-body Hamilton operator H^e is calculated using a very general ansatz of many-body wave functions in the high-dimensional configurational space. Then the wave functions are varied and the minimum of the expectation value $\langle \Phi | H^e | \Phi \rangle / \langle \Phi | \Phi \rangle$ is determined. Due to the availability of fast computers and several methodological developments in recent years this method has gained in importance. It will be discussed in part II of this lecture.

Now we will discuss density-functional theory in detail. This will be done step by step to clarify the physical contents of the theory. Thus, we begin with the Hartree and Hartree-Fock theory and then proceed, via Thomas-Fermi theory, to density-functional theory.

3.1 Hartree Approximation

The ansatz of Hartree shows how a theory evolves or can evolve. Often initially an intuitive feeling is present. Only after that one attempts to derive things in a mathematical way. Hartree (Proc. Camb. Phil. Soc. **24**, 89, 111, 426 (1928)) started from the following idea:

The effect of the electron-electron interaction on a certain electron at position \mathbf{r} should approximately be given by the electrostatic potential, which is generated by all other electrons on average at position \mathbf{r} , i.e., it should approximately be possible to replace the potential $V^{e-e}(\{\mathbf{r}_i\})$ of the many-body Schrödinger equation by

$$V^{e-e}(\{\mathbf{r}_i\}) \overset{!}{\approx} \sum_{k=1}^N v^{\text{Hartree}}(\mathbf{r}_k) \quad (3.3)$$

with

$$v^{\text{Hartree}}(\mathbf{r}) = \frac{e^2}{4\pi\epsilon_0} \int \frac{n(\mathbf{r}')}{|\mathbf{r} - \mathbf{r}'|} d^3\mathbf{r}' \quad . \quad (3.4)$$

Then the many-body Hamilton operator decomposes into N single-particle operators

$$H^e = \sum_{k=1}^N h(\mathbf{r}_k) \quad . \quad (3.5)$$

Each electron would then be described by an effective single-particle Schrödinger equation with a Hamilton operator

$$h = -\frac{\hbar^2}{2m} \nabla^2 + v(\mathbf{r}) + v^{\text{Hartree}}(\mathbf{r}) \quad . \quad (3.6)$$

The validity of Eqs. (3.3) – (3.6) may seem to be reasonable. Often, however, this approach is an (often drastic) approximation. Only a more precise treatment can show how problematic this approximation is, and this shall be done now.

Mathematical Derivation of the Hartree Equations

Starting from the general many-body equation, Eqs. (3.3) – (3.6) shall be derived. In particular the approximation connected with Eq. (3.6) shall be identified. Before we start, we note that H^e does not contain the spin of the electrons explicitly and therefore, also no coupling between the spin and position is included. Thus, for the eigenfunctions of H^e we must have

$$\Phi_\nu(\{\mathbf{r}_i\sigma_i\}) = \Phi_\nu(\{\mathbf{r}_i\}) \chi_\nu(\{\sigma_i\}) \quad . \quad (3.7)$$

To take into account orbital as well as spin quantum numbers, from now on we will label the set k of quantum numbers as follows

$$\nu \equiv o_\nu s_\nu \quad ,$$

with o_ν representing the orbital quantum numbers of set ν and s_ν the spin quantum numbers. In the free electron gas (cf. Chapter 2) o_ν represents all possible values of the 3 numbers: k_x, k_y, k_z . For each state s_ν is \uparrow or \downarrow .

For the spin component we have (because H^e does not contain spin-orbit and spin-spin coupling)

$$\chi_\nu(\{\sigma_i\}) = \chi_{s_1}(\sigma_1) \chi_{s_2}(\sigma_2) \dots \chi_{s_N}(\sigma_N) \quad . \quad (3.8)$$

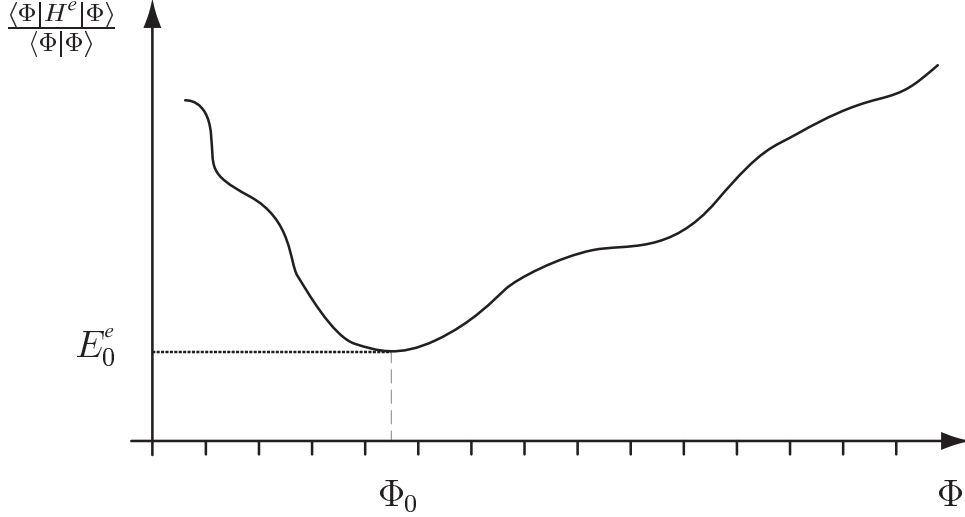


Figure 3.1: Schematic representation of the expectation value of the Hamilton operator as a “function” of the vectors of the Hilbert space. The dashes at the Φ -axis label the wave functions of type Φ^{Hartree} . They cannot reach the function Φ_0 , but can get close to it.

Here, we have $\chi_{\uparrow}(\sigma) = \begin{cases} 1 & \text{for } \sigma = +1/2 \\ 0 & \text{for } \sigma = -1/2 \end{cases}$ and $\chi_{\downarrow}(\sigma) = \begin{cases} 0 & \text{for } \sigma = +1/2 \\ 1 & \text{for } \sigma = -1/2 \end{cases}$, i.e. σ labels two components of the Pauli spinors, $\begin{pmatrix} 1 \\ 0 \end{pmatrix}$ and $\begin{pmatrix} 0 \\ 1 \end{pmatrix}$, respectively. For the spatial part such a product ansatz is invalid, because H^e due to the electron-electron interaction couples the positions of “different” electrons. For the lowest eigenvalue of the Schrödinger equation the variational principle holds, i.e., for the ground state of H^e we have

$$E_0^e \leq \frac{\langle \Phi | H^e | \Phi \rangle}{\langle \Phi | \Phi \rangle} \quad , \quad (3.9)$$

where the Φ are arbitrary functions of the N -particle Hilbert space, which can be differentiated twice and can be normalized. If we constrain the set of functions Φ and consider the Hilbert space defined by the subset given by the eigenfunctions of H^e , we most probably will not obtain E_0^e exactly. Consequently, the ansatz for independent particles

$$\Phi(\{\mathbf{r}_i\}) \approx \Phi^{\text{Hartree}}(\{\mathbf{r}_i\}) = \varphi_{o_1}(\mathbf{r}_1)\varphi_{o_2}(\mathbf{r}_2) \dots \varphi_{o_N}(\mathbf{r}_N) \quad (3.10)$$

in general is an approximation. Functions that can be written as Eq. (3.10) do not span the full Hilbert space of the functions $\Phi(\{\mathbf{r}_i\})$, which can be differentiated twice and can be normalized. A certain restriction of the set of the allowed functions is acceptable, but we also note that an estimation (determination) of E_0^e using the variational principle is “dangerous”, i.e., it is unknown, how close to E_0^e the result will be. Generally we are not interested in the exact value of E_0^e , but an error of 0.1 eV could be acceptable. Schematically, the variational principle can be described by Fig. 3.1. Because the Hartree ansatz (Eq. (3.10)) for sure is an approximation, we have

$$E_0^e < \frac{\langle \Phi^{\text{Hartree}} | H^e | \Phi^{\text{Hartree}} \rangle}{\langle \Phi^{\text{Hartree}} | \Phi^{\text{Hartree}} \rangle} \quad . \quad (3.11)$$

Due to the normalization condition we have

$$\langle \Phi^{\text{Hartree}} | \Phi^{\text{Hartree}} \rangle = \int \dots \int |\Phi^{\text{Hartree}}(\{\mathbf{r}_i\})|^2 d^3\mathbf{r}_1 \dots d^3\mathbf{r}_N = 1 \quad , \quad (3.12)$$

$$\langle \varphi_{o_i} | \varphi_{o_i} \rangle = \int |\varphi_{o_i}(\mathbf{r})|^2 d^3\mathbf{r} = 1 \quad . \quad (3.13)$$

Orthogonality of the different φ_{o_i} is not required, because we do not want to restrict Φ^{Hartree} any further than we have already done by Eq. (3.10). However, we will obtain that it is – quasi automatically – fulfilled. With the Hartree ansatz (Eq. (3.10)) the expectation value of the energy is

$$\begin{aligned} \langle \Phi^{\text{Hartree}} | H^e | \Phi^{\text{Hartree}} \rangle &= \int \varphi_{o_1}^*(\mathbf{r}_1) \varphi_{o_2}^*(\mathbf{r}_2) \dots \varphi_{o_N}^*(\mathbf{r}_N) \left[\sum_{k=1}^N \frac{-\hbar^2}{2m} \nabla_{\mathbf{r}_k}^2 + v(\mathbf{r}_k) \right] \\ &\quad \varphi_{o_1}(\mathbf{r}_1) \varphi_{o_2}(\mathbf{r}_2) \dots \varphi_{o_N}(\mathbf{r}_N) d^3\mathbf{r}_1 \dots d^3\mathbf{r}_N \\ &+ \frac{1}{2} \frac{e^2}{4\pi\epsilon_0} \int \varphi_{o_1}^*(\mathbf{r}_1) \varphi_{o_2}^*(\mathbf{r}_2) \dots \varphi_{o_N}^*(\mathbf{r}_N) \left[\sum_{\substack{k,k'=1 \\ k \neq k'}}^{N,N} \frac{1}{|\mathbf{r}_k - \mathbf{r}_{k'}|} \right] \\ &\quad \varphi_{o_1}(\mathbf{r}_1) \varphi_{o_2}(\mathbf{r}_2) \dots \varphi_{o_N}(\mathbf{r}_N) d^3\mathbf{r}_1 \dots d^3\mathbf{r}_N \quad . \\ &= \sum_{k=1}^N \int \varphi_{o_k}^*(\mathbf{r}_k) \left\{ -\frac{\hbar^2}{2m} \nabla^2 + v(\mathbf{r}_k) \right\} \varphi_{o_k}(\mathbf{r}_k) d^3\mathbf{r}_k \\ &+ \frac{1}{2} \frac{e^2}{4\pi\epsilon_0} \sum_{\substack{k,k'=1 \\ k \neq k'}}^{N,N} \iint \varphi_{o_k}^*(\mathbf{r}_k) \frac{\varphi_{o_{k'}}^*(\mathbf{r}_{k'}) \varphi_{o_{k'}}(\mathbf{r}_{k'}) \varphi_{o_k}(\mathbf{r}_k) d^3\mathbf{r}_k d^3\mathbf{r}_{k'}}{|\mathbf{r}_k - \mathbf{r}_{k'}|} \quad (3.15) \end{aligned}$$

Equation (3.14) can be understood as an energy functional:

$$\langle \Phi^{\text{Hartree}} | H^e | \Phi^{\text{Hartree}} \rangle \stackrel{!}{=} \tilde{E}^{\text{Hartree}} [\varphi_{o_1}, \varphi_{o_2} \dots \varphi_{o_N}, \varphi_{o_1}^*, \varphi_{o_2}^* \dots \varphi_{o_N}^*] \quad (3.16)$$

Here φ and φ^* are considered as two independent functions. Alternatively, the real and the imaginary part of φ could be considered as separate variables.

Ansatz (Eq. (3.10)) represents a significant restriction to the possible functions. Still, we will continue and determine “the best” single-particle functions from this set of functions, i.e., those single-particle functions, which minimize $\tilde{E}^{\text{Hartree}}[\varphi_{o_1} \dots \varphi_{o_N}^*]$. The hope is that the minimum of $\langle \Phi^{\text{Hartree}} | H^e | \Phi^{\text{Hartree}} \rangle$ will be rather close to the true ground state energy E_0^e . Thus, we vary the expression (Eq. (3.14)) with respect to the functions $\varphi_{o_i}^*(\mathbf{r})$ and $\varphi_{o_i}(\mathbf{r})$. The variation is not fully free, because only those functions can be considered, that can be normalized to one. This constraint (Eq. (3.13)) can be taken into account in the variational problem using the method of Lagrange multipliers. Then we obtain an equation to determine the best $\varphi_{o_i}(\mathbf{r})$:

$$\begin{aligned} Q[\varphi_{o_1}, \dots, \varphi_{o_N}, \varphi_{o_1}^*, \dots, \varphi_{o_N}^*] &= \tilde{E}^{\text{Hartree}}[\varphi_{o_1} \dots \varphi_{o_N}, \varphi_{o_1}^* \dots \varphi_{o_N}^*] \\ &\quad - \sum_{k=1}^N \{ \epsilon_{o_k} (1 - \langle \varphi_{o_k} | \varphi_{o_k} \rangle) \} \equiv \text{minimum} \quad , \quad (3.17) \end{aligned}$$

where the ϵ_{o_k} are the Lagrange-multipliers.

Equation (3.16) can be formulated in the following way: We search for the minimum of the functional Q , and for the minimum we have:

$$\begin{aligned} \delta Q = Q [\varphi_{o_1}, \varphi_{o_2}, \dots, \varphi_{o_N}, \varphi_{o_1}^*, \varphi_{o_2}^*, \dots, \varphi_{o_i}^* + \delta\varphi_{o_i}^*, \dots, \varphi_{o_N}^*] \\ - Q [\varphi_{o_1}, \dots, \varphi_{o_N}, \varphi_{o_1}^*, \dots, \varphi_{o_i}^*, \dots, \varphi_{o_N}^*] = 0 \quad , \end{aligned} \quad (3.18)$$

for an arbitrary variation $\delta\varphi_{o_i}^*$, $i = 1 \dots N$, or $\delta\varphi_{o_i}$, $i = 1 \dots N$.

Therefore, if we vary $\varphi_{o_i}^*(\mathbf{r})$, with Eq. (3.16) we obtain

$$\left\langle \delta\varphi_{o_i} \left| -\frac{\hbar^2}{2m} \nabla^2 + v(\mathbf{r}) \right| \varphi_{o_i} \right\rangle + \sum_{\substack{k=1 \\ k \neq i}}^N \frac{e^2}{4\pi\epsilon_0} \left\langle \delta\varphi_{o_i} \varphi_{o_k} \left| \frac{1}{|\mathbf{r}_k - \mathbf{r}_i|} \right| \varphi_{o_k} \varphi_{o_i} \right\rangle = \epsilon_{o_i} \langle \delta\varphi_{o_i} | \varphi_{o_i} \rangle \quad . \quad (3.19)$$

Because the constraint (normalization of the φ_{o_i}) is taken into account by the method of the Lagrange-multipliers, this equation is valid for arbitrary variations $\delta\varphi_{o_i}$. Thus, the equation used to determine the functions $\varphi_{o_i}(\mathbf{r})$ is

$$\left[-\frac{\hbar^2}{2m} \nabla^2 + v(\mathbf{r}) \right] \varphi_{o_i}(\mathbf{r}) + \sum_{\substack{k=1 \\ k \neq i}}^N \frac{e^2}{4\pi\epsilon_0} \left\langle \varphi_{o_k} \left| \frac{1}{|\mathbf{r}_k - \mathbf{r}|} \right| \varphi_{o_k} \right\rangle \varphi_{o_i}(\mathbf{r}) = \epsilon_{o_i} \varphi_{o_i}(\mathbf{r}) \quad . \quad (3.20)$$

We rewrite this equation and obtain

$$\left[-\frac{\hbar^2}{2m} \nabla^2 + v(\mathbf{r}) + v^{\text{Hartree}}(\mathbf{r}) + v_{o_i}^{\text{SIC}}(\mathbf{r}) \right] \varphi_{o_i}(\mathbf{r}) = \epsilon_{o_i} \varphi_{o_i}(\mathbf{r}) \quad , \quad (3.21)$$

where

$$v^{\text{Hartree}}(\mathbf{r}) = \frac{e^2}{4\pi\epsilon_0} \int \frac{n(\mathbf{r}')}{|\mathbf{r} - \mathbf{r}'|} d^3\mathbf{r}' \quad (3.22)$$

with

$$n(\mathbf{r}) = \langle \Phi | \sum_{k=1}^N \delta(\mathbf{r} - \mathbf{r}_k) | \Phi \rangle = \sum_{k=1}^N |\varphi_{o_k}(\mathbf{r})|^2 \quad , \quad (3.23)$$

and

$$v_{o_i}^{\text{SIC}}(\mathbf{r}) = -\frac{e^2}{4\pi\epsilon_0} \int \frac{|\varphi_{o_i}(\mathbf{r}')|^2}{|\mathbf{r} - \mathbf{r}'|} d^3\mathbf{r}' \quad . \quad (3.24)$$

$n(\mathbf{r})$ is the particle density of all electrons and $-en(\mathbf{r})$ is the charge density of all electrons. The first equals sign in Eq. (3.22) holds in general, i.e., this is the quantum mechanical definition of the electron density. The second equals sign is valid only for independent particles and for the Hartree approximation.

The term $v^{\text{Hartree}}(\mathbf{r})$, generally called the Hartree potential, can also be expressed in the differential form of electrostatics (Poisson equation):

$$\nabla^2 v^{\text{Hartree}}(\mathbf{r}) = -\frac{e^2}{\epsilon_0} n(\mathbf{r}) \quad (3.25)$$

The potential $v_{\sigma_i}^{\text{SIC}}(\mathbf{r})$ is the self-interaction correction of the Hartree potential. It takes into account that an electron in orbital $\varphi_{o_i}(\mathbf{r})$ shall not interact with itself, but only with the $(N - 1)$ remaining electrons of the system. Equation (3.20) is now “sufficiently simple” to be solved using modern numerical methods. Often the potential $v_{\sigma_i}^{\text{SIC}}(\mathbf{r})$ is then neglected. However, since recent years it became clear that this additional approximation is typically not justified. If the functions $\varphi_{o_i}(\mathbf{r})$ were known, we could calculate the total energy from Eq. (3.14) or the electron distribution using Eq. (3.22). The latter can be compared to measurements (e.g. X-ray diffraction). Additionally, using the charge distribution of the electrons, the nature of the forces, which stabilize the solid, can be understood. One finds that several quantities obtained from the Hartree approximation agree well with experimental data. Further, we find that the negative values of the Lagrange parameters ϵ_{o_i} , introduced due to the normalization, agree approximately with measured ionization energies. An exact discussion of the physical meaning of the Lagrange parameters will be given later (in the context of the Hartree-Fock theory).

Obviously, the Hartree Eq. (3.20) is no ordinary single-particle equation. Formally, it can be written as a single-particle equation,

$$\left\{ -\frac{\hbar^2}{2m} \nabla^2 + v^{\text{eff}}(\mathbf{r}) \right\} \varphi_{o_i}(\mathbf{r}) = \epsilon_{o_i} \varphi_{o_i}(\mathbf{r}) \quad . \quad (3.26)$$

However, the “effective potential” itself depends on the solutions $\varphi_{o_i}(\mathbf{r})$. Therefore, Eq. (3.25) is an effective (but not a true) single-particle equation. This, for example, implies that the total energy is not equal to the sum of the ϵ_{o_i} , which would be the case for non-interacting particles in the single-particle states $\varphi_{o_i}(\mathbf{r})$.

Nevertheless, using the φ_{o_i} via Eq. (3.14) the total energy can be obtained. How can an equation like Eq. (3.25) be solved, if the potential

$$v^{\text{eff}}(\mathbf{r}) = v(\mathbf{r}) + v^{\text{Hartree}}(\mathbf{r}) + v_{\sigma_i}^{\text{SIC}}(\mathbf{r}) \quad (3.27)$$

initially is unknown, because $n(\mathbf{r})$ is not known? For this purpose the so-called self-consistent field method (SCF) is applied. First, one starts with a reasonable guess, i.e., one estimates $n(\mathbf{r})$. Then the density is improved step by step until the correct result is obtained.

A first crude approximation for $n(\mathbf{r})$ of a solid is obtained by assuming that it can be written as a simple superposition of the electron densities of the individual atoms

$$n^{\text{start}}(\mathbf{r}) = \sum_{I=1}^M n_I^{\text{Atom}}(|\mathbf{r} - \mathbf{R}_I|) \quad . \quad (3.28)$$

This is correct for large interatomic distances, but it is a severe approximation when the electron densities of different atoms overlap. Nevertheless, Eq. (3.27) is a possible and not bad “zeroth approximation”. Once a “zeroth approximation” has been made, one proceeds as shown in Fig. 3.2. At the end of such a calculation the wave functions $\varphi_{o_k}(\mathbf{r})$ and

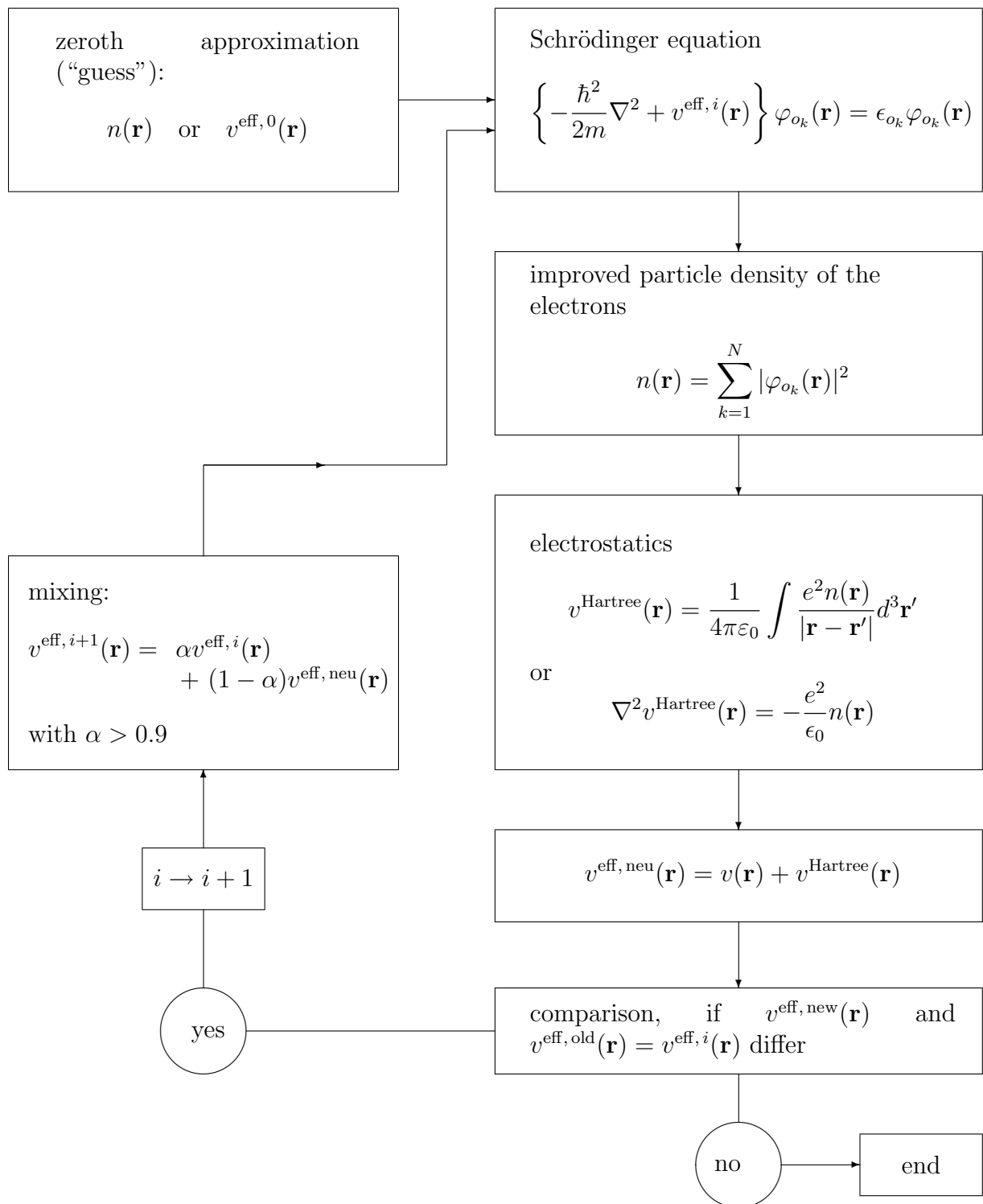


Figure 3.2: Scheme of the self-consistent field method for the solution of the Hartree equation. Here, v^{SIC} has been neglected. Analogous diagrams exist for Hartree-Fock and density-functional theory.

the potential $v^{\text{eff}}(\mathbf{r})$ are *self-consistent*, i.e., their differences in two subsequent iterations are arbitrarily small. Typically, between 5 and 50 iterations are required.

3.2 Hartree-Fock Approximation

The Hartree wave function (Eq. (3.10)) has an important disadvantage: It does not satisfy the Pauli principle. Due to the variational principle, this does not necessarily have a drastic impact on the calculated energy, but for sure it would be better, to remove or reduce this disadvantage. In a many-electron system there is an important interaction between the particles, which in the single-particle picture is formulated in the following way: A single-particle wave function can be occupied by only one electron. More generally, in the many-body picture, the Pauli principle states that the N -particle wave function of fermions has to be antisymmetric with respect to the interchange of all coordinates (spatial and spin) of two particles.

In order to fulfill the Pauli principle, Fock suggested to replace the wave function used in Hartree theory by a suitable linear combination, a so-called Slater determinant²

$$\Phi^{\text{HF}}(\{\mathbf{r}_i\sigma_i\}) = \frac{1}{\sqrt{N!}} \begin{vmatrix} \varphi_{o_1s_1}(\mathbf{r}_1\sigma_1) \cdots \varphi_{o_Ns_N}(\mathbf{r}_1\sigma_1) \\ \varphi_{o_1s_1}(\mathbf{r}_2\sigma_2) \cdots \varphi_{o_Ns_N}(\mathbf{r}_2\sigma_2) \\ \cdots \\ \varphi_{o_1s_1}(\mathbf{r}_N\sigma_N) \cdots \varphi_{o_Ns_N}(\mathbf{r}_N\sigma_N) \end{vmatrix} . \quad (3.29)$$

The factor $1/\sqrt{N!}$ ensures the normalization of the many-body wave function. The many-body wave function (Eq. (3.28)) changes sign on interchange of the coordinates (spatial and spin) of two particles. For a determinant this is obvious, because the interchange of two particles corresponds to the interchange of two rows of the determinant.

For two-electron systems (e.g. H^- or He) the wave function reads

$$\Phi^{\text{HF}} = \frac{1}{\sqrt{1 \times 2}} (\varphi_1(\mathbf{r}_1\sigma_1)\varphi_2(\mathbf{r}_2\sigma_2) - \varphi_2(\mathbf{r}_1\sigma_1)\varphi_1(\mathbf{r}_2\sigma_2)) \quad , \quad (3.30)$$

where the one-particle states $i =: (o_i s_i)$ can be, for instance, $1 =: (o_1 \uparrow)$, $2 =: (o_1 \downarrow)$ (two electrons with opposite spin in the same orbital) or $1 =: (o_1 \uparrow)$, $2 =: (o_2 \uparrow)$ (two electrons with the same spin in different orbitals).

²From here on we label the one-particle states by quantum numbers o_i instead of k_i to emphasize that they refer to the position-space component of these states.

And also the normalization is fulfilled:

$$\begin{aligned}
\langle \Phi^{\text{HF}} | \Phi^{\text{HF}} \rangle &= \frac{1}{2!} \sum_{\sigma_1, \sigma_2} \iint \left\{ \varphi_1^*(\mathbf{r}_1 \sigma_1) \varphi_2^*(\mathbf{r}_2 \sigma_2) \varphi_1(\mathbf{r}_1 \sigma_1) \varphi_2(\mathbf{r}_2 \sigma_2) \right. \\
&\quad - \varphi_1^*(\mathbf{r}_1 \sigma_1) \varphi_2^*(\mathbf{r}_2 \sigma_2) \varphi_1(\mathbf{r}_2 \sigma_2) \varphi_2(\mathbf{r}_1 \sigma_1) \\
&\quad - \varphi_1^*(\mathbf{r}_2 \sigma_2) \varphi_2^*(\mathbf{r}_1 \sigma_1) \varphi_1(\mathbf{r}_1 \sigma_1) \varphi_2(\mathbf{r}_2 \sigma_2) \\
&\quad \left. + \varphi_1^*(\mathbf{r}_2 \sigma_2) \varphi_2^*(\mathbf{r}_1 \sigma_1) \varphi_1(\mathbf{r}_2 \sigma_2) \varphi_2(\mathbf{r}_1 \sigma_1) \right\} d^3 \mathbf{r}_1 d^3 \mathbf{r}_2 \\
&= \frac{1}{2} (1 + 0 + 0 + 1) \\
&= 1 \quad .
\end{aligned} \tag{3.31}$$

The single-particle functions shall be normalized and orthogonal,

$$\langle \varphi_{o_i s_i} | \varphi_{o_j s_j} \rangle = \delta_{o_i, o_j} \delta_{s_i, s_j} \quad \text{with} \quad \varphi_{o_i s_i}(\mathbf{r}, \sigma) = \varphi_{o_i s_i}(\mathbf{r}) \chi_{s_i}(\sigma) \quad . \tag{3.32}$$

Note that the spatial functions for spin \uparrow and spin \downarrow states do not have to be the same. In Hartree theory the spatial functions were assumed to be independent of the spin states so that the spin quantum numbers s_i could be omitted. In Hartree-Fock theory this is not the case anymore.³

Now we proceed in the same way as in the Hartree theory, i.e., we will make use of the variational principle $\langle \Phi | H^e | \Phi \rangle = E[\Phi] \geq E_0^e$. It should be noted that ansatz (Eq. (3.28)) still is not general. It allows for an infinite number of possibilities, because the $\varphi_{o_i s_i}(\mathbf{r}, \sigma)$ are arbitrary functions (which can be normalized), but still the set of all vectors in Hilbert space that can be written like Eq. (3.28), do only form a subset of the Hilbert space of the N -particle problem. Many vectors in Hilbert space can only be expressed as a linear combination of Slater determinants. Consequently, again we will not necessarily obtain the ground state energy exactly, but often an approximation will be obtained. However, most probably the approximation will be better than the approximation obtained in Hartree theory, because now the subset of the Hilbert space satisfies the quantum mechanical properties (Pauli principle) of the electrons. Similar to Hartree theory, using Eq.

³Because the (non-relativistic) Hamilton operator of Eq. (3.1) commutes with the operators for the total spin and its z -projection, the exact solutions of the many-electron Schrödinger equation should be eigenfunctions of all of these operators. In principle, this imposes constraints on the form of Φ and the one-particle orbitals. On the other hand, such (spin symmetry) constraints typically lead to higher (i.e. poorer) ground state energies compared to freely varied orbitals. In the context of Hartree-Fock theory, one may make restrict the orbitals $\varphi_{o_i \uparrow} \equiv \varphi_{o_i \downarrow}$ to ensure that Φ^{HF} has the proper spin symmetry (say, for a singlet or triplet He atom). This approach is often referred to as “restricted open-shell Hartree-Fock” (RHF). Or, one may allow the spin-up and -down orbitals to differ. For systems with an unequal number of spin-up and -down electrons, such “unrestricted Hartree-Fock” (UHF) calculations yield indeed lower ground state energies than RHF. The price is that Φ^{UHF} in general does not describe a pure spin state but a mixture of different spin states.

(3.28) we now obtain the expectation value of the energy

$$\begin{aligned}
E^{\text{HF}}[\Phi^{\text{HF}}] &= \langle \Phi^{\text{HF}} | H^e | \Phi^{\text{HF}} \rangle \\
&= \sum_{i=1}^N \sum_{\sigma} \int \varphi_{o_i s_i}^*(\mathbf{r}, \sigma) \left\{ -\frac{\hbar^2}{2m} \nabla^2 + v(\mathbf{r}) \right\} \varphi_{o_i s_i}(\mathbf{r}, \sigma) d^3 \mathbf{r} \\
&\quad + \frac{1}{2} \frac{e^2}{4\pi\epsilon_0} \sum_{\substack{i,j \\ i \neq j}}^{N,N} \sum_{\sigma, \sigma'} \iint \frac{\varphi_{o_i s_i}^*(\mathbf{r}', \sigma') \varphi_{o_j s_j}^*(\mathbf{r}, \sigma) \varphi_{o_i s_i}(\mathbf{r}', \sigma') \varphi_{o_j s_j}(\mathbf{r}, \sigma)}{|\mathbf{r} - \mathbf{r}'|} d^3 \mathbf{r} d^3 \mathbf{r}' \\
&\quad - \frac{1}{2} \frac{e^2}{4\pi\epsilon_0} \sum_{\substack{i,j \\ i \neq j}}^{N,N} \sum_{\sigma, \sigma'} \iint \frac{\varphi_{o_j s_j}^*(\mathbf{r}', \sigma') \varphi_{o_i s_i}^*(\mathbf{r}, \sigma) \varphi_{o_i s_i}(\mathbf{r}', \sigma') \varphi_{o_j s_j}(\mathbf{r}, \sigma)}{|\mathbf{r} - \mathbf{r}'|} d^3 \mathbf{r} d^3 \mathbf{r}' \quad .
\end{aligned} \tag{3.33}$$

The sums over the spins vanish, because $\varphi_{o_i s_i}(\mathbf{r}, \sigma) = \varphi_{o_i s_i}(\mathbf{r}) \chi_{s_i}(\sigma)$ and

$$\sum_{\sigma} \chi_{s_i}^*(\sigma) \chi_{s_j}(\sigma) = \delta_{s_i, s_j} \quad . \tag{3.34}$$

In the first line of Eq. (3.32) we obtain

$$\sum_{\sigma} \chi_{s_i}^*(\sigma) \chi_{s_i}(\sigma) = 1 \quad . \tag{3.35}$$

In the second line we obtain

$$\sum_{\sigma, \sigma'} \chi_{s_i}^*(\sigma') \chi_{s_i}(\sigma') \chi_{s_j}^*(\sigma) \chi_{s_j}(\sigma) = 1 \quad . \tag{3.36}$$

In the third line we obtain

$$\sum_{\sigma, \sigma'} \chi_{s_j}^*(\sigma') \chi_{s_i}^*(\sigma) \chi_{s_i}(\sigma') \chi_{s_j}(\sigma) = \sum_{\sigma} \delta_{s_i, s_j} \chi_{s_i}^*(\sigma) \chi_{s_j}(\sigma) = \delta_{s_i, s_j} \quad . \tag{3.37}$$

This means that in Eq. (3.32) all sums, $\sum_{\sigma, \sigma'}$, can be removed. Only in the last line this sum has to be replaced by a Kronecker symbol. A comparison of Eq. (3.28) with the corresponding equation of Hartree theory (Eq. (3.14)) shows that we now have obtained an additional term

$$\tilde{E}^{\text{x}}[\{\varphi_{o_i s_i}^*, \varphi_{o_i s_i}\}] = -\frac{1}{2} \frac{e^2}{4\pi\epsilon_0} \sum_{\substack{i,j \\ i \neq j}}^{N,N} \delta_{s_i, s_j} \iint \frac{\varphi_{o_i s_i}^*(\mathbf{r}) \varphi_{o_j s_j}^*(\mathbf{r}') \varphi_{o_i s_i}(\mathbf{r}') \varphi_{o_j s_j}(\mathbf{r})}{|\mathbf{r} - \mathbf{r}'|} d^3 \mathbf{r} d^3 \mathbf{r}' \quad . \tag{3.38}$$

This term enters because of the inclusion of the exchange interaction (Pauli principle). Thus the letter x is used as index. It is an abbreviation for the word “exchange”.

This term has a negative sign. Compared to Hartree theory it therefore lowers the energy. Now it is clear that Hartree-Fock theory is a better approximation than Hartree theory. In Eq. (3.28) the condition $i \neq j$ in both sums can be omitted, because for $i = j$ the last two terms cancel each other. By summing over the spins we obtain

$$\begin{aligned}
E^{\text{HF}}[\{\varphi_{o_i s_i}^*, \varphi_{o_i s_i}\}] &= T_s[\{\varphi_{o_i s_i}^*, \varphi_{o_i s_i}\}] + E^{e-\text{Ion}}[\{\varphi_{o_i s_i}^*, \varphi_{o_i s_i}\}] \\
&\quad + E^{\text{Hartree}}[\{\varphi_{o_i s_i}^*, \varphi_{o_i s_i}\}] + E^{\text{x}}[\{\varphi_{o_i s_i}^*, \varphi_{o_i s_i}\}] \quad , \tag{3.39}
\end{aligned}$$

with

$$T_s[\{\varphi_{o_i s_i}^*, \varphi_{o_i s_i}\}] = \sum_{i=1}^N \int \varphi_{o_i s_i}^*(\mathbf{r}) \left\{ -\frac{\hbar^2}{2m} \nabla^2 \right\} \varphi_{o_i s_i}(\mathbf{r}) d^3\mathbf{r} \quad , \quad (3.40)$$

the functional of the kinetic energy of non-interacting electrons in the single-particle states $\varphi_{o_i s_i}(\mathbf{r})$. The other quantities are:

$$E^{e-Ion}[\{\varphi_{o_i s_i}^*, \varphi_{o_i s_i}\}] = \int v(\mathbf{r}) n(\mathbf{r}) d^3\mathbf{r} \quad , \quad (3.41)$$

$$E^{\text{Hartree}}[\{\varphi_{o_i s_i}^*, \varphi_{o_i s_i}\}] = \frac{1}{2} \frac{e^2}{4\pi\epsilon_0} \iint \frac{n(\mathbf{r})n(\mathbf{r}')}{|\mathbf{r} - \mathbf{r}'|} d^3\mathbf{r} d^3\mathbf{r}' \quad , \quad (3.42)$$

and

$$E^x[\{\varphi_{o_i s_i}^*, \varphi_{o_i s_i}\}] = -\frac{1}{2} \frac{e^2}{4\pi\epsilon_0} \sum_{i,j}^{N,N} \delta_{s_i, s_j} \iint \frac{\varphi_{o_i s_i}^*(\mathbf{r}) \varphi_{o_j s_j}^*(\mathbf{r}') \varphi_{o_i s_i}(\mathbf{r}') \varphi_{o_j s_j}(\mathbf{r})}{|\mathbf{r} - \mathbf{r}'|} d^3\mathbf{r} d^3\mathbf{r}' \quad . \quad (3.43)$$

The electron density is

$$n(\mathbf{r}) = \sum_{i=1}^N |\varphi_{o_i s_i}(\mathbf{r})|^2 \quad . \quad (3.44)$$

For the last term in Eq. (3.42) we have written E^x (without tilde): $E^x = \tilde{E}^x - E^{\text{SIC}}$. Here, E^{SIC} is the term $i = j$, which does not appear in Eq. (3.37). Nowadays the quantity E^x is called exchange energy. Consequently, E^{Hartree} now contains the self-interaction of the electrons, while E^x takes into account the correction of this self-interaction, and additionally E^x makes sure the Pauli principle is fulfilled.

The “best” functions $\varphi_{o_i s_i}(\mathbf{r})$, i.e., the functions yielding the lowest energy, are obtained if Eq. (3.42) is varied in the $\varphi_{o_i s_i}^*(\mathbf{r})$ or in the $\varphi_{o_i s_i}(\mathbf{r})$, respectively. This again has to be done taking into account the normalization and the orthogonality of the $\varphi_{o_i s_i}(\mathbf{r})$. Both have been used already in the construction of Eq. (3.32) and (3.38). We have

$$\delta \left\{ E^{\text{HF}}[\{\varphi_{o_i s_i}^*, \varphi_{o_i s_i}\}] + \sum_{i,j}^{N,N} \lambda_{o_i s_i, o_j s_j} [\delta_{o_i s_i, o_j s_j} - \langle \varphi_{o_i} | \varphi_{o_j} \rangle] \right\} = \delta Q = 0 \quad . \quad (3.45)$$

In the derivation of the Hartree theory only the normalization has been considered as a constraint. This is sufficient here as well; but mathematically it is easier to consider both, orthogonality and normalization as constraints (cf. Slater “The Self-consistent Field ...”, Vol. 2, Chapter 17). The functional in the curly brackets in Eq. (3.44) we call $Q[\varphi_{o_1 s_1}^*, \dots, \varphi_{o_N s_N}^*, \varphi_{o_1 s_1}, \dots, \varphi_{o_N s_N}]$. If we form the functional derivative of this functional⁴ Q and take into account that $\varphi_{o_i s_i}^*$ and $\varphi_{o_i s_i}$ have to be treated as independent variables (which are given by their real and imaginary parts, i.e., by two functions), for the variation of $\varphi_{o_i s_i}^*$

$$\frac{\delta}{\delta \varphi_{o_k s_k}^*(\mathbf{r})} Q[\{\varphi_{o_i s_i}^*, \varphi_{o_i s_i}\}] = 0 \quad \text{for} \quad k = 1 \dots N \quad , \quad (3.46)$$

⁴Note: $\frac{\delta}{\delta f(x)} \int f(x') g(x') dx' = g(x)$.

we obtain the set of equations

$$\begin{aligned} & \left\{ -\frac{\hbar^2}{2m} \nabla^2 + v(\mathbf{r}) + v^{\text{Hartree}}(\mathbf{r}) \right\} \varphi_{o_k s_k}(\mathbf{r}) - \frac{e^2}{4\pi\epsilon_0} \sum_{j=1}^N \delta_{s_k, s_j} \int \frac{\varphi_{o_j s_j}^*(\mathbf{r}') \varphi_{o_k s_k}(\mathbf{r}') \varphi_{o_j s_j}(\mathbf{r})}{|\mathbf{r} - \mathbf{r}'|} d^3 \mathbf{r}' \\ & = \sum_{j=1}^N \lambda_{o_k s_k, o_j s_j} \varphi_{o_j s_j}(\mathbf{r}) \quad , \end{aligned} \quad (3.47)$$

with

$$v^{\text{Hartree}}(\mathbf{r}) = \frac{e^2}{4\pi\epsilon_0} \int \frac{n(\mathbf{r}')}{|\mathbf{r} - \mathbf{r}'|} d^3 \mathbf{r}' \quad . \quad (3.48)$$

At a first glance, this equation looks unfamiliar. Due to the exchange term and due to the right side it does not look like a Schrödinger equation. However, it can be easily shown that it can be written in a familiar form. To show this we investigate the matrix $\lambda_{o_j s_j, o_i s_i}$. Multiplying Eq. (3.46) from the left by $\varphi_{o_l s_l}^*(\mathbf{r})$ and integrate over \mathbf{r} , we obtain

$$A_{lk} + B_{lk} = \lambda_{o_l s_l, o_k s_k} \quad , \quad (3.49)$$

where

$$A_{lk} = \int \varphi_{o_l s_l}^*(\mathbf{r}) \left\{ -\frac{\hbar^2}{2m} \nabla^2 + v(\mathbf{r}) + v^{\text{Hartree}}(\mathbf{r}) \right\} \varphi_{o_k s_k}(\mathbf{r}) d^3 \mathbf{r} \quad (3.50)$$

and

$$B_{lk} = -\frac{e^2}{4\pi\epsilon_0} \sum_{j=1}^N \delta_{s_k, s_j} \iint \frac{\varphi_{o_l s_l}^*(\mathbf{r}) \varphi_{o_j s_j}^*(\mathbf{r}') \varphi_{o_k s_k}(\mathbf{r}') \varphi_{o_j s_j}(\mathbf{r})}{|\mathbf{r} - \mathbf{r}'|} d^3 \mathbf{r} d^3 \mathbf{r}' \quad . \quad (3.51)$$

The matrix A defined this way is obviously Hermitian, i.e., we have $A_{lk} = A_{kl}^*$. If we take the complex conjugate of B we obtain

$$B_{kl}^* = -\frac{e^2}{4\pi\epsilon_0} \sum_{j=1}^N \delta_{s_j, s_k} \iint \frac{\varphi_{o_k s_k}(\mathbf{r}) \varphi_{o_j s_j}(\mathbf{r}') \varphi_{o_l s_l}^*(\mathbf{r}') \varphi_{o_j s_j}^*(\mathbf{r})}{|\mathbf{r} - \mathbf{r}'|} d^3 \mathbf{r} d^3 \mathbf{r}' = B_{lk} \quad . \quad (3.52)$$

Therefore, also B is Hermitian and thus $\lambda_{o_l s_l, o_k s_k}$ as well. It follows that there must be a unitary transformation

$$\sum_{o_l} U_{o_k, o_l} \varphi_{o_k}(\mathbf{r}) = \tilde{\varphi}_{o_k}(\mathbf{r}) \quad (3.53)$$

and

$$\sum_{o_m, o_n} U_{o_k, o_m}^\dagger \lambda_{o_m s_l, o_n s_k} U_{o_n, o_l} = \epsilon_{o_k s_k} \delta_{o_l s_l, o_k s_k} \quad , \quad (3.54)$$

so that matrix λ is transformed into a real, diagonal matrix. We obtain the equation to determine the $\tilde{\varphi}_{o_k s_k}(\mathbf{r})$

$$\left\{ -\frac{\hbar^2}{2m} \nabla^2 + v(\mathbf{r}) + v^{\text{Hartree}}(\mathbf{r}) + v_k^x(\mathbf{r}) \right\} \tilde{\varphi}_{o_k s_k}(\mathbf{r}) = \epsilon_{o_k s_k} \tilde{\varphi}_{o_k s_k}(\mathbf{r}) \quad (3.55)$$

with

$$v_k^x(\mathbf{r})\tilde{\varphi}_{o_k s_k}(\mathbf{r}) = -\frac{e^2}{4\pi\epsilon_0} \sum_{i=1}^N \delta_{s_i s_k} \int \frac{\tilde{\varphi}_{o_i s_i}^*(\mathbf{r}')\tilde{\varphi}_{o_k s_k}(\mathbf{r}')\tilde{\varphi}_{o_i s_i}(\mathbf{r})}{|\mathbf{r} - \mathbf{r}'|} d^3\mathbf{r}' \quad . \quad (3.56)$$

Equation (3.54) is called the *Hartree-Fock equation*. Once the single-particle wave functions $\{\tilde{\varphi}_{o_i s_i}\}$ have been obtained using Eq. (3.54), in the next step the total energy can be calculated using Eq. (3.38).

The exchange term $v_k^x(\mathbf{r})$ does not look like a normal potential, because it is an integral operator. In 1951 Slater pointed out that it can be written in a familiar form. For this purpose (Eq. (3.55)) is multiplied by

$$\frac{\tilde{\varphi}_{o_k s_k}(\mathbf{r})}{\tilde{\varphi}_{o_k s_k}(\mathbf{r})} = 1 \quad . \quad (3.57)$$

Using the definition

$$n_k^{\text{HF}}(\mathbf{r}, \mathbf{r}') = \sum_{i=1}^N \delta_{s_i, s_k} \frac{\tilde{\varphi}_{o_i s_i}^*(\mathbf{r}')\tilde{\varphi}_{o_k s_k}(\mathbf{r}')\tilde{\varphi}_{o_i s_i}(\mathbf{r})}{\tilde{\varphi}_{o_k s_k}(\mathbf{r})} \quad (3.58)$$

for the exchange particle density the exchange potential adopts the following form

$$v_k^x(\mathbf{r}) = -\frac{e^2}{4\pi\epsilon_0} \int \frac{n_k^{\text{HF}}(\mathbf{r}, \mathbf{r}')}{|\mathbf{r} - \mathbf{r}'|} d^3\mathbf{r}' \quad . \quad (3.59)$$

Now, the potential v_k^x is almost a “normal” multiplicative operator, but it is different for each particle. $v^{\text{Hartree}} + v_k^x$ describes the interaction of electron k with the other electrons. This interaction, v_k^x , is present only for those electrons, which have the same spin, i.e., $s_i = s_k$. In principle, the expression (Eq. (3.57)) is not defined at the points where $\tilde{\varphi}_{o_k s_k}(\mathbf{r})$ are zero, but this is not a problem, because $n_k^{\text{HF}}(\mathbf{r}, \mathbf{r}')$ can be extended continuously. From now on, when talking about the Hartree-Fock equation, we mean Eq. (3.54), and we will now leave away the tilde on the $\varphi_{o_k s_k}(\mathbf{r})$.

3.3 The Exchange Interaction

Here, the physical meaning of the Hartree and the Hartree-Fock equations will be investigated in more detail. In particular the exchange energy will be made plausible, and the problems of Hartree-Fock theory will be discussed, i.e., which physical many-body effects are missing in this theory. The effective single-particle Hamilton operator of the Hartree and of the Hartree-Fock equations is:

$$h = -\frac{\hbar^2}{2m}\nabla^2 + v(\mathbf{r}) + v^{\text{Hartree}}(\mathbf{r}) + \begin{cases} -\frac{e^2}{4\pi\epsilon_0} \int \frac{n_k^{\text{H}}(\mathbf{r}')}{|\mathbf{r} - \mathbf{r}'|} d^3\mathbf{r}' = v_k^{\text{SIC}}(\mathbf{r}) & \text{Hartree,} \\ -\frac{e^2}{4\pi\epsilon_0} \int \frac{n_k^{\text{HF}}(\mathbf{r}, \mathbf{r}')}{|\mathbf{r} - \mathbf{r}'|} d^3\mathbf{r}' = v_k^x(\mathbf{r}) & \text{Hartree-Fock,} \end{cases} \quad (3.60)$$

with

$$n_k^H(\mathbf{r}') = |\varphi_{o_k}(\mathbf{r}')|^2 \quad (3.61)$$

and $n_k^{\text{HF}}(\mathbf{r}, \mathbf{r}')$ from Eq. (3.57). Nowadays, v_k^{SIC} is often neglected, and the ansatz $v^{\text{eff}} = v + v^{\text{Hartree}}$ is termed Hartree approximation. We will not introduce this additional approximation here.

We have

$$\int n_k^H(\mathbf{r}') d^3\mathbf{r}' = 1 \quad (3.62)$$

$$\int n_k^{\text{HF}}(\mathbf{r}, \mathbf{r}') d^3\mathbf{r}' = 1 \quad . \quad (3.63)$$

Both densities $n_k^H(\mathbf{r}')$ and $n_k^{\text{HF}}(\mathbf{r}, \mathbf{r}')$ represent one electron, i.e., in both cases the self-interaction included in v^{Hartree} is removed. Equation (3.62) is an important sum rule, which also holds for the exact theory. However, $n_k^{\text{HF}}(\mathbf{r}, \mathbf{r}')$ contains more than just the correction of the self-interaction. We will investigate this for a simple system now. Because now we are dealing with the electron-electron interaction (and not with the electron-ion interaction), we investigate a system, in which the potential of the lattice components (i.e., of the ions) varies only weakly. Thus we set $v(\mathbf{r}) = v \equiv \text{constant}$. We want to use this to demonstrate the meaning of the exchange interaction. For such a jellium system the Hartree-Fock equations are solved by plane waves. This will be the result of our discussion (but we note in passing that there are also more complex solutions: “spin density waves”). Therefore, the single-particle wave functions are

$$\varphi_{o_i s_i}(\mathbf{r}) = \frac{1}{\sqrt{V_g}} e^{i\mathbf{k}_i \cdot \mathbf{r}} \quad . \quad (3.64)$$

With these wave functions we obtain:

$$n_k^H(\mathbf{r}') = \frac{1}{V_g} = \text{constant} \quad , \quad (3.65)$$

i.e., the density n_k^H and the electron k , respectively, is smeared out uniformly over the whole volume. The particle density interacting with the Hartree particle k is

$$n(\mathbf{r}') - n_k^H(\mathbf{r}') = \frac{N}{V_g} - \frac{1}{V_g} \quad . \quad (3.66)$$

If particle k is located at $\mathbf{r} = 0$, the distribution of the other electrons is as shown in Fig. 3.3. Strictly speaking the line in Fig. 3.3 is at $(1 - \frac{1}{N})$. But because N is arbitrarily large, this cannot be distinguished from 1.

Therefore, for extended wave functions, $v_k^{\text{SIC}}(\mathbf{r})$ is negligible.

The corresponding particle density interacting with an electron in single-particle state $\varphi_{o_k s_k}$ in the Hartree-Fock theory is

$$n(\mathbf{r}') - n_k^{\text{HF}}(\mathbf{r}, \mathbf{r}') \quad . \quad (3.67)$$

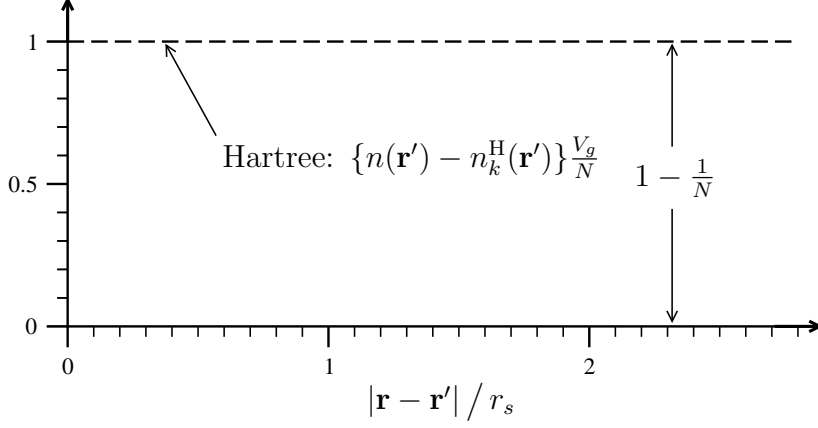


Figure 3.3: Distribution of the $(N - 1)$ electrons seen by particle $\varphi_k(\mathbf{r})$, which is located at $\mathbf{r} = 0$ (in the Hartree approximation and for jellium).

If particle k is at position \mathbf{r} , then the $(N - 1)$ other particles have a distribution, which is given by Eq. (3.66). Like in the Hartree approximation (Eq. (3.66)) also contains exactly $N - 1$ particles. What does this density look like?

$$n_k^{\text{HF}}(\mathbf{r}, \mathbf{r}') = \sum_{i=1}^N \delta_{s_i, s_k} \frac{\varphi_{o_i s_i}^*(\mathbf{r}') \varphi_{o_k s_k}(\mathbf{r}') \varphi_{o_i s_i}(\mathbf{r})}{\varphi_{o_k s_k}(\mathbf{r})} \quad (3.68)$$

$$= \frac{1}{V_g} \sum_{\mathbf{k}_i}^{\frac{N}{2}} e^{-i\mathbf{k}_i \mathbf{r}'} e^{i\mathbf{k}_k \mathbf{r}'} e^{i\mathbf{k}_i \mathbf{r}} e^{-i\mathbf{k}_k \mathbf{r}} \quad (3.69)$$

$$= \frac{1}{V_g} \sum_{\mathbf{k}_i}^{\frac{N}{2}} e^{i(\mathbf{k}_i - \mathbf{k}_k)(\mathbf{r} - \mathbf{r}')} \quad (3.70)$$

In order to simplify the representation, here we have assumed that the system is nonmagnetic and therefore each spatial state $\varphi_{o_i}(\mathbf{r})$ is occupied by two electrons. Because n_k^{HF} is different for each state, one obtains a better impression of the meaning of Eq. (3.69), if one averages over all electrons:

$$\bar{n}^{\text{HF}}(\mathbf{r}, \mathbf{r}') \stackrel{!}{=} \sum_{k=1}^N \frac{\varphi_{o_k}^*(\mathbf{r}) n_k^{\text{HF}}(\mathbf{r}, \mathbf{r}') \varphi_{o_k}(\mathbf{r})}{n(\mathbf{r})} \quad (3.71)$$

$$= \frac{V_g}{N} \frac{1}{V_g} \frac{1}{V_g} 2 \sum_{\mathbf{k}_k}^{\frac{N}{2}} e^{-i\mathbf{k}_k(\mathbf{r} - \mathbf{r}')} \sum_{\mathbf{k}_i}^{\frac{N}{2}} e^{i\mathbf{k}_i(\mathbf{r} - \mathbf{r}')} \quad (3.72)$$

The sum over the vectors \mathbf{k}_i and \mathbf{k}_k can be evaluated easily, if one changes from a discrete to a continuous representation (cf. the discussion following Eq. (2.18)):

$$\sum_{\mathbf{k}_i}^{\frac{N}{2}} \rightarrow \int_0^{k_{\text{F}}} \frac{V_g}{(2\pi)^3} d^3 \mathbf{k} \quad (3.73)$$

We obtain

$$\frac{V_g}{(2\pi)^3} \int_0^{k_{\text{F}}} e^{i\mathbf{k}(\mathbf{r} - \mathbf{r}')} d^3 \mathbf{k} = \frac{3}{2} N \frac{(k_{\text{F}} \hat{r}) \cos(k_{\text{F}} \hat{r}) - \sin(k_{\text{F}} \hat{r})}{(k_{\text{F}} \hat{r})^3} \quad (3.74)$$

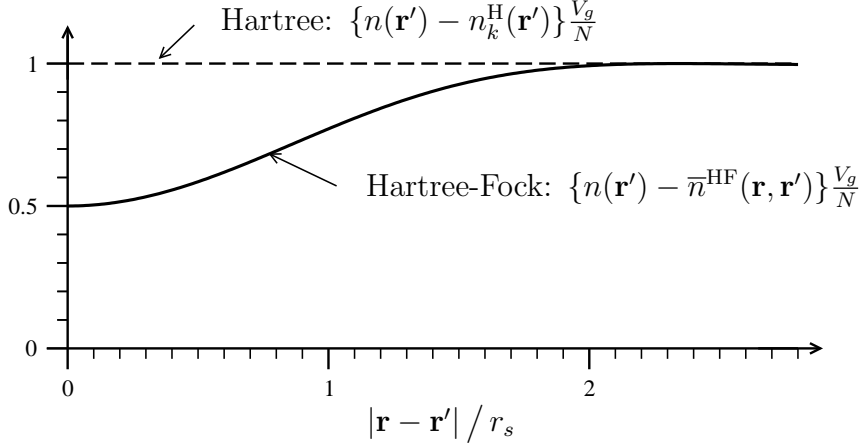


Figure 3.4: Distribution (averaged) of the $(N - 1)$ other electrons with respect to a particle that is located at position $\mathbf{r} = 0$ (in the Hartree-Fock approximation and for jellium).

with $\hat{r} = |\mathbf{r} - \mathbf{r}'|$.

It follows:

$$\bar{n}^{\text{HF}}(\hat{r}) = \frac{9}{2} \frac{N}{V_g} \left(\frac{(k_F \hat{r}) \cos(k_F \hat{r}) - \sin(k_F \hat{r})}{(k_F \hat{r})^3} \right)^2, \quad (3.75)$$

\bar{n}^{HF} therefore is spherically symmetric. The particle density of the other electrons felt by a (averaged) Hartree-Fock particle, looks like that shown in Fig. 3.4. The concentration of the electrons of like spin is lowered in the neighborhood of the investigated electron. This is formulated in the following way: An electron is surrounded by its exchange hole. The quantity $n_k^{\text{HF}}(\mathbf{r}, \mathbf{r}')$ is called particle density (with respect to \mathbf{r}') of the exchange hole of an electron at position \mathbf{r} .

The difference between the Hartree and the Hartree-Fock approximation (cf. Fig. 3.4, or the equations (3.64) and (3.74)) is that $n_k^{\text{H}}(\mathbf{r}')$ only depends on \mathbf{r}' , i.e., it is the same for each position \mathbf{r} of the observed particle. But $n_k^{\text{HF}}(\mathbf{r}, \mathbf{r}')$ and $\bar{n}^{\text{HF}}(\mathbf{r}, \mathbf{r}')$ depends on the position of the particle, i.e., on the position of the particle for which we are actually solving the Hartree-Fock equation using n_k^{HF} . n_k^{HF} fulfills the Pauli principle: If the investigated electron k is at position \mathbf{r} , then all other electrons of like spin are displaced from position \mathbf{r} . Due to the Pauli principle the electrons of like spin do not move independently of each other, but their motion is correlated, because in its neighborhood an electron displaces the other electrons. Although we have solved the time-independent Schrödinger equation, this dynamic Pauli correlation is taken into account. This is because the Pauli interaction is not explicitly included in the Hamilton operator, but is taken into account via the constraint of an “antisymmetric wave function”. Another correlation should appear (in an exact theory) due to the Coulomb repulsion for all electrons, i.e., also for electrons of unlike spins there must be a displacement of electrons. But this Coulomb repulsion is included only in an averaged way in Hartree as well as in Hartree-Fock theory, so that the correlation resulting from the Coulomb repulsion is missing in both theories. Hartree-Fock therefore contains a part of the correlation, the so-called Pauli correlation. Nevertheless, it is commonly agreed that the term correlation is used for all that is missing in Hartree-

Fock. This usage is not very fortunate, but it has become generally accepted⁵.

For the exchange potential (cf. Eq. (3.58)) of a jellium system we obtain (with plane waves as eigenfunctions) for the dependence of v^x on state \mathbf{k}_m the result shown in Fig. 3.5. In Chapter 2.3 we have set the potential as spatially constant and the same (state-independent) for *all* (free) electrons. Here we will see how far this can be justified for interacting (real) electrons.

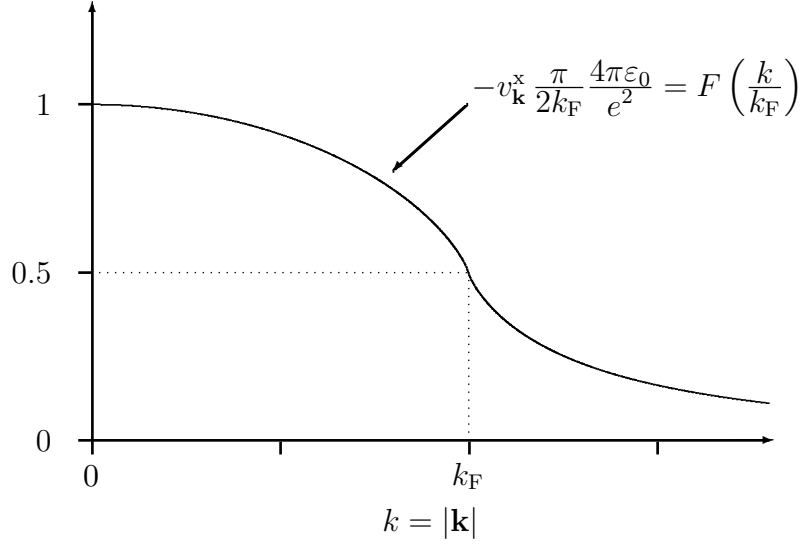


Figure 3.5: The exchange potential as a function of state \mathbf{k} for a jellium system.

The calculation goes as follows:

$$\begin{aligned} v_{\mathbf{k}}^x(\mathbf{r}) &= -\frac{e^2}{4\pi\epsilon_0} \int \frac{n_{\mathbf{k}}^{\text{HF}}(\mathbf{r} - \mathbf{r}')}{|\mathbf{r} - \mathbf{r}'|} d^3\mathbf{r}' \quad , \\ &= -\frac{e^2}{4\pi\epsilon_0} \frac{1}{(2\pi)^3} \int_0^{k_F} \int \frac{e^{i(\mathbf{k}' - \mathbf{k})\hat{\mathbf{r}}}}{|\hat{\mathbf{r}}|} d^3\hat{\mathbf{r}} d^3\mathbf{k}' \quad , \end{aligned} \quad (3.76)$$

where $\hat{\mathbf{r}} = \mathbf{r} - \mathbf{r}'$. We have

$$\frac{1}{|\mathbf{r} - \mathbf{r}'|} = 4\pi \frac{1}{(2\pi)^3} \int \frac{e^{i\mathbf{q}(\mathbf{r} - \mathbf{r}')}}{q^2} d^3\mathbf{q} \quad . \quad (3.77)$$

Thus, we obtain

$$v_{\mathbf{k}}^x = -\frac{e^2}{4\pi\epsilon_0} \frac{4\pi}{(2\pi)^3} \int_0^{k_F} \frac{1}{|\mathbf{k} - \mathbf{k}'|^2} d^3\mathbf{k}' \quad . \quad (3.78)$$

We have used

$$\int e^{i(\mathbf{q} - \mathbf{k} + \mathbf{k}')\hat{\mathbf{r}}} d^3\hat{\mathbf{r}} = (2\pi)^3 \delta(\mathbf{q} + \mathbf{k}' - \mathbf{k}) \quad . \quad (3.79)$$

⁵In the field of density-functional theory the definition is modified.

If the integration is done, one obtains

$$v_{\mathbf{k}}^x = -\frac{e^2}{4\pi\epsilon_0} \frac{2k_F}{\pi} F\left(\frac{k}{k_F}\right) \quad , \quad (3.80)$$

where

$$F(x) = \frac{1}{2} + \frac{1-x^2}{4x} \ln \left| \frac{1+x}{1-x} \right| \quad . \quad (3.81)$$

The function $F\left(\frac{k}{k_F}\right)$ is shown in Fig. 3.5.

For the further discussion of Hartree-Fock theory we have a look at the eigenvalues of the Hartree-Fock equation. In the jellium approximation it follows:

$$\langle \varphi_{\mathbf{k}} | h | \varphi_{\mathbf{k}} \rangle = \epsilon(\mathbf{k}) = \frac{\hbar^2 \mathbf{k}^2}{2m} + \langle \varphi_{\mathbf{k}} | v_{\mathbf{k}}^x | \varphi_{\mathbf{k}} \rangle \quad . \quad (3.82)$$

Here, the zero point of the energy was set to the average electrostatic potential:

$$v(\mathbf{r}) + \frac{e^2}{4\pi\epsilon_0} \int \frac{n(\mathbf{r}')}{|\mathbf{r} - \mathbf{r}'|} d^3\mathbf{r}' = 0 \quad . \quad (3.83)$$

The expectation value of the exchange potential is given by Eq. (3.77):

$$\langle \varphi_{\mathbf{k}} | v_{\mathbf{k}}^x | \varphi_{\mathbf{k}} \rangle = v_{\mathbf{k}}^x \langle \varphi_{\mathbf{k}} | \varphi_{\mathbf{k}} \rangle = -\frac{e^2}{4\pi\epsilon_0} \frac{2k_F}{\pi} F\left(\frac{k}{k_F}\right) \quad , \quad (3.84)$$

and for Eq. (3.81) we obtain:

$$\epsilon(\mathbf{k}) = \frac{\hbar^2 \mathbf{k}^2}{2m} - \frac{e^2}{4\pi\epsilon_0} \frac{2k_F}{\pi} F\left(\frac{k}{k_F}\right) \quad (3.85)$$

with $F(x)$ from Eq. (3.80).

This derivation shows that plane waves are in fact eigenfunctions of the Hartree-Fock Hamilton operator, i.e., they diagonalize the Hartree-Fock operator. However, we do not have the dispersion relation of free electrons anymore, but there is an additional term, which depends on k and which gives rise to a lowering of the single-particle energies. If we now compare the relation (Eq. (3.83)) of Hartree-Fock theory with the one of free electrons ($v^{\text{eff}}(\mathbf{r}) = \text{constant}$) or with Hartree theory, we obtain Fig. 3.6.

In Fig. 3.6 it can be seen:

1. For very small \mathbf{k} the dispersion of Hartree-Fock particles is parabolic. The curvature of this parabola is different from the one of free electrons. If \mathbf{k} is very small we obtain

$$\epsilon(\mathbf{k}) = \frac{\hbar^2 \mathbf{k}^2}{2m^*} + C \quad \text{for} \quad |\mathbf{k}| \rightarrow 0 \quad . \quad (3.86)$$

For the effective mass of the Hartree-Fock particles we have:

$$\frac{m^*}{m} = \frac{1}{1 + 0.22 (r_s/a_B)} \quad \text{for} \quad |\mathbf{k}| \rightarrow 0 \quad , \quad (3.87)$$

for $k \rightarrow 0$, m^* is smaller than m (r_s is typically between 2 and 3 bohr).

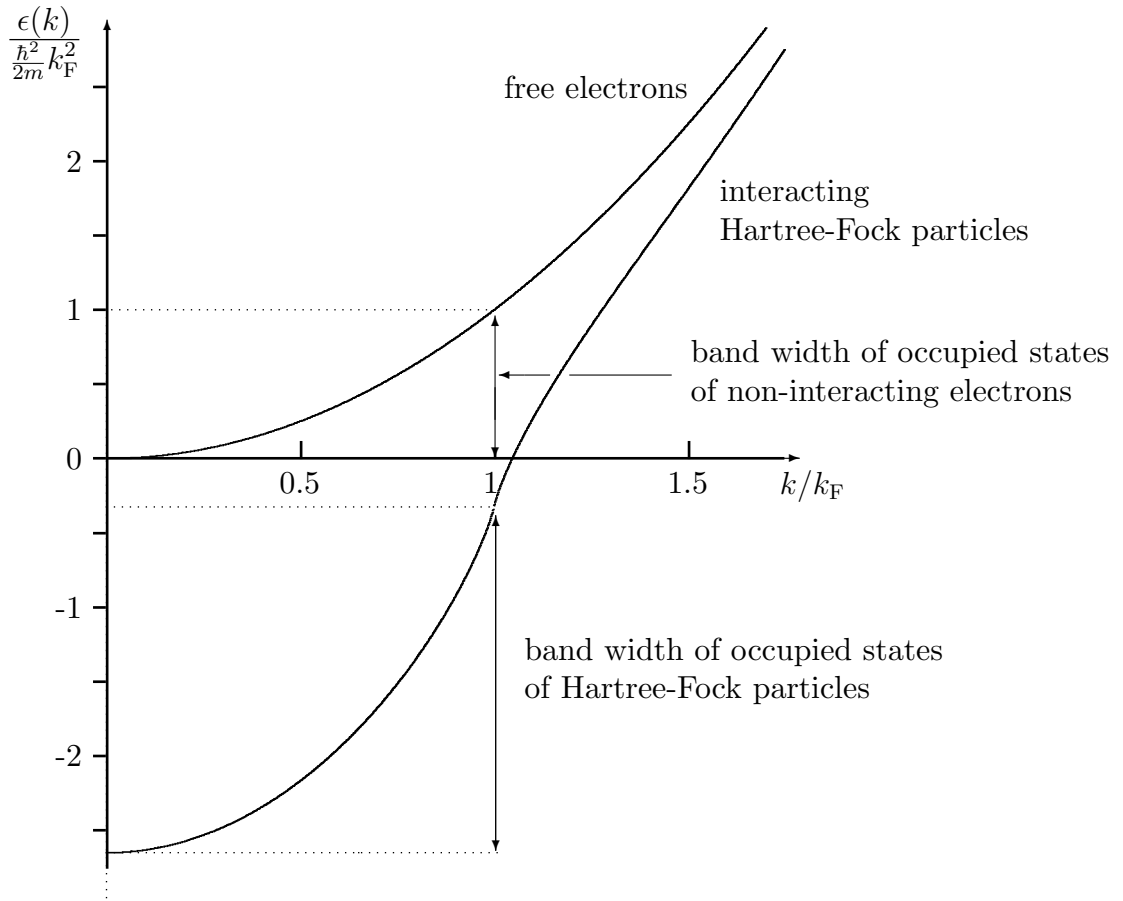


Figure 3.6: Dispersion of the single-particle energies in jellium for free electrons (or Hartree particles) and for Hartree-Fock particles (Eq. (3.83)), shown here for the density parameter ($r_s = 4$ bohr).

2. The band width of the occupied states is significantly larger for Hartree-Fock particles than for Hartree particles, a factor 2.33 in Fig. 3.6.
3. For $k = k_F$ there is an obviously unphysical result:

The derivation

$$\frac{\partial \epsilon(\mathbf{k})}{\partial k} \rightarrow \infty \quad \text{for} \quad k \rightarrow k_F \quad (3.88)$$

becomes logarithmically infinite. This has consequences for metallic properties and for the heat capacity. Both are described mainly by the electrons close to the Fermi energy. The reason for the singularity is in the $\frac{1}{|\mathbf{r}-\mathbf{r}'|}$ behavior of the electron-electron interaction. If the interaction was screened, e.g.

$$\frac{e^{-\lambda(|\mathbf{r}-\mathbf{r}'|)}}{|\mathbf{r}-\mathbf{r}'|}, \quad (3.89)$$

the singularity would not exist (cf. Ashcroft-Mermin, p. 337).

4. The potential v_k^x is typically in the range of 5-15 eV. Because many phenomena in solid-state physics are determined by energy differences in the order of 0.1-0.5 eV, an exact treatment of the exchange interaction is crucial.

3.4 Koopmans' Theorem⁶

In the discussion of the Hartree equation we pointed out that the Lagrange parameters ϵ_{o_i} seem to correspond (at least approximately) to ionization energies. This statement will be investigated in more detail now for the Hartree-Fock equation.

The energy, which is required to remove an electron from state k in an N electron system is

$$I_k = E_k^{N-1} - E^N = \langle \Phi_k^{N-1} | H^{e,N-1} | \Phi_k^{N-1} \rangle - \langle \Phi^N | H^{e,N} | \Phi^N \rangle \quad (3.90)$$

Here we assume that the removed electron is excited to the zero point of the energy (the vacuum level), and there is a free particle of zero kinetic energy. Φ^N is the ground state wave function of the N electron system and Φ_k^{N-1} the wave function of the $N-1$ electron system, the state k being unoccupied. If state k is the highest occupied state of the N electron system (i.e., state N), then I_k is the ionization energy. In order to investigate Eq. (3.90) we make the following assumptions:

- 1) Removing an electron has no influence on lattice geometry, or more precisely, we assume that the electron removal happens very fast (e.g. by optical excitation), so that the lattice components do move only after the ionization (Franck-Condon principle).
- 2) The many-body wave functions shall be single Slater determinants (i.e., the discussion refers to the Hartree-Fock approximation).
- 3) Removing the k -th electron does not affect the single-particle wave functions of the other electrons. This assumption is reasonable, as long as the number of electrons is large and the density $|\varphi_{o_k}(\mathbf{r})|^2$ of the electron being removed is rather extended. Then $v^{\text{Hartree}}(\mathbf{r})$ and $n_j^{\text{HF}}(\mathbf{r}, \mathbf{r}')$ remain basically unchanged, and, consequently also all φ_{o_i, s_i} remain essentially unchanged.

In particular assumptions 2) and 3) are rather drastic. These two assumptions mean that the wave function Φ^{N-1} is derived from the wave function Φ^N by deleting line k and column k in the Slater determinant Φ^N . Then we obtain, using Eq. (3.89), (3.32), and (3.54)

$$\begin{aligned} I_k = & \langle \Phi_k^{N-1} | \sum_{\substack{i=1 \\ i \neq k}}^N -\frac{\hbar^2}{2m} \nabla_{\mathbf{r}_i}^2 + v(\mathbf{r}_i) | \Phi_k^{N-1} \rangle + \frac{1}{2} \frac{e^2}{4\pi\epsilon_0} \langle \Phi_k^{N-1} | \sum_{\substack{i,j=1 \\ i \neq j \\ i,j \neq k}}^{N,N} \frac{1}{|\mathbf{r}_i - \mathbf{r}_j|} | \Phi_k^{N-1} \rangle \\ & - \langle \Phi^N | \sum_{i=1}^N -\frac{\hbar^2}{2m} \nabla_{\mathbf{r}_i}^2 + v(\mathbf{r}_i) | \Phi^N \rangle - \frac{1}{2} \frac{e^2}{4\pi\epsilon_0} \langle \Phi^N | \sum_{\substack{i,j=1 \\ i \neq j}}^{N,N} \frac{1}{|\mathbf{r}_i - \mathbf{r}_j|} | \Phi^N \rangle \end{aligned}$$

$$\begin{aligned}
&\approx -\langle \varphi_{o_k s_k} | -\frac{\hbar^2}{2m} \nabla^2 + v(\mathbf{r}) | \varphi_{o_k s_k} \rangle \\
&\quad - \frac{e^2}{4\pi\epsilon_0} \sum_{\substack{i=1 \\ i \neq k}}^N \iint \frac{\varphi_{o_k s_k}^*(\mathbf{r}') \varphi_{o_i s_i}^*(\mathbf{r}) \varphi_{o_i s_i}(\mathbf{r}) \varphi_{o_k s_k}(\mathbf{r}')}{|\mathbf{r} - \mathbf{r}'|} d^3\mathbf{r} d^3\mathbf{r}' \\
&\quad + \frac{e^2}{4\pi\epsilon_0} \sum_{\substack{i=1 \\ i \neq k}}^N \delta_{s_k, s_i} \iint \frac{\varphi_{o_k s_k}^*(\mathbf{r}) \varphi_{o_i s_i}^*(\mathbf{r}') \varphi_{o_i s_i}(\mathbf{r}) \varphi_{o_k s_k}(\mathbf{r}')}{|\mathbf{r} - \mathbf{r}'|} d^3\mathbf{r} d^3\mathbf{r}' \\
&= -\langle \varphi_{o_k s_k} | h^{\text{HF}} | \varphi_{o_k s_k} \rangle \\
&= -\epsilon_{o_k s_k} \quad .
\end{aligned} \tag{3.91}$$

Thus what we had assumed before is valid approximately, indeed: The meaning of the quantities introduced as Lagrange parameters ϵ_{o_k} or $\epsilon_{o_k s_k}$ is (approximately) the negative value of the energy that is required to remove an electron from orbital k . It follows that also excitation energies, i.e., a transition from an occupied state i to an unoccupied state j is (approximately) determined by the ϵ_{o_k} :

$$\Delta E_{i \rightarrow j} \approx \epsilon_j - \epsilon_i \tag{3.92}$$

These statements (Eq. (3.91)) and (Eq. (3.92)) are called Koopmans' theorem. They are valid approximately for the valence electrons of atoms and for extended states of solids. However, when one excites an electron from a localized state, one does not only obtain a single discrete line. Due to many-body effects (electronic relaxation and excitations) one obtains several "peaks". Then Koopmans' theorem (approximately) gives the center of mass of the function $I_k(\epsilon)$.

3.5 The X_α Method

(Hartree-Fock-Slater Method)

Initially, the Hartree-Fock method was applied to atoms without major difficulties. For solids, however, it was realized that it is very complicated⁷. This is only due to the exchange term. Because of these difficulties in 1951 Slater suggested (Phys. Rev. **81**, 385 (1951); **82**, 5381 (1951)), to simplify this term. This simplification, although introduced ad hoc, was very successful. Later, i.e., by density-functional theory, it was realized that the treatment introduced by Slater as a simplification in fact corresponds to an important physical theorem and is not an approximation but even an improvement of Hartree-Fock theory.

The difficulty in Hartree-Fock theory is that the exchange potential is state-dependent. For jellium the expectation value of the exchange potential $v_{\mathbf{k}}^x$ is given by Eq. (3.79) and it reads

⁷In recent years there have been several better Hartree-Fock calculations for solids: Stollhoff (1987), Gigy-Baldereschi (1987), Louie (1988). In particular Dovesi *et al.* have developed a Hartree-Fock program ("CRYSTAL") for solids. The next step is to take into account "exact exchange" in the context of density-functional theory.

$$v_{\mathbf{k}}^x = -\frac{e^2}{4\pi\epsilon_0} \frac{2k_{\text{F}}}{\pi} k_{\text{F}} F \left(\frac{k}{k_{\text{F}}} \right) \quad \text{with} \quad k_{\text{F}} = \sqrt[3]{3\pi^2 n} \quad . \quad (3.93)$$

The complicated aspect of the exchange potential is that it is different for different states \mathbf{k} . Slater therefore introduced the idea to average over all \mathbf{k} to obtain a (state-independent) “average potential”. However, how should such “average” be performed? If one averages over all occupied states the function $F(k/k_{\text{F}})$ becomes the number 0.75. But one could also claim that only the states at k_{F} are important: Electrons can react to external perturbations only by transitions to excited states, and the energetically lowest excitations happen at ϵ_{F} (or k_{F}). At k_{F} F has the value 0.5. Exactly this value ($F = 0.5$) is also obtained, if one averages over all states in the expression for the total energy (Eq. (3.42)), *before* the functional derivative $\delta E^{\text{HF}}/\delta\varphi$ is calculated. This is because a variation after averaging mainly refers to the Fermi edge. One obtains:

$$v_{F=\frac{3}{4}}^x(\mathbf{r}) = -\frac{3}{2\pi} \frac{e^2}{4\pi\epsilon_0} \sqrt[3]{3\pi^2 n(\mathbf{r})} \quad \begin{array}{l} \text{averaging over all occupied} \\ \text{states of the Hartree-Fock} \\ \text{equation } (F = 0.75). \end{array} \quad (3.94)$$

$$v_{F=\frac{1}{2}}^x(\mathbf{r}) = -\frac{1}{\pi} \frac{e^2}{4\pi\epsilon_0} \sqrt[3]{3\pi^2 n(\mathbf{r})} \quad \begin{array}{l} \text{Averaging in the expression of} \\ \text{the total energy or by taking} \\ \text{into account only the states at } k_{\text{F}} \\ \text{of the Hartree-Fock equation} \\ (F = 0.5). \end{array} \quad (3.95)$$

Now in $n(\mathbf{r})$ we have again noted the \mathbf{r} dependence, to indicate that the discussion is also valid for slowly varying densities. Because Hartree-Fock theory is not exact anyway (Coulomb correlation is missing), Slater suggested to introduce the following quantity for the impractical exchange potential

$$v^{x\alpha}(\mathbf{r}) = -\alpha \frac{3}{2\pi} \frac{e^2}{4\pi\epsilon_0} \sqrt[3]{3\pi^2 n(\mathbf{r})} \quad , \quad (3.96)$$

where α is a parameter of value

$$\frac{2}{3} < \alpha < 1 \quad . \quad (3.97)$$

The higher value (i.e., $\alpha = 1$) corresponds to the exchange potential originally derived by Slater ($F = 0.75$). Today, from the point of view of density-functional theory, the potential for $\alpha = 2/3$ (for $F = 0.5$) would be called exchange potential. In the seventies α was determined for atomic calculations and then transferred to solids and molecules (K. Schwarz, Vienna). If α is chosen to obtain a good agreement with experimental total energies one finds that α should obtain a value of $\approx \frac{2}{3}$. Slater believed that the obtained $\alpha \approx \frac{2}{3}$ -exchange potential represents an improvement, because the Coulomb correlation is taken into account semi-empirically. Today this is interpreted differently [cf. Kohn, Sham, Phys. Rev. **140**, A 1193 (1965), Gaspar, Acta Phys. Acad. Sci. Hung. **3**, 263 (1954)].

From a puristic theoretician’s point of view Slater’s empirical treatment was not satisfying, because the derivation was not really justified. Still this treatment had impressive

success. The X_α -potential is illustrated in Fig. 3.7. It gives an impression of the dependence on the density and of the strength of the exchange interaction. Most metals have a density of $r_s = 2$ bohr, or $n = 0.03$ bohr $^{-3}$. Here, the exchange potential has a value of about 7 eV, and consequently one recognizes that for an accurate theoretical treatment in general it will be very important to take into account the exchange potential precisely.

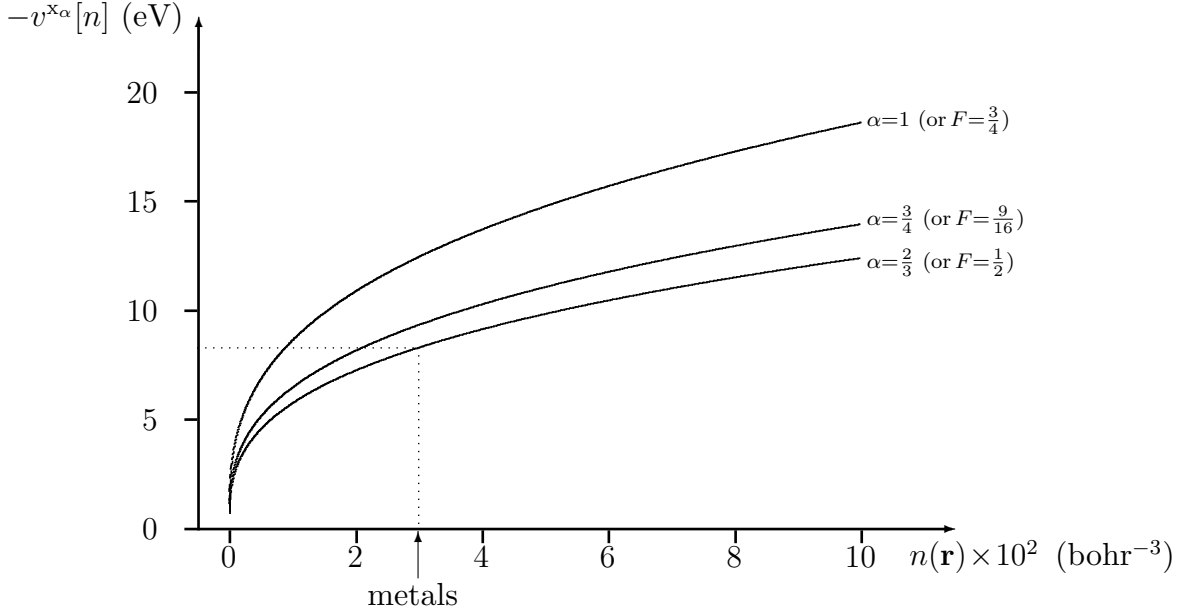


Figure 3.7: The X_α -potential as a function of the density n (atomic units). the density, as usual, depends on the position, the value n is different for each \mathbf{r} . And for this value of n , the figure gives $v^{x_\alpha}(\mathbf{r})$.

3.6 Thomas-Fermi Theory and the Concept of Screening

The basic concept behind this approach is very useful. The main reason for solving the Hamilton operator of the solid is to learn something about the distribution of the electrons of the solid in the many-body ground state Φ , i.e., about the electron density:

$$n(\mathbf{r}) = \left\langle \Phi \left| \sum_{i=1}^N \delta(\mathbf{r} - \mathbf{r}_i) \right| \Phi \right\rangle . \quad (3.98)$$

The question arises if it is really necessary to calculate the many-body wave function Φ . When thinking of the approaches of Hartree, Hartree-Fock, and Hartree-Fock-Slater, one could ask, if one really has to calculate $\sim 10^{23}$ single-particle wave functions $\varphi_{o_i}(\mathbf{r})$, in order to calculate

$$n(\mathbf{r}) = \sum_{i=1}^N |\varphi_{o_i}(\mathbf{r})|^2 , \quad (3.99)$$

or if $n(\mathbf{r})$ can be calculated directly. We start from the effective single-particle equation

$$\left\{ -\frac{\hbar^2}{2m} \nabla^2 + v^{\text{eff}}(\mathbf{r}) \right\} \varphi_i(\mathbf{r}) = \epsilon_i \varphi_i(\mathbf{r}) \quad , \quad (3.100)$$

where the effective potential is taken e.g. from the Hartree or Hartree-Fock-Slater theory. We ask ourselves if it is possible to calculate the density directly from the potential $v(\mathbf{r})$, without calculating the wave function and without solving the Schrödinger equation. In this context we note that $n(\mathbf{r})$ is a functional of the external potential $v(\mathbf{r})$: $v(\mathbf{r})$ defines the many-body Hamilton operator and the latter determines everything, also $n(\mathbf{r})$. It is unclear, however, if the particle density $n(\mathbf{r})$ can be expressed explicitly as a functional of the potential of the ions (lattice components). To continue, we start with the jellium model: Then the single-particle wave functions are plane waves, and the expectation value of the single-particle Hamiltonian is:

$$\epsilon_i = \frac{\hbar^2}{2m} k_i^2 + v^{\text{eff}} \quad . \quad (3.101)$$

For the highest occupied state, i.e., for the weakest bound electron, we have:

$$\frac{\hbar^2}{2m} k_F^2 + v^{\text{eff}} = \epsilon_N = \mu \quad . \quad (3.102)$$

The fact that $\epsilon_N = \mu$ will be shown below. For a non-jellium system, as long as the potential $v^{\text{eff}}(\mathbf{r})$ varies slowly in \mathbf{r} , Eq. (3.101) is still valid, but only approximately. Actually, one should replace $v^{\text{eff}}(\mathbf{r})$ by $\langle \varphi_{o_N} | v^{\text{eff}} | \varphi_{o_N} \rangle$. Because this is not done here, the following derivation should be considered as a semi-classical approximation.

For the jellium system (and for slowly varying densities) we can define a (position dependent) Fermi- \mathbf{k} -vector (cf. Eq. (2.30)),

$$k_F(\mathbf{r}) = \sqrt[3]{3\pi^2 n(\mathbf{r})} \quad (3.103)$$

and obtain the following equation for the electron of the highest energy:

$$\frac{\hbar^2}{2m} (3\pi^2 n(\mathbf{r}))^{2/3} + v^{\text{eff}}(\mathbf{r}) = \mu \quad . \quad (3.104)$$

Since μ is the energy of the weakest bound electron, it has to be spatially constant. The first term of the left side of Eq. (3.103) is the kinetic, the second the potential energy. This equation enables us for a given μ to calculate the density $n(\mathbf{r})$ from $v(\mathbf{r})$ without solving a Schrödinger equation. The $\sim 10^{23}$ particles do not appear explicitly as individual particles. Equation (3.104) tells that there is a discrete relation between $v^{\text{eff}}(\mathbf{r})$ and $n(\mathbf{r})$, at least for jellium, or close to jellium systems

Equation (3.103) is called the *Thomas-Fermi equation*. For $v^{\text{eff}} = v + v^{\text{Hartree}}$ it is equivalent to the Hartree equation, and for $v^{\text{eff}} = v + v^{\text{Hartree}} + v^{\text{x}\alpha}$ it is equivalent to the Hartree-Fock-Slater Equation.

The Thomas-Fermi equation (3.102) can also be derived from a variational principle. This shall be done here for the Hartree theory. We have:

$$\begin{aligned}
E^e &= \langle \Phi | H^e | \Phi \rangle \\
&= \sum_{i=1}^N \left\langle \varphi_{o_i} \left| -\frac{\hbar^2}{2m} \nabla^2 \right| \varphi_{o_i} \right\rangle + \int v(\mathbf{r}) n(\mathbf{r}) d^3\mathbf{r} + \frac{e^2}{4\pi\epsilon_0} \frac{1}{2} \iint \frac{n(\mathbf{r})n(\mathbf{r}')}{|\mathbf{r} - \mathbf{r}'|} d^3\mathbf{r} d^3\mathbf{r}' \quad ,
\end{aligned} \tag{3.105}$$

and for jellium we have:

$$\begin{aligned}
\sum_{i=1}^N \left\langle \varphi_{o_i} \left| -\frac{\hbar^2}{2m} \nabla^2 \right| \varphi_{o_i} \right\rangle &= \frac{V_g}{V_g(2\pi)^3} 2 \int_0^{k_F} \frac{\hbar^2}{2m} k^2 d^3\mathbf{k} \\
&= 4\pi \frac{2}{(2\pi)^3} \frac{\hbar^2}{2m} \int_0^{k_F} k^4 dk = \frac{1}{5\pi^2} \frac{\hbar^2}{2m} k_F^5 \\
&= \frac{1}{5\pi^2} \frac{\hbar^2}{2m} (3\pi^2 n)^{5/3} = T_s^{\text{Jellium}}[n] \quad .
\end{aligned} \tag{3.106}$$

Thus, we have found that for jellium and probably also for slowly and weakly varying densities $n(\mathbf{r})$, the expectation value $\langle \Phi | H^e | \Phi \rangle$ can be written as a functional of the density (at least in the Hartree approximation). Then for jellium we obtain

$$\frac{\delta T_s^{\text{Jellium}}[n]}{\delta n(\mathbf{r})} = \frac{\hbar^2}{2m} (3\pi^2 n(\mathbf{r}))^{2/3} \quad . \tag{3.107}$$

Because the total energy of the ground state is $E_0^e = \text{Min}_{\Phi^N} \langle \Phi^N | H^e | \Phi^N \rangle$, we write

$$E_0^e = \text{Min}_{n(\mathbf{r})} E^e[n] \quad . \tag{3.108}$$

With the assumption that the total number of particles remains constant, the minimization is written as

$$\frac{\delta \{ E^e[n] - \mu (\int n(\mathbf{r}) d^3\mathbf{r} - N) \}}{\delta n(\mathbf{r})} = 0 \quad . \tag{3.109}$$

Here μ is the Lagrange parameter taking care of the constraint that the total number of electrons is N . Equation (3.108) apparently is equal to the Thomas-Fermi equation

$$\mu = \frac{\hbar^2}{2m} (3\pi^2 n(\mathbf{r}))^{2/3} + v^{\text{eff}}(\mathbf{r}) \quad , \tag{3.110}$$

with

$$v^{\text{eff}}(\mathbf{r}) = v(\mathbf{r}) + \frac{e^2}{4\pi\epsilon_0} \int \frac{n(\mathbf{r}')}{|\mathbf{r} - \mathbf{r}'|} d^3\mathbf{r}' \quad . \tag{3.111}$$

We did not prove that the variational principle is really valid (Eq. (3.108)), but we have “simply” assumed its validity. Further, it should be mentioned that in addition to the condition of the conservation of the particle number actually other constraints would be important as well, namely that only densities $n(\mathbf{r})$ must be considered that are physically meaningful, e.g.: $n(\mathbf{r})$ must be real and always positive.

We had already see that μ is the energy of the weakest bound electron. Let is look again at the meaning in terms of the variational principle. Equation (3.109) gives

$$\frac{\delta E^e[n]}{\delta n(\mathbf{r})} = \mu \quad ,$$

and if we specify this variation to a change in electron number, we obtain as a special case

$$\frac{d E^e}{d N} = \mu$$

which is, in fact, the definition of the chemical potential. Consequently, μ is the chemical potential, i.e., the energy required to change the particle number.

The Concept of Screening

Equation (3.103) shows that $n(\mathbf{r})$ is a functional of $v^{\text{eff}}(\mathbf{r})$:

$$n(\mathbf{r}) = F_1[v^{\text{eff}}(\mathbf{r}); \mu] \quad (3.112)$$

$$= \frac{1}{3\pi^2} \left[\frac{2m}{\hbar^2} (\mu - v^{\text{eff}}(\mathbf{r})) \right]^{3/2} . \quad (3.113)$$

Now we introduce a small perturbation

$$v^{\text{eff}}(\mathbf{r}) \longrightarrow v^{\text{eff}}(\mathbf{r}) + \Delta v^{\text{eff}}(\mathbf{r}) \quad . \quad (3.114)$$

Here μ shall remain unchanged, i.e., the energy, that is required to remove the weakest bound electron shall stay the same as it was without perturbation, because the perturbation is small. This will hold, e.g. when Δv^{eff} is a spatially localized perturbation of the potential in a macroscopic system, e.g. a defect atom in a semiconductor. Now we ask, how the particle density will change

$$n(\mathbf{r}) \longrightarrow \tilde{n}(\mathbf{r}) = n(\mathbf{r}) + \Delta n(\mathbf{r}) \quad . \quad (3.115)$$

For the perturbed system we have the Thomas-Fermi equation for \tilde{n} :

$$\mu = \frac{\hbar^2}{2m} [3\pi^2 \tilde{n}(\mathbf{r})]^{2/3} + v^{\text{eff}}(\mathbf{r}) + \Delta v^{\text{eff}}(\mathbf{r}) \quad , \quad (3.116)$$

and the comparison with Eq. (3.113) yields

$$\tilde{n}(\mathbf{r}) = F_1[v^{\text{eff}} + \Delta v^{\text{eff}}; \mu] = F_1[v^{\text{eff}}(\mathbf{r}); \mu - \Delta v^{\text{eff}}(\mathbf{r})] \quad . \quad (3.117)$$

Now we call $\mu - v^{\text{eff}} = \alpha$ and expand (3.117) in a Taylor series around the point $\alpha = \mu$. This yields

$$\tilde{n}(\mathbf{r}) = F_1[v^{\text{eff}}(\mathbf{r}); \alpha] \Big|_{\alpha=\mu} - \frac{\partial F_1[v^{\text{eff}}(\mathbf{r}); \alpha]}{\partial \alpha} \Big|_{\alpha=\mu} \cdot \Delta v^{\text{eff}}(\mathbf{r}) + O([\Delta v^{\text{eff}}]^2) \quad . \quad (3.118)$$

It follows

$$\begin{aligned} \Delta n(\mathbf{r}) &= \tilde{n}(\mathbf{r}) - n(\mathbf{r}) \\ &= - \frac{\partial F_1[v^{\text{eff}}(\mathbf{r}); \alpha]}{\partial \alpha} \Big|_{\alpha=\mu} \cdot \Delta v^{\text{eff}}(\mathbf{r}) + O([\Delta v^{\text{eff}}]^2) \quad . \end{aligned} \quad (3.119)$$

Actually we are interested in the relation between $v(\mathbf{r})$ and $n(\mathbf{r})$, or between $\Delta v(\mathbf{r})$ and $\Delta n(\mathbf{r})$. To obtain this relation, we consider here the Hartree approximation. Then we have:

$$\Delta v^{\text{eff}}(\mathbf{r}) = \Delta v(\mathbf{r}) + \frac{e^2}{4\pi\epsilon_0} \int \frac{\Delta n(\mathbf{r}')}{|\mathbf{r} - \mathbf{r}'|} d^3\mathbf{r}' \quad (3.120)$$

or with the Poisson equation,

$$\nabla^2(\Delta v^{\text{eff}}(\mathbf{r})) = \nabla^2(\Delta v(\mathbf{r})) - \frac{e^2}{\epsilon_0} \Delta n(\mathbf{r}) \quad . \quad (3.121)$$

In the Fourier representation we have:

$$\Delta n(\mathbf{k}) = \frac{\epsilon_0}{e^2} k^2 [\Delta v^{\text{eff}}(\mathbf{k}) - \Delta v(\mathbf{k})] = - \left. \frac{\partial F_1[v^{\text{eff}}(\mathbf{r}); \alpha]}{\partial \alpha} \right|_{\alpha=\mu} \cdot \Delta v^{\text{eff}}(\mathbf{k}) \quad . \quad (3.122)$$

If we set $\left. \frac{\partial F_1}{\partial \alpha} \right|_{\alpha=\mu} = \frac{\epsilon_0}{e^2} k_0^2$, we obtain

$$\frac{k^2 + k_0^2}{k^2} \Delta v^{\text{eff}}(\mathbf{k}) = \Delta v(\mathbf{k}) \quad . \quad (3.123)$$

The quantity k_0 is called the Thomas-Fermi wave vector. We have now derived an equation, which (in the Hartree approximation and for a jellium-type system) describes the relation between the origin of the perturbation (change of the potential of the ions) and the potential (effective potential) acting on the single-particle wave functions. This equation corresponds closely to a description, which is known from electrodynamics: The relation between the strength of an electric field \mathbf{E} and the dielectric displacement \mathbf{D} is

$$\mathbf{D} = \epsilon \mathbf{E} \quad , \quad (3.124)$$

where ϵ is the dielectric constant (generally a tensor). Therefore, we can and want to continue our investigation by starting from the relation $\Delta v(\mathbf{r}) \rightleftharpoons \Delta v^{\text{eff}}(\mathbf{r})$, and considering in terms of a microscopic materials equation of electrodynamics. In the context of Thomas-Fermi theory in \mathbf{k} -space we write (cf. Eq. (3.123)):

$$\Delta v(\mathbf{k}) = \epsilon(\mathbf{k}) \Delta v^{\text{eff}}(\mathbf{k}) \quad (3.125)$$

with the Thomas-Fermi dielectric constant

$$\epsilon(\mathbf{k}) = \frac{\mathbf{k}^2 + k_0^2}{\mathbf{k}^2} \quad . \quad (3.126)$$

For small values of \mathbf{k}^2 , i.e., large wave lengths, the jellium approximation is well justified and then equations (3.125) and (3.126) are equivalent to the Hartree theory. Still k_0 is unknown, but it will be determined below (Eq. (3.137)). In real space we obtain

$$\Delta v(\mathbf{r}) = \int \epsilon(\mathbf{r}, \mathbf{r}') \Delta v^{\text{eff}}(\mathbf{r}') d^3\mathbf{r}' \quad . \quad (3.127)$$

All the many-body quantum mechanics is now hidden in the dielectric constant. In case we were dealing with a spatially isotropic, uniform and homogenous system, we would have:

$$\epsilon(\mathbf{r}, \mathbf{r}') = \epsilon(|\mathbf{r} - \mathbf{r}'|) \quad . \quad (3.128)$$

To demonstrate the scientific content of the Thomas-Fermi theory we will now discuss the screening in the neighborhood of a point charge in a solid (e.g. a defect in a crystal). We start from:

$$\Delta v(\mathbf{r}) = \frac{-e^2 Z}{4\pi\epsilon_0 r} \quad . \quad (3.129)$$

In \mathbf{k} -space we obtain

$$\Delta v(\mathbf{k}) = \frac{-e^2 Z}{4\pi\epsilon_0 k^2} \quad , \quad (3.130)$$

and for the effective potential we obtain:

$$\Delta v^{\text{eff}}(\mathbf{k}) = \frac{k^2}{k^2 + k_0^2} \Delta v(\mathbf{k}) = \frac{-e^2 Z}{4\pi\epsilon_0} \frac{Z}{k^2 + k_0^2} \quad . \quad (3.131)$$

When we go back into real space, we have

$$\Delta v^{\text{eff}}(\mathbf{r}) = \frac{-e^2 Z}{4\pi\epsilon_0} \frac{Z}{r} e^{-k_0 r} \quad . \quad (3.132)$$

Now it is clear that not an “external” perturbation charge $Z \cdot e$, with a potential $\frac{-e^2 Z}{4\pi\epsilon_0 r}$ is acting on the electron, but a *screened* Coulomb potential (Eq. (3.132)). This potential is also called Yukawa potential (the name originates from the theory of mesons, where this potential also plays a role). The Thomas-Fermi wave vector k_0 determines the strength of the screening. When $1/k_0$ becomes infinite, then there is no screening. The effective potential of Eq. (3.132) is shown in Fig. 3.8.

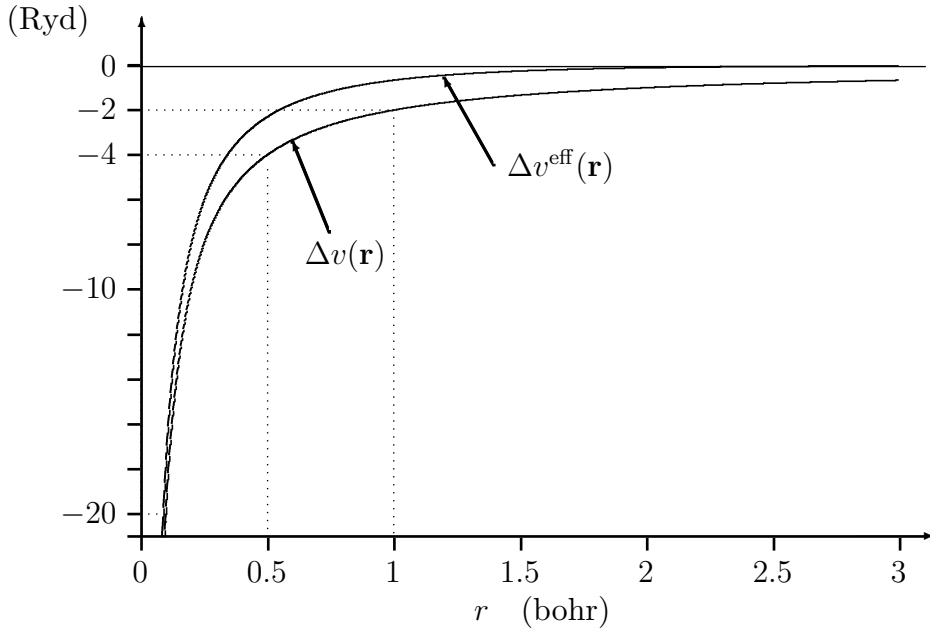


Figure 3.8: Change of the effective potential induced by a point charge at $\mathbf{r} = 0$ with $Z = 1$. In the Thomas-Fermi approximation with $k_0 = 1.1 \text{ bohr}^{-1}$, i.e. for $r_s \simeq 2 \text{ bohr}$.

This polarization charge density, $\Delta n(\mathbf{r})$, i.e., the change of the electron density induced by the perturbation, according to Eq. (3.124) with (3.133) is:

$$\Delta n(\mathbf{k}) = -\frac{\varepsilon_0}{e^2} k_0^2 \Delta v^{\text{eff}}(\mathbf{k}) = Z \frac{k_0^2}{k^2 + k_0^2} \cdot \frac{1}{4\pi} \quad . \quad (3.133)$$

In real space we obtain the result,

$$\Delta n(\mathbf{r}) = Z \frac{k_0^2}{4\pi} \frac{e^{-k_0 r}}{r} \quad , \quad (3.134)$$

which is shown in Fig. 3.9. Physically this result means that a positive perturbation charge at $\mathbf{r} = 0$ induces an attraction of the valence electrons of the solid to the perturbation charge. This increases the negative charge density in the neighborhood of $\mathbf{r} = 0$, and the perturbation is screened. One says that the “valence charge density is polarized”.

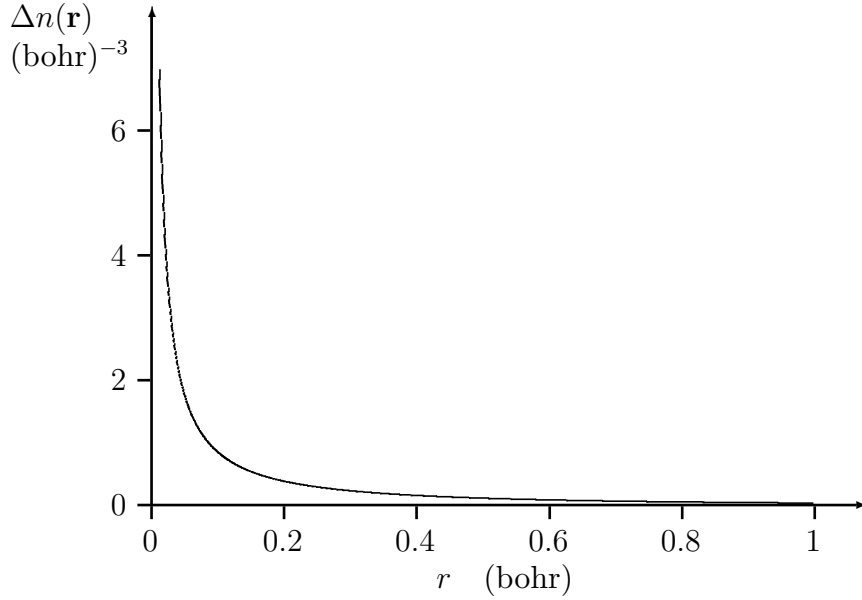


Figure 3.9: Change of the electron density induced by a positive point charge at $\mathbf{r} = 0$ with $Z = 1$. In the Thomas-Fermi approximation with $k_0 = 1.1 \text{ bohr}^{-1}$ and $r_s \simeq 2 \text{ bohr}$.

The area under the curve is equal to $Z = \int \Delta n(\mathbf{r}) d^3\mathbf{r}$, i.e., the charge belonging to $\Delta n(\mathbf{r})$, is exactly equal to the perturbation charge, but with an opposite sign. How important, or how efficient is this screening; i.e., how large is k_0 for realistic systems?

$$\begin{aligned} \frac{\varepsilon_0}{e^2} k_0^2 &= \left. \frac{\partial F_1[v^{\text{eff}}(\mathbf{r}); \alpha]}{\partial \alpha} \right|_{\alpha=\mu} = \left. \frac{\partial}{\partial \alpha} \frac{1}{3\pi^2} \left\{ \frac{2m}{\hbar^2} (\alpha - v^{\text{eff}}) \right\}^{3/2} \right|_{\alpha=\mu} \\ &= \left. \frac{3}{2} \frac{2m}{\hbar^2 3\pi^2} \left\{ \frac{2m}{\hbar^2} (\alpha - v^{\text{eff}}) \right\}^{1/2} \right|_{\alpha=\mu} = \frac{m}{\hbar^2 \pi^2} k_F \quad . \quad (3.135) \end{aligned}$$

We have:

$$k_0^2 = \frac{e^2}{\varepsilon_0} \frac{m}{\hbar^2 \pi^2} k_F = \frac{e^2}{\varepsilon_0} \frac{m}{\hbar^2 \pi^2} [3\pi^2 n]^{1/3} \quad (3.136)$$

If we express the density by the density parameter r_s , we have

$$k_0 = \frac{2.95}{\sqrt{r_s/a_B}} \text{\AA}^{-1} \quad . \quad (3.137)$$

Because r_s is generally in the range $1 \dots 6$ bohr, the screening happens very fast, i.e., on a length scale of $1/k_0 \approx 0.5 \text{\AA}$. This length is comparable to, or even shorter than, the distance between the atoms in a crystal (typically $2\text{--}3 \text{\AA}$). A more accurate calculation yields *qualitatively* the same result. But there are also significant differences. A more accurate calculation (which is significantly more complicated) is shown in Fig. 3.10. The reasons for the differences to Fig. 3.9 are that now not $T^{\text{Jellium}}[n]$, but the correct kinetic energy has been used. Further, no semiclassical approximation for v^{eff} has been assumed, and no Taylor-series expansion and approximation for $F_1[v^{\text{eff}}; \alpha]$ has been used, and the exchange interaction has been taken into account. The correct kinetic energy, T , yields oscillations (Friedel oscillations).

The basic idea of Thomas-Fermi theory to calculate $n(\mathbf{r})$ directly from $v(\mathbf{r})$ is for sure interesting. However, generally the mentioned approximations are too drastic. Improvements of the kinetic energy term (cf. Eq. (3.106)) have been suggested by C.F. Weizsäcker. The correction term is proportional to $|\nabla n(\mathbf{r})|^2/n(\mathbf{r})$.

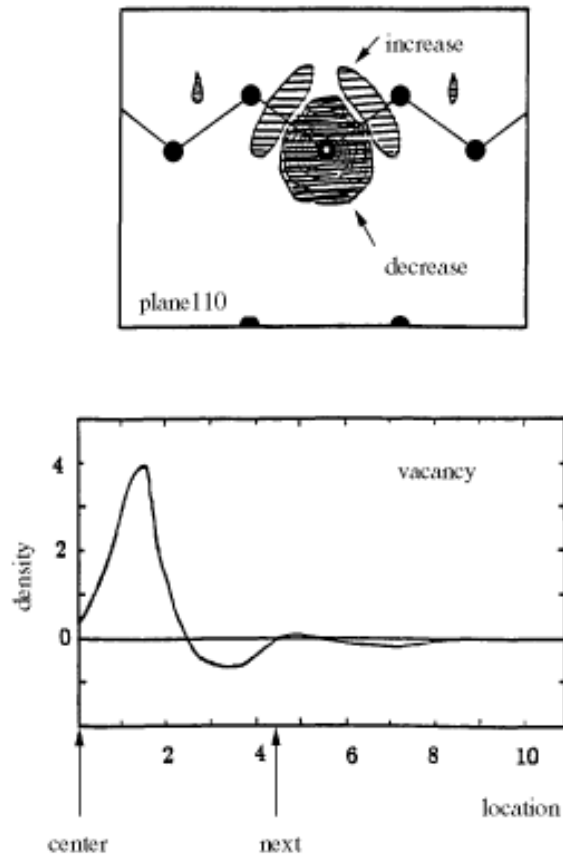


Figure 3.10: Change in the charge density induced by a defect atom (arsenic) in a silicon crystal. The top figure shows a contour plot in the (110) plane, and the bottom shows the density change along the [111] direction.

3.7 Density-Functional Theory⁸

We are still interested in the properties of a solid, which is described by the many-body Hamilton operator

$$H^e = \sum_{i=1}^N -\frac{\hbar^2}{2m} \nabla_{\mathbf{r}_i}^2 + v(\mathbf{r}_i) + \frac{1}{2} \frac{e^2}{4\pi\epsilon_0} \sum_{\substack{i,j \\ i \neq j}}^{N,N} \frac{1}{|\mathbf{r}_i - \mathbf{r}_j|} \quad . \quad (3.138)$$

We will assume that the ground state of

$$H^e \Phi = E^e \Phi \quad (3.139)$$

is non-degenerate. Further we will assume that the system is non-magnetic, i.e., the particle density of the spin-up and spin-down electrons shall be the same:

$$n_{\uparrow}(\mathbf{r}) = n_{\downarrow}(\mathbf{r}) \quad , \quad (3.140)$$

where for the total particle density as usual we have:

$$n(\mathbf{r}) = n_{\uparrow}(\mathbf{r}) + n_{\downarrow}(\mathbf{r}) \quad (3.141)$$

$$= \left\langle \Phi \left| \sum_{i=1}^N \delta(\mathbf{r} - \mathbf{r}_i) \right| \Phi \right\rangle \quad . \quad (3.142)$$

From (3.140) and (3.141) we then obtain

$$n_{\uparrow}(\mathbf{r}) = n_{\downarrow}(\mathbf{r}) = \frac{n(\mathbf{r})}{2} \quad (3.143)$$

The assumptions of a “non-degenerate ground state” and Eqs. (3.141) and (3.143) can also be omitted, but the following discussion is simpler when they are made. First, we give the theorem of Hohenberg und Kohn, and subsequently we will prove its validity:

The expectation value of H^e is a functional of the particle density $n(\mathbf{r})$:

$$\langle \Phi | H^e | \Phi \rangle = E_v[n] = \int v(\mathbf{r}) n(\mathbf{r}) d^3\mathbf{r} + F[n] \quad . \quad (3.144)$$

Here the functional $F[n]$ does not depend explicitly on $v(\mathbf{r})$.

Proof of this statement: It is immediately clear that $F = \langle \Phi | T^e + V^{e-e} | \Phi \rangle$ is a functional of Φ , but initially it is surprising that it is supposed to be a functional of $n(\mathbf{r})$. Now we will show that Φ is a functional of $n(\mathbf{r})$, as long as we constrain ourselves to functions, which are defined according to Eq. (3.144) and Φ is the ground state wave function of an *arbitrary* N -particle problem. Because of the word “arbitrary”, i.e., $v(\mathbf{r})$ is arbitrary,

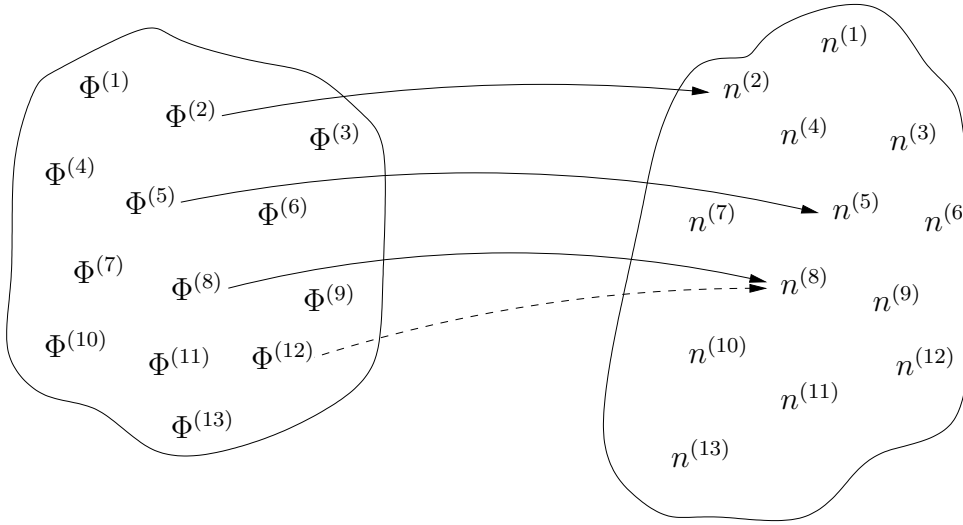
⁸References: P. Hohenberg, W. Kohn, Phys. Rev. **136**, B 864 (1964); W. Kohn, L. Sham, Phys. Rev. A **140**, 1133 (1965); M. Levy, Proc. Natl. Acad. Sci. USA **76**, 6062 (1979); R.M. Dreizler, E.K.U. Gross, Density Functional Theory (Springer, 1990); R.G. Parr, W. Yang, Density-Functional Theory of Atoms and Molecules (Oxford University Press 1994); R.O. Jones and O. Gunnarsson, Rev. Mod. Phys. **61**, 689 (1989)

this is not a constraint of physical relevance. Mathematically, however, this is a noticeable restriction.

The opposite of our goal is known: $n(\mathbf{r})$ is a functional of Φ :

$$n(\mathbf{r}) = \left\langle \Phi \left| \sum_{i=1}^N \delta(\mathbf{r} - \mathbf{r}_i) \right| \Phi \right\rangle . \quad (3.145)$$

The question to be answered is: Is the mapping of Eq. (3.144) reversibly unique (cf. Fig. 3.11)?



The set of non-degenerate ground state wave functions Φ of arbitrary N -particle Hamilton operators of type of Eq. (3.1) or Eq. (3.142).

The set of the particle densities $n(\mathbf{r})$, which belong to non-degenerate ground states of the N -particle problem.

Figure 3.11: Relation between wave functions and particle densities. The Hohenberg-Kohn theorem states that the dashed case does not exist, i.e., two different many-body wave functions have to yield different densities.

The proof of the theorem of Hohenberg and Kohn and of the statement $\Phi = \Phi[n]$ is done following the principle “reductio ad absurdum”:

Starting point: $v(\mathbf{r})$ and $\tilde{v}(\mathbf{r})$ shall be two physically different potentials, i.e., we have

$$v(\mathbf{r}) - \tilde{v}(\mathbf{r}) \neq \text{constant} . \quad (3.146)$$

These two potentials define two Hamilton operators H^e and \tilde{H}^e (for simplicity we constrain ourselves to operators, that have a non-degenerate ground state (for a more general discussion we refer to the work of Levy).

Assumption 1: Both Hamilton operators have the same ground state wave function. It follows

$$(\tilde{H}^e - H^e)\Phi_0 = \sum_{i=1}^N \{\tilde{v}(\mathbf{r}_i) - v(\mathbf{r}_i)\} \Phi_0 = (\tilde{E}_0^e - E_0^e)\Phi_0 \quad , \quad (3.147)$$

and from this one obtains (with the exception of a discrete number of points, for which Φ_0 is zero)

$$\sum_{i=1}^N \{\tilde{v}(\mathbf{r}_i) - v(\mathbf{r}_i)\} = \tilde{E}_0^e - E_0^e \quad . \quad (3.148)$$

This means that $\tilde{v}(\mathbf{r}) - v(\mathbf{r})$ is constant which is in contradiction to the starting point. It follows: Our assumption 1 that H^e and \tilde{H}^e have the same eigenfunction, is wrong. Therefore, we have that Φ_0 and $\tilde{\Phi}_0$ are different.

Assumption 2: We assume that Φ_0 and $\tilde{\Phi}_0$ (even though $\Phi_0 \neq \tilde{\Phi}_0$) both can give rise to the same particle density $n(\mathbf{r})$. This corresponds to the dashed arrows in Fig. 3.11. We then get

$$E_0^e = \langle \Phi_0 | H^e | \Phi_0 \rangle < \langle \tilde{\Phi}_0 | H^e | \tilde{\Phi}_0 \rangle = \left\langle \tilde{\Phi}_0 \left| \tilde{H}^e - \sum_{i=1}^N \tilde{v}(\mathbf{r}_i) + \sum_{i=1}^N v(\mathbf{r}_i) \right| \tilde{\Phi}_0 \right\rangle \quad , \quad (3.149)$$

therefore,

$$E_0^e < \tilde{E}_0^e + \left\langle \tilde{\Phi}_0 \left| \sum_{i=1}^N \{v(\mathbf{r}_i) - \tilde{v}(\mathbf{r}_i)\} \right| \tilde{\Phi}_0 \right\rangle \quad (3.150)$$

and

$$E_0^e < \tilde{E}_0^e + \int \{v(\mathbf{r}) - \tilde{v}(\mathbf{r})\} n(\mathbf{r}) d^3\mathbf{r} \quad . \quad (3.151)$$

Similarly, we obtain for $\tilde{E}_0^e = \langle \tilde{\Phi}_0 | \tilde{H}^e | \tilde{\Phi}_0 \rangle$:

$$\tilde{E}_0^e < E_0^e - \int \{v(\mathbf{r}) - \tilde{v}(\mathbf{r})\} n(\mathbf{r}) d^3\mathbf{r} \quad (3.152)$$

If we add equations (3.151) and (3.152), we obtain

$$E_0^e + \tilde{E}_0^e < E_0^e + \tilde{E}_0^e \quad , \quad (3.153)$$

a contradiction. This means that assumption 2 is wrong. Thus we have proven:

Two different ground states Φ_0 and $\tilde{\Phi}_0$ must yield two different particle densities $n(\mathbf{r})$ and $\tilde{n}(\mathbf{r})$. This has the following consequences:

- a) $E_v[n] \stackrel{!}{=} \langle \Phi | H^e | \Phi \rangle$ is a functional of $n(\mathbf{r})$. In fact, what we had shown was even more general, namely: $\Phi = \Phi[n]$. Here, the functionals are only defined for the set of particle densities, that can be constructed from a ground state wave function of an arbitrary N -particle Hamilton operator H^e , where $v(\mathbf{r})$ is an arbitrary function (cf. Fig. 3.11).

b) In the expression

$$E_v[n] = \int n(\mathbf{r})v(\mathbf{r}) d^3\mathbf{r} + F[n] \quad (3.154)$$

$F[n]$ is a universal functional of $n(\mathbf{r})$. This means that the functional F is independent of the “external” potential $v(\mathbf{r})$.

c) $E_v[n]$ obtains under the constraint

$$\int n(\mathbf{r})d^3\mathbf{r} = N \quad (3.155)$$

a minimum for the correct particle density. This minimum defines the ground state energy and the ground state electron density n_0 :

$$E_0^e = \text{Min}_{n(\mathbf{r})} E_v[n] = E_v[n_0] \quad . \quad (3.156)$$

Thus, the variational principle for $\langle \Phi | H^e | \Phi \rangle$ can exactly be reformulated in terms of a variational principle for $E_v[n]$. The new variational principle is:

$$\delta \left\{ E_v[n] - \mu \left(\int n(\mathbf{r})d^3\mathbf{r} - N \right) \right\} = 0 \quad , \quad (3.157)$$

or

$$\left. \frac{\delta E_v[n]}{\delta n(\mathbf{r})} \right|_{n_0} = \mu \quad . \quad (3.158)$$

Here the constraint of a constant total number of particles being equal to N is taken into account by the method of Lagrange multipliers, i.e., we have included the condition

$$\int n(\mathbf{r})d^3\mathbf{r} = N \quad . \quad (3.159)$$

Still some physically important conditions are missing, e.g. that $n(\mathbf{r}) \geq 0$ and that $n(\mathbf{r})$ has to be continuous. These are necessary conditions, which have to be fulfilled by the functions of the range of $E_v[n]$, and which we will have to take into account when doing the variation in an actual calculation. Compared to Hartree and Hartree-Fock theory we achieved a significant advantage: Earlier we had to insert a wave function depending on 10^{23} coordinates in the functional to be minimized. This treatment led to obvious difficulties and approximations, which were introduced *before* the actual variation was performed. Now we have to insert functions depending on three coordinates only into the functional, and, up to now, i.e., up to Eq. (3.158), we have introduced *no* approximation.

We have shown: The ground state electron density determines the many-body Hamiltonian, uniquely. As the many-body Hamiltonian determines everything, we can also tell – in principle – the ground state electron density determines everything: the ground state, all excited states, all physical properties.

So far, we have shown that the functional $E_v[n]$ does exist. However, we have not shown how it looks like. In fact, we also have not shown that it can be written as a closed mathematical expression.

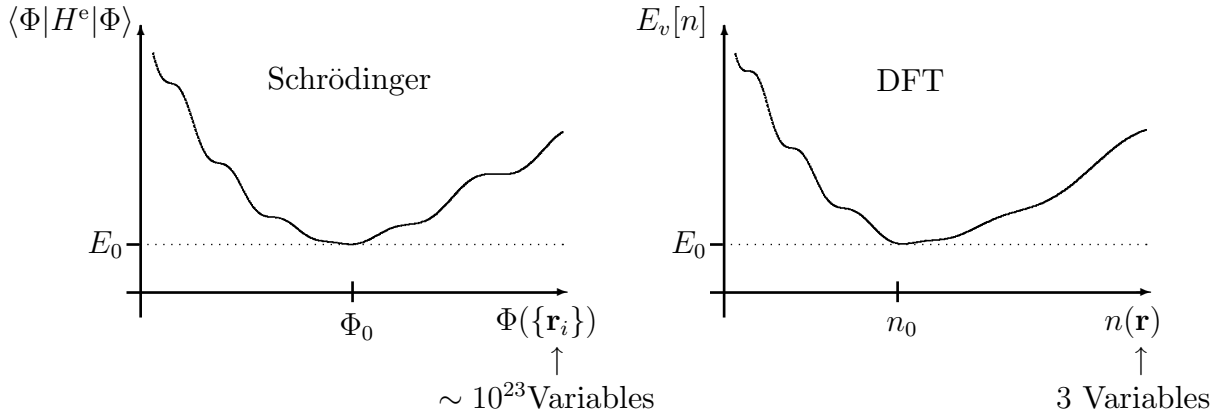


Figure 3.12: Schematic figure for the variational principle of $\langle \Phi | H^e | \Phi \rangle$ and $E_v[n]$.

For the actual variation Kohn and Sham suggested the following procedure. We write:

$$E_v[n] = T_s[n] + \int v(\mathbf{r})n(\mathbf{r})d^3\mathbf{r} + E^{\text{Hartree}}[n] + E^{\text{xc}}[n] \quad (3.160)$$

with

$$E^{\text{Hartree}}[n] = \frac{1}{2} \frac{e^2}{4\pi\epsilon_0} \iint \frac{n(\mathbf{r})n(\mathbf{r}')}{|\mathbf{r} - \mathbf{r}'|} d^3\mathbf{r}d^3\mathbf{r}' \quad . \quad (3.161)$$

$T_s[n]$ is the kinetic energy functional of non-interacting electrons. Although generally it is not explicitly known as a function of $n(\mathbf{r})$, it will be introduced here. In fact, $T_s[n]$ cannot be written down in a closed mathematical form as a functional of the density. However, we know a series expansion:

$$T_s[n] = \frac{1}{5\pi^2} \frac{\hbar^2}{2m} (3\pi^2 n(\mathbf{r}))^{5/3} + \mathcal{O}(\nabla n(\mathbf{r})) \quad , \quad (3.162)$$

where the first term is the result for jellium, i.e. when $\nabla n(\mathbf{r}) = 0$.

$$\frac{\delta T_s}{\delta n(\mathbf{r})} = \frac{\hbar^2}{2m} (3\pi^2 n(\mathbf{r}))^{2/3} \quad (3.163)$$

was used in the Thomas-Fermi theory, i.e. for jellium.

Introducing here $T_s[n]$ – the exact one, not Thomas-Fermi – is still an approximation in mathematical terms. There may be physically reasonable densities that ly outside the range of definition of $T_s[n]$. However, from a physicist's point of view it appears to be plausible that all physically meaningful densities can be constructed from

$$\left(-\frac{\hbar^2}{2m} \nabla^2 + \tilde{v}(\mathbf{r}) \right) \varphi_{o_i}(\mathbf{r}) = \epsilon_{o_i} \varphi_{o_i}(\mathbf{r}) \quad , \quad (3.164)$$

$$\text{with } n(\mathbf{r}) = \sum_{i=1}^N |\varphi_{o_i}(\mathbf{r})|^2 \quad (3.165)$$

and arbitrary $\tilde{v}(\mathbf{r})$. For such densities the kinetic energy is

$$T_s[n] = \sum_{i=1}^N \langle \varphi_{o_i} | -\frac{\hbar^2}{2m} \nabla^2 | \varphi_{o_i} \rangle \quad . \quad (3.166)$$

We note that Eq. (3.164) formally describes the ground state of a system of non-interacting electrons moving in the potential $\tilde{v}(\mathbf{r})$.⁹

For the exchange-correlation functional we obtain

$$\begin{aligned} E^{\text{xc}}[n] &= \langle \Phi | H^e | \Phi \rangle - \int v(\mathbf{r})n(\mathbf{r})d^3\mathbf{r} - T_s[n] - E^{\text{Hartree}}[n] \\ &= F[n] - T_s[n] - E^{\text{Hartree}}[n] \quad . \end{aligned} \quad (3.167)$$

The variational principle Eq. (3.158) applied to the energy functional Eq. (3.160) yields

$$\left. \frac{\delta T_s[n]}{\delta n(\mathbf{r})} \right|_{n_0} + v^{\text{eff}}([n_0], \mathbf{r}) = \mu \quad (3.168)$$

with

$$\begin{aligned} v^{\text{eff}}([n], \mathbf{r}) &= \frac{\delta \left\{ \int v(\mathbf{r})n(\mathbf{r})d^3\mathbf{r} + E^{\text{Hartree}}[n] + E^{\text{xc}}[n] \right\}}{\delta n(\mathbf{r})} \\ &= v(\mathbf{r}) + \frac{e^2}{4\pi\epsilon_0} \int \frac{n(\mathbf{r}')}{|\mathbf{r} - \mathbf{r}'|} d^3\mathbf{r}' + \frac{\delta E^{\text{xc}}[n]}{\delta n(\mathbf{r})} \quad . \end{aligned} \quad (3.169)$$

We note that Eq. (3.168) determines the ground state density of *interacting* electrons. Formally, it is an equation for *non-interacting* electrons moving in the potential $v^{\text{eff}}([n], \mathbf{r})$, because per definition $T_s[n]$ is the kinetic energy of non-interacting electrons of density $n(\mathbf{r})$ (see Eqs. (3.164) – (3.166)). It seems plausible that the set of densities defined this way covers all physically reasonable densities or at least come arbitrarily close. As long as $T_s[n]$ is a well behaved functional, the assumption (of “being arbitrarily close”) should be sufficient. But this point still has not been discussed conclusively in the literature.

From Eq. (3.168) we obtain the equivalent single-particle Schrödinger equation

$$\left\{ -\frac{\hbar^2}{2m} \nabla^2 + v^{\text{eff}}([n], \mathbf{r}) \right\} \varphi_{o_i}(\mathbf{r}) = \epsilon_{o_i} \varphi_{o_i}(\mathbf{r}) \quad . \quad (3.170)$$

Obviously, this is an *effective* single-particle equation, because v^{eff} depends on the solutions that we are seeking.

Equation (3.170) together with Eq. (3.165) and (3.169) is called the *Kohn-Sham equation*. It is solved using an SCF procedure. Although the functional $T_s[n]$ is not explicitly known as a functional in n , we can, by replacing Eq. (3.168) by the equivalent Eq. (3.170), still

⁹For non-interacting electrons the Hamiltonian is $H' = \sum_{i=1}^N \left(-\frac{\hbar^2}{2m} \nabla_{\mathbf{r}_i}^2 + \tilde{v}(\mathbf{r}_i) \right)$ and the many-body wavefunction $\Phi(\{\mathbf{r}_i\})$ is a Slater-determinant. The ground state for N such particles is determined by minimization with respect to the single-particle orbitals, $\frac{\delta}{\delta \varphi_{o_i}(\mathbf{r})} \left\{ \langle \Phi | H | \Phi \rangle - \epsilon_{o_i} \left(\int n(\mathbf{r})d^3\mathbf{r} - N \right) \right\} = \left\{ -\frac{\hbar^2}{2m} \nabla^2 + \tilde{v}(\mathbf{r}) - \epsilon_{o_i} \right\} \varphi_{o_i}(\mathbf{r}) \equiv 0$ (and *c.c.*), i.e. Eq. (3.164). According to the Hohenberg-Kohn theorem, we can also obtain the ground state from the density functional $E'_v[n] = \int n(\mathbf{r})\tilde{v}(\mathbf{r})d^3\mathbf{r} + T_s[n]$, i.e. $T_s[n]$ defines the functional $F[n]$ of Eq. (3.154) for non-interacting electrons. The variational principle, Eq. (3.158), then yields $\left. \frac{\delta E'_v[n]}{\delta n(\mathbf{r})} \right|_{n_0} = \left. \frac{\delta T_s[n]}{\delta n(\mathbf{r})} \right|_{n_0} + \tilde{v}(\mathbf{r}) = \mu$.

treat it exactly. This has the technical disadvantage that we end up with the N single-particle functions, which we wanted to avoid. For the evaluation of the total energy $E_v[n]$ we need $T_s[n]$. The calculation of $T_s[n]$ is done using one of the two following equations. Generally, for non-interacting particles we have:

$$T_s[n] = \sum_{i=1}^N \langle \varphi_{o_i} \left| -\frac{\hbar^2}{2m} \nabla^2 \right| \varphi_{o_i} \rangle \quad , \quad (3.171)$$

$$= \sum_{i=1}^N \epsilon_{o_i} - \int v^{\text{eff}}[n^{\text{in}}](\mathbf{r}) n(\mathbf{r}) d^3\mathbf{r} \quad . \quad (3.172)$$

Here $v^{\text{eff}}(\mathbf{r})$ is determined from Eq. (3.169), and ϵ_{o_i} is obtained from Eq. (3.170). Thus, we have proven that T_s is a functional of n . Here v^{eff} has to be calculated from a density $n^{\text{in}}(\mathbf{r})$, because if we interpret $T_s[n]$ as a *functional*, v^{eff} has to be exactly the potential, which generates the ϵ_{o_i} and the $\varphi_{o_i}(\mathbf{r})$ and $n(\mathbf{r})$. Generally, $n^{\text{in}}(\mathbf{r})$, which is used for the calculation of $v^{\text{eff}}(\mathbf{r})$ will differ from $n(\mathbf{r})$. Only at the end of the SCF cycle both densities are the same.

As a side remark we note that the self-consistent solution of the variational principle would not be changed if $T_s[n]$ was not be used, but e.g.

$$\tilde{T}[n] = \sum_{i=1}^N \epsilon_{o_i} - \int v^{\text{eff}}([n], \mathbf{r}) n(\mathbf{r}) d^3\mathbf{r} \quad , \quad (3.173)$$

or different equations, which differ only by $O(n^{\text{in}} - n)$ from $T_s[n]$. But here we continue using $T_s[n]$.

Up to now no approximation has been introduced (apart from the reasonable assumption described by Eq. (3.165)). Therefore we have – in contrast to Hartree and Hartree-Fock – first made use of the variational principle of the ground state, and now we will start to think about approximations.

In Hartree and Hartree-Fock theory *first* an approximation (ansatz of the wave function) was introduced and then the expectation value of H^e was investigated. Experience shows that it is particularly important to treat $T_s[n]$ as accurately as possible, in order to obtain e.g. the shell structure of the electrons in atoms (*s*-, *p*-, *d*-electrons), which cannot be described with Thomas-Fermi theory. The Kohn-Sham ansatz permits one to treat $T_s[n]$ exactly.

Using Eq. (3.171) or (3.172) we can evaluate $T_s[n]$ without knowing the functional explicitly. Just one thing remains unknown: $E^{\text{xc}}[n]$ and $v^{\text{xc}}(\mathbf{r}) = \frac{\delta E^{\text{xc}}[n]}{\delta n(\mathbf{r})}$. We know that $E^{\text{xc}}[n]$ is a universal functional¹⁰, i.e., the functional does not depend on the system: The hydrogen atom, the diamond crystal etc. are described by the same functional. Unfortunately, we do not know the exact form of $E^{\text{xc}}[n]$. It is also not clear, if the functional can be given in a simple, closed form at all, or if E^{xc} is similar to T_s . Analogous to the

¹⁰Strictly, $F[n]$ is a universal functional in n . Because $F[n] = T_s[n] + E^{\text{Hartree}}[n] + E^{\text{xc}}[n]$, cf. Eq. (3.165), this is also valid for $E^{\text{xc}}[n]$.

Thomas-Fermi-Weizsäcker ansatz for $T_s[n]$, we consider a series expansion starting from jellium (the homogeneous, interacting electron gas, where we have $v(\mathbf{r}) = \text{constant}$ and $n(\mathbf{r}) = \text{constant}$),

$$E^{\text{xc}}[n] = E^{\text{xc-jellium}}[n] + O(\nabla n) \quad . \quad (3.174)$$

We rewrite the exchange-correlation energy as follows

$$E^{\text{xc}}[n] = \int \epsilon^{\text{xc}}[n] n(\mathbf{r}) d^3\mathbf{r} \quad , \quad (3.175)$$

and

$$E^{\text{xc-jellium}}[n] = \int \epsilon^{\text{xc-jellium}}[n] n(\mathbf{r}) d^3\mathbf{r} \quad . \quad (3.176)$$

Here $\epsilon^{\text{xc-jellium}}[n]$ is the exchange-correlation energy per particle in a jellium system of constant density n . Because $n(\mathbf{r})$ is constant, i.e., n is just a number, $\epsilon^{\text{xc-jellium}}$ then is a *function* of the density: $\epsilon^{\text{xc-jellium}}(n)$. We generalize this expression to the following statement: For systems with a slowly varying density, $E^{\text{xc}}[n]$ can be replaced by

$$E^{\text{xc-LDA}}[n] = \int n(\mathbf{r}) \epsilon^{\text{xc-jellium}}(n(\mathbf{r})) d^3\mathbf{r} \quad . \quad (3.177)$$

Here n is the local density, i.e., the density at position \mathbf{r} .

“Slowly varying” means that the system can be regarded as a collection of jellium systems, where neighboring systems have only slightly different densities. Therefore, in a strict sense, $n(\mathbf{r})$ at a scale of $\frac{2\pi}{k_F}$ must change only marginally. $\frac{2\pi}{k_F}$ is the shortest wave length, appearing in the occupied states of a jellium system. Generally, for real systems this “mathematical requirement” for $n(\mathbf{r})$ is not fulfilled, i.e., $\frac{2\pi}{k_F} \approx 5\text{\AA}$ is of the same order as the interatomic distances. Still, experience shows that the ansatz Eq. (3.177)

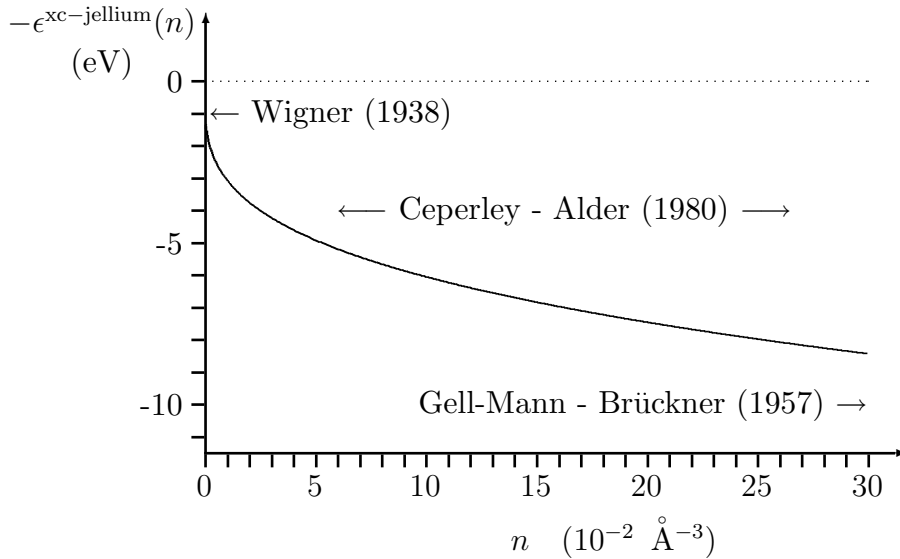


Figure 3.13: The exchange-correlation energy per particle for jellium systems of density n .

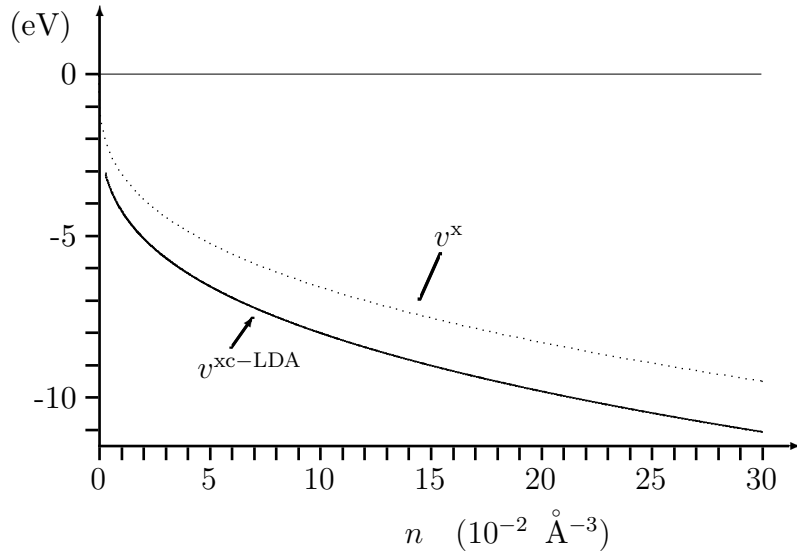


Figure 3.14: Exchange potential ($F = 0.5$ or $\alpha = 2/3$, cf. Eq. (3.85)) and the exchange-correlation potential as a function of the electron-density. The difference of both is the correlation potential.

works surprisingly well. This will be explained later. As a side remark we note that for $T_s[n]$ a local-density approximation is very poor, but for $E^{\text{xc}}[n]$ such an approximation is apparently acceptable.

The approximation (3.177) is called the *local-density approximation* (LDA). In this approximation each point in space (only for $E^{\text{xc}}[n]$) is treated like a jellium system. For the density at this point $n(\mathbf{r})$ then $E^{\text{xc}}[n]$ for jellium of density n is inserted. For this the function $\epsilon^{\text{xc-jellium}}(n)$ is required. What does $\epsilon^{\text{xc-jellium}}(n)$ look like? Already in 1938 Wigner determined ϵ^{xc} for jellium in the limit of small densities (Trans. Faraday Soc. **34**, 678 (1938)). In 1957 Gell-Mann and Brückner discussed the limit of high densities using many-body theories (Phys. Rev. **106**, 364 (1957)). In 1980 it became possible using computer calculations to address also the range in between (Ceperley, Alder, Phys. Rev. Lett. **45**, 566 (1980)). Today, the function $\epsilon^{\text{xc-jellium}}(n)$, or $\epsilon^{\text{xc-jellium}}(r_s)$ ($r_s = \sqrt[3]{\frac{3}{4\pi n}}$), is numerically well known. It is shown in Fig. 3.13. Table 3.1 gives the average electron density and the corresponding r_s parameter for some metals.

If we know $\epsilon^{\text{xc}}[n]$, the exchange-correlation potential of the Kohn-Sham equation can be calculated:

$$\begin{aligned}
 v^{\text{xc-LDA}}(\mathbf{r}) &= \frac{\delta E^{\text{xc-LDA}}[n]}{\delta n(\mathbf{r})} = \frac{\partial}{\partial n} \left(n \epsilon^{\text{xc-jellium}}(n) \right) \Bigg|_{n=n(\mathbf{r})} \\
 &= \epsilon^{\text{xc-jellium}}(n) + n \frac{\partial \epsilon^{\text{xc-jellium}}(n)}{\partial n} \Bigg|_{n=n(\mathbf{r})} .
 \end{aligned} \tag{3.178}$$

Figure 3.14 shows the correct v^{xc} potential for jellium in comparison to the previous Hartree-Fock-Slater result.

atom	number of valence electrons in the atom	number of atoms per primitive unit cell	lattice constant (Å)	average density (10^{22} cm^{-3})	r_s (bohr)
Li	1	1	3.49	4.70	3.25
Na	1	1	4.23	2.65	3.93
K	1	1	5.23	1.40	4.86
Cs	1	1	6.05	0.91	5.62
Cu	1	1	3.61	8.47	2.67
Ag	1	1	4.09	5.86	3.02
Al	3	1	4.05	18.1	2.07
Ga	3	1	4.51	15.4	2.19

Table 3.1: Average electron density of metals. For Cu and Ag the electrons of the $3d$ - and $4d$ -shells have not been counted as valence electrons. For several problems this approximation is too crude.

In order to interpret the exchange-correlation potential of DFT-LDA theory, we proceed like for Hartree and Hartree-Fock (cf. the discussion of Fig. 3.4). We write:

$$E^{\text{Hartree}}[n] + E^{\text{xc}}[n] = \frac{e^2}{8\pi\epsilon_0} \int n(\mathbf{r}) \int \frac{n(\mathbf{r}') - n^{\text{xc}}(\mathbf{r}, \mathbf{r}')}{|\mathbf{r} - \mathbf{r}'|} d^3\mathbf{r} d^3\mathbf{r}' . \quad (3.179)$$

The density $n - n^{\text{xc}}$ is shown in Fig. 3.15. The interpretation is to view the exchange-correlation energy as a correction of the Coulomb interaction of the Hartree term, i.e., a particle at position \mathbf{r} does not interact with particles being distributed like $n(\mathbf{r}')$, but it feels a particle distribution $n(\mathbf{r}') - n^{\text{xc}}(\mathbf{r}, \mathbf{r}')$.¹¹ For the corresponding terms in the effective potential we have:

$$\begin{aligned} v^{\text{Hartree}}(\mathbf{r}) + v^{\text{xc}}(\mathbf{r}) &= \frac{\delta}{\delta n(\mathbf{r})} (E^{\text{Hartree}}[n] + E^{\text{xc}}[n]) \\ &= \frac{e^2}{4\pi\epsilon_0} \int \frac{n(\mathbf{r}') - n^{\text{xc}}(\mathbf{r}, \mathbf{r}')}{|\mathbf{r} - \mathbf{r}'|} d^3\mathbf{r}' - \frac{e^2}{8\pi\epsilon_0} \iint \frac{n(\mathbf{r}') \left(\frac{\delta}{\delta n(\mathbf{r})} \frac{n^{\text{xc}}(\mathbf{r}, \mathbf{r}'')}{n(\mathbf{r}'')} \right) n(\mathbf{r}'')}{|\mathbf{r} - \mathbf{r}'|} d^3\mathbf{r}' d^3\mathbf{r}'' , \end{aligned} \quad (3.180)$$

where the first term again shows that a particle at position \mathbf{r} interacts with a particle distribution $n(\mathbf{r}') - n^{\text{xc}}(\mathbf{r}, \mathbf{r}')$. The second term includes in addition changes of the particle distribution n^{xc} when the density is varied.

¹¹Here we have expressed the exchange-correlation energy as $-\frac{1}{2} \frac{e^2}{4\pi\epsilon_0} \iint \frac{n(\mathbf{r})n^{\text{xc}}(\mathbf{r}, \mathbf{r}')}{|\mathbf{r} - \mathbf{r}'|} d^3\mathbf{r} d^3\mathbf{r}'$. In the literature, exchange-correlation is often discussed in terms of the so-called exchange-correlation hole $h^{\text{xc}}(\mathbf{r}, \mathbf{r}') \equiv -n^{\text{xc}}(\mathbf{r}, \mathbf{r}')$. The function $n(\mathbf{r})n(\mathbf{r}') - n^{\text{xc}}(\mathbf{r}, \mathbf{r}')$ is identical to the (coupling constant averaged) pair-correlation function, i.e. the probability of finding an electron at position \mathbf{r}' if there is already one at \mathbf{r} .

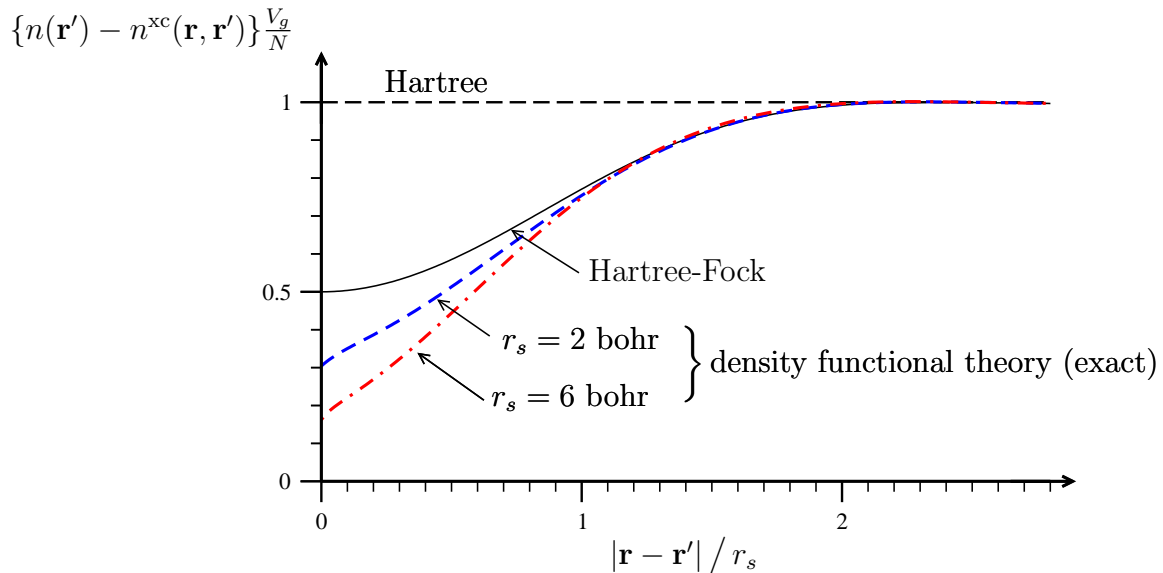


Figure 3.15: Distribution of the $N - 1$ other electrons with respect to a particle that is located at position $\mathbf{r} = 0$, i.e. the pair-correlation function (for jellium).

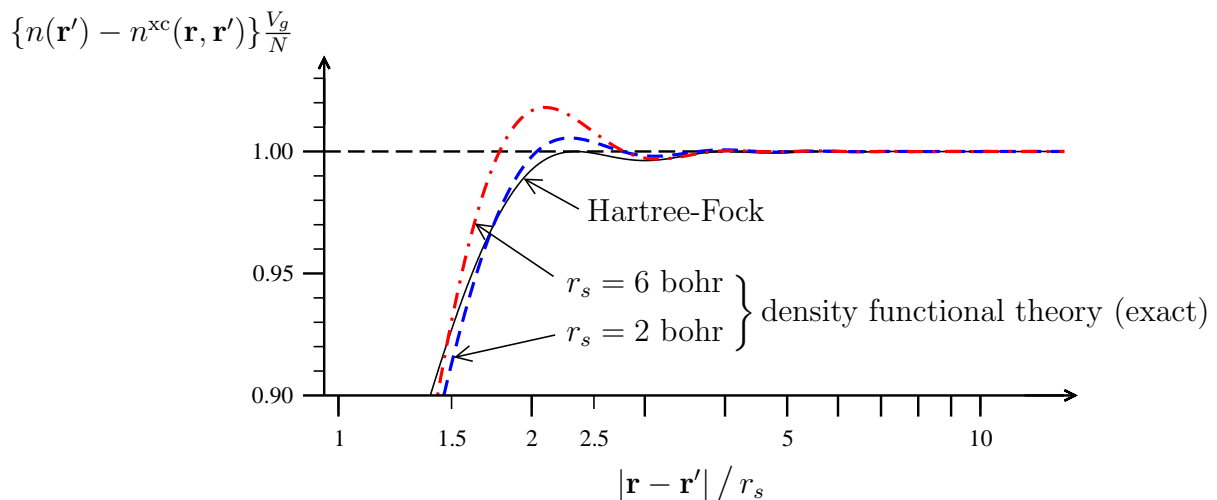


Figure 3.16: Like Fig. 3.15, but for larger electron-electron separations.

In the neighborhood of a particle the density is reduced. The origins of this reduction are the Pauli principle and the Coulomb repulsion. Strictly, this reduction has to be explained by a dynamical treatment. This is the origin of the term correlation (of the motion). But in a time-independent theory dynamic correlation can also be described as mentioned above. We summarize: Hartree theory does not include correlation, i.e., a Hartree particle sees a distribution of the other particles, which is independent of its position. Hartree-Fock theory includes the correlation of electrons of like spin originating from the Pauli principle. This “Pauli correlation” is called exchange interaction. In principle density-functional theory is exact (and for jellium it can be carried out numerically exact). It contains exchange as well as the correlation caused by the Coulomb repulsion. But since the functional $E^{\text{xc}}[n]$ in its general form is unknown, DFT combined with the LDA is accurate only for interacting electronic systems of slowly varying densities. For inhomogeneous systems the LDA is an approximation, but a surprisingly good one! For no

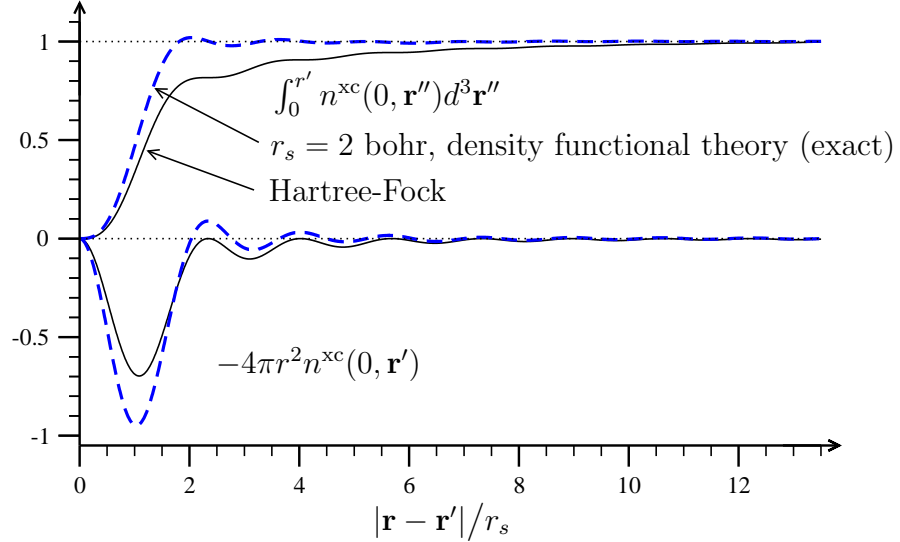


Figure 3.17: Exchange-correlation hole $-n^{\text{xc}}(0, \mathbf{r}')$ of an electron at position $\mathbf{r} = 0$ (for jellium). The lower part of the plot shows how many electrons are removed from, or shifted into, a spherical shell $r' \pm \delta r'$ due to exchange and correlation, respectively. The top part shows how $n^{\text{xc}}(0, \mathbf{r}')$ integrates up to satisfy the sum rule Eq. (3.181).

interacting many-body problem Hartree is exact and the Hartree-Fock approximation is exactly right only for those systems, for which the ground state is one Slater determinant.

Surprisingly, it turned out that DFT-LDA yields rather reliable results also for systems of strongly varying densities. This can be made plausible: The LDA can be understood as an approximation for the *shape* of the exchange-correlation hole, and because in E^{xc} and in v^{xc} only the integral over n^{xc} enters, the errors in the shape of the exchange-correlation hole cancel to some extent¹².

The exchange-correlation hole $-n^{\text{xc}}(\mathbf{r}, \mathbf{r}')$, i.e. the reduction of electron density $n(\mathbf{r}') - n^{\text{xc}}(\mathbf{r}, \mathbf{r}')$ around the position of an electron at \mathbf{r} , is a plausible consequence of the Pauli exclusion principle and Coulomb repulsions. Figure 3.15 illustrates their effect for jellium. In Hartree theory the electrons are essentially treated as if they moved independently from one another (like in an ideal gas of non-interacting fermions), i.e. their exchange-correlation hole is zero. The effect of the Pauli exclusion principle is to reduce the probability of finding electrons with the spin σ around an electron at position \mathbf{r} with the same spin σ ; therefore the probability of finding two electrons at the same position is 0.5 (for jellium with $n_{\uparrow} = n_{\downarrow}$). Coulomb repulsion pushes the electrons further apart and thus reduces the pair-correlation function (deepen the exchange-correlation hole) at short electron-electron separations and increases it at larger separations (see Fig.). At $\mathbf{r} = \mathbf{r}'$ the pair-correlation function displays a “cusp”, i.e. a finite slope, which is a consequence of the the $1/r$ singularity of the Coulomb interaction. Here, in Fig. 3.15, we also see the quantum mechanical nature of the electron. For a classical particle the density of the exchange-correlation hole must go to zero at $\mathbf{r} = \mathbf{r}'$, because when a particle is at position

¹²For a detailed discussion cf. Barth, Williams, in “The inhomogeneous electron gas”, also R.O. Jones and O. Gunnarsson, Rev. Mod. Phys. **61**, 689 (1989).

\mathbf{r} not other particle can be at the same position. In quantum mechanics the uncertainty principle weakens the meaning of “particle at position \mathbf{r} ” and therefore $n(\mathbf{r}') - n^{\text{xc}}(\mathbf{r}, \mathbf{r}')$ is non-zero at $\mathbf{r} = \mathbf{r}'$.

Without proof, we also state another strict property of $n^{\text{xc}}(\mathbf{r}, \mathbf{r}')$: As each electron of the N -electron problem interacts with the $(N - 1)$ other electrons, and because

$$\int n(\mathbf{r}') d^3\mathbf{r}' = N \quad ,$$

it follows that

$$\int n^{\text{xc}}(\mathbf{r}, \mathbf{r}') d^3\mathbf{r}' = 1 \quad . \quad (3.181)$$

This sum rule is illustrated in Fig. 3.17 for jellium. Any reasonable approximation to $E^{\text{xc}}[n]$ must fulfil this condition, for instance it is fulfilled by the LDA.

3.7.1 Meaning of the Kohn-Sham Single-Particle Energies ϵ_{o_k} – The DFT Analog of Koopmans’ Theorem –

Density-functional theory was derived with the goal that $n(\mathbf{r})$ and $E_0^e = \text{Min}_{n(\mathbf{r})} E_v[n]$ are physical quantities. There was no meaning assigned to $\varphi_{o_k}(\mathbf{r})$ or ϵ_{o_k} . These appeared in the theory as technical quantities, somewhat similar to the single-particle energies which appeared in Hartree-Fock theory. Only via Koopmans’ theorem we found out that the Hartree-Fock single-particle energies are approximate ionization energies.

Often one reads that in DFT Koopmans’ theorem is not valid and that the single-particle energies of the Kohn-Sham equation have no physical meaning. In narrow terms this statement is right. However, we like to emphasize that there is a theorem in DFT that is practically equivalent to Koopmans’ theorem. As mentioned above, i.e. considering the derivation of the Kohn-Sham equation, the Kohn-Sham single-particle energies do not seem to have a *direct* physical meaning. However, we found that the ϵ_{o_k} are nevertheless required, i.e. in the expression of the kinetic energy when the total energy has to be calculated (cf. Eq. (3.172)). Only the highest occupied Kohn-Sham level has a direct physical meaning: The highest occupied level (of the exact DFT) is the ionization energy (Almbladh, v. Barth, Phys. Rev. B **31**, 3231 (1985)).

In order to clarify the physical meaning of the Kohn-Sham single-particle energies we introduce occupation numbers:

$$n(\mathbf{r}) = \sum_{k=1}^N |\varphi_{o_k}(\mathbf{r})|^2 \quad (3.182)$$

$$= \sum_{k=1}^{\infty} f_{o_k} |\varphi_{o_k}(\mathbf{r})|^2 \quad . \quad (3.183)$$

At zero temperature we have

$$f_{o_k} = \begin{cases} 1 & \text{for } k = 1 \dots N \\ 0 & \text{otherwise} \quad , \end{cases} \quad (3.184)$$

and

$$T_s[n] = \sum_{k=1}^{\infty} f_{o_k} \epsilon_{o_k} - \int v^{\text{eff}}(\mathbf{r}) n(\mathbf{r}) d^3\mathbf{r} \quad . \quad (3.185)$$

Strictly, $E_v[n]$ is defined only for $f_{o_k} = 0$ or 1. Now we will assume that the range of the f_{o_k} can be extended to non-integer occupations. For example, for a finite temperature description the occupation numbers would be given by the Fermi function. This extension of the f_{o_k} is obviously not a problem for all parts of the energy functional, except for E^{xc} , as we do not know it exactly. However, for all known approximations of E^{xc} this extension of the range of possible f_{o_k} is unproblematic. We then get

$$\frac{\partial E_v[n]}{\partial f_{o_k}} = \int \frac{\delta E_v[n]}{\delta n(\mathbf{r})} \frac{\partial n(\mathbf{r})}{\partial f_{o_k}} d^3\mathbf{r} \quad , \quad (3.186)$$

where

$$\frac{\partial n(\mathbf{r})}{\partial f_{o_k}} = |\varphi_{o_k}(\mathbf{r})|^2 \quad , \quad (3.187)$$

because the φ_{o_k} (for a given v^{eff}) do not depend explicitly on the occupation numbers. We do not want to assume here that the variational principle $\frac{\delta E_v[n]}{\delta n(\mathbf{r})} = \mu$ is fulfilled, and therefore calculate $\frac{\delta E_v[n]}{\delta n(\mathbf{r})}$:

$$\frac{\delta E_v[n]}{\delta n(\mathbf{r})} = \frac{\delta T_s[n]}{\delta n(\mathbf{r})} + v^{\text{Hartree}}(\mathbf{r}) + v^{\text{xc}}(\mathbf{r}) + v(\mathbf{r}) \quad (3.188)$$

$$= \frac{\delta T_s[n]}{\delta n(\mathbf{r})} + v^{\text{eff}}(\mathbf{r}) \quad . \quad (3.189)$$

It follows that

$$\begin{aligned} \frac{\partial E_v[n]}{\partial f_{o_k}} &= \int \frac{\delta E_v[n]}{\delta n(\mathbf{r})} \frac{\partial n(\mathbf{r})}{\partial f_{o_k}} d^3\mathbf{r} \\ &= \int \frac{\delta T_s[n]}{\delta n(\mathbf{r})} |\varphi_{o_k}(\mathbf{r})|^2 d^3\mathbf{r} + \int v^{\text{eff}}(\mathbf{r}) |\varphi_{o_k}(\mathbf{r})|^2 d^3\mathbf{r} \quad . \end{aligned} \quad (3.190)$$

Because

$$\int \frac{\delta T_s[n]}{\delta n(\mathbf{r})} |\varphi_{o_k}(\mathbf{r})|^2 d^3\mathbf{r} = \frac{\partial T_s[n]}{\partial f_{o_k}} \quad , \quad (3.191)$$

and with

$$\frac{\partial T_s}{\partial f_{o_k}} = \epsilon_{o_k} - \int v^{\text{eff}}(\mathbf{r}) |\varphi_{o_k}(\mathbf{r})|^2 d^3\mathbf{r} \quad , \quad (3.192)$$

we obtain the result

$$\frac{\partial E_v[n]}{\partial f_{o_k}} = \epsilon_{o_k} \quad . \quad (3.193)$$

This equation also holds for the highest occupied state, $k = N$, which, at least in metals, is called the Fermi energy:

$$\frac{\partial E_v[n]}{\partial f_{o_N}} = \epsilon_{o_N} = \epsilon_{\text{F}} \quad , \quad (3.194)$$

and because $\frac{\delta E_v[n]}{\delta n(\mathbf{r})} = \mu$ it follows that $\mu = \epsilon_{\text{F}}$. Figure 3.18 shows an example for ϵ_{o_k} as function of the occupation number. However, here the local spin-density approximation

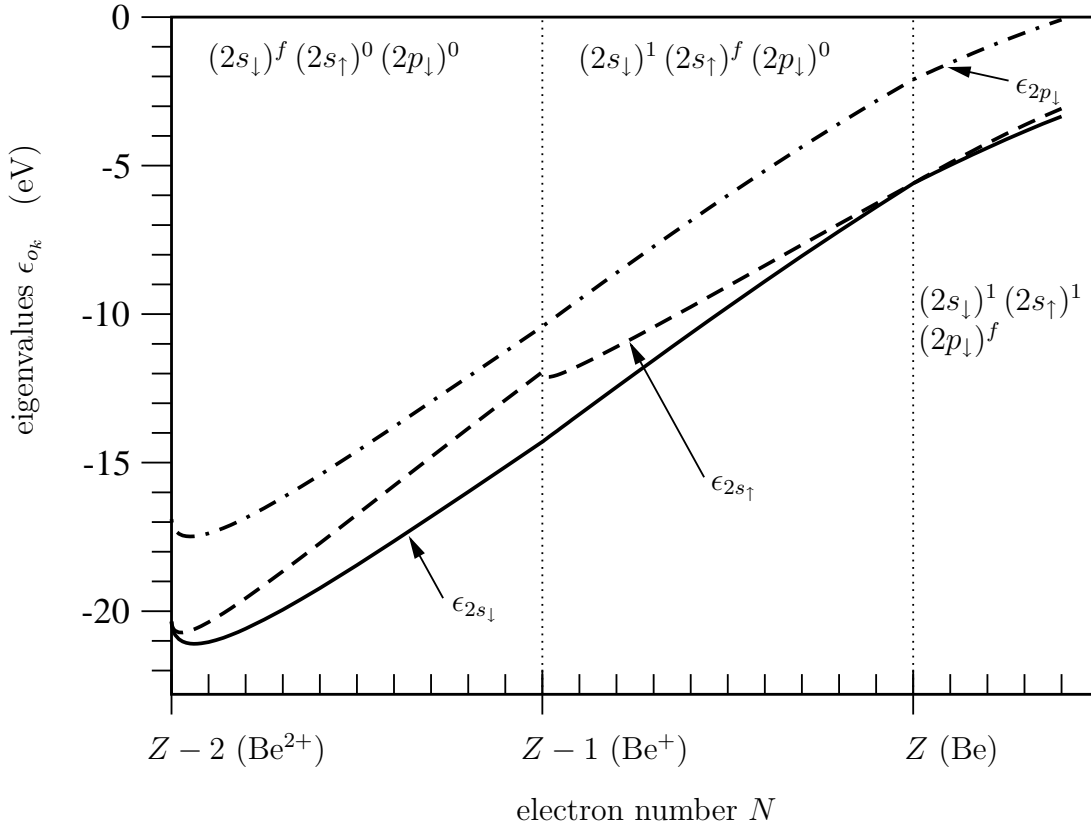


Figure 3.18: The function $\epsilon_{o_k}(N)$ for the $2s$ and $2p$ states of the Be atom ($Z = 4$) as a function of the electron number (from $N = 2$ to $N = 4.4$). The neutral Be atom has the configuration $1s^2 2s^2$. At first the occupation of the $2s_{\downarrow}$ level is changed from zero to one (from left to right). Then the occupation of the $2s_{\uparrow}$ level is changed and then that of the $2p_{\downarrow}$ level. The local spin-density approximation is employed.

for E^{xc} has been used. This represents an improvement over the ansatz $n_{\uparrow} = n_{\downarrow}$, and it will be discussed in Section 3.7.3 below. Due to the kinetic energy, the functions $\epsilon_{o_k}(f)$ are not differentiable at some points. These points are found at integer values of N where a new spin channel or a new shell is added.

Now we look at an ionization event, i.e., the transition from the ground state Φ^N to the state Φ_k^{N-1} plus a free electron of zero energy. The index k of the wave function marks that the level k is no more occupied. In the exact meaning of the word, ionization refers to the highest level, i.e. $o_k = o_N$. However, in general (e.g. by photoemission) one can also remove more strongly bound electrons.

The ionization energy is

$$I_k = E_k^{N-1} - E^N \quad (3.195)$$

$$= - \int_0^1 \frac{\partial E_v[n]}{\partial f_{o_k}} df_{o_k} \quad (3.196)$$

$$= - \int_0^1 \epsilon_{o_k}(f_{o_k}) df_{o_k} \quad (3.197)$$

Here we assume that the geometry of the lattice is not changed by the ionization. For the ionization from extended levels of a solid this assumption is justified. And in general it represents the Franck-Condon principle which states that the displacement of the nuclei follows the electronic excitation (or the ionization) with some delay. Using the mean value theorem of calculus we obtain:

$$I_k = -\epsilon_{o_k}(0.5) \quad . \quad (3.198)$$

This expression is called Slater-Janak-“transition-state”. When a calculation is carried out and the level k is occupied by only half an electron, the energy ϵ_{o_k} approximately equals the ionization energy. If the functions $\varphi_k(\mathbf{r})$ are extended, $n(\mathbf{r})$ and therefore also $v^{\text{eff}}(\mathbf{r})$ and thus also the values of ϵ_{o_k} practically will not change, if the occupation of a level, f_{o_k} , is changed. Then we have $\epsilon_{o_k}(f_{o_k} = 1) \approx \epsilon_{o_k}(f_{o_k} = 0.5)$ and the single-particle levels correspond to the ionization energies: $I_k = -\epsilon_{o_k}$. Thus, we get the same result as obtained by Koopmans’ theorem of Hartree-Fock theory, and the proof is even more plausible here in DFT than it was before in Hartree-Fock theory.

We mention here only in passing another shortcoming of the LDA, besides the mentioned poor correction of the electron self-interaction. It can be shown that the true $E^{\text{xc}}[n]$ functional has kinks at integer values of N when plotted as a continuous function of the number of electrons. This is somewhat analogous to $T_s[n]$ which also has kinks due to the level structure of the Kohn-Sham eigenvalues (e.g. the shell structure of atomic orbitals). These kinks in $E^{\text{xc}}[n]$ give rise to discontinuities in $\frac{\delta E^{\text{xc}}}{\delta n} = v^{\text{xc}}$ when studied as a function of particle number. We may get back to this point and the current theories for excited states at the end of the semester. The LDA does not have such kinks in E^{xc} or discontinuities in v^{xc} .

Experience shows that although $E_0^e = \min_{n(\mathbf{r})} E_v[n]$ is affected by the approximation to the xc-functional, I (as an energy difference) is often rather accurate; the errors of the LDA cancel to some extent in the calculation of the difference. This is reasonable but not proven. It shall be illustrated now for the (extreme) example of the hydrogen atom. There is hardly any similarity between the hydrogen atom and the many-body problem of an extended solid. But it points to the problems of the LDA and the error compensation. In density-functional theory we have:

$$\left\{ -\frac{\hbar^2}{2m} \nabla^2 - \frac{e^2}{4\pi\epsilon_0} \frac{1}{r} + \frac{e^2}{4\pi\epsilon_0} \int \frac{n(\mathbf{r}')}{|\mathbf{r} - \mathbf{r}'|} d^3\mathbf{r}' + v^{\text{xc}}(\mathbf{r}) \right\} \varphi(\mathbf{r}) = \epsilon \varphi(\mathbf{r}) \quad (3.199)$$

In an exact calculation for the ground state of a hydrogen atom we have:

$$\frac{e^2}{4\pi\epsilon_0} \int \frac{n(\mathbf{r}')}{|\mathbf{r} - \mathbf{r}'|} d^3\mathbf{r}' + v^{\text{xc}}(\mathbf{r}) = 0 \quad , \quad (3.200)$$

because in a one-electron system there is no electron-electron interaction. The corresponding (exact) lowest energy value then is $\epsilon_{1s} = -13.6$ eV. In the LDA, however, the two terms in Eq. 3.200 do not cancel. The eigenvalue obtained from the LDA therefore is significantly above the exact eigenvalue: $\epsilon_{1s}^{\text{LDA}} = -6.4$ eV. Thus, for the hydrogen atom the jellium approximation for v^{xc} is very bad. Quite obviously, the orbital of a hydrogen atom is not extended but very localized. Nevertheless, even here we see that differences of total energies are rather good: $I \approx -\epsilon_{1s}^{\text{LDA}} \left(\frac{1}{2}\right) = +12.4$ eV. Generally we have: Due to

the poorly corrected self-interaction in the LDA the eigenvalues ϵ_k^{LDA} are too high, i.e., they correspond to too small ionization energies. This is the more true, the more a state is localized¹³. Consequently, for localized states the ϵ_{o_k} are no good approximation for ionization energies, but in general $\epsilon_{o_k}(0.5)$ is a rather good approximation.

3.7.2 Hellmann-Feynman Theorem

Already in 1933 the theory was very close to an invention of DFT. Back then, i.e. 31 years before the Hohenberg-Kohn paper, it was shown that forces acting on nuclei are only due to electrostatic interactions between the nuclear charges and the electron *density*. When \mathbf{F}_K is the force acting on atom (or nucleus) K , i.e.

$$\mathbf{F}_K = -\frac{\partial E_v[n]}{\partial \mathbf{R}_K} \quad (3.201)$$

in the language of DFT, Hellmann (1933, 1937) and Feynman (1939) showed within an exact derivation, starting from the many-body Schrödinger equation that

$$-\frac{\partial E_v[n]}{\partial \mathbf{R}_K} = \mathbf{F}_K = -\int \frac{\partial v(\mathbf{r}, \{\mathbf{R}_I\})}{\partial \mathbf{R}_K} n(\mathbf{r}) d^3\mathbf{r} \quad . \quad (3.202)$$

Starting from DFT, the proof is simple and will be done in the exercises (see also Scheffler, Vigneron, Bachelet, Phys. Rev. B **31**, 6541 (1985)).

¹³Taking into account the spin in the LSDA improves the value for the ionization energies of the hydrogen atom at the “transition-state” for half-occupation slightly: $I \approx -\epsilon_1^{\text{LSDA}}(\frac{1}{2}) = 13.35$ eV, $\epsilon_1(1) = -7.32$ eV and $\Delta E^e = 13.1$ eV, for the H-atom.

3.7.3 Spin Polarization

References:

Kohn and Sham (1965), Barth, Hedin (1972), Rajagopal, Callaway (1973), Levy.

Strictly, the ground state density alone defines the full problem: The ground state density determines the many-body Hamilton operator, which determines everything. However, the dependence of the total energy on the density is very complicated, and possibly cannot be represented in a closed mathematical form. Therefore, it is reasonable to soften the puristic approach and to start, e.g. for magnetic systems, with densities for spin up and spin down electrons as independent variables. This establishes the spin-density-functional theory (SDFT) and is an important and simple improvement of DFT. In this way, also magnetic effects can be described. For non-magnetic systems SDFT and DFT are identical. In the spin-density-functional theory the *density matrix* is used as the basic variable:

$$n_{s,s'}(\mathbf{r}) = \langle \Phi | \Psi_s^+(\mathbf{r}) \Psi_{s'}(\mathbf{r}) | \Phi \rangle \quad (3.203)$$

here s and s' represent the spin orientations of individual particles: \uparrow or \downarrow . $\Psi_s^+(\mathbf{r})$ and $\Psi_{s'}(\mathbf{r})$ are field operators, i.e., creation of a particle at position \mathbf{r} with spin s and annihilation of a particle at position \mathbf{r} with spin s' . Φ is the ground state wave function of the N electron system. The particle density (the basic variable in DFT) is

$$n(\mathbf{r}) = n_{\uparrow}(\mathbf{r}) + n_{\downarrow}(\mathbf{r}) \quad , \quad (3.204)$$

and the magnetization density is

$$m(\mathbf{r}) = \mu_B \{n_{\uparrow}(\mathbf{r}) - n_{\downarrow}(\mathbf{r})\} \quad . \quad (3.205)$$

Here, instead of $n_{\uparrow\downarrow}$ I have used only n_{\uparrow} and instead of $n_{\downarrow\downarrow}$ only n_{\downarrow} . Thus, we only need the diagonal elements. The Bohr magneton μ_B is defined as

$$\mu_B = \frac{e\hbar}{2mc} \quad . \quad (3.206)$$

Now we want to use

$$n_{\uparrow}(\mathbf{r}) = \langle \Phi | \sum_{k=1}^N \delta_{s_k, \uparrow} \delta(\mathbf{r} - \mathbf{r}_k) | \Phi \rangle \quad (3.207)$$

and

$$n_{\downarrow}(\mathbf{r}) = \langle \Phi | \sum_{k=1}^N \delta_{s_k, \downarrow} \delta(\mathbf{r} - \mathbf{r}_k) | \Phi \rangle \quad (3.208)$$

as the basic variables. Exactly analogous to standard DFT we obtain a single-particle equation:

$$\left\{ -\frac{\hbar^2}{2m} \nabla^2 + v_{s_k}^{\text{eff}}(\mathbf{r}) \right\} \varphi_{o_k s_k}(\mathbf{r}) = \epsilon_{o_k s_k} \varphi_{o_k s_k}(\mathbf{r}) \quad . \quad (3.209)$$

The wave functions $\varphi_{o_k \uparrow}$ and $\varphi_{o_k \downarrow}$ are now determined from two different equations, but these equations are coupled, because the effective potential depends on n_{\uparrow} and n_{\downarrow} :

$$v_{s_k}^{\text{eff}}(\mathbf{r}) = v(\mathbf{r}) + \frac{e^2}{4\pi\epsilon_0} \int \frac{n(\mathbf{r}')}{|\mathbf{r} - \mathbf{r}'|} d^3\mathbf{r}' + v_{s_k}^{\text{xc}}(\mathbf{r}) \quad , \quad (3.210)$$

with

$$v_{s_k}^{\text{xc}}(\mathbf{r}) = \frac{\delta E^{\text{xc}}[n_{\uparrow}, n_{\downarrow}]}{\delta n_{s_k}(\mathbf{r})} \quad , \quad (3.211)$$

and

$$n_{s_k}(\mathbf{r}) = \sum_{i=1}^N \delta_{s_k, s_i} |\varphi_{o_i s_i}(\mathbf{r})|^2 \quad . \quad (3.212)$$

The exchange-correlation potential now depends on the spin orientation. For practical calculations the local spin-density approximation is introduced:

$$E^{\text{xc-LSDA}} = \int n(\mathbf{r}) \epsilon^{\text{xc-jellium}}(n(\mathbf{r}), m(\mathbf{r})) d^3\mathbf{r} \quad . \quad (3.213)$$

Here, $\epsilon^{\text{xc-jellium}}(n, m)$ is the exchange-correlation energy per particle of a homogeneous electron gas of constant particle density n and constant magnetization density m . The exchange-correlation potential of the LSDA depends on the local electron density in a similar way as in LDA. However, the exchange and the correlation contribution of $v_{s_k}^{\text{xc-LSDA}}(\mathbf{r})$ or $\epsilon^{\text{xc-LSDA}}$ additionally depend on the spin-orientation.

Apart from spin-density theory also other generalizations have been investigated: Velocity-dependent forces, spin-orbit-coupling, relativistic formulation (\rightarrow Dirac equation). These will not be discussed here (cf. Rajagopal, Calloway, Phys. Rev. B **87**, 1912 (1973); MacDonald, Vosko: J. Phys. C **11**, L943 (1978); Rajagopal, J. Phys. C **11**, L943 (1978)).

3.7.4 Two Examples

Finally, we will demonstrate for two *examples*, which type of information can be obtained using DFT-LDA and SDFT-LSDA calculations. Later, at the detailed discussion and explanation of the nature of cohesion of solids we will use such calculations again.

Before 1980 systematic high-quality DFT calculation were not possible, partly due to the lack of efficient and reliable algorithms, partly due to the lack of computational power. Therefore, it was often not understood how the electron density is distributed in the crystal and how the solid is stabilized. It was, for example, not clear, why silicon does exist in the diamond structure or why silver has a fcc structure. Using parameter-free, self-consistent DFT calculations an initial understanding was obtained. However, we are still at the beginning, but with good perspectives: Efficient algorithms and powerful hardware are available, and compared to 1980 the efficiency of state-of-the-art algorithms is very much higher. The main advantage of such parameter-free, self-consistent DFT calculations is that the results can be analyzed in detail, i.e., which parts are essential for the stabilization of the solid and which are not. Such theoretical investigations of static and low-frequency dynamical properties usually are performed via the self-consistent calculation of the Kohn-Sham equation. The self-consistent field procedure is almost identical to the Hartree approximation discussed before (cf. Fig. 3.2), but now the effective potential additionally contains exchange and correlation. The only external parameters given (by the scientist) are the nuclear charge (i.e., the decision of the material, e.g. Si or Ag). In general, the lattice geometry will be varied in order to find the most stable geometry, i.e., the lowest

energy structure, and to analyze $n(\mathbf{r})$ for this structure. For these calculations there are still several serious practical problems that are not visible in Fig. 3.2. These problems are:

1. The solution of the effective Schrödinger equation. For this purpose suitable methods have to be developed (cf. Chapter 5). Such an equation cannot be solved analytically (except for the hydrogen atom and the linear harmonic oscillator).
2. The calculation of $n(\mathbf{r})$ as an integral or the summation of the $|\varphi_{o_i}(\mathbf{r})|^2$, respectively.
3. The calculation of the Poisson Eq. (3.104) for arbitrary charge densities $-en(\mathbf{r})$.
4. Approximations for the exchange-correlation functional $E^{\text{xc}}[n]$.

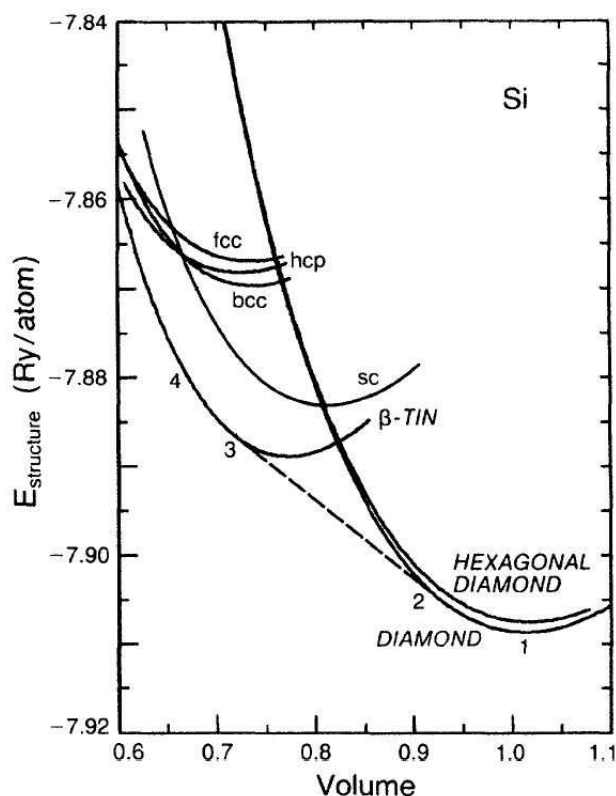


Figure 3.19: Density-functional theory calculations (using the local-density approximation for the exchange-correlation energy) of the total energy for various crystal structures of silicon as function of the volume per atom. The volume-axis is normalized such that the value 1.0 corresponds to the experimental result known for the diamond structure of Si. (M.T. Yin and M.L. Cohen, "Theory of static structural properties, crystal stability, and phase transformations: Application to Si and Ge", Phys. Rev. B **26**, 5668-5687 (1982)).

Figure 3.19 shows a "historic figure", namely what I consider to be the first convincing example demonstrating what type of problems can be tackled by density-functional theory calculations¹⁴. These are calculations performed in the group of Marvin Cohen

¹⁴Another early, impressive example of the power of density-functional theory calculation is the book by V.L. Moruzzi, J.F. Janak, and A. R. Williams, "Calculated Electronic Properties of Metals", Pergamon Press (1978).

in Berkeley. The figure shows the total energy for silicon as function of the volume per atom, where the volume was normalized such that 1.0 is that of the experimentally known result for Si in the diamond structure. The results show clearly that the lowest energy of all considered structures is indeed found for the diamond structure, and the minimum of the theoretical curve is very close to the experimental result. If the volume is reduced the figure also reveals that there is a phase transition that eventually brings the system into the beta-tin structure. The slope of the common tangent of two curves for the beta-tin and the diamond structures gives the pressure at which the phase transition sets in. This common tangent is called the Gibbs construction. Such calculations can predict and explain why solids behave as they do, and new materials of hitherto unknown structure or composition can be investigated as well.

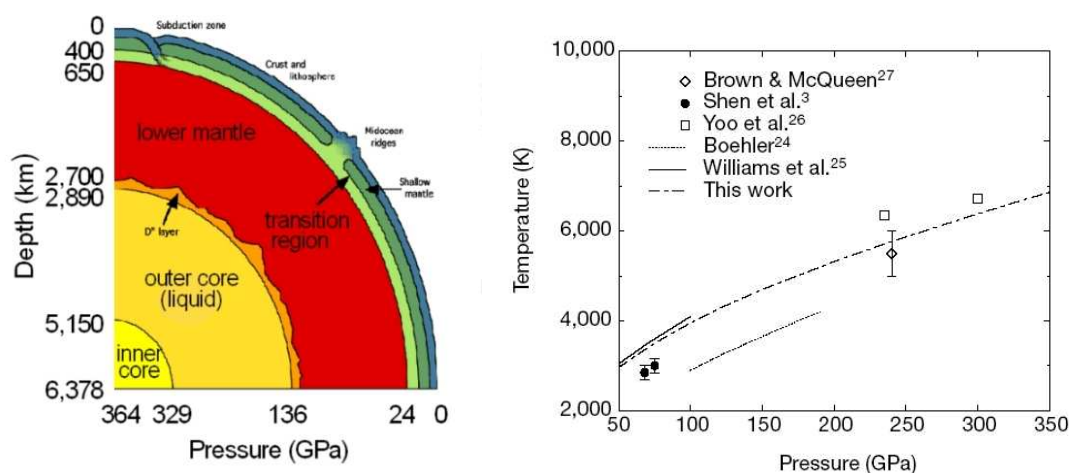


Figure 3.20: A cut through the earth showing the various shells (left) and the calculated melting curve for iron. (D. Alfè, G.D. Price, and M.J. Gillan, “Melting curve of Iron at Earth’s core pressures from ab-initio calculations”, *Nature* **401**, 462-464 (1999).)

In Fig. 3.20 I show a more recent example and this demonstrates how density-functional theory calculations can tell us things about geology that we cannot learn otherwise. Save knowledge about the earth only exists about the crust and the upper mantle. However, it is interesting and indeed important to know more about the central region of our planet, as this, for example contains information about the origin, the development, and the future of the earth. One aspect here also is the question what determines the earth magnetic field and its fluctuations and changes. The structure of the earth (left side in Figure 3.18) is known from measurements of the propagation, time delays, phase differences of earth quake waves, as these are reflected when the composition or the aggregate state in the earth change. The inner core of the earth is most likely solid and then we have the outer core which is liquid. We know the depth and we also quite accurately can estimate the pressure that is present at the phase boundary between the solid and the liquid core. The material down there is mostly iron probably with some fraction of O, S, Se and C. Unclear, however, is the temperature at this place.

In fact, we don’t know at what temperature does iron melt when it is put under such a high pressure of 330 GPa, and we have no idea how such melt may behave. What is

the local structure and what is the viscosity of the melt at such extreme conditions? The problem is that such pressure can hardly be reached in the laboratory. With a diamond anvil cell one gets somewhat close, i.e., to 200 GPa, but not to 330 GPa.

Density-functional theory calculations by Alfè et al. (see also <http://chianti.geol.ucl.ac.uk/~dario/> and <http://chianti.geol.ucl.ac.uk/~dario/resint.htm>) have shown that the melting temperature of iron at 330 GPa is 6.670 K (cf. Fig. 3.18, right). Thus, this must be the temperature at the interface between the inner and the outer core. In simple words one could say, that DFT was used as a thermometer to determine the temperature at an inaccessible place.

Furthermore, the authors studied the viscosity. The previously existing experimental estimates differed by many orders of magnitude. The DFT work showed that liquid iron in the outer core should have a local coordination similar to that of the hcp structure, and the viscosity is only by a factor of 10 higher than that of liquid iron at standard pressure. This is actually on the lowest side of the previous experimental estimates. Of course there are also some uncertainties in the theoretical result. These arise, because a somewhat small supercell was used, the exchange-correlation functional was, of course, treated approximately, and the authors studies pure iron, i.e., without the O, S, etc. fractions that must be there as well. All together the uncertainty of the calculated viscosity may be a factor of 3. This is still a much lower uncertainty than that of experimental studies.

It is now clear that in the outer core local circulations and turbulent convection will occur. At most of the previous, experimentally estimated values for the viscosity this would not be possible.

3.8 Summary (Electron-Electron Interaction)

Chapter 3 was “only” concerned about the properties of the electronic ground state, e.g. the basic equations that one has to solve to learn about the total energy (internal energy), density of the electrons, screening, lattice structure, lattice constant, elastic properties, lattice vibrations, and approximate electronic excitations. In the following summary of the most important equations we assume for clarity that spin polarization is absent, i.e.,

$$n_{\uparrow}(\mathbf{r}) = n_{\downarrow}(\mathbf{r}) = \frac{n(\mathbf{r})}{2} \quad . \quad (3.214)$$

The Hamilton operator of the electrons is

$$H^e = T^e + V^{e-Ion} + V^{e-e} \quad (3.215)$$

$$= \sum_{i=1}^N -\frac{\hbar^2}{2m} \nabla_{\mathbf{r}_i}^2 + \sum_{i=1}^N v(\mathbf{r}_i) + \frac{1}{2} \frac{e^2}{4\pi\epsilon_0} \sum_{\substack{i,j=1 \\ i \neq j}}^{N,N} \frac{1}{|\mathbf{r}_i - \mathbf{r}_j|} \quad . \quad (3.216)$$

The total energy is

$$E_0 = E_0^e + E^{\text{Ion-Ion}} \quad \text{with} \quad E_0^e = \text{Min}_{\Phi} \langle \Phi | H^e | \Phi \rangle \quad . \quad (3.217)$$

The density-functional theory of Hohenberg and Kohn means that the many-body Schrödinger equation with the Hamilton operator (Eq. (3.215)) can be transformed into a self-consistent field theory. Hohenberg and Kohn have shown that

$$\langle \Phi | H^e | \Phi \rangle = \int v(\mathbf{r})n(\mathbf{r})d^3\mathbf{r} + F[n] = E_v[n] \quad (3.218)$$

with the particle density of the electrons

$$n(\mathbf{r}) = \sum_{i=1}^N \langle \Phi | \delta(\mathbf{r} - \mathbf{r}_i) | \Phi \rangle \quad (3.219)$$

and

$$F[n] = \langle \Phi | T^e + V^{e-e} | \Phi \rangle \quad (3.220)$$

For a given external potential $v(\mathbf{r})$ and taking into account the conservation of the number of particles ($\int n(\mathbf{r})d^3\mathbf{r} = N$), $E_v[n]$ assumes a minimum at the correct particle density $n_0(\mathbf{r})$, and at the value E_0^e for the energy of the electronic ground state. We have:

$$\left. \frac{\delta T_s[n]}{\delta n(\mathbf{r})} \right|_{n_0} + v^{\text{eff}}(\mathbf{r}) = \mu \quad (3.221)$$

Here $T_s[n]$ is the kinetic energy functional of independent (non-interacting) particles. It must not be confused with $T^e = \langle \Phi | T^e | \Phi \rangle$, which is defined for interacting systems. We have:

$$\frac{\delta T_s[n]}{\delta n(\mathbf{r})} = \frac{\hbar^2}{2m} (3\pi^2 n(\mathbf{r}))^{2/3} + O(\nabla n(\mathbf{r})) \quad (3.222)$$

It should be noted, however, that this series expansion converges slowly and is therefore probably not useful; using only the Thomas-Fermi approximation to the kinetic energy is very inaccurate.

For $v^{\text{eff}}(\mathbf{r})$ we have:

$$v^{\text{eff}}(\mathbf{r}) = v(\mathbf{r}) + \frac{e^2}{4\pi\epsilon_0} \int \frac{n(\mathbf{r}')}{|\mathbf{r} - \mathbf{r}'|} d^3\mathbf{r}' + \frac{\delta E^{\text{xc}}[n]}{\delta n(\mathbf{r})} \quad (3.223)$$

where $E^{\text{xc}}[n]$ is the exchange-correlation functional. We have:

$$E^{\text{xc}}[n] = \langle \Phi | H^e | \Phi \rangle - \int v(\mathbf{r})n(\mathbf{r})d^3\mathbf{r} - T_s[n] - \frac{1}{2} \frac{1}{4\pi\epsilon_0} \iint \frac{n(\mathbf{r})n(\mathbf{r}')}{|\mathbf{r} - \mathbf{r}'|} d^3\mathbf{r}d^3\mathbf{r}' \quad (3.224)$$

The quantity μ introduced as a Lagrange parameter in Eq. (3.221) is the chemical potential of the electrons.

The particle density of Eq. (3.219) can also be determined using the Kohn-Sham equation:

$$\left\{ -\frac{\hbar^2}{2m} \nabla^2 + v^{\text{eff}}(\mathbf{r}) \right\} \varphi_{o_k}(\mathbf{r}) = \epsilon_{o_k} \varphi_{o_k}(\mathbf{r}) \quad (3.225)$$

with

$$n(\mathbf{r}) = \sum_{k=1}^N |\varphi_{o_k}(\mathbf{r})|^2 \quad (3.226)$$

Equation (3.221) means: In principle it is possible to determine $n(\mathbf{r})$ directly from $v(\mathbf{r})$, i.e., the many-body wave function $\Phi(\mathbf{r}_1\sigma_1, \dots, \mathbf{r}_n\sigma_N)$ is not required explicitly.

The problem with the calculation is that the functional $T_s[n]$ is not explicitly known, or that the known approximations are inaccurate or very complicated. Although the functional $T_s[n]$ cannot be given in a closed mathematical form, its value is calculated exactly when the Kohn-Sham equation is used. Experience shows that the exact calculation of $T_s[n]$ is very important.

$E^{\text{xc}}[n]$ is also not known exactly. A known approximation for $E^{\text{xc}}[n]$ and for $v^{\text{xc}}(\mathbf{r}) = \frac{\delta E^{\text{xc}}[n]}{\delta n(\mathbf{r})}$ is the “local-density approximation” (LDA).

Equation (3.225) means that the many-body problem of the Hamilton operator of Eq. (3.215) can be brought into the form of a single-particle equation to be solved self-consistently. The potential, in which the N independent quasi particles $\varphi_{o_k}(\mathbf{r})$ move, $v^{\text{eff}}(\mathbf{r})$, is local (i.e., it is multiplicative) and is identical for all particles. In practical calculations the only approximation introduced concerns $E^{\text{xc}}[n]$.

Approximations:

1. Local-density approximation (LDA):

$$E^{\text{xc}}[n] = \int n(\mathbf{r}) \epsilon^{\text{xc}}[n](\mathbf{r}) d^3\mathbf{r} \quad \rightarrow \quad E^{\text{xc-LDA}}[n] = \int n(\mathbf{r}) \epsilon^{\text{xc-jellium}}(n(\mathbf{r})) d^3\mathbf{r} \quad (3.227)$$

$\epsilon^{\text{xc-jellium}}(n)$ is the exchange-correlation energy per particle of the homogeneous electron gas (jellium) of density n . Strictly, Eq. (3.227) is valid only for slowly varying densities. Experience with this approximation for calculations of atoms, molecules and solids shows that Eq. (3.227) in general can also be applied to these systems.

2. The Hartree-Fock approximation is obtained from Eq. (3.223) and (3.225), when

$$\frac{\delta E^{\text{xc}}[n]}{\delta n(\mathbf{r})} = v^{\text{xc}}(\mathbf{r}) \quad (3.228)$$

is replaced by

$$v_k^{\text{x}}(\mathbf{r}) = -\frac{e^2}{4\pi\epsilon_0} \int \frac{n_k^{\text{HF}}(\mathbf{r}, \mathbf{r}')}{|\mathbf{r} - \mathbf{r}'|} d^3\mathbf{r}' \quad (3.229)$$

$$n_k^{\text{HF}}(\mathbf{r}, \mathbf{r}') = \sum_{i=1}^N \delta_{s_i, s_k} \frac{\varphi_{o_i s_i}^*(\mathbf{r}') \varphi_{o_k s_k}(\mathbf{r}') \varphi_{o_i s_i}(\mathbf{r})}{\varphi_{o_k s_k}(\mathbf{r})} \quad (3.230)$$

is called *exchange particle density*. This approximation is obtained, if the many-body wave function is constructed from *one* Slater determinant.

Problems:

- a) $v_k^{\text{x}}(\mathbf{r})$ depends on the index (quantum number) of the wave function to be calculated.

- b) $v_k^x(\mathbf{r})$ contains only exchange, i.e., the correlation of the electrons due to the Pauli principle. The correlation arising from the Coulomb repulsion between electrons is missing.
3. The Hartree approximation is obtained when $E^{xc}[n]$ and $v^{xc}(\mathbf{r})$ are neglected. Strictly, $v^{xc}(\mathbf{r})$ should be replaced by

$$v_k^{\text{SIC}}(\mathbf{r}) = -\frac{e^2}{4\pi\epsilon_0} \int \frac{|\varphi_{o_k}|^2}{|\mathbf{r} - \mathbf{r}'|} d^3\mathbf{r}' \quad , \quad (3.231)$$

which is, however, typically ignored. This approximation is obtained, if the many-body wave function is constructed as a simple product of single-particle functions.

4. The Thomas-Fermi approximation is obtained from Eq. (3.221), (3.222) and (3.224), if the following approximation is introduced:
- a) in $T_s[n]$ $O(\nabla n)$ is neglected
 - b) in $E^{xc}[n]$ $O(\nabla n)$ is neglected

Problems: The approximation for $T_s[n]$ generally yields an error of 10% in the total energy. The shell structure of the atoms is not described.

Chapter 4

Lattice Periodicity

4.1 Symmetry

In part 3 we saw that the many-body problem can be reduced exactly to the self-consistent solution of effective single-particle equations:

$$h\varphi_{o_i}(\mathbf{r}) = \epsilon_{o_i}\varphi_{o_i}(\mathbf{r}) \quad (4.1)$$

with

$$h = -\frac{\hbar^2}{2m}\nabla^2 + v^{\text{eff}}(\mathbf{r}) \quad . \quad (4.2)$$

In the effective potential, the electrostatic potential of the nuclei depends on the atomic positions, the Hartree and the exchange-correlation potential are determined by the charge density of the electrons. Since the densities depend on the positions of the atoms, the symmetry properties of $v^{\text{eff}}(\mathbf{r})$ are determined the arrangement of the lattice components (nuclei), i.e., by the symmetry of $v(\mathbf{r})$. Note that this does not always mean that the symmetry of $v^{\text{eff}}(\mathbf{r})$ has to be the *same* as that of any given system of nuclei. In principle, the charge density (and thus, $v^{\text{eff}}(\mathbf{r})$) could have a lower symmetry than a given arrangement of nuclei.¹ However, this will then lead to residual forces on the nuclei, “pulling” them into the same (lower) symmetry state as $v^{\text{eff}}(\mathbf{r})$. In general, the symmetries of $v(\mathbf{r})$, $n(\mathbf{r})$ and $v^{\text{eff}}(\mathbf{r})$ will thus be consistent with one another when the nuclei are at their equilibrium position. Since the operator ∇^2 is invariant with respect to translation, rotation and inversion in real space, the symmetry of h is determined only by $v^{\text{eff}}(\mathbf{r})$. Now we will see what we can learn from such investigations of the symmetry. In order to study the properties depending on the periodic arrangement of the atoms, we first have to introduce several definitions. The fundamental property of a *crystal* or a crystalline solid is the regular arrangement of its constituents, i.e., the nuclei. “Periodicity” and “order” are not synonyms, and the most recent definition by the “International Union of Crystallography” therefore reads: “A crystal is a solid having an essentially discrete diffraction pattern.” Periodic crystals form a subset. At this point we note that in nature crystals are more frequent than expected: Not only diamond and quartz are crystals. Also metals often have a crystalline structure, although their outer shape usually is not so pronounced as, e.g. for salts or for minerals.

A periodic crystal is characterized by the fact that by a certain translation it is mapped onto itself. A translation is defined by a vector

$$\mathbf{R}_n = n_1\mathbf{a}_1 + n_2\mathbf{a}_2 + n_3\mathbf{a}_3 \quad , \quad (4.3)$$

¹So-called spin or charge density waves in periodic crystals are an example for cases where the nuclei may have a different (higher) translational symmetry (see below) than the resulting $v^{\text{eff}}(\mathbf{r})$. Examples are the so-called *Peierls instability*, or the magnetic ground state of Cr, where the periodicity of the electronic spin density extends over many unit cells of the actual nuclear subsystem.

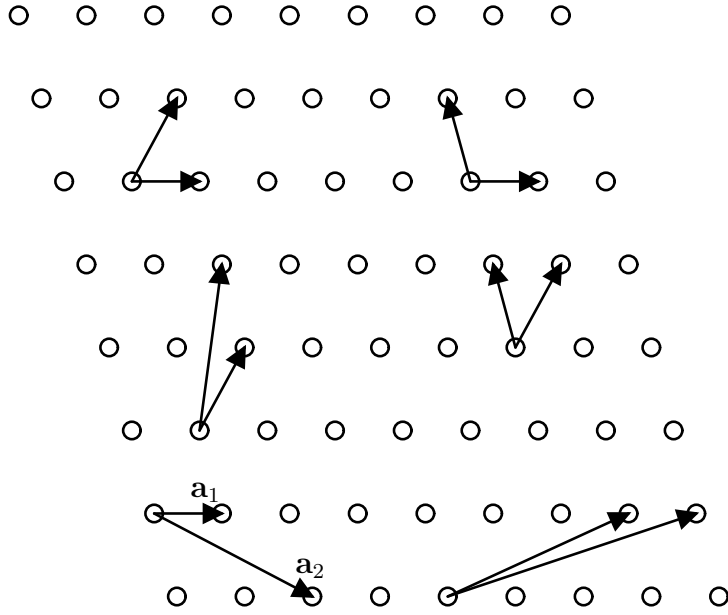


Figure 4.1: A two-dimensional Bravais lattice. The choice of the primitive vectors $\mathbf{a}_1, \mathbf{a}_2$ is not unique.

where $n_i \in \mathbb{Z}$ and the vectors \mathbf{a}_i are linearly independent. For the translation operator we have

$$T_{\mathbf{R}_n} f(\mathbf{r}) = f(\mathbf{r} + \mathbf{R}_n) \quad , \quad (4.4)$$

where $f(\mathbf{r})$ is an arbitrary function. We have

$$T_{\mathbf{R}_n} v^{\text{eff}}(\mathbf{r}) = v^{\text{eff}}(\mathbf{r} + \mathbf{R}_n) = v^{\text{eff}}(\mathbf{r}) \quad (4.5)$$

and

$$T_{\mathbf{R}_n} \nabla^2 f(\mathbf{r}) = \nabla^2 f(\mathbf{r} + \mathbf{R}_n) = \nabla^2 T_{\mathbf{R}_n} f(\mathbf{r}) \quad . \quad (4.6)$$

This means that $T_{\mathbf{R}_n}$ and h commute: Then for the Hamilton operator h we have

$$T_{\mathbf{R}_n} h \varphi_{o_i}(\mathbf{r}) = h \varphi_{o_i}(\mathbf{r} + \mathbf{R}_n) = h T_{\mathbf{R}_n} \varphi_{o_i}(\mathbf{r}) = \epsilon_{o_i} \varphi_{o_i}(\mathbf{r} + \mathbf{R}_n) \quad . \quad (4.7)$$

The vectors \mathbf{a}_i introduced above are called primitive vectors. The set of *points* defined by $\{\mathbf{R}_n\}$ is called a *Bravais lattice* (cf. Fig. 4.1). For obvious reasons the term Bravais lattice is often also used for the set of *vectors* $\{\mathbf{R}_n\}$. The choice of the primitive vectors is not unique, generally the shortest primitive translations are chosen. The points of the Bravais lattice do not need to correspond to the positions of individual atoms. As a warning we mention that not every apparently symmetric set of points constitutes a Bravais lattice (cf. the example in Fig. 4.2). Apart from translations, which shift all points in space, generally the structure of a crystal is also invariant with respect to symmetry operations that keep at least one point fixed, so-called *point symmetries* (details will be given later). The smallest structural unit of a crystal is called the *primitive cell* or the *primitive unit cell*. If the *primitive unit cell* is shifted by all vectors of the Bravais lattice, the full space is filled without gaps or overlap. Similar to the definition of primitive vectors the definition of the primitive unit cell is not unique. A primitive unit cell contains exactly one point of the Bravais lattice. Thus, a possible choice for the primitive unit cell would be the

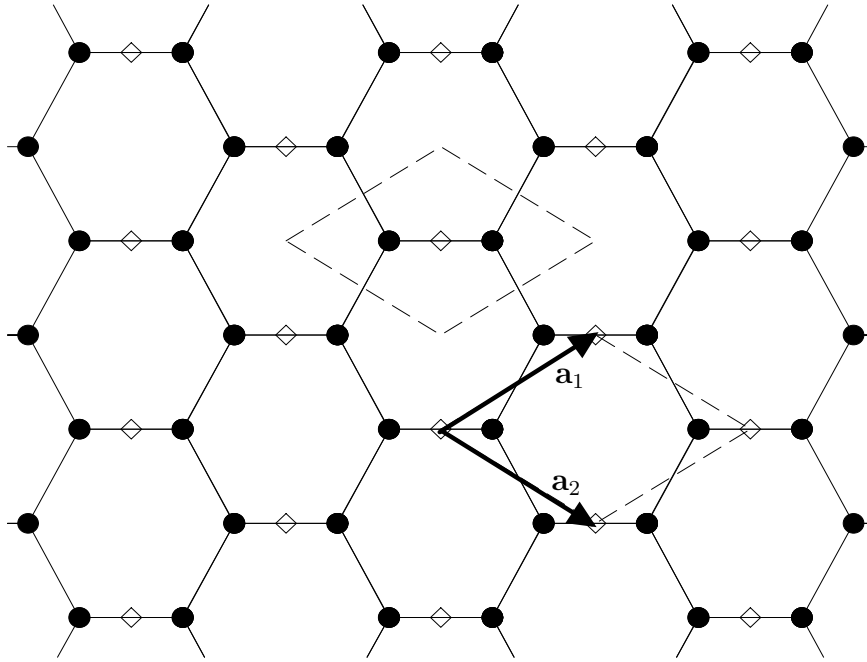


Figure 4.2: The crossing points of the honeycomb structure do not form a Bravais lattice, but the centers of the dumbbells do. Thus, the hexagonal structure is also called a *Bravais lattice with basis*, i.e., for each point of the Bravais lattice in this case there are two atoms, which in this context are called basis.

body spanned by the shortest primitive vectors. This choice has the disadvantage that the primitive unit cell defined this way often does not have the same symmetry (point symmetry) as the Bravais lattice. But there is always a primitive unit cell, which has the same symmetry with respect to reflection, rotations and inversion as the Bravais lattice. This is the Wigner-Seitz cell: It consists of the region, which is closer to a certain Bravais lattice point than to all other Bravais lattice points. The Wigner-Seitz cell has the same symmetry as the Bravais lattice. For the construction of the Wigner-Seitz cell, one starts with an arbitrary point of the Bravais lattice. The surface is obtained by connecting this lattice point with its nearest neighbors. In the middle of the connecting line a plane perpendicular to this line is constructed. A two-dimensional example is shown in Fig. 4.3, and some three-dimensional examples are shown in Fig. 4.4.

Often it is more illustrative to construct a crystal structure from larger unit cells instead of primitive cells (*“conventional unit cells”*). Four important examples for Bravais lattices are the sc (simple cubic), fcc (face-centered cubic), bcc (body-centered cubic) and the hexagonal Bravais lattice (cf. Fig. 4.4).

Apart from translations $T_{\mathbf{R}_n}$ there may be further *symmetry operations of the crystal*:

- 1) R_ϕ rotation
 - 1a) C_n normal rotation by $\phi = \frac{2\pi}{n}$
 - 1b) S_n improper rotation
- 2) σ reflection

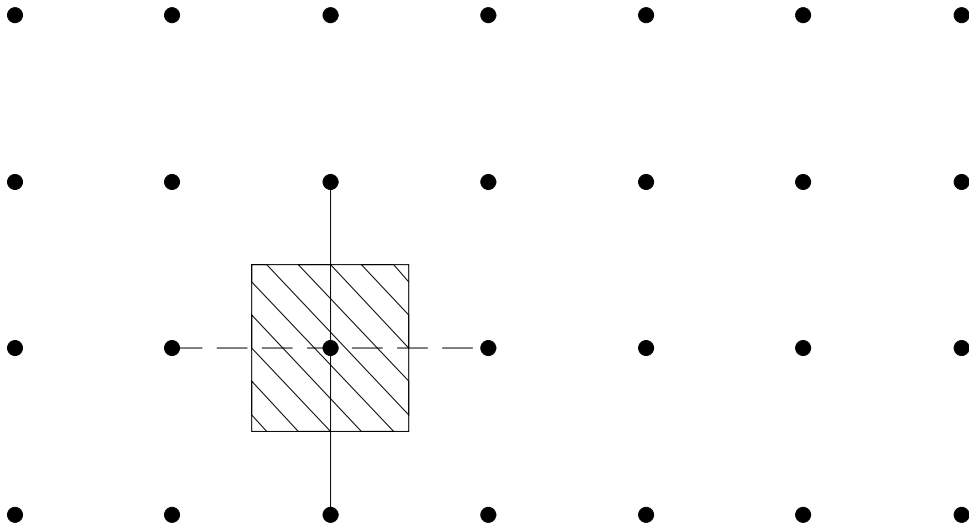


Figure 4.3: The Wigner-Seitz cell of a square net of points.

- 3) $i = S_2$ inversion
- 4) \widehat{TR}_ϕ screw rotation
- 5) $\widehat{T}\sigma$ glide reflection

Generally, the term “rotation” includes “normal rotations” as well as improper rotations. An improper rotation is the following combination of operations: First, rotate about a certain axis by the angle ϕ and then reflect at the plane perpendicular to this axis. Screw rotation and glide reflection are combinations of rotations and reflections and non-primitive translations. The example of a glide reflection is shown in Fig. 4.5.

If we want to distinguish between proper and improper rotations, instead of the symbol R_ϕ we use the following symbols: Operator of the normal rotation: C_n . Operator of the improper rotation: S_n . The letter C results from “cyclic”. The Index n gives the rotation angle ϕ as $\phi = 2\pi/n$.

The operation of inversion at the origin, i.e., $x \rightarrow -x$, $y \rightarrow -y$, $z \rightarrow -z$ is labeled by the letter i . We have: $i = S_2$ -reflections are labeled by the letter σ . They can be composed of a rotation and an improper rotation: $\sigma = C_n^{-1} \otimes S_n$.

It can easily be seen that the set of symmetry operations of a body has group properties. Therefore, we have the four laws (O,A,N,I):

- 1) There is an operation \otimes :

$$a, b \in \mathbf{G} \rightarrow a \otimes b = c \in \mathbf{G}$$

- 2) The associative law is valid:

$$a \otimes (b \otimes c) = (a \otimes b) \otimes c$$

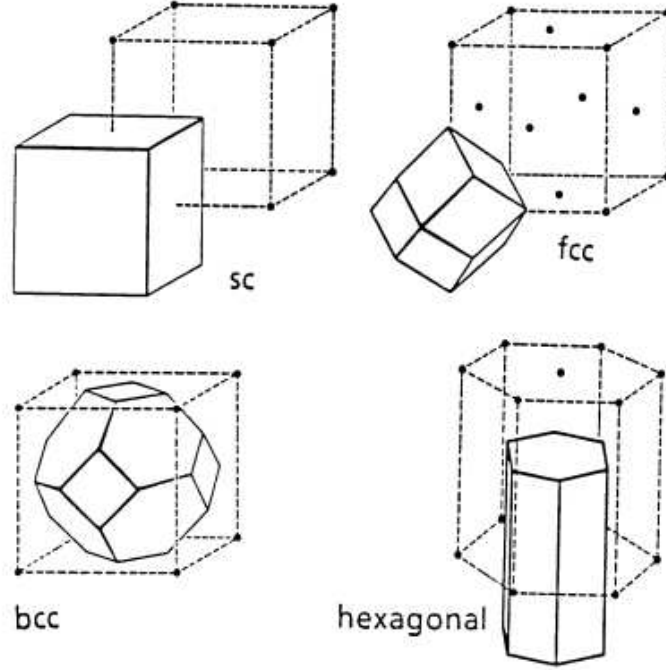


Figure 4.4: Some Bravais lattices and the corresponding Wigner-Seitz cells.

3) There is a neutral element E :

$$a \otimes E = E \otimes a = a$$

4) For each element in \mathbf{G} there is an inverse element:

$$a \otimes a^{-1} = E = a^{-1} \otimes a$$

For the elements of the Bravais lattice, i.e., for the translations, additionally we have the commutative law $a \otimes b = b \otimes a$:

$$T_{\mathbf{R}_m} + T_{\mathbf{R}_n} = T_{\mathbf{R}_n} + T_{\mathbf{R}_m} = T_{\mathbf{R}_n + \mathbf{R}_m} \quad (4.8)$$

Thus, the translational group is Abelian.

A subset \mathbf{U} of \mathbf{G} , that is closed with respect to the operation \otimes and itself has group properties, is called a *subgroup*. The set of elements, which is generated by operating all elements of \mathbf{U} on a given element a of the group, is called a *coset* (notation $a \otimes \mathbf{U}$). The cosets themselves are not groups. For non-Abelian groups one has to distinguish between right ($\mathbf{U} \otimes a$) and left cosets ($a \otimes \mathbf{U}$). If, in a special case, right and left cosets of a subgroup \mathbf{U} are the same, the subgroup \mathbf{U} is called a *normal divisor* of \mathbf{G} .

As an example for a point symmetry we now investigate the point group of a cube. The group is labeled O_h , the letter O referring to “octahedra”. This point group is rather important. Many important crystals have this point symmetry or at least the symmetry of a subgroup of O_h . The sc, fcc, and bcc Bravais lattices have O_h symmetry.

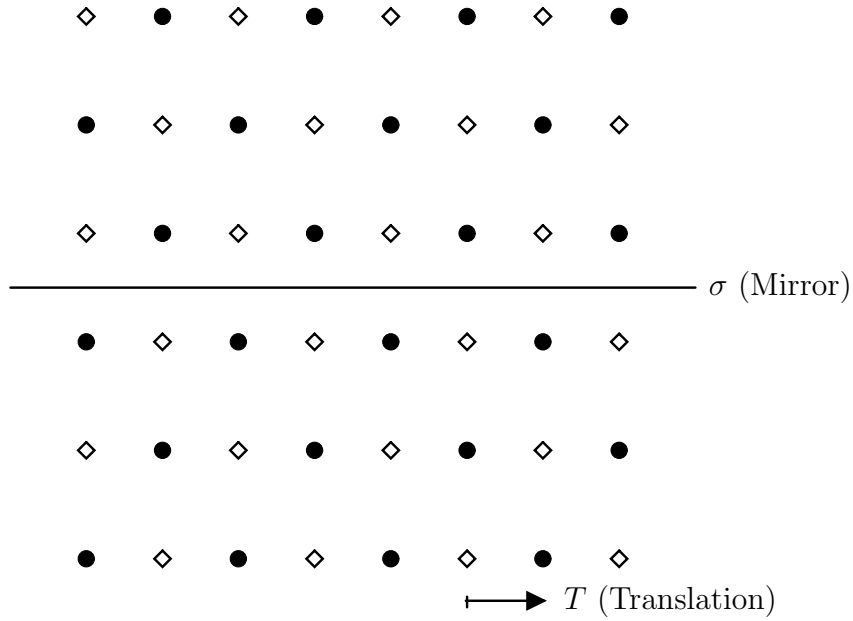


Figure 4.5: The system of two atom types is mapped on itself by a combination of translation T and reflection (glide reflection symmetry). The translation T and the reflection σ alone would not be symmetry operations. In this example the glide reflection is identical to a screw rotation. For the screw rotation a translation and a rotation (here by 180°) are combined.

symbol	operation	number
E	unit operation	1
C_4	rotation around the x -, $-x$ -, y -, $-y$ -, z - or $-z$ -axis by $2\pi/4$	6
C_2	rotation around the x -, y - or z -axis by $2\pi/2$	3
C_2	rotation around the six axes cutting the edges of the cube in the middle by $2\pi/2$	6
C_3	rotation around the four space diagonals by $\pm 2\pi/3$	8
$\otimes i$	all operations given up to here $\otimes i$	24

Table 4.1: The 48 symmetry operations of the cube, i.e., the point group O_h .

In Table 4.1 the symmetry operations are described. Reflections do not appear explicitly in the table, but they are included in the symmetry operations of O_h . We have $\sigma_v = i \otimes C_2$ and $\sigma_d = i \otimes C_2'$. The index at σ indicates if the plane is crossing the cube vertically (v) or diagonally (d).

As another term we introduce is the *class of conjugate elements* (often just called class). Two symmetry operations a and b are part of such a class if there is an element c of this group, so that we have

$$a = c^{-1}bc \quad (4.9)$$

a and b are then called “similar symmetry operations” or “conjugate operations”. Symmetry operations of the “same kind” are in one class. In Table 4.1 we already intuitively summarized the symmetry operations according to classes. Only in the last row we con-

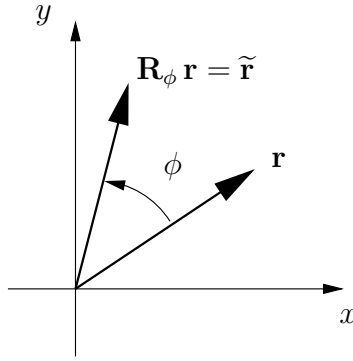


Figure 4.6: Operator R_ϕ . Here: Rotation about the z -axis by the angle ϕ .

sidered 5 classes together. This can easily be validated. The group O_h has 10 classes. The group O (this is the subgroup of O_h , which does not contain i) has 5 classes. The neutral element is always a class by itself.

The total of all symmetry operations (translations, point symmetries, and combinations of both), which map the Bravais lattice (including a possibly existing basis) on itself, form the *space group* of the crystal. If we label the operator of a rotation (by the angle ϕ) with R_ϕ (cf. Fig. 4.6), an arbitrary element of the space group can be labeled by $(R_\phi; T_{\mathbf{D}})$. We have:

$$(R_\phi; T_{\mathbf{D}})f(\mathbf{r}) = f(\tilde{\mathbf{r}} + \mathbf{D}) \quad (4.10)$$

with $\tilde{\mathbf{r}} = R_\phi \mathbf{r}$. Because \mathbf{D} appears in a combination of rotation and translation operations, it is not necessarily an element of the Bravais lattice (cf. Fig. 4.5).

It can be shown that the space group contains the required group properties. In particular it has to be closed with respect to all operations, which are defined as:

$$(R_{\phi_2}; T_{\mathbf{D}_2})(R_{\phi_1}; T_{\mathbf{D}_1}) = (R_{\phi_2} R_{\phi_1}; T_{R_{\phi_2} \mathbf{D}_1 + \mathbf{D}_2}) \quad (4.11)$$

For the inverse element we have:

$$(R_\phi; T_{\mathbf{D}})^{-1} = (R_\phi^{-1}; T_{-R_\phi^{-1} \mathbf{D}}) \quad (4.12)$$

For Bravais lattices we have: The total number of the different² symmetry operations is finite: There are, e.g. only four rotations: C_2 , C_3 , C_4 , and C_6 . In periodic solids there is no rotational axis with a 5-fold symmetry or a symmetry of higher than 6 (due to translational invariance).

Proof:

The vectors of the Bravais lattice are

$$\mathbf{R}_n = n_1 \mathbf{a}_1 + n_2 \mathbf{a}_2 + n_3 \mathbf{a}_3 \quad (4.13)$$

²The operations $T_{\mathbf{R}_n}$ and $NT_{\mathbf{R}_n}$ or C_n and $2C_n, 3C_n, \dots$ are considered the same.

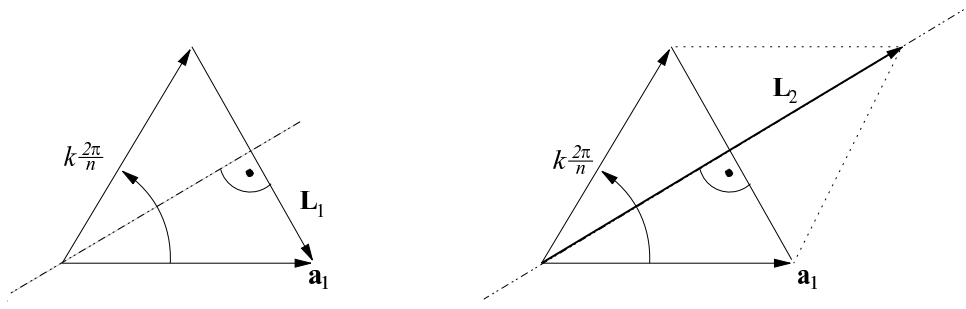


Figure 4.7: Visualization of Equations (4.19) and (4.20).

Further, the crystal shall have (at least) one rotational axis C_n , and for the moment we leave it open, what n may be. $C_n \mathbf{R}_n$ then also is an element of the Bravais lattice. The vectors

$$\mathbf{R}'_n = \mathbf{R}_n - C_n \mathbf{R}_n \quad (4.14)$$

are perpendicular to the rotational axis and are of course also part of the Bravais lattice. The shortest of these vectors shall be labeled with \mathbf{a}_1 . The vectors $(kC_n)\mathbf{a}_1$ with $k = 1 \dots n$ are then also elements of the Bravais lattice; (kC_n) means that the rotation is performed k -times. They all have the same length as \mathbf{a}_1 . Now we consider two vectors of different lengths:

$$|\mathbf{a}_1 - (kC_n)\mathbf{a}_1| = L_1 \quad (4.15)$$

and

$$|\mathbf{a}_1 + (kC_n)\mathbf{a}_1| = L_2 \quad . \quad (4.16)$$

Because \mathbf{a}_1 is the shortest vector perpendicular to the rotational axis, we have

$$L_1 \geq |\mathbf{a}_1| \quad (4.17)$$

and

$$L_2 \geq |\mathbf{a}_1| \quad . \quad (4.18)$$

Alternatively, it would be possible that L_1 or L_2 are zero. In Fig. 4.7 it can be seen that for $k = 1 \dots n$

$$\left| \sin \left(\frac{k\pi}{n} \right) \right| = \frac{L_1}{2|\mathbf{a}_1|} \quad (4.19)$$

and

$$\left| \cos \left(\frac{k\pi}{n} \right) \right| = \frac{L_2}{2|\mathbf{a}_1|} \quad . \quad (4.20)$$

With condition (Eq. (4.17)) follows:

$$\left| \sin \left(\frac{k\pi}{n} \right) \right| = \frac{L_1}{2|\mathbf{a}_1|} \geq \frac{1}{2} = \sin(30^\circ) \quad (4.21)$$

for all numbers $k \leq n$. This means that we must have $\frac{k\pi}{n} \geq \pi/6$, i.e., n must not be larger than 6.

\tilde{G}_1	A_1	A_2	\dots	A_N
A_1	$A_1 \otimes A_1$	$A_1 \otimes A_2$	\dots	$A_1 \otimes A_N$
A_2	$A_2 \otimes A_1$	\dots	\dots	\dots
\vdots	\dots	\dots	\dots	\dots
A_N	$A_N \otimes A_1$	\dots	\dots	$A_N \otimes A_N$

Table 4.2: Multiplication table of a group \tilde{G}_1 consisting of N elements. Each product $A_i \otimes A_j$ is equal to an element of the group, i.e., $A_i \otimes A_j = A_k$.

From Eq. (4.18) we obtain

$$\left| \cos \left(\frac{k\pi}{n} \right) \right| \geq \frac{1}{2} = \cos(60^\circ) \quad (4.22)$$

If we set $k = 2$, we obtain a contradiction; thus $n = 5$ is also impossible. Therefore, we have proven that for a Bravais lattice only point symmetries with rotations C_2, C_3, C_4 , and C_6 can exist.

A cell with C_5 or one with C_n and $n > 6$ cannot fill space completely or without overlap. This was noted already in 1619 by Johannes Kepler. However, in 1984 in rapidly cooled aluminium-manganese-melts diffraction images of 5-fold symmetry were measured (Phys. Rev. Letters, **53**, 1951 (1984)) and also 12-fold (Phys. Rev. Letters, May 1988) symmetries were found. These are not periodic crystals although these are ordered systems. These “new lattices” are called quasi-crystals (cf. e.g. Physikalische Blätter 1986, S. 373 and S. 368, Fig. 3). A certain analogy to the three-dimensional quasi crystals in two dimensions are the so-called Penrose-patterns (cf e.g. Spektrum der Wissenschaft, Juli 1999). This effect is also known from tiling walls or floors. When tiles of five-fold symmetry are used one also needs other tiles to fill some areas.

From the very limited number of possible rotation axes for Bravais lattices it follows: For Bravais lattices there are only 7 different point groups (7 crystal systems). We first have to explain what is meant by the term “different”, or what is meant by the term “the same”. Two groups are equivalent, if they contain the same number of elements and if their multiplication tables are identical. The multiplication table of a point group is defined in Table 4.2. Instead of the term “point group of the Bravais lattice” we also use the term “crystal system” as a synonym. One of the 7 point groups, i.e., the group O_h , has already been examined.

In Table 4.3 the 7 crystal systems are listed, where we reduce the symmetry of the sample body (with the exception of the hexagonal point group) when going from row N to $N + 1$. When considering the space groups one finds that for Bravais lattices (with mono-atomic basis) there are only 14 different space groups. This has been investigated by Frankheim in 1842, but he made a mistake (he found 15), in 1845 Bravais found the correct number.

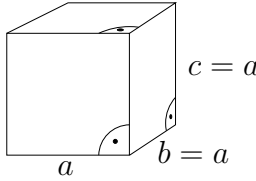
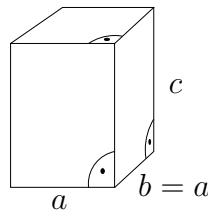
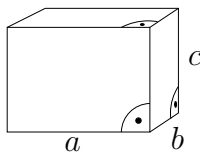
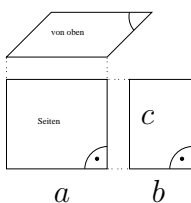
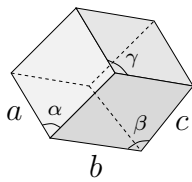
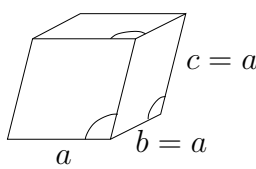
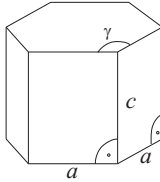
crystal system	crystal axes	example	Bravais lattice
cubic	$\alpha = \beta = \gamma = 90^\circ$ $a = b = c$		sc, fcc, bcc,
tetragonal	$\alpha = \beta = \gamma = 90^\circ$ $a = b \neq c$		simple tetragonal, centered tetragonal,
orthorhombic (rhombic)	$\alpha = \beta = \gamma = 90^\circ$ $a \neq b \neq c$		simple, face centered, body centered, face centered, (Basis: upper/lower facet)
monoclinic	$\alpha = \gamma = 90^\circ \neq \beta$ $a \neq b \neq c$		simple monoclinic, centered monoclinic,
triclinic	$\alpha \neq \beta \neq \gamma$ $a \neq b \neq c$	 Parallelepiped (Spat), opposite facets are parallel	simple triclinic,
trigonal	$\alpha = \beta = \gamma \neq 90^\circ$ $a = b = c$		simple trigonal,
hexagonal	$\alpha = \beta = 90^\circ$ $\gamma = 120^\circ$ $a = b \neq c$		simple hexagonal.

Table 4.3: The 7 Crystal Systems and 14 Bravais Lattices.

crystal system	number of Bravais lattices	number of point groups	name of the point groups
cubic	3	5	O_h, O, T_h, T, T_d
tetragonal	2	7	$C_4, S_4, C_{4h}, D_4, C_{4v}, D_{2d}, D_{4h}$
orthorhombic	4	3	D_2, C_{2v}, D_{2h}
monoclinic	2	3	C_2, C_S, C_{2h}
triclinic	1	2	C_1, C_i
trigonal	1	5	$C_3, C_{3i}, D_3, C_{3v}, D_{3d}$
hexagonal	1	7	$C_6, C_{6h}, D_6, C_{6v}, D_{3h}, D_{6h}, C_{3h}$
	$\Sigma = 14$	$\Sigma = 32$	

Table 4.4: Bravais lattices and point groups of the crystal structures.

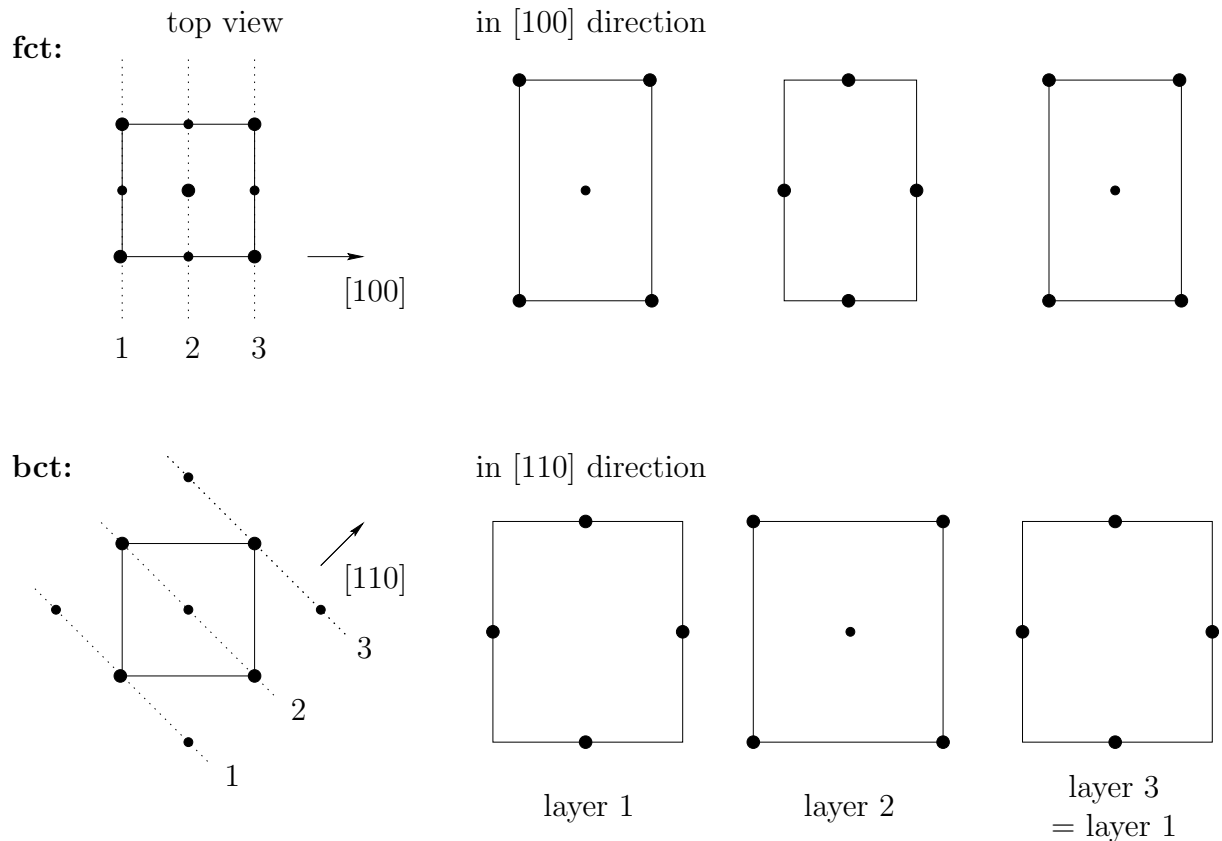


Figure 4.8: Layer sequence of a fct and of a bct lattice (at the left: projection onto the (001) plane). Both lattices can be represented as a ct lattice.

There are further Bravais lattices, that may come to mind analogous to sc-, fcc-, and bcc-lattices. They are not included in the table, because they are equivalent to the ones listed. For example, a face-centered and a body-centered tetragonal Bravais lattice are identical (cf. Fig. 4.8).

This is a first crude classification of all possible periodic crystals in the 14 Bravais lattices. For each crystal there is a Bravais lattice and a crystal system. In case each point of the Bravais lattice has an inner structure (e.g. the dumbbells of Fig. 4.2), i.e., if it has a basis, then the point symmetry of the crystal is lower than the symmetry of the Bravais lattice. Generally, we have: The point group of a crystal is a subgroup of the *crystal system*. For the cubic crystal system O_h , e.g. there are 5 subgroups, which can be present in real crystals. These are the groups O_h , O (like O_h , but without inversion i), T_d (the point group of a tetrahedron: $E, 8C_3, 3C_2, 6\sigma_d, 6S_4$), T (the point group of a tetrahedron, without reflection symmetry: $E, 3C_2, 4C_3^+, 4C_3^-$), the group $T_h = T \otimes i$, which in addition to T contains also the operations $i, 8S_6, 3\sigma_d$. We have used $\sigma_d = C_2 \otimes i$ and $S_4 = C_4 \otimes i$. Thus, if the “inner atomic structure” of the individual points of the Bravais lattice are taken into account, one finds: There are 32 crystalline point groups, which are compatible with the translational properties of a crystal (cf. Table 4.4) and there are 230 space groups.

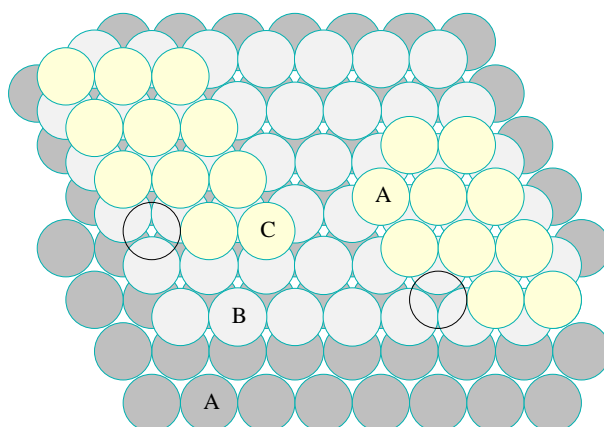


Figure 4.9: Close-packed structures hcp (left, layer sequence ABCABC...) and fcc (right, layer sequence ABAB...).

If one thinks of the crystal as being composed of hard spheres and these spheres are close-packed, one obtains a structure with the first two layers as shown in Fig. 4.9. The first layer has a 6-fold symmetry and each sphere has 6 neighbors. The spheres of the second layer are located in the hollow sites of the first layer. For the third layer there are two different possibilities: The spheres could be on top of the gaps (site b) or above the spheres of the second-last layer (site a). In the second case the arrangement of the third layer is equal to the first, and we obtain a layer sequence ABABAB... . This is the hcp-structure. In case b) a layer sequence of ABC... can be obtained. This is the fcc-structure.

fcc- and hcp-structures are mostly adopted by systems without directional bonds between structural elements (in simple Bravais lattices without basis these are the atoms). Then energetically it will be favored if each structural element can form bonds to as many

neighbors as possible. In the fcc- and hcp-structure each structural element has twelve nearest neighbors.

In Fig. 4.10 some important crystal structures are listed (from Ashcroft-Mermin). Further some crystals adopting these structures and their lattice constants are given. Except for the last example, the hexagonal structure, these are all cubic crystal systems.

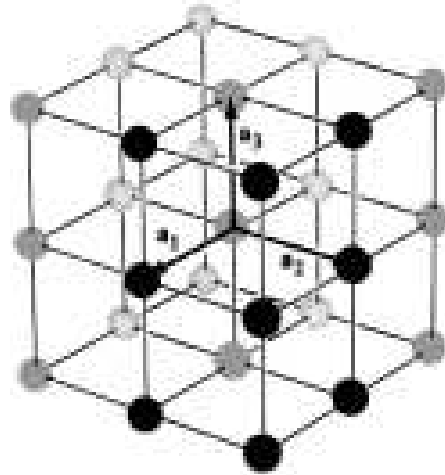
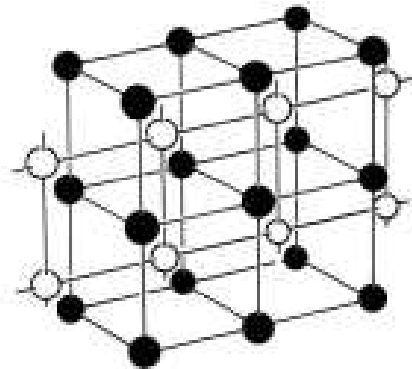
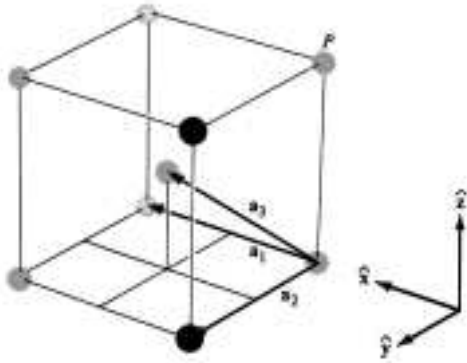


Figure 4.10: Some important crystal structures. a) Simple cubic (sc) Bravais lattice, (e.g. α -Polonium).



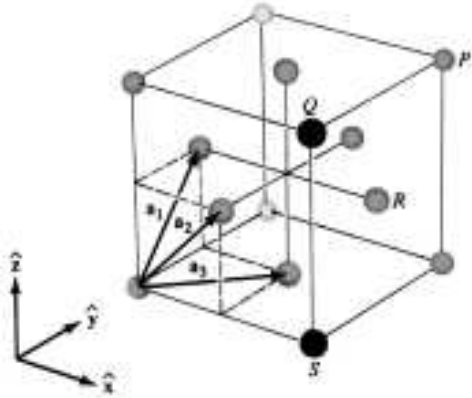
CRYSTAL	a (Å)	CRYSTAL	a (Å)
CsCl	4.12	TlCl	3.83
CsBr	4.29	TlBr	3.97
CsI	4.57	TlI	4.20

Fig. 4.10 – b) CsCl structure (sc with a diatomic basis).



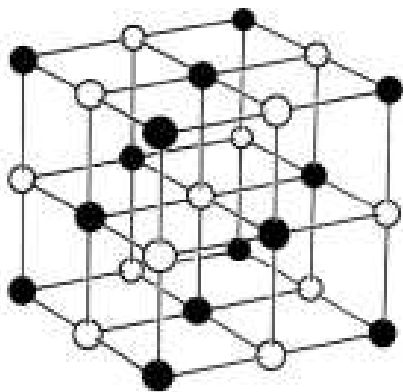
ELEMENT	a (Å)	ELEMENT	a (Å)	ELEMENT	a (Å)
Ba	5.02	Li	3.49 (78 K)	Ta	3.31
Cr	2.88	Mo	3.15	Tl	3.88
Cs	6.05 (78 K)	Na	4.23 (5 K)	V	3.02
Fe	2.87	Nb	3.30	W	3.16
K	5.23 (5 K)	Rb	5.59 (5 K)		

Fig. 4.10 – c) body-centered cubic Bravais lattice (bcc).



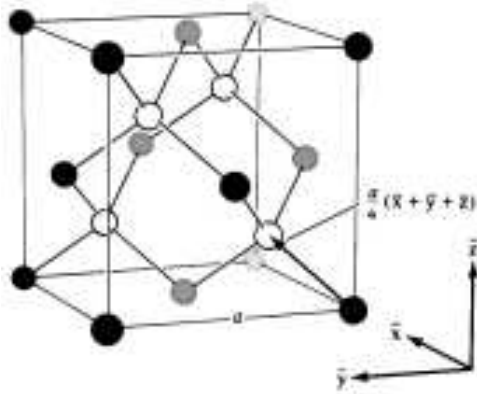
ELEMENT	a (Å)	ELEMENT	a (Å)	ELEMENT	a (Å)
Ar	5.26 (4.2 K)	Ir	3.84	Pt	3.92
Ag	4.09	Kr	5.72 (58 K)	δ -Pu	4.64
Al	4.05	La	5.30	Rh	3.80
Au	4.08	Ne	4.43 (4.2 K)	Sc	4.54
Cu	5.58	Ni	3.52	Sr	6.08
Ce	5.16	Pb	4.95	Th	5.08
β -Co	3.55	Pd	3.89	Xe (58 K)	6.20
Cu	3.61	Pr	5.16	Yb	5.49

Fig. 4.10 – d) face-centred cubic Bravais lattice (fcc).



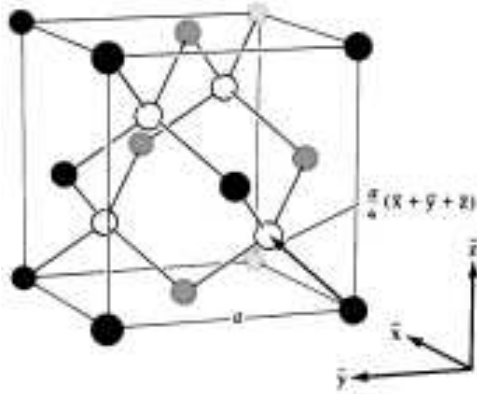
CRYSTAL	a (Å)	CRYSTAL	a (Å)	CRYSTAL	a (Å)
LiF	4.02	RbF	5.64	CaS	5.69
LiCl	5.13	RbCl	6.58	CaSe	5.91
LiBr	5.50	RbBr	6.85	CaTe	6.34
LiI	6.00	RbI	7.34	SrO	5.16
NaF	4.62	CsF	6.01	SrS	6.02
NaCl	5.64	AgF	4.92	SrSe	6.23
NaBr	5.97	AgCl	5.55	SrTe	6.47
NaI	6.47	AgBr	5.77	BaO	5.52
KF	5.35	MgO	4.21	BaS	6.39
KCl	6.29	MgS	5.20	BaSe	6.60
KBr	6.60	MgSe	5.45	BaTe	6.99
KI	7.07	CaO	4.81		

Fig. 4.10 – e) NaCl structure (fcc with a diatomic basis),



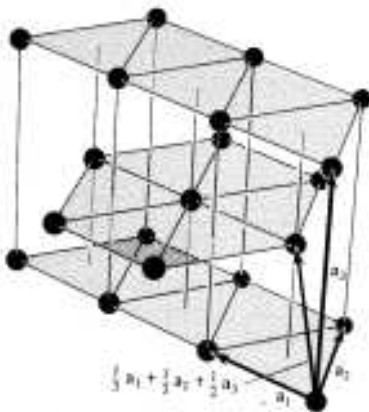
ELEMENT	CUBE SIDE a (Å)
C (diamond)	3,57
Si	5,43
Ge	5,66
α -Sn (grey)	6,49

Fig. 4.10 – f) Diamond structure (fcc with a diatomic basis).



CRYSTAL	a (Å)	CRYSTAL	a (Å)	CRYSTAL	a (Å)
CuF	4,26	ZnS	5,41	AlSb	6,13
CuCl	5,41	ZnSe	5,67	GaP	5,45
CuBr	5,69	ZnTe	6,09	GaAs	5,65
CuI	6,04	CdS	5,82	GaSb	6,12
AgI	6,47	CdTe	6,48	InP	5,87
BeS	4,85	HgS	5,85	InAs	6,04
BeSe	5,07	HgSe	6,08	InSb	6,48
BeTe	5,54	HgTe	6,43	SiC	4,35
MnS (red)	5,60	AlP	5,45		
MnSe	5,82	AlAs	5,62		

Fig. 4.10 – g) Zincblende structure (fcc with a diatomic basis of different species).



ELEMENT	a (Å)	c	c/a	ELEMENT	a (Å)	c	c/a
Be	2,29	3,58	1,56	Os	2,74	4,32	1,58
Cd	2,98	5,62	1,89	Pr	3,67	5,92	1,61
Ce	3,65	5,96	1,63	Re	2,76	4,46	1,62
α -Co	2,51	4,07	1,62	Ru	2,70	4,28	1,59
Dy	3,59	5,65	1,57	Sc	3,31	5,27	1,59
Er	3,56	5,59	1,57	Tb	3,60	5,69	1,58
Gd	3,64	5,78	1,59	Ti	2,95	4,69	1,59
He (2 K)	3,57	5,83	1,63	Tl	3,46	5,53	1,60
Hf	3,20	5,06	1,58	Tm	3,54	5,55	1,57
Ho	3,58	5,62	1,57	Y	3,65	5,73	1,57
La	3,75	6,07	1,62	Zn	2,66	4,95	1,86
Lu	3,50	5,55	1,59	Zr	3,23	5,15	1,59
Mg	3,21	5,21	1,62				
Nd	3,66	5,90	1,61	"Ideal"			1,63

Fig. 4.10 – h) Hexagonal closed packed structure (hcp, hexagonal Bravais lattice with a diatomic basis). The table lists the lattice parameters for some elements with hexagonal closed-packed structure (hcp), cf. Fig. 4.9.

	Bravais lattice	crystal structure
point symmetry	7 crystal systems	32 crystalline point groups
point symmetry and translational symmetry	14 Bravais lattices	230 crystalline space groups

Table 4.5: The space groups.

4.2 The Bloch Theorem

What can we learn from the symmetry properties of $v^{\text{eff}}(\mathbf{r})$ for the solution of the Kohn-Sham equation? In this paragraph we take into account (at first) the translational invariance of the periodic crystal. For the Kohn-Sham equation the Hamilton operator of the crystal and the translations of the Bravais lattice commute (cf. Eq. (4.7)).

Thus, the functions $\varphi_{o_i}(\mathbf{r})$ and $T_{\mathbf{R}_n}\varphi_{o_i}(\mathbf{r})$ are both eigenfunctions of h , and they have the same eigenvalue. In order to analyze this we will distinguish two cases:

- a) The eigenvalue ϵ_{o_i} is non-degenerate.

Then the functions $\varphi_{o_i}(\mathbf{r})$ and $T_{\mathbf{R}_n}\varphi_{o_i}(\mathbf{r})$ are physically equivalent. They can differ by a phase factor only:

$$T_{\mathbf{R}_n}\varphi_{o_i}(\mathbf{r}) = e^{i\alpha}\varphi_{o_i}(\mathbf{r}) \quad , \quad (4.23)$$

where α is an arbitrary real number, which can depend on \mathbf{R}_n .

In order to investigate the properties of the function $\alpha(\mathbf{R}_n)$ in more detail, we apply two translational operators \mathbf{R}_n and \mathbf{R}_m and obtain

$$T_{\mathbf{R}_m}T_{\mathbf{R}_n}\varphi_{o_i}(\mathbf{r}) = e^{i\alpha(\mathbf{R}_m)}e^{i\alpha(\mathbf{R}_n)}\varphi_{o_i}(\mathbf{r}) \quad . \quad (4.24)$$

Further we have

$$T_{\mathbf{R}_m+\mathbf{R}_n}\varphi_{o_i}(\mathbf{r}) = e^{i\alpha(\mathbf{R}_m+\mathbf{R}_n)}\varphi_{o_i}(\mathbf{r}) \quad . \quad (4.25)$$

For the phase function α we obtain

$$\alpha(\mathbf{R}_m + \mathbf{R}_n) = \alpha(\mathbf{R}_m) + \alpha(\mathbf{R}_n) \quad , \quad (4.26)$$

and we have

$$\alpha(j\mathbf{R}_n) = j\alpha(\mathbf{R}_n) \quad (4.27)$$

with j being an arbitrary integer number. The function $\alpha(\mathbf{R}_n)$ therefore is linear in \mathbf{R}_n . Thus, it has the form

$$\alpha(\mathbf{R}_n) = \mathbf{k}\mathbf{R}_n \quad . \quad (4.28)$$

Therefore, we have

$$T_{\mathbf{R}_n}\varphi_{o_i}(\mathbf{r}) = \varphi_{o_i}(\mathbf{r} + \mathbf{R}_n) = e^{i\mathbf{k}\mathbf{R}_n}\varphi_{o_i}(\mathbf{r}) \quad (4.29)$$

This is the eigenvalue equation of the translation operator. The eigenvalues of $T_{\mathbf{R}_n}$ are $e^{i\mathbf{k}\mathbf{R}_n}$. The introduced vector \mathbf{k} labels the eigenvalues of $T_{\mathbf{R}_n}$ and thus also the eigenfunctions of $\varphi_{o_i}(\mathbf{r})$.

b) The eigenvalue ϵ_{o_i} shall be degenerate.

As a second possibility we have to investigate the case that the eigenvalue is f -fold degenerate. For the f eigenfunctions φ_l we have: The functions $\varphi_l(\mathbf{r})$ and $T_{\mathbf{R}_n}\varphi_l(\mathbf{r})$ with $l = 1 \dots f$ have the same energy eigenvalue ϵ_{o_i} . This means:

$$T_{\mathbf{R}_n}\varphi_l(\mathbf{r}) = \sum_{m=1}^f \Gamma_{m,l}\varphi_l(\mathbf{r}) \quad (4.30)$$

The matrices $\Gamma_{m,l}$ are called representation of the translational group:

$$\Gamma_{m,l} = \langle \varphi_m | T_{\mathbf{R}_n} | \varphi_l \rangle \quad (4.31)$$

The translations $T_{\mathbf{R}_n}$ form an Abelian group. This means: Since the group of the $T_{\mathbf{R}_n}$ is Abelian, in the space $\{\varphi_l\}$ with $l \in \{1 \dots f\}$ there is a similarity transformation of $\varphi_l(\mathbf{r})$ to $\tilde{\varphi}_l(\mathbf{r})$ and thus of $\Gamma_{m,l}$ to $\tilde{\Gamma}_{m,l}$, such that the matrix $\tilde{\Gamma}_{m,l}$ is diagonal.³ This is also formulated as follows: The irreducible representation of an Abelian group is one-dimensional. Then, we can write:

$$T_{\mathbf{R}_n}\tilde{\varphi}_l(\mathbf{r}) = \tilde{\Gamma}_{l,l}\tilde{\varphi}_l(\mathbf{r}) \quad (4.32)$$

Formally, this equation is the same as (4.29), and it follows that

$$\tilde{\Gamma}_{l,l} = e^{i\mathbf{k}\mathbf{R}_n} \quad (4.33)$$

We summarize:

The translational operators of the Bravais lattice commute with h . $T_{\mathbf{R}_n}$ and h therefore have the same eigenfunctions. The eigenfunctions and eigenvalues of h can be labeled by the eigenvalues of $T_{\mathbf{R}_n}$ or, better, by the vector \mathbf{k} : From now on we will write $\varphi_{\mathbf{k}}(\mathbf{r})$ and $\epsilon(\mathbf{k})$. \mathbf{k} contains three quantum numbers. This labeling is not necessarily complete. The statement that for the eigenfunctions of a crystal we have

$$T_{\mathbf{R}_n}\varphi_{\mathbf{k}}(\mathbf{r}) = \varphi_{\mathbf{k}}(\mathbf{r} + \mathbf{R}_n) = e^{i\mathbf{k}\mathbf{R}_n}\varphi_{\mathbf{k}}(\mathbf{r}) \quad (4.34)$$

is called *Bloch theorem*.⁴ In order to understand the meaning and the consequences of the Bloch theorem, we have a look at the equation

$$\varphi_{\mathbf{k}}(\mathbf{r}) = e^{i\mathbf{k}\mathbf{r}}u_{\mathbf{k}}(\mathbf{r}) \quad (4.35)$$

At first this is a very general ansatz for the eigenfunctions of h , because we have made no assumptions for $u_{\mathbf{k}}(\mathbf{r})$. We have:

$$T_{\mathbf{R}_n}\varphi_{\mathbf{k}}(\mathbf{r}) = e^{i\mathbf{k}(\mathbf{r}+\mathbf{R}_n)}u_{\mathbf{k}}(\mathbf{r} + \mathbf{R}_n) \quad (4.36)$$

Because for $\varphi_{\mathbf{k}}(\mathbf{r})$ the Bloch's theorem is valid, we obtain

$$T_{\mathbf{R}_n}\varphi_{\mathbf{k}}(\mathbf{r}) = e^{i\mathbf{k}\mathbf{R}_n}\varphi_{\mathbf{k}}(\mathbf{r}) \quad (4.37)$$

$$= e^{i\mathbf{k}\mathbf{R}_n}e^{i\mathbf{k}\mathbf{r}}u_{\mathbf{k}}(\mathbf{r}) \quad (4.38)$$

³For the proof of this we refer to text books on group theory (e.g. Tinkham).

⁴This was found by Bloch during his PhD thesis, which he carried out in the group of Seitz, but initially he was not aware of the importance of this result.

From this we obtain the equation

$$u_{\mathbf{k}}(\mathbf{r} + \mathbf{R}_n) = u_{\mathbf{k}}(\mathbf{r}) \quad (4.39)$$

The function $u_{\mathbf{k}}(\mathbf{r})$ has the periodicity of the Bravais lattice. This can be formulated as follows: The solutions of the single-particle Schrödinger equation of a periodic crystal have the form of a plane wave that is modulated by a function with lattice periodicity. $\varphi_{\mathbf{k}}(\mathbf{r})$ generally does not have the periodicity of the lattice, but $|\varphi_{\mathbf{k}}(\mathbf{r})|^2$. This gives rise to a second formulation of Bloch's theorem: Due to the translational invariance of the Hamilton operator the eigenfunctions have the following form:

$$\varphi_{\mathbf{k}}(\mathbf{r}) = e^{i\mathbf{k}\mathbf{r}} u_{\mathbf{k}}(\mathbf{r}) \quad \text{with } u_{\mathbf{k}}(\mathbf{r}) \text{ having the periodicity of the Bravais lattice} \quad (4.40)$$

This form of the eigenfunctions of h gives a hint to the physical meaning of the vectors \mathbf{k} . When looking at the special case $v^{\text{eff}}(\mathbf{r}) = \text{constant}$ we know that the solutions are simple plane waves:

$$\varphi_{\mathbf{k}}(\mathbf{r}) = \frac{1}{\sqrt{V_g}} e^{i\mathbf{k}\mathbf{r}} \quad (4.41)$$

I.e., in this case the function $u_{\mathbf{k}}(\mathbf{r})$ is constant. V_g is the volume of the base region. This means: When going to a constant potential (infinitesimal translational invariance) \mathbf{k} becomes identical to the wave vector. We note that the vector \mathbf{k} , as appearing here, (for crystals) is not uniquely defined. This is because different vectors \mathbf{k} yield the same eigenvalue $e^{i\mathbf{k}\mathbf{R}_n}$ of $T_{\mathbf{R}_n}$. This will be investigated more closely now.

4.3 The Reciprocal Lattice

Since the vector \mathbf{k} appears in a scalar product and in an exponent, it is not uniquely defined. We have

$$e^{i\mathbf{k}'\mathbf{R}_n} = e^{i\mathbf{k}\mathbf{R}_n} \quad \text{for } \mathbf{k}' = \mathbf{k} + \mathbf{G}_m \quad , \quad (4.42)$$

if

$$\mathbf{G}_m \mathbf{R}_n = 2\pi N \quad \text{with } N \text{ integer} \quad . \quad (4.43)$$

All vectors \mathbf{k}' defined by Eq. (4.42) label the same eigenvalue and the same eigenfunction of $T_{\mathbf{R}_n}$. How does the set of \mathbf{G} -vectors defined by (4.42) look like? We define:

$$\begin{aligned} \mathbf{b}_1 &= \frac{2\pi}{\Omega} (\mathbf{a}_2 \times \mathbf{a}_3) \\ \mathbf{b}_2 &= \frac{2\pi}{\Omega} (\mathbf{a}_3 \times \mathbf{a}_1) \\ \mathbf{b}_3 &= \frac{2\pi}{\Omega} (\mathbf{a}_1 \times \mathbf{a}_2) \end{aligned} \quad (4.44)$$

Here the vectors \mathbf{a}_i shall be the primitive vectors and $\Omega = \mathbf{a}_1(\mathbf{a}_2 \times \mathbf{a}_3)$ is the volume of the primitive unit cell. The vectors \mathbf{G}_m then are

$$\mathbf{G}_m = m_1 \mathbf{b}_1 + m_2 \mathbf{b}_2 + m_3 \mathbf{b}_3 \quad (4.45)$$

direct lattice	reciprocal lattice
sc	sc
hexagonal	hexagonal
fcc	bcc
bcc	fcc

Table 4.6: Four important Bravais lattices in direct space and the corresponding Bravais lattices in reciprocal space.

with m_i being an integer number. This lattice of \mathbf{G}_m -vectors defined in \mathbf{k} space is called the reciprocal lattice. (Vectors in real space have the dimension length. Vectors in reciprocal space have the dimension $1/\text{length}$.)

The vectors of the reciprocal lattice satisfy the condition (Eq. (4.43)), and the basis vectors of the reciprocal lattice are defined by Eq. (4.44), or by

$$\mathbf{a}_i \mathbf{b}_j = 2\pi \delta_{i,j} \quad . \quad (4.46)$$

The set $\{\mathbf{k} + \mathbf{G}_m\}$ with an arbitrary vector \mathbf{G}_m from reciprocal space labels the eigenfunctions and eigenvalues of the single-particle Schrödinger equation. In order to label this set we use the shortest vector of the set $\{\mathbf{k} + \mathbf{G}_m\}$. From the definition (4.45) we obtain that the reciprocal lattice is a Bravais lattice. Therefore we consider only those \mathbf{k} -vectors, which are closer to point $\mathbf{k} = 0$ (or $\mathbf{G} = 0$) than to any other point of the reciprocal lattice. Such a region of the reciprocal lattice is called “first Brillouin zone” (the corresponding region of the direct lattice is called the “Wigner-Seitz cell”). A two-dimensional example is shown in Fig. 4.11. The construction of Brillouin zones for three-dimensional Bravais lattices is somewhat more complex, but of course also just geometry.

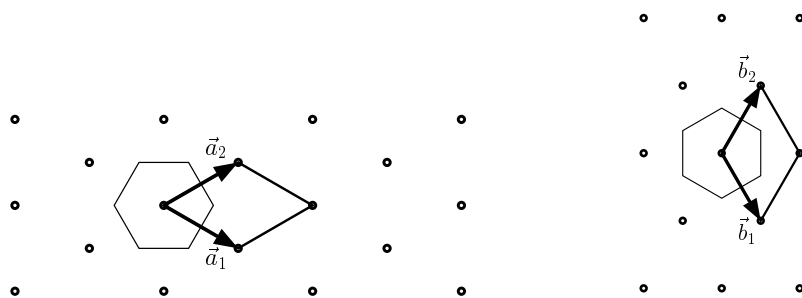


Figure 4.11: A two-dimensional rhombic point lattice. On the left the direct lattice and the Wigner-Seitz cell are shown, and on the right the corresponding reciprocal lattice with the first Brillouin zone.

It can easily be confirmed that the relations between the direct and the reciprocal lattice noted in Table 4.6 are valid. Fig. 4.12 shows the 1st Brillouin zone of four important direct lattices: sc, fcc, bcc, and hexagonal. The point $\mathbf{k} = 0$ is always called Γ . Other directions and points also have specific labels. Later we will need $\epsilon(\mathbf{k})$ for the full range of the Brillouin-Zone of the crystal. For this purpose it is often sufficient to investigate

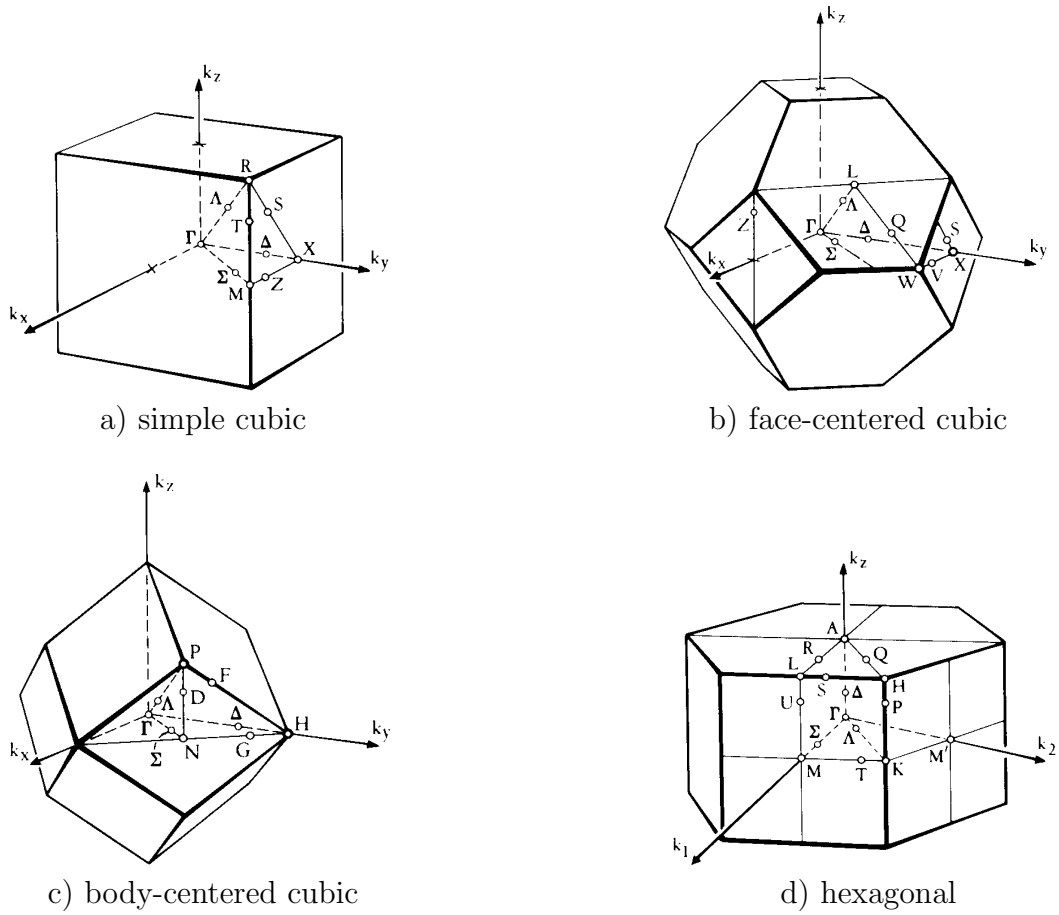


Figure 4.12: Brillouin zones for the simple cubic a), face-centered cubic b), body-centered cubic c), and hexagonal lattice d). The most important symmetry points and lines and their labels are shown.

the function along certain directions or in a small part of the 1st Brillouin zone. The rest is determined by the point symmetry of the lattice. This will be discussed later. Now we will investigate the physical meaning of the reciprocal lattice and of the 1. Brillouin zone for the wave functions of the effective single-particle Schrödinger equation. Due to the translational invariance for the effective potential, $v^{\text{eff}}(\mathbf{r} + \mathbf{R}_n) = v^{\text{eff}}(\mathbf{r})$, only the vectors of the reciprocal lattice appear in the Fourier expansion:

$$v^{\text{eff}}(\mathbf{r}) = \sum_l v^{\text{eff}}(\mathbf{G}_l) e^{i\mathbf{G}_l \mathbf{r}} \quad (4.47)$$

with $\mathbf{G}_l \mathbf{R}_n = 2\pi N$.

For the eigenfunctions of the Schrödinger equation we obtain in a similar way:

$$\varphi_{\mathbf{k}}(\mathbf{r}) = e^{i\mathbf{k}\mathbf{r}} u_{\mathbf{k}}(\mathbf{r}) = e^{i\mathbf{k}\mathbf{r}} \sum_m C_{\mathbf{G}_m}(\mathbf{k}) e^{i\mathbf{G}_m \mathbf{r}} \quad (4.48)$$

Then, the Kohn-Sham equation in reciprocal space is:

$$\begin{aligned} & \sum_m \frac{\hbar^2}{2m} (\mathbf{k} + \mathbf{G}_m)^2 C_{\mathbf{G}_m}(\mathbf{k}) e^{i(\mathbf{k} + \mathbf{G}_m)\mathbf{r}} + \sum_l v^{\text{eff}}(\mathbf{G}_l) \sum_m C_{\mathbf{G}_m}(\mathbf{k}) e^{i(\mathbf{k} + \mathbf{G}_m + \mathbf{G}_l)\mathbf{r}} \\ &= \epsilon(\mathbf{k}) \sum_m C_{\mathbf{G}_m}(\mathbf{k}) e^{i(\mathbf{k} + \mathbf{G}_m)\mathbf{r}} \end{aligned} \quad (4.49)$$

For the $C_{\mathbf{G}_m}(\mathbf{k})$ this means:

$$\frac{\hbar^2}{2m} (\mathbf{k} + \mathbf{G}_n)^2 C_{\mathbf{G}_n}(\mathbf{k}) + \sum_m v^{\text{eff}}(\mathbf{G}_n - \mathbf{G}_m) C_{\mathbf{G}_m}(\mathbf{k}) = \epsilon(\mathbf{k}) C_{\mathbf{G}_n}(\mathbf{k}) \quad (4.50)$$

For any chosen \mathbf{k} = vector of the 1st Brillouin zone this is a set of equations, which for a certain (given) \mathbf{k} allows for the calculation of the expansion coefficients $C_{\mathbf{G}_n}(\mathbf{k})$. Only those coefficients $C_{\mathbf{G}_n}(\mathbf{k})$ (or plane waves $e^{i(\mathbf{k} + \mathbf{G}_n)\mathbf{r}}$) are coupled by the periodic potential $v^{\text{eff}}(\mathbf{G}_n - \mathbf{G}_m)$, which differ by a reciprocal lattice vector. Equation (4.48) means that a plane wave $e^{i\mathbf{k}\mathbf{r}}$ in the solid does not exist alone, but due to diffraction at the periodic potential plane waves $e^{i(\mathbf{k} + \mathbf{G}_m)\mathbf{r}}$ are added. Equation (4.50) can also be written in matrix form:

$$\sum_m h_{n,m} C_{\mathbf{G}_m}(\mathbf{k}) = \epsilon(\mathbf{k}) C_{\mathbf{G}_n}(\mathbf{k}) \quad (4.51)$$

with

$$h_{n,m} = \frac{\hbar^2}{2m} (\mathbf{k} + \mathbf{G}_n)^2 \delta_{n,m} + v^{\text{eff}}(\mathbf{G}_n - \mathbf{G}_m) \quad (4.52)$$

This means that for each vector \mathbf{k} one matrix equation has to be solved, which provides a number of eigenfunctions and eigenvalues. Therefore, next to \mathbf{k} another quantum number will be introduced and we write: $\varphi_{n,\mathbf{k}}(\mathbf{r})$, $\epsilon_n(\mathbf{k})$. We find that equation (4.50) or (4.51) and (4.52) are often quite useful for real systems and can be calculated. This is in particular pronounced if it is combined with the so-called pseudopotential theory (cf. part V). The main problem is the dimension of the matrix of Eq. (4.53), and in particular the calculation of the non-diagonal elements or the sums in Eq. (4.50). We find that $v^{\text{eff}}(\mathbf{G}_l)$ rapidly decreases with increasing length of the \mathbf{G}_l and often only the first terms in $v^{\text{eff}}(\mathbf{G}_l)$ differ from zero. If this is true, then the evaluation of Eq. (4.50) or (4.51) and (4.52) is possible, because the non-diagonal part of the matrix $h_{n,m}$ is then of finite size. We have introduced two quantum numbers: the vector \mathbf{k} , which is limited to the first Brillouin zone and the discrete index n . In order to illustrate this on a simple level, we examine a one-dimensional example and a very weakly varying potential. Then, the energies are

$$\epsilon_n(\mathbf{k}) \approx \frac{\hbar^2}{2m} (\mathbf{k} + \mathbf{G}_n)^2 \quad . \quad (4.53)$$

Figure 4.13 shows the parabola for $\mathbf{G} = 0$ as a dotted line. We have found that due to periodicity it is reasonable and sufficient to constrain \mathbf{k} to the first Brillouin zone. This is possible if we look at $\mathbf{k} + \mathbf{G}_n$, i.e., if we fold back parts, which are outside the first Brillouin zone, of the dotted curve, by a suitable vector \mathbf{G}_n . The part of Fig. 4.14 in the range of the 1st Brillouin zone, or the function $\epsilon_n(\mathbf{k})$ is called the “band structure”.

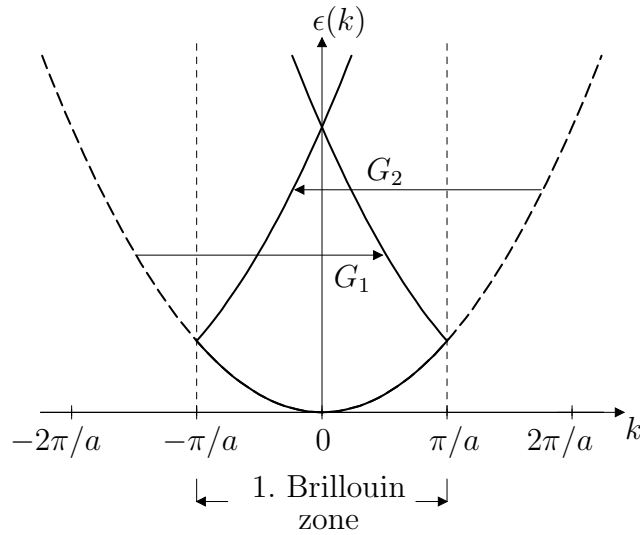


Figure 4.13: First Brillouin zone of a one-dimensional lattice of lattice constant a . \mathbf{G}_1 and \mathbf{G}_2 are the shortest non-zero reciprocal lattice vectors (length $2\pi/a$). The straight line gives the function $\epsilon_n(\mathbf{k})$.

For the further discussion of the importance of the reciprocal lattice we have taken a side view at a crystal (cf. Fig. 4.14). We can see that the Bravais point lattice can also be regarded as a regular arrangement of planes. There is a close relation between the vectors of the reciprocal lattice and such parallel planes (the straight, the dashed-dotted and the dashed planes in Fig. 4.14): For each family of lattice planes being separated by a distance d there are reciprocal lattice vectors perpendicular to these planes. The shortest of these reciprocal lattice vectors has the length $2\pi/d$. The inverse of this statement is also true: For each reciprocal lattice vector \mathbf{G} there is a family of lattice planes perpendicular to \mathbf{G} . This close relation between planes of the crystal and the reciprocal lattice vectors implies that one generally can label the planes in the crystal lattice by the shortest reciprocal lattice vector being perpendicular to these planes.

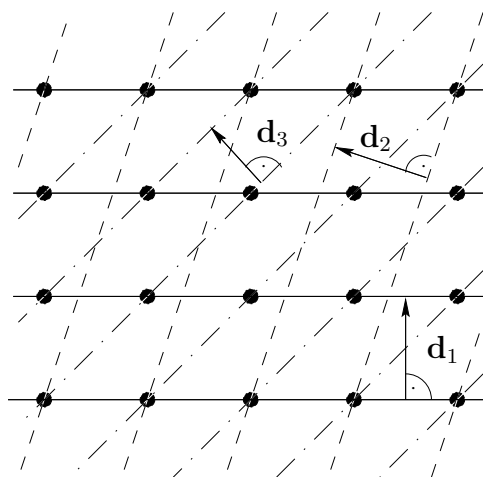


Figure 4.14: Side view of a crystal (i.e., of the Bravais point lattice)

These labels are called *Miller indices*. In general, they are defined by the coordinates of

the shortest possible reciprocal lattice vector of the *Bravais lattice* perpendicular to this plane; by definition, they are always integer numbers and have no common factor. Note that, usually, the Miller indices in any cubic lattice are referred to by the *conventional* (cubic) cell, which for the fcc- and bcc-lattices is a sc lattice with a basis. Figure 4.15 shows three important lattice planes for cubic crystals and their labels. In fcc and bcc lattices, this convention leads to a formal disconnection between lattice planes and actual reciprocal lattice vectors: Since the primitive cells (one atom per cell) of both lattices are smaller than the conventional cell (2 atoms for bcc, 4 atoms for fcc), some of their reciprocal lattice vectors appear to be missing when written down in a in the “simple cubic” notation. For example, for the bcc lattice we find that only (i, j, k) with $i + j + k = \text{even number}$ is allowed, for the fcc lattice the indices of reciprocal lattice vectors have to be either all odd or all even numbers. Thus, the fcc, bcc, and sc lattices all have (111) lattice planes as denoted by Miller indices and shown in Fig. 4.15, but the shortest corresponding reciprocal lattice vector in bcc would have the indices (222).

Now we have a look at the origin of a reflection of electrons at (or in) a crystal, the crystal being composed of planes. At first we imagine that a plane wave of electrons or X-rays propagates with wave vector \mathbf{k} . From the discussion of Eq. (4.48) we know that this wave is not a stationary state (eigenstate). This is obtained without solving the Schrödinger equation.

The wave is reflected at the crystal planes (cf. Fig. 4.16). We have constructive interference (Bragg reflection), if the path difference of the waves scattered at different planes is a multiple of the wave vector,

$$2d \sin \theta = m\lambda = m \frac{2\pi}{|\mathbf{k}|} \quad , \quad (4.54)$$

where m is an arbitrary integer number and λ the wave length of the plane waves.

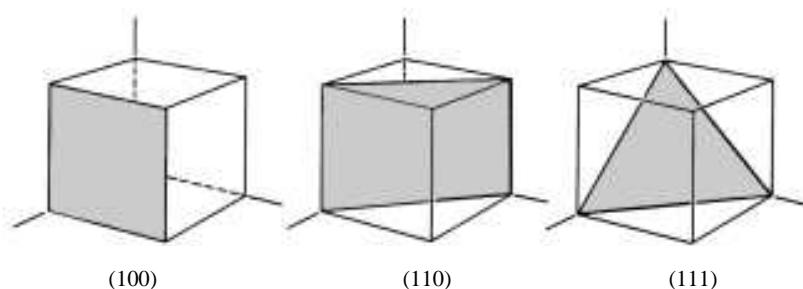


Figure 4.15: Important crystal planes in a cubic crystal

We rewrite this condition by using that there are reciprocal lattice vectors which are perpendicular to the planes of interest and which have the following length:

$$|\mathbf{G}_m| = m \frac{2\pi}{d} \quad (4.55)$$

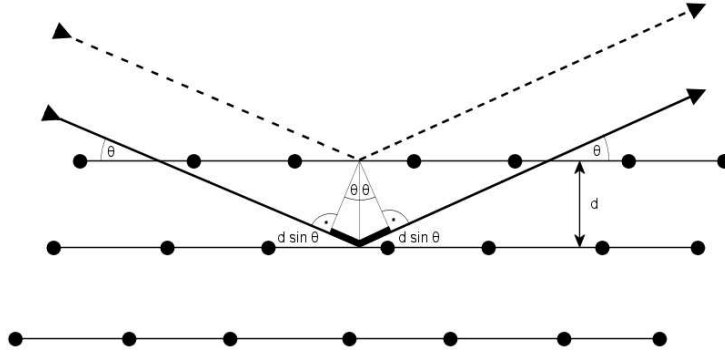


Figure 4.16: Bragg reflection at a crystal

From Eq. (4.54) we obtain

$$2d \frac{\mathbf{G}_m \mathbf{k}}{|\mathbf{G}_m| |\mathbf{k}|} = m \frac{2\pi}{|\mathbf{k}|} \quad . \quad (4.56)$$

Here, we use that

$$\mathbf{k} \mathbf{G}_m = |\mathbf{k}| |\mathbf{G}_m| \sin \theta \quad .$$

The condition for constructive interference (cf. Eq. (4.56)) can also be written as:

$$2\mathbf{k} \mathbf{G}_m = |\mathbf{G}_m|^2 \quad (4.57)$$

or

$$\mathbf{k}^2 = (\mathbf{k} - \mathbf{G}_m)^2 \quad . \quad (4.58)$$

This means: Waves with wave vectors \mathbf{k} fulfilling the requirement (Eq. (4.58)) (i.e., the Bragg condition), cannot propagate in the crystal. They are reflected in other directions. The condition (Eq. (4.58)) is obviously fulfilled at the border of the Brillouin zone, i.e., $\mathbf{k} = \frac{\mathbf{G}_m}{2}$.

Chapter 5

The Band Structure of the Electrons

5.1 Introduction

In the Fourier representation, i.e., in the basis of plane waves,

$$\chi_n(\mathbf{k}) = \frac{1}{\sqrt{V_g}} e^{i(\mathbf{k} + \mathbf{G}_n)\mathbf{r}} \quad (5.1)$$

the Hamilton operator of the Kohn-Sham equation has the form:

$$h_{n,m} = \frac{\hbar^2}{2m} (\mathbf{k} + \mathbf{G}_n)^2 \delta_{n,m} + v^{\text{eff}}(\mathbf{G}_n - \mathbf{G}_m). \quad (5.2)$$

$v^{\text{eff}}(\mathbf{G}_n - \mathbf{G}_m)$ decreases with increasing length $|\mathbf{G}_n - \mathbf{G}_m|$, and thus $h_{n,m}$ is basically diagonal for large $|\mathbf{G}_n - \mathbf{G}_m|$. The corresponding eigenvalue equation enables the calculation of the energies and eigenfunctions for given \mathbf{k} .

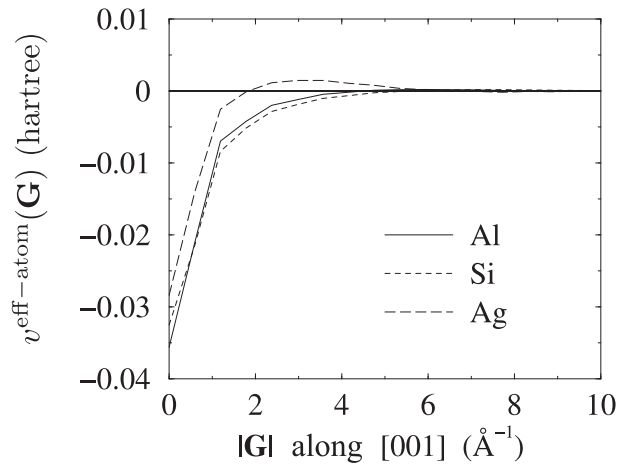


Figure 5.1: Fourier representation of the atomic potentials of Al, Si and Ag.

In Fig. 5.1 we show the function $v^{\text{eff}}(\mathbf{G})$ for three examples: Al, Si, and Ag. In fact, the figure shows the potential¹ of atoms and therefore, v^{eff} is defined for continuous values of $|\mathbf{G}|$. For a solid we have roughly

$$v^{\text{eff}}(\mathbf{r}) = \sum_{I=1}^M v^{\text{eff-atom}}(\mathbf{r} - \mathbf{R}_I) \quad ,$$

and then, in the Fourier representation $v^{\text{eff-atom}}$ is only needed at discrete reciprocal lattice vectors. These are determined by the lattice structure, and we have: $\frac{2\pi}{a} = 1.55 \text{ \AA}^{-1}$

¹To be precise, Fig. 5.1 shows the effective potential for atomic pseudopotentials. The definition of pseudopotentials is given in Section *tba.* below.

(Al), 1.16 \AA^{-1} (Si), and 1.54 \AA^{-1} (Ag).

If *all* Fourier components $v^{\text{eff}}(\mathbf{G}_l)$ are small, we obtain the dispersion of free electrons:

$$\epsilon_n(\mathbf{k}) = \frac{\hbar^2}{2m}(\mathbf{k} + \mathbf{G}_n)^2. \quad (5.3)$$

$\epsilon_n(\mathbf{k})$ as a function of \mathbf{k} is called the energy band n . For the one-dimensional case we have shown this dispersion before (cf. Fig. 4.13). However, the one-dimensional case is not typical, because in this case at most two-fold degeneracy can be present. Therefore, we will now discuss a two-dimensional example, which shows all the important characteristics of a band structure – even those of three-dimensional structures. We will investigate a hexagonal lattice. The 1st Brillouin zone and the labels of special \mathbf{k} -points are shown in Fig. 5.2. If we now evaluate Eq. (5.3), we obtain the band structure of free electrons, as shown in Fig. 5.3, for $\mathbf{G}_0 = (0, 0) = \Gamma$, $\mathbf{G}_1 = \frac{2\pi}{a}(0, 1)$, $\mathbf{G}_2 = \frac{2\pi}{a}(\cos 30^\circ, \sin 30^\circ) = \frac{2\pi}{a}(\frac{\sqrt{3}}{2}, \frac{1}{2})$, $\mathbf{G}_3 = \frac{2\pi}{a}(\cos 30^\circ, -\sin 30^\circ) = \frac{2\pi}{a}(\frac{\sqrt{3}}{2}, -\frac{1}{2})$, etc. Here, we restrict ourselves to the boundary of the so-called *irreducible wedge*, which is hatched in Fig. 5.2. By reflection and rotation of this wedge the full 1st Brillouin zone can be obtained.

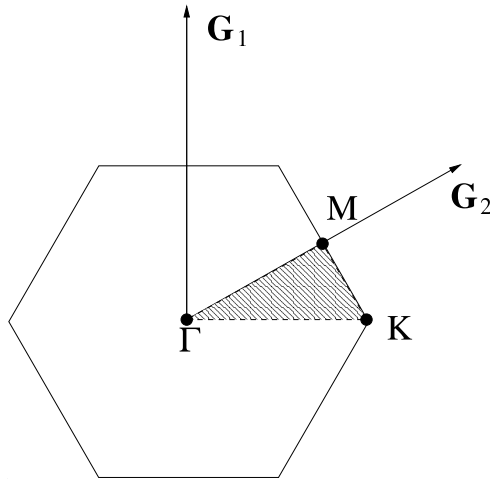


Figure 5.2: Brillouin zone of a hexagonal cell. Special \mathbf{k} -points are shown. The hatched area is the irreducible part.

The point \mathbf{K} is at $\frac{1}{3}(\mathbf{G}_2 + \mathbf{G}_3) = \frac{2\pi}{a}(\frac{1}{\sqrt{3}}, 0)$, and along the $\overline{\Gamma\mathbf{K}}$ -direction we have $\mathbf{k} = (k_x, 0)$. We obtain the results:

$$\begin{aligned} n = 0, \quad \text{i.e., } \mathbf{G}_0 : \quad \epsilon_0(\mathbf{k}) &= \frac{\hbar^2}{2m} k_x^2 \\ &\epsilon_0(\Gamma) = 0 \\ &\epsilon_0(\mathbf{K}) = \frac{\hbar^2}{2m} \left(\frac{2\pi}{a} \frac{1}{\sqrt{3}}\right)^2 \\ n = 1, \quad \text{i.e., } \mathbf{G}_1 : \quad \epsilon_1(\mathbf{k}) &= \frac{\hbar^2}{2m} \left(k_x^2 + \left(\frac{2\pi}{a}\right)^2\right) \\ &\epsilon_1(\Gamma) = \frac{\hbar^2}{2m} \left(\frac{2\pi}{a}\right)^2 \\ &\epsilon_1(\mathbf{K}) = \frac{\hbar^2}{2m} \left(\frac{1}{3} + 1\right) \cdot \left(\frac{2\pi}{a}\right)^2 \end{aligned}$$

$$\begin{aligned}
n = 2, \text{ i.e., } \mathbf{G}_2: \quad \epsilon_2(\mathbf{k}) &= \frac{\hbar^2}{2m} \left\{ \left(k_x + \frac{2\pi}{a} \frac{\sqrt{3}}{2} \right)^2 + \left(\frac{2\pi}{a} \right)^2 \cdot \frac{1}{4} \right\} \\
\epsilon_2(\Gamma) &= \frac{\hbar^2}{2m} \left(\frac{2\pi}{a} \right)^2 \left(\frac{3}{4} + \frac{1}{4} \right) \\
&= \frac{\hbar^2}{2m} \left(\frac{2\pi}{a} \right)^2 = \epsilon_1(\Gamma) \\
\epsilon_2(\mathbf{K}) &= \frac{\hbar^2}{2m} \left(\frac{2\pi}{a} \right)^2 \cdot \frac{7}{3}
\end{aligned}$$

etc.

The result for $\epsilon_n(\mathbf{k})$ is shown in Fig. 5.3. Even for free electrons the band structure – just because of the reduction to the 1st Brillouin zone – looks rather complicated.

Which modifications can we expect, if the potential – which has been zero so far – slightly differs from zero? This will be investigated in more detail now.

Plane waves with different \mathbf{G}_n are coupled by the crystal potential (Bragg-condition, hybridization of states), i.e., wave functions and eigenvalues are different:

$$\begin{aligned}
\frac{1}{\sqrt{V_g}} e^{i(\mathbf{k}+\mathbf{G}_n)\mathbf{r}} &\longrightarrow \varphi_{n,\mathbf{k}}(\mathbf{r}) = \sum_l c_{\mathbf{G}_n}(\mathbf{l}) e^{i(\mathbf{k}+\mathbf{G}_l)\mathbf{r}}, \\
\epsilon_n(\mathbf{k}) &\longrightarrow \epsilon_n(\mathbf{k}) + \Delta_n(\mathbf{k}) \quad .
\end{aligned}$$

For non-degenerate states the change of the energy levels is small ($\sim v^{\text{eff}}(\mathbf{G}_n)^2$), but it is larger for degenerate states² ($\sim v^{\text{eff}}$):

$$\Delta_n(\mathbf{k}) = \pm |v^{\text{eff}}(\mathbf{G}_n)| \quad . \quad (5.4)$$

Equation (5.4) describes the band structure close to the boundary of the 1st Brillouin zone. This is illustrated in Fig. 5.4. The representation of $\epsilon_n(\mathbf{k})$ in the domain of the 1st Brillouin zone is called a *reduced zone scheme*. Due to the equivalence of \mathbf{k} and $(\mathbf{k} + \mathbf{G})$ we can consider the bands $\epsilon_n(\mathbf{k})$ also as periodic functions in \mathbf{k} -space, as shown in Fig. 5.5 for a one-dimensional example. However, the “repeated zone scheme” and the “extended

²cf. e.g. Ashcroft/Mermin, Chapter 9 or Madelung, Chapters 18–19.

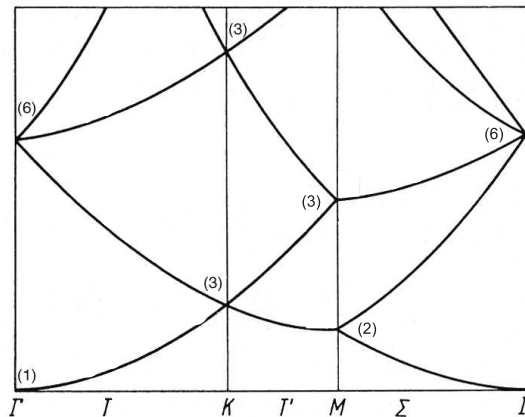


Figure 5.3: Band structure of free electrons in a hexagonal lattice. The numbers in brackets give the degeneracy.

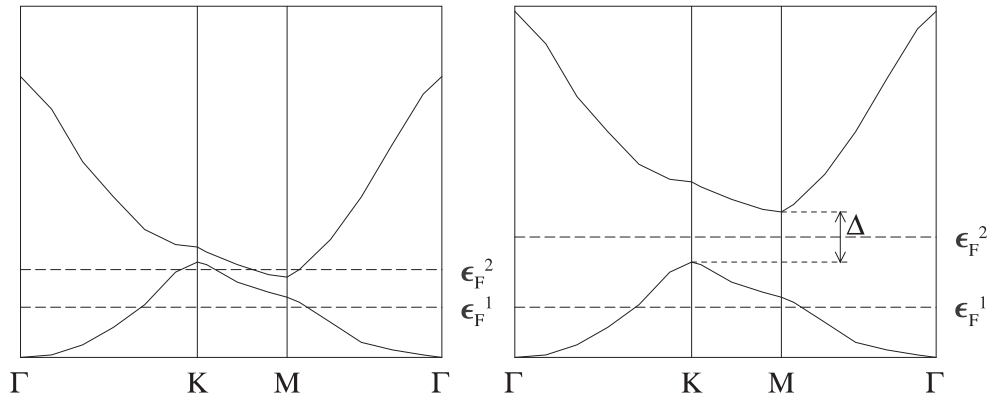


Figure 5.4: The band structure of *nearly* free electrons in a hexagonal lattice for two different systems and two different Fermi energies: ϵ_F^1 for 1 electron per cell and ϵ_F^2 for 2 electrons per cell.

zone scheme” illustrated in Fig. 5.5 are very rarely used.

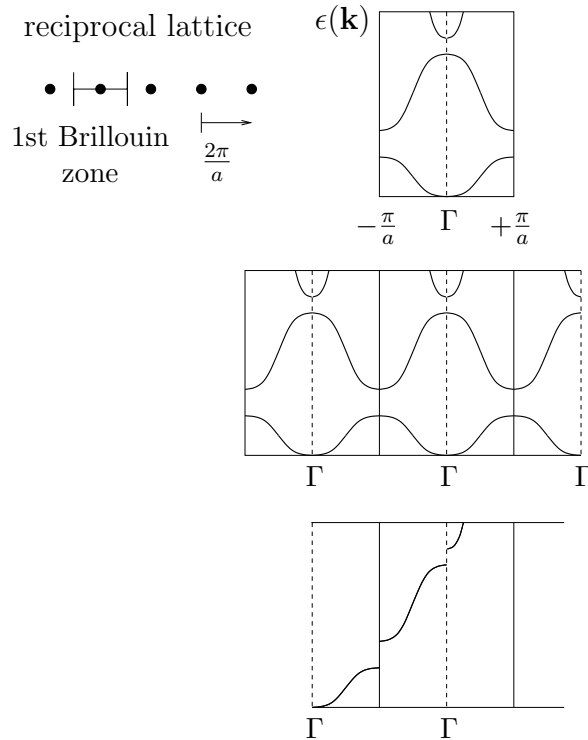


Figure 5.5: Three possible representations for $\epsilon_n(\mathbf{k})$ (one-dimensional example). **Top:** reduced zone scheme. **Middle:** repeated zone scheme. **Bottom:** extended zone scheme.

5.1.1 What Can We Learn from a Band Structure?

First we note that in a N electron system at $T = 0$ K the N lowest-energy states are occupied, i.e., each state $\varphi_{n,\mathbf{k}}(\mathbf{r})$ can be filled by two electrons: \uparrow and \downarrow . One band, i.e., a

function $\epsilon_n(\mathbf{k})$ with fixed n but variable \mathbf{k} ($\mathbf{k} \in 1\text{st BZ}$), can be occupied by

$$2 \int_{1.\text{BZ}} \frac{V_g}{(2\pi)^3} d^3k \quad (5.5)$$

electrons. The factor 2 takes into account the spin.

We have:

$$2 \int_{1.\text{BZ}} \frac{V_g}{(2\pi)^3} d^3k = 2 \frac{V_g}{(2\pi)^3} \frac{(2\pi)^3}{\Omega} = 2 \frac{V_g}{\Omega} = 2\hat{N} \quad . \quad (5.6)$$

One band can be filled by $2\hat{N}$ electrons, where \hat{N} is the number of unit cells in the base volume V_g , and Ω is the volume of the unit cell. Thus, one band can be filled by 2 electrons per primitive unit cell.

The number of electrons per primitive unit cell and the band structure determine important electric and optical properties of a solid, and we will now consider three special systems:

- **System #1: One electron per cell.**

This can be, for example, alkali metals or noble metals (Cu, Ag, Au). The lowest band of the band structure is then half filled, i.e., the Fermi energy is in the middle of the band (cf. Fig. 5.4, ϵ_F^1). Thus, directly above the highest occupied state there are unoccupied states. The energy required to excite an electron (to give it a higher kinetic energy), therefore is arbitrarily small. Such a system is an electric conductor.

- **System #2: Two electrons per cell and a band structure as in Fig. 5.4, left.**

If $\Delta < 0$, like in the left figure of Fig. 5.4, the Fermi energy is at ϵ_F^2 . Thus, the second band is partially filled while a fraction of the first band remains unoccupied. Also in this case the Fermi edge cuts bands, and thus also this system is a metal.

- **System #3: Two electrons per cell, and $\Delta > 0$ (Fig. 5.4, left).**

Then, the lowest band is filled, and the Fermi energy is in the band gap above this band. The band occupied at $T = 0K$ is called *valence band* (VB), the unoccupied band above the band gap is called *conduction band* (CB). The position of the Fermi energy is then set equal to the chemical potential at $T = 0K$. In this case the electrons require an energy of at least $E_{\text{gap}} = \Delta^{\text{KS}} + \Delta_{\text{xc}}$ for the excitation from an occupied to an unoccupied state. Here, Δ^{KS} is given by the Kohn-Sham eigenvalues calculated for the N -particle ground state:

$$\Delta^{\text{KS}} = \epsilon_{\text{LB}}^N - \epsilon_{\text{VB}}^N \quad .$$

The quantity Δ_{xc} is introduced here because in principle Δ^{KS} does not correspond to an excitation. We will come back to this point in Section *tba.* below. Systems with $E_{\text{gap}} \neq 0$ consequently are not electric conductors, but, depending on the size of the band gap $\Delta^{\text{KS}} + \Delta_{\text{xc}}$, they are called insulators or semiconductors.

The size of the band gap determines, for instance, the appearance of the material. The measured band gap is the difference between the ionization energy I (removal of an electron from the highest level of the valence band) and the affinity A (addition of an electron in the lowest level of the conduction band)³:

$$E_{\text{gap}} = I - A \quad , \quad (5.7)$$

$$A = E^N - E^{N+1} \quad , \quad (5.8)$$

$$I = E^{N-1} - E^N \quad . \quad (5.9)$$

From this we obtain

$$\begin{aligned} E_{\text{gap}} &= E^{N-1} - E^N + E^{N+1} - E^N \\ &= E^{N-1} + E^{N+1} - 2E^N \quad . \end{aligned} \quad (5.10)$$

Thus, for a correct evaluation of the band gap we need information for three different systems: The $N - 1$, N , and the $N + 1$ particle system. The Kohn-Sham eigenvalues are typically only evaluated for the N -particle system.

On the other hand for the Kohn-Sham eigenvalues we have:

$$A = E^N - E^{N+1} \approx -\epsilon_{\text{CB}}^{N+\frac{1}{2}} \quad , \quad (5.11)$$

$$I = E^{N-1} - E^N \approx -\epsilon_{\text{VB}}^{N+\frac{1}{2}} \quad , \quad (5.12)$$

where we assumed that $E^{\tilde{N}}$ is continuous and differentiable for $E^{N-1} < \tilde{N} < E^N$ and $E^N < \tilde{N} < E^{N+1}$. For integer values of \tilde{N} this may not be the case (c.f. the discussion on the Janak-Slater transition state, Eq. (3.197)).

For the band gap we then obtain

$$E_{\text{gap}} \approx \epsilon_{\text{CB}}^{N+\frac{1}{2}} - \epsilon_{\text{VB}}^{N-\frac{1}{2}} \quad (5.13)$$

$$= \epsilon_{\text{CB}}^N - \epsilon_{\text{VB}}^N + \Delta_{\text{xc}} \quad . \quad (5.14)$$

In the last line we used the Kohn-Sham eigenvalues only for the N -particle ground state and called the correction term Δ_{xc} .

At this point it is still controversially discussed if for the exact DFT the correction Δ_{xc} is there at all and, if it is, how big it may be.⁴ For the known approximations of the xc functional it is quite clear, however, that the difference of the Kohn-Sham eigenvalues ($\epsilon_{\text{CB}}^N - \epsilon_{\text{VB}}^N$) and the measured experimental band gap is indeed noticeable but much of this difference is due to the approximate treatment of xc. For the LDA, for example, the Kohn-Sham band gap underestimates the experimental band gap by about 50%. At this point, the only practical way to calculate a band gap is to leave DFT and to employ the many-body perturbation theory. Here, the so-called GW approximation (G is the Green function and W is the screened Coulomb interaction) is the state-of-the-art approach (see Section *tba.* below).

³ I and A are both defined as positive quantities.

⁴For a recent discussion see P. Mori-Sanchez, A. J. Cohen, W. Yang, Phys. Rev. Lett. **100**, 146401 (2008).

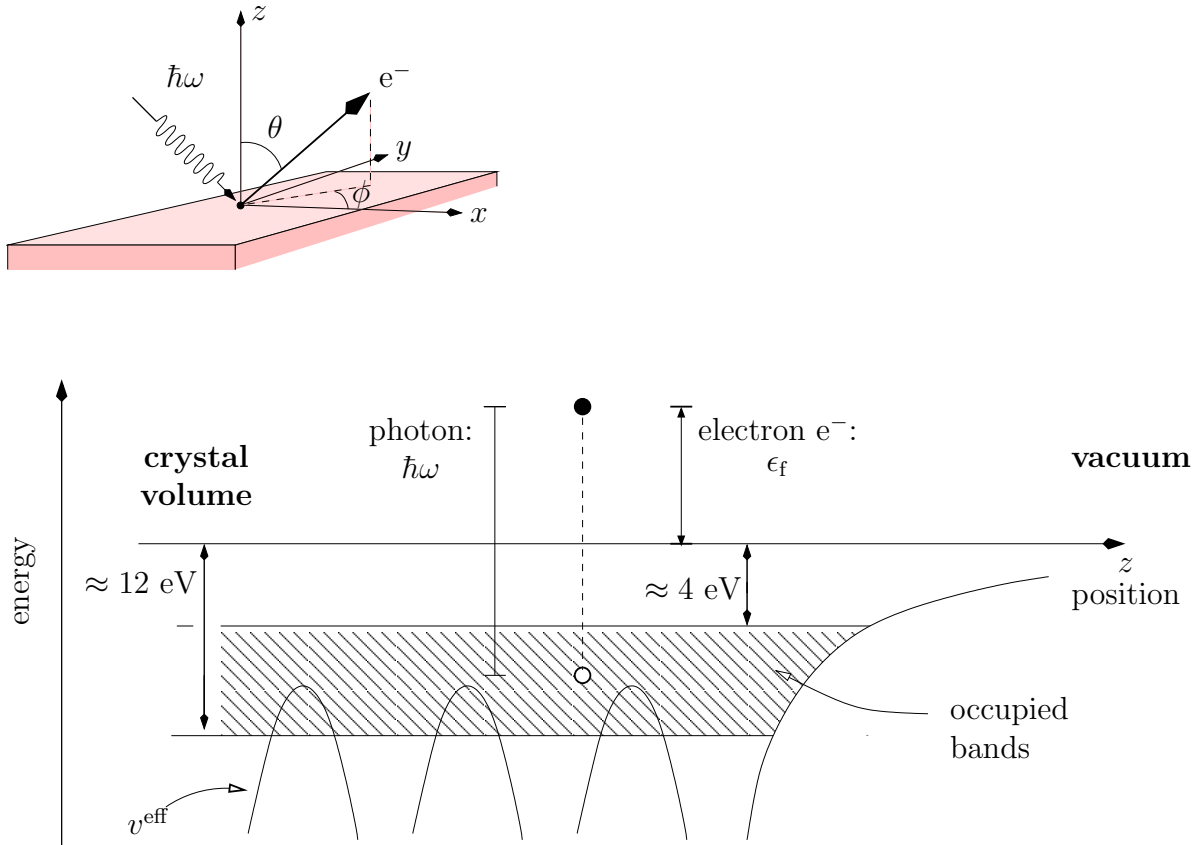


Figure 5.6: By measuring the intensity $I(\epsilon_f, \theta, \phi, \hbar\omega, e)$ of the electrons emitted by an optical excitation $\hbar\omega$ (ϵ_f is the kinetic energy of the emitted electrons in vacuum; \mathbf{e} and $\hbar\omega$ are the electric field vector and the energy of the light), information on the occupied states of the band structure can be obtained.

The quantity E_{gap} determines the appearance of the materials. If E_{gap} is lower than the energy of visible light⁵, the solid looks like a metal (e.g. Si: $E_{\text{gap}} = 1.1$ eV, or GaAs: $E_{\text{gap}} = 1.45$ eV). If the band gap is in the range of visible light or larger, the solid is transparent to light (e.g. GaP: $E_{\text{gap}} = 2.35$ eV looks orange because blue light is absorbed; diamond is clear and colorless: $E_{\text{gap}} \approx 6$ eV). For semiconductors E_{gap} is in the order of $0.5 \dots 5$ eV, so that at room temperature some electrons are excited (at 300 K we have $k_B \cdot T = 0.026$ eV). For insulators we have: $E_{\text{gap}} \gg k_B \cdot T$. The term “semiconductor” is not well defined, i.e., strictly speaking a semiconductor is an insulator with a not too large band gap. In my view this is, however, not a useful definition. Much more relevant is the following: A semiconductor is an insulator that can be doped (i.e., impurity atoms can be added) to generate charge carriers in the valence band and/or in the conduction band.

At the end of this paragraph we note that the band structure $\epsilon_n(\mathbf{k})$ can be studied experimentally. Angle-resolved photo emission (cf. Figs. 5.6 and 5.7) measures the electrons leaving the solid upon irradiation with light of energy $\hbar\omega$, mostly UV or X-rays. More precisely: One measures the kinetic energy ϵ_f of these electrons, the direction of their mo-

⁵Visible light is in the energy range $1.65 \text{ eV} < \hbar\omega < 3.1 \text{ eV}$.

tion \mathbf{k}_f and their number per unit time (the index “f” (“final”) refers to the final state). From this the energy of the occupied states $\epsilon_n(\mathbf{k}) \approx \epsilon_f - \hbar\omega$ and of the corresponding \mathbf{k} -vectors can be determined. Such experiments require a tunable light frequency and thus a synchrotron. They are carried out for example at BESSY in Berlin, and at many other “synchrotron light sources” in the world.

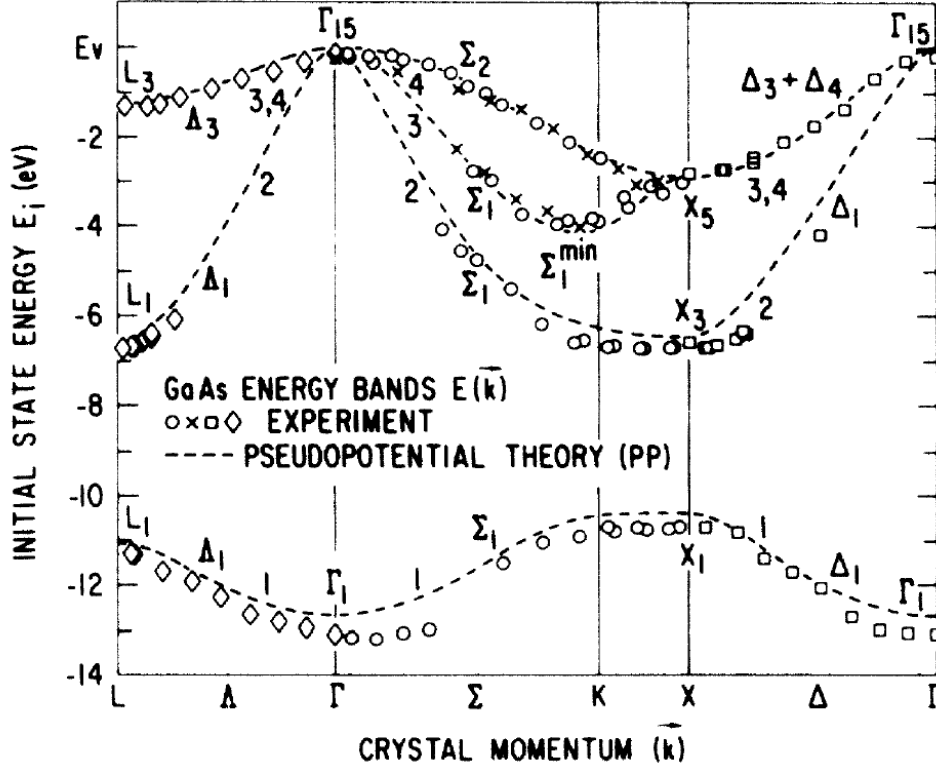


Figure 5.7: Comparison of a calculated empirical-pseudopotential band structure for GaAs (J.C. Phillips and K.C. Pandey, *Phys. Rev. Lett.* **30**, 787 (1973)) (dashed curve) with data measured by angle-resolved photo emission (T.C. Chiang, J.A. Knapp, M. Aono, and D.E. Eastman, *Phys. Rev. B* **21**, 3515 (1980)). For more recent band structures of the Kohn-Sham eigenvalues and using the LDA or the GGA the agreement is less good. In particular, the Kohn-Sham band gap between the top of the valence band and the bottom of the conduction band (not shown in the figure) is typically much smaller than the experimental one (at least when the LDA or GGA are used).

The theoretical band structure of Fig. 5.7 agrees very well with the experimental data. This clearly proves that the theory captures the right physics. However, the excellent quantitative agreement is also a consequence of the fact that this here was an *empirical* theory. *Ab initio* calculations are doing slightly worse for the bands. For the band gap, between VB and CB (not shown in Fig. 5.7), DFT is so far not doing well.

5.2 General Properties of $\epsilon_n(\mathbf{k})$

5.2.1 Continuity of $\epsilon_n(\mathbf{k})$ and Meaning of the First and Second Derivatives of $\epsilon_n(\mathbf{k})$

With

$$\varphi_{n,\mathbf{k}}(\mathbf{r}) = e^{i\mathbf{k}\mathbf{r}} u_{n,\mathbf{k}}(\mathbf{r}) \quad (5.15)$$

we have

$$\begin{aligned} h\varphi_{n,\mathbf{k}}(\mathbf{r}) &= \left[-\frac{\hbar^2}{2m} \nabla^2 + v^{\text{eff}}(\mathbf{r}) \right] e^{i\mathbf{k}\mathbf{r}} u_{n,\mathbf{k}}(\mathbf{r}) \\ &= e^{i\mathbf{k}\mathbf{r}} \left[-\frac{\hbar^2}{2m} \nabla^2 + v^{\text{eff}}(\mathbf{r}) + \frac{\hbar^2}{2m} k^2 - 2\frac{\hbar^2}{2m} i\mathbf{k}\nabla \right] u_{n,\mathbf{k}}(\mathbf{r}) \\ &= \epsilon_n(\mathbf{k}) e^{i\mathbf{k}\mathbf{r}} u_{n,\mathbf{k}}(\mathbf{r}) \quad . \end{aligned} \quad (5.16)$$

Thus

$$\epsilon_n(\mathbf{k}) = \int_{V_g} u_{n,\mathbf{k}}^*(\mathbf{r}) \cdot \tilde{h} u_{n,\mathbf{k}}(\mathbf{r}) d^3\mathbf{r} \quad , \quad (5.17)$$

with

$$\tilde{h}(\mathbf{k}) \equiv \left[-\frac{\hbar^2}{2m} \nabla^2 + v^{\text{eff}}(\mathbf{r}) + \frac{\hbar^2}{2m} k^2 - 2\frac{\hbar^2}{2m} i\mathbf{k}\nabla \right] \quad . \quad (5.18)$$

Thus, $\tilde{h}(\mathbf{k})$ determines the eigenvalue problem for given vectors $\mathbf{k} \in \text{BZ}$:

$$\tilde{h}(\mathbf{k}) u_{n,\mathbf{k}} = \epsilon_n(\mathbf{k}) u_{n,\mathbf{k}} \quad , \quad (5.19)$$

for which we only have to consider one primitive unit cell because $u_{n,\mathbf{k}}(\mathbf{r})$ is periodic. In order to investigate the analytical properties of $\epsilon_n(\mathbf{k})$ we look at the neighborhood of an arbitrary point \mathbf{k} . For $\mathbf{k} + \boldsymbol{\kappa}$ we then have

$$\epsilon_n(\mathbf{k} + \boldsymbol{\kappa}) = \int u_{n,\mathbf{k}+\boldsymbol{\kappa}}^*(\mathbf{r}) \tilde{h}(\mathbf{k} + \boldsymbol{\kappa}) u_{n,\mathbf{k}+\boldsymbol{\kappa}}(\mathbf{r}) d^3r \quad . \quad (5.20)$$

As long as $|\boldsymbol{\kappa}|$ is small, the difference between $\tilde{h}(\mathbf{k})$ and $\tilde{h}(\mathbf{k} + \boldsymbol{\kappa})$

$$\tilde{h}(\mathbf{k} + \boldsymbol{\kappa}) - \tilde{h}(\mathbf{k}) = \frac{\hbar^2}{2m} (\boldsymbol{\kappa}^2 + 2\mathbf{k}\boldsymbol{\kappa}) - \frac{\hbar^2}{2m} 2i\boldsymbol{\kappa}\nabla \quad (5.21)$$

is also small. It seems reasonable to calculate the energy $\epsilon_n(\mathbf{k} + \boldsymbol{\kappa})$ by perturbation theory, i.e., to expand the functions $u_{n,\mathbf{k}+\boldsymbol{\kappa}}(\mathbf{r})$ with respect to the functions $u_{n,\mathbf{k}}(\mathbf{r})$ of the unperturbed problem:

$$\begin{aligned} \epsilon_n(\mathbf{k} + \boldsymbol{\kappa}) &= \underbrace{\int u_{n,\mathbf{k}}^*(\mathbf{r}) \tilde{h}(\mathbf{k}) u_{n,\mathbf{k}}(\mathbf{r}) d^3r}_{0. \text{ Order}} \\ &\quad + \underbrace{\int u_{n,\mathbf{k}}^*(\mathbf{r}) \left\{ \frac{\hbar^2}{2m} (\boldsymbol{\kappa}^2 + 2\mathbf{k}\boldsymbol{\kappa}) - \frac{\hbar^2}{2m} 2i\boldsymbol{\kappa}\nabla \right\} u_{n,\mathbf{k}}(\mathbf{r}) d^3r}_{1. \text{ Order}} \end{aligned}$$

$$\begin{aligned}
& + \underbrace{\sum_{m \neq n} \frac{\left| \int u_{n,\mathbf{k}}^*(\mathbf{r}) \left\{ \frac{\hbar^2}{2m} (\kappa^2 + 2\mathbf{k}\boldsymbol{\kappa}) - \frac{\hbar^2}{2m} 2i\boldsymbol{\kappa}\nabla \right\} u_{m,\mathbf{k}}(\mathbf{r}) d^3r \right|^2}{\epsilon_n(\mathbf{k}) - \epsilon_m(\mathbf{k})}}_{2. \text{ Order}} \\
& + O(\kappa^3) \quad . \quad (5.22)
\end{aligned}$$

For convenience we now introduce the matrix element of the momentum operator:

$$\begin{aligned}
\mathbf{p}_{nm} & = \langle \varphi_{n,\mathbf{k}}(\mathbf{r}) | \frac{\hbar}{i} \nabla | \varphi_{m,\mathbf{k}}(\mathbf{r}) \rangle \\
& = \langle u_{n,\mathbf{k}}(\mathbf{r}) | \hbar \mathbf{k} + \frac{\hbar}{i} \nabla | u_{m,\mathbf{k}}(\mathbf{r}) \rangle \quad , \quad (5.23)
\end{aligned}$$

where the second equals sign is obtained from Bloch theorem. If we put Eq. (5.23) in Eq. (5.22) we obtain:

$$\begin{aligned}
\epsilon_n(\mathbf{k} + \boldsymbol{\kappa}) - \epsilon_n(\mathbf{k}) & = \frac{\hbar}{m} \boldsymbol{\kappa} \mathbf{p}_{nn} + \frac{\hbar^2}{2m} \kappa^2 \\
& + \frac{\hbar^2}{2m} \sum_{m \neq n} \frac{|\boldsymbol{\kappa} \mathbf{p}_{nm}|^2}{\epsilon_n(\mathbf{k}) - \epsilon_m(\mathbf{k})} + O(\kappa^3) \quad . \quad (5.24)
\end{aligned}$$

The limit $|\boldsymbol{\kappa}| \rightarrow 0$ illustrates that $\epsilon_n(\mathbf{k})$ is continuous as a function of \mathbf{k} , and that it is differentiable. Furthermore, we obtain the gradient $\nabla_{\mathbf{k}}$ of $\epsilon_n(\mathbf{k})$:

$$\mathbf{p}_{nn} = \frac{m}{\hbar} \nabla_{\mathbf{k}} \epsilon_n(\mathbf{k}) \quad . \quad (5.25)$$

The expectation value of the momentum operator therefore is not $\sim \mathbf{k}$, like for free electrons, but it is given by the gradient of the function $\epsilon_n(\mathbf{k})$. This is a rather important modification and, e.g., it may occur that \mathbf{p}_{nn} decreases with increasing \mathbf{k} .

For the second derivative of the energy $\epsilon_n(\mathbf{k})$ with respect to \mathbf{k} from Eq. (5.24) in the limit $|\boldsymbol{\kappa}| \rightarrow 0$ we obtain:

$$\frac{\partial^2}{\partial k_\alpha \partial k_\beta} \epsilon_n(\mathbf{k}) = \frac{\hbar^2}{m} \delta_{\alpha\beta} + \frac{\hbar^2}{m} \sum_{m \neq n} \frac{\text{Re}(p_{\alpha,nm} p_{\beta,nm}^*)}{\epsilon_n(\mathbf{k}) - \epsilon_m(\mathbf{k})} \quad . \quad (5.26)$$

For free electrons the second term on the right side of Eq. (5.26) vanishes, and the expression corresponds to the inverse of the inert mass of an electron. Close to maxima or minima of the band structure Bloch electrons behave as if they had a direction-dependent mass given by the tensor (5.26): This effective mass contains the effects due to the electron-lattice interaction and the electron-electron interaction. Using this concept (Eq. 5.26) and if we are interested in electronic states and their behavior at band extrema, the Hamilton operator can be simplified:

$$h = -\frac{\hbar^2}{2m} \nabla^2 + v^{\text{eff}}(\mathbf{r}) \quad \longrightarrow \quad \hat{h} = -\frac{\hbar^2}{2m^*} \nabla^2 \quad , \quad (5.27)$$

with

$$\frac{1}{m^*} = \frac{1}{\hbar^2} \frac{\partial^2 \epsilon_n(\mathbf{k})}{\partial k_\alpha \partial k_\beta} \quad . \quad (5.28)$$

Here $\frac{1}{m^*}$ is a tensor and the expression is reasonable only in the part of the Brillouin zone, where $\epsilon_n(\mathbf{k})$ to a good approximation has a parabolic shape. This is obviously a severe limitation, but in some later parts of this lecture the concept of the effective mass will prove useful.

In Fig. 5.8 we show the lower edges of the conduction bands of two semiconductors. An electron at the bottom of the conduction band of silicon (left figure) has a larger effective mass than an electron at the bottom of the conduction band in GaAs (right figure). Thus, the conduction band electrons in GaAs mobility is larger.

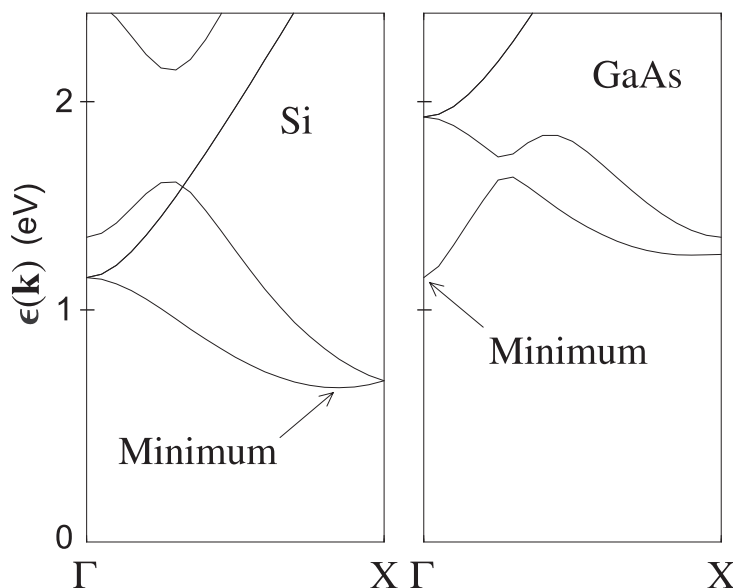


Figure 5.8: Band structure of the lower conduction band for two semiconductors, left Si and right GaAs. For the left system at the minimum the curvature is small. Thus, $1/m_{\text{eff}}$ is small, i.e., m_{eff} is large and the mobility of the charge carriers in this state is low. For the right system at the minimum the opposite is true, i.e., the mobility of the charge carriers at the minimum of the right system is high.

5.2.2 Time Reversal Symmetry

Further important properties of $\epsilon_n(\mathbf{k})$ are found when we consider the operation of time reversal T_t ⁶:

$$T_t: t \longrightarrow -t \quad . \quad (5.29)$$

This operator reverses the state of motion. For the time-independent Schrödinger equation this has the consequence that, since the position operator is invariant, spin and momentum operator change signs.

At first we want to investigate a system *without spin-orbit-coupling*, for which we have the Hamilton operator:

$$h = h^* \quad . \quad (5.30)$$

⁶cf. Madelung I., p. 107; Tinkham, p. 143.

We investigate two possibly different eigenfunctions of h , $\varphi_n(\mathbf{k}, \mathbf{r})$ and $\varphi_n^*(\mathbf{k}, \mathbf{r})$. Both functions are degenerate, because we have

$$h\varphi_n(\mathbf{k}, \mathbf{r}) = \epsilon_n(\mathbf{k})\varphi_n(\mathbf{k}, \mathbf{r}) \quad , \quad (5.31)$$

and with Eq. (5.30) conjugate complex:

$$h^*\varphi_n^*(\mathbf{r}) = h\varphi_n^*(\mathbf{k}, \mathbf{r}) = \epsilon_n(\mathbf{k})\varphi_n^*(\mathbf{k}, \mathbf{r}) \quad . \quad (5.32)$$

Are $\varphi_n(\mathbf{k}, \mathbf{r})$ and $\varphi_n^*(\mathbf{k}, \mathbf{r})$ physically different eigenfunctions? To answer this question we apply the translation operator to both functions:

$$T_{\mathbf{R}_I}\varphi_n(\mathbf{k}, \mathbf{r}) = e^{i\mathbf{k}\mathbf{R}_I}\varphi_n(\mathbf{k}, \mathbf{r}) \quad , \quad (5.33)$$

or

$$T_{\mathbf{R}_I}\varphi_n^*(\mathbf{k}, \mathbf{r}) = e^{-i\mathbf{k}\mathbf{R}_I}\varphi_n^*(\mathbf{k}, \mathbf{r}) \quad . \quad (5.34)$$

On the other hand we have:

$$T_{\mathbf{R}_I}\varphi_n(-\mathbf{k}, \mathbf{r}) = e_I^{-i\mathbf{k}\mathbf{R}}\varphi_n(-\mathbf{k}, \mathbf{r}) \quad . \quad (5.35)$$

For $\varphi_n(\mathbf{k}, \mathbf{r})$ we thus have the quantum numbers n and \mathbf{k} . On the other hand, for $\varphi_n^*(\mathbf{k}, \mathbf{r})$ and for $\varphi_n(-\mathbf{k}, \mathbf{r})$ the quantum numbers are n and $-\mathbf{k}$. Thus, $\varphi_n^*(\mathbf{k}, \mathbf{r})$ is identical to $\varphi_n(-\mathbf{k}, \mathbf{r})$. The energies of $\varphi_n(\mathbf{k}, \mathbf{r})$ and of $\varphi_n(-\mathbf{k}, \mathbf{r}) = \varphi_n^*(\mathbf{k}, \mathbf{r})$ are $\epsilon_n(\mathbf{k})$ and $\epsilon_n(-\mathbf{k})$, and with Eq. (5.31) we obtain:

$$\epsilon_n(\mathbf{k}) = \epsilon_n(-\mathbf{k}) \quad . \quad (5.36)$$

This degeneracy is often given also because of spatial inversion symmetry, but what we have just found is also valid if the crystal does not have spatial inversion symmetry.

Now we investigate the Hamilton operator of a single-particle problem *with Spin-Orbit-Coupling*:

$$h = \left[-\frac{\hbar^2}{2m}\nabla^2 + v^{\text{eff}}(\mathbf{r}) \right] \begin{pmatrix} 1 & 0 \\ 0 & 1 \end{pmatrix} + \frac{\hbar^2}{4m^2c^2}\boldsymbol{\sigma}(\nabla v^{\text{eff}}(\mathbf{r}) \times \frac{\hbar}{i}\nabla) \quad , \quad (5.37)$$

where the components of $\boldsymbol{\sigma}$ have the form

$$\sigma_x = \begin{pmatrix} 0 & 1 \\ 1 & 0 \end{pmatrix} \quad , \quad \sigma_y = \begin{pmatrix} 0 & -i \\ i & 0 \end{pmatrix} \quad , \quad \sigma_z = \begin{pmatrix} 1 & 0 \\ 0 & -1 \end{pmatrix} \quad . \quad (5.38)$$

To understand how the time-reversal operator acts on the various terms we note that “physical” operators can be separated into two classes, operators commuting with T_t , like e.g. the position operator:

$$T_t\mathbf{r} = \mathbf{r}T_t \quad , \quad (5.39)$$

and operators anticommutating with T_t , like e.g. the momentum and spin operators:

$$T_t\mathbf{p} = T_t\frac{\hbar}{i}\nabla = -\frac{\hbar}{i}\nabla T_t \quad , \quad (5.40)$$

$$T_t \boldsymbol{\sigma} = -\boldsymbol{\sigma} T_t \quad . \quad (5.41)$$

For the Hamilton operator without an external magnetic field we then have

$$[h, T_t] = 0 \quad , \quad (5.42)$$

which means

$$h\varphi = \epsilon\varphi \quad , \quad (5.43)$$

and

$$h(T_t\varphi) = \epsilon(T_t\varphi) \quad . \quad (5.44)$$

As long as φ and $T_t\varphi$ are linearly independent, both functions are degenerate. According to the definitions given above T_t can be defined by the following equation:

$$T_t = -i\sigma_y K \quad , \quad (5.45)$$

where K is the conjugator

$$K\varphi = \varphi^* \quad . \quad (5.46)$$

One can easily prove that the operator T_t defined this way has the required properties (note: σ_y acts on the two components of a spinor, not on \mathbf{r} or ∇):

$$(-i\sigma_y K)\mathbf{r} = \mathbf{r}(-i\sigma_y K) \quad (5.47)$$

$$(-i\sigma_y K)\frac{\hbar}{i}\nabla = -\frac{\hbar}{i}\nabla(-i\sigma_y K) \quad (5.48)$$

$$(-i\sigma_y K)\sigma_x = -\sigma_x(-i\sigma_y K) \quad (5.49)$$

etc.

In our single-particle problem the spin state is well defined. If we investigate a wave function with “spin up” (in the limit of \mathbf{j} - \mathbf{j} -coupling of the many-body system), we obtain:

$$T_t \begin{bmatrix} \psi \\ 0 \end{bmatrix} = -i\sigma_y K \begin{bmatrix} \psi \\ 0 \end{bmatrix} = \begin{bmatrix} 0 \\ \psi^* \end{bmatrix} \quad (5.50)$$

and analogous for “spin down”

$$T_t \begin{bmatrix} 0 \\ \psi \end{bmatrix} = - \begin{bmatrix} \psi^* \\ 0 \end{bmatrix} \quad . \quad (5.51)$$

Thus we have:

$$T_t^2\psi(\mathbf{r}, \sigma) = -\psi(\mathbf{r}, \sigma) \quad . \quad (5.52)$$

It is clear that ψ and $T_t\psi$ are orthogonal to each other, wave functions for “spin up” and “spin down”, respectively. Therefore, as noted in Eq. (5.43) and (5.44), generally we have that $\varphi_{n,\mathbf{k}}$ and $T_t\varphi_{n,\mathbf{k}}$ are linearly independent functions and that the energy level $\epsilon_n(\mathbf{k})$ is twofold degenerate.

Therefore, the eigenvalue ϵ of a single-particle problem is – independent of spatial symmetry – two-fold degenerate because of time-reversal symmetry:

$$\epsilon_n(\mathbf{k}, \uparrow) = \epsilon_n(-\mathbf{k}, \downarrow) \quad . \quad (5.53)$$

As long as spin polarization can be neglected, we have further:

$$\epsilon_n(\mathbf{k}, \uparrow) = \epsilon_n(\mathbf{k}, \downarrow) = \epsilon_n(-\mathbf{k}, \uparrow) = \epsilon_n(-\mathbf{k}, \downarrow) \quad , \quad (5.54)$$

i.e., 4-fold degeneracy!

5.2.3 The Fermi Surface

For metals at $T = 0\text{K}$ all single particle states with $\epsilon_n(\mathbf{k}) \leq \epsilon_F$ are occupied. This is in fact the definition of ϵ_F : For a finite N electron system we have $\epsilon_F = \epsilon_N$. For metals (infinite and periodic) there is a *Fermi surface*. It is defined by the equation

$$\epsilon_n(\mathbf{k}) = \epsilon_F \quad . \quad (5.55)$$

The Fermi surface is a surface of constant energy in \mathbf{k} -space. It separates the occupied from the unoccupied states. The Fermi surface consequently exists only for metals, because, if ϵ_F is in a band gap, condition (5.55) is never fulfilled. Then there is no Fermi surface. At first we investigate the Fermi surface for the example of electrons in jellium. The band

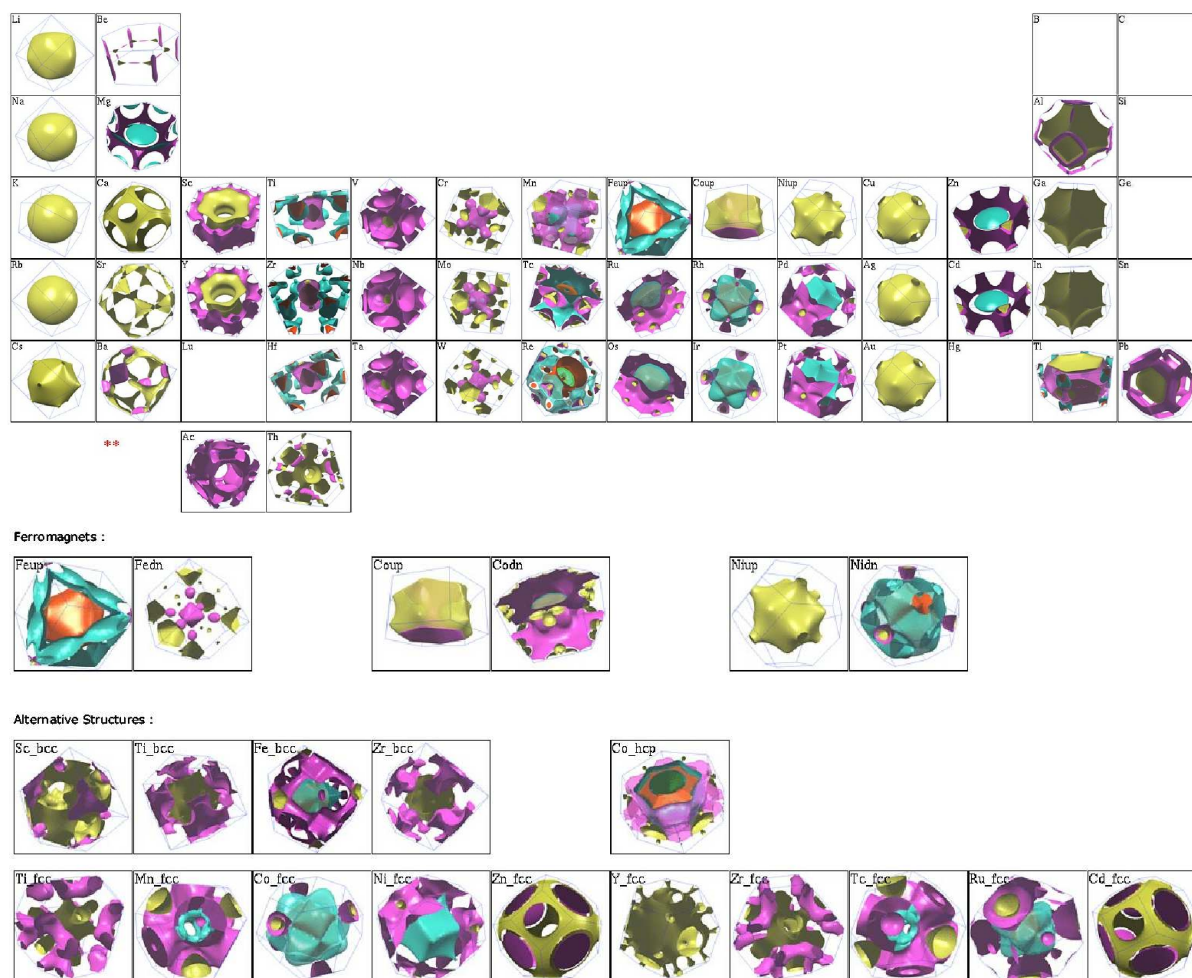


Figure 5.9: The Fermi Surface Database <http://www.phys.ufl.edu/fermisurface>

structure is given by

$$\epsilon(\mathbf{k}) = \frac{\hbar^2}{2m} k^2 \quad , \quad (5.56)$$

the Fermi-surface is thus the surface of a sphere of radius $|\mathbf{k}| = k_F = \sqrt{\frac{2m}{\hbar^2} \epsilon_F}$.

For nearly-free electrons in a periodic system the band structure looks more complicated and the Fermi surface as well. We have:

$$\epsilon_n(\mathbf{k}) = \frac{\hbar^2}{2m} (\mathbf{k} + \mathbf{G}_n)^2 \stackrel{!}{=} \epsilon_F \quad . \quad (5.57)$$

Sometimes only one band index n will contribute to the Fermi surface, but in general different n will contribute different sections.

And for the realistic materials, i.e., $v^{\text{eff}}(\mathbf{r}) \neq \text{const.}$, the Fermi surface looks again more complicated. Figure 5.9 shows some examples from “The Fermi Surface Database”. More details can be found on that webpage.

For the further, very detailed discussion of Fermi surfaces I refer to the Ashcroft-Mermin chapters 9, 14 and 15. This can be presented hardly better than there.

5.3 The LCAO (linear combination of atomic orbitals) Method

In part 5.1 we assumed that the potential of the solid, v^{eff} , is not particularly strong, and that the band structure is only a weak modification of the dispersion relation of free electrons. This led to the band structure in the approximation of nearly free electrons. This treatment is in principle exact, but typically $v^{\text{eff}}(\mathbf{r}) = \sum_{\mathbf{G}} v^{\text{eff}}(\mathbf{G}) e^{i\mathbf{G}\mathbf{r}}$ will have a very large number of Fourier components.

To get a feeling for the wave functions and energies, and for the forces that hold the solid together, also another point of view is possible. For this we now want to start with well separated atoms and investigate what happens if these atoms are brought closer together. In fact the situation present in a solid is rather in the middle between the properties of atoms or molecules and the ones describing the behavior of nearly free electrons. The various modern numerical methods for the calculation of the electronic structure of solids therefore combine both aspects in their methodology. Such methods, in particular the ab initio pseudopotential theory, the linearized muffin-tin orbital method (LMTO) and the linearized augmented plane waves method (LAPW) are discussed in this Chapter.

We start by reminding the reader about the **H₂ molecule**: Since the Hamilton operator (and the potential) has a reflection symmetry, we have: the eigenstates have to be either symmetric or antisymmetric with respect to this reflection plane. If we assume that the molecular eigenstates are linear combinations of the atomic $1s$ states $\hat{\varphi}_{1s}$ (cf. Fig. 5.10),

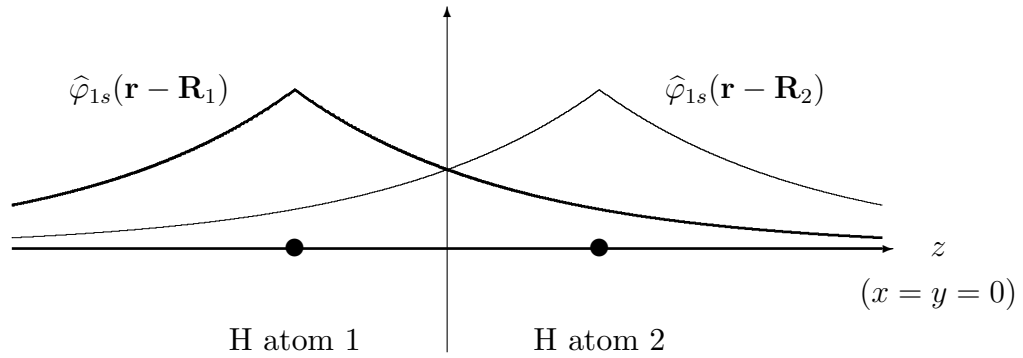


Figure 5.10: Schematic presentation of the atomic eigenstates of two H atoms in the H_2 molecule.

we have

$$\varphi_{1s}^b(\mathbf{r}) = \frac{1}{\sqrt{A}} (\hat{\varphi}_{1s}(\mathbf{r} - \mathbf{R}_1) + \hat{\varphi}_{1s}(\mathbf{r} - \mathbf{R}_2)) \quad , \quad (5.58)$$

$$\varphi_{1s}^a(\mathbf{r}) = \frac{1}{\sqrt{A}} (\hat{\varphi}_{1s}(\mathbf{r} - \mathbf{R}_1) - \hat{\varphi}_{1s}(\mathbf{r} - \mathbf{R}_2)) \quad , \quad (5.59)$$

where $1/\sqrt{A}$ ensures the normalization of the φ^b , φ^a to 1. This is illustrated in Fig. 5.11 and Fig. 5.12 shows the corresponding energy levels.

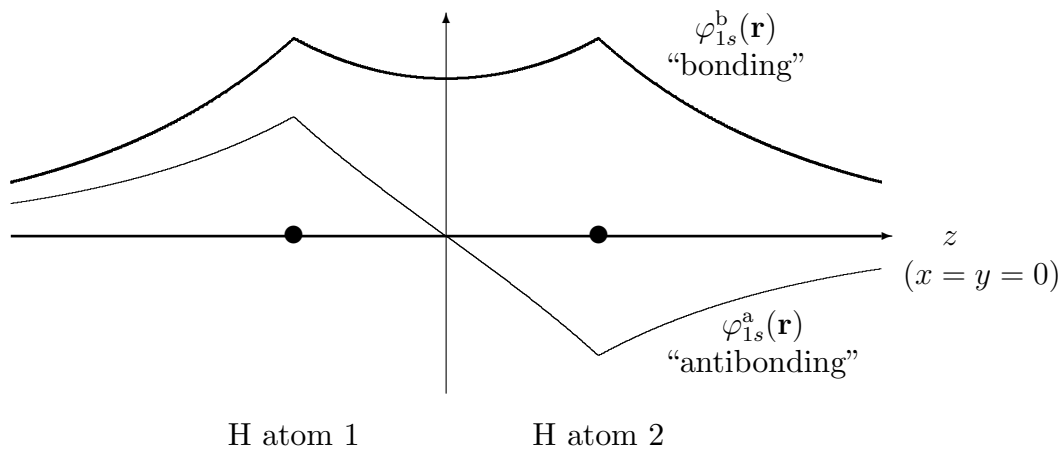


Figure 5.11: Schematic presentation of the electronic eigenstates in the H_2 molecule.

Thus, when the atoms get closer to each other, so that the wave functions start to overlap, there is a splitting of the energy levels:

ϵ_b : low energy (thus favored)

φ^b : $\oplus\oplus$: the electron density $|\phi_b|^2$ charge has a maximum between the nuclei

ϵ_a : high energy (thus unfavored)

φ^a : $\oplus\ominus$: the electron density $|\phi_a|^2$ is zero between the nuclei

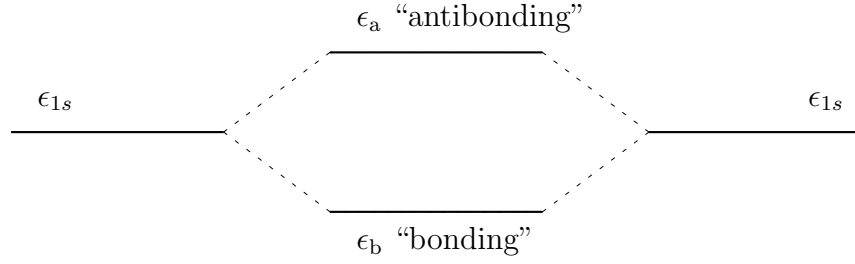


Figure 5.12: Schematic presentation of the electronic energy levels in the H_2 molecule

We now use the same concept to describe a solid, i.e. we use such atom-centered basis functions as basis set. The LCAO basis set for the representation of the wave functions in a solid or molecule is defined by:

$$\chi_\alpha(\mathbf{k}, \mathbf{r}) = \frac{1}{\sqrt{A}} \sum_{\mathbf{R}_I}^M \gamma_I(\mathbf{k}) \hat{\varphi}_\alpha(\mathbf{r} - \mathbf{R}_I) \quad (5.60)$$

with

- M : Number of atoms in the base region
- $\hat{\varphi}_\alpha(\mathbf{r} - \mathbf{R}_I)$: atom-like function,
centered at position \mathbf{R}_I , (e.g.
numerical solution of the atomic Kohn-Sham equation,
or Gaussians, or LMTOs with $\alpha = 1s, 2s, 2p, \dots$)

From the translation invariance in a periodic crystal it follows (Bloch's theorem) that

$$\gamma_I(\mathbf{k}) = e^{i\mathbf{k}\mathbf{R}_I} \quad . \quad (5.61)$$

Thus, there is an infinite number of phases: $e^{i\mathbf{k}\mathbf{R}_I} = +1 \dots -1$. Here, the value $+1$ refers to $\mathbf{k} = \mathbf{0}$ and the value -1 to the edge of the Brillouin zone: $\mathbf{k} = \frac{1}{2}\mathbf{G}$.

For normalization we choose the condition

$$\langle \hat{\varphi}_\alpha(\mathbf{r}) | \hat{\varphi}_\beta(\mathbf{r}) \rangle = \delta_{\alpha,\beta} \quad (5.62)$$

and

$$A = M = \text{number of atoms} \quad . \quad (5.63)$$

This yields that

$$\langle \chi_\alpha(\mathbf{k}, \mathbf{r}) | \chi_\beta(\mathbf{k}, \mathbf{r}) \rangle \longrightarrow \delta_{\alpha,\beta} \quad ,$$

when the lattice constant goes to ∞ .

The eigenfunctions of the single-particle hamiltonian are then written

$$\varphi_n(\mathbf{k}, \mathbf{r}) = \sum_{\beta} c_{n\beta}(\mathbf{k}) \chi_\beta(\mathbf{k}, \mathbf{r}) \quad (5.64)$$

and the matrix equation of the Kohn-Sham equation is

$$\sum_{\beta} [h_{\alpha\beta} - S_{\alpha\beta} \epsilon_n(\mathbf{k})] c_{n\beta}(\mathbf{k}) = 0 \quad , \quad (5.65)$$

with

$$h_{\alpha\beta} = \langle \chi_\alpha(\mathbf{k}, \mathbf{r}) | h | \chi_\beta(\mathbf{k}, \mathbf{r}) \rangle \quad (5.66)$$

$$= \frac{1}{M} \sum_{\mathbf{R}_I, \mathbf{R}_J} e^{i\mathbf{k}(\mathbf{R}_I - \mathbf{R}_J)} \langle \hat{\varphi}_\alpha(\mathbf{r} - \mathbf{R}_I) | h | \hat{\varphi}_\beta(\mathbf{r} - \mathbf{R}_J) \rangle$$

$$= \sum_{\mathbf{R}_I} e^{i\mathbf{k}\mathbf{R}_I} \underbrace{\langle \hat{\varphi}_\alpha(\mathbf{r} - \mathbf{R}_I) | h | \hat{\varphi}_\beta(\mathbf{r}) \rangle}_{\epsilon_{\alpha\beta}(\mathbf{R}_I)} \quad (5.67)$$

$$S_{\alpha\beta} = \langle \chi_\alpha(\mathbf{k}, \mathbf{r}) | \chi_\beta(\mathbf{k}, \mathbf{r}) \rangle \quad (5.68)$$

$$= \sum_{\mathbf{R}_I} e^{i\mathbf{k}\mathbf{R}_I} \underbrace{\langle \hat{\varphi}_\alpha(\mathbf{r} - \mathbf{R}_I) | \hat{\varphi}_\beta(\mathbf{r}) \rangle}_{s_{\alpha\beta}(\mathbf{R}_I)} . \quad (5.69)$$

The advantage of the LCAO method, i.e., of using atomic or atom-like orbitals for $\varphi_\alpha(\mathbf{r})$ is that these are very localized. The quantities $\epsilon_{\alpha\beta}(\mathbf{R}_I)$ and $s_{\alpha\beta}(\mathbf{R}_I)$ thus differ from zero only for very few \mathbf{R}_I (often only for $|\mathbf{R}_I| \leq 2$ or 3 interatomic distances). This results in a high numerical efficiency and good scaling with system size. Another advantage of the LCAO method is that the number of basis functions and consequently the dimension of the matrices in Eq. (5.65) can be kept very small. For a solid of hydrogen atoms or of alkali atoms (Na, Cs) as a first approximation (or for a qualitative discussion) it is sufficient to use only one basis function per atom:

$$\begin{aligned} \text{H} &: 1s \\ \text{Li} &: 2s \\ &: \\ \text{Cs} &: 6s \end{aligned} \quad (5.70)$$

For C, Si, Ge, GaAs one has to use at least four orbitals per atom:

$$\begin{aligned} \text{C} &: 2s, 2p_x, 2p_y, 2p_z \\ \text{Si} &: 3s, 3p_x, 3p_y, 3p_z \\ &: \end{aligned} \quad (5.71)$$

The “minimum basis sets” in the examples (5.70) and (5.71) allow for a qualitative description, for a more accurate quantitative description further orbitals have to be included.

What happens, when the atoms get closer to each other? Then the electronic energy levels of the atoms split. This is sketched in Fig. 5.13. For smaller distances the sharp energy levels become *energy bands*. The total number of all states is constant, i.e., independent of the distance of the atoms.

In the spirit of such LCAO basis sets and considering a “minimum basis” we now like to construct the band structure of a simple material.

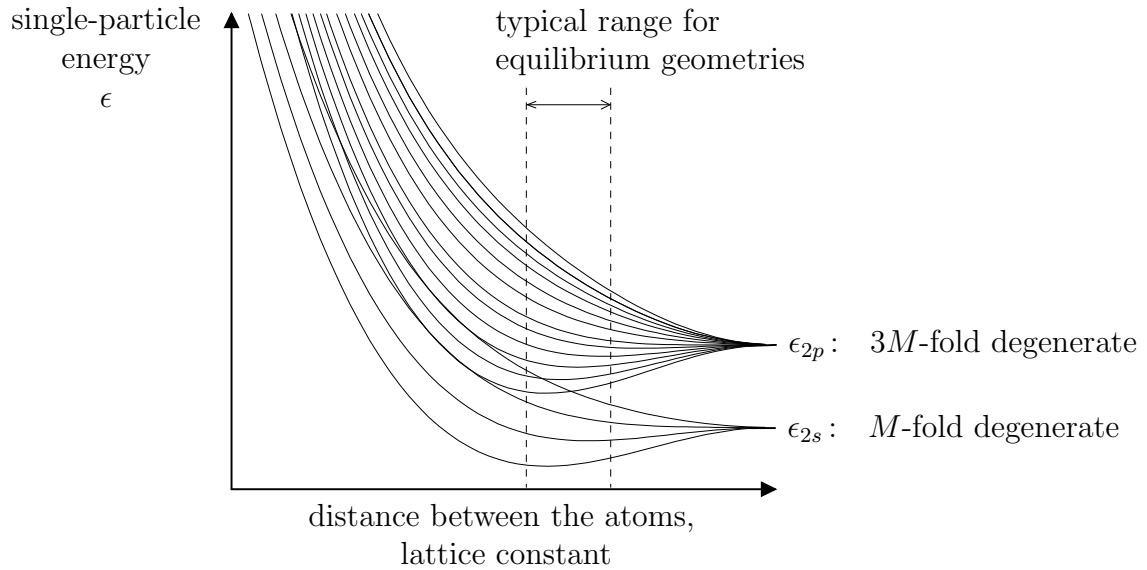


Figure 5.13: Schematic presentation of the energy levels of a solid as function of the interatomic distance. For large distances one obtains the energy levels of the free atoms.

5.3.1 Band Structure and Analysis of the Contributions to Chemical Bonding

We discuss a two-dimensional example. Although in part 5.1 we have used the hexagonal lattice, I now want to talk about the square lattice. Because of the orthogonality of the lattice vectors the discussion is somewhat simpler, cf. Fig. 5.14.

In a qualitative or semi-quantitative description of an s -band we will now just use one s -orbital per atom. An estimate of the relative energies at high symmetry points in the Brillouin zone is compiled in Table 5.1. Knowing about the continuity of the functions $\epsilon_n(\mathbf{k})$ we can now draw the qualitative band structure (Fig. 5.15).

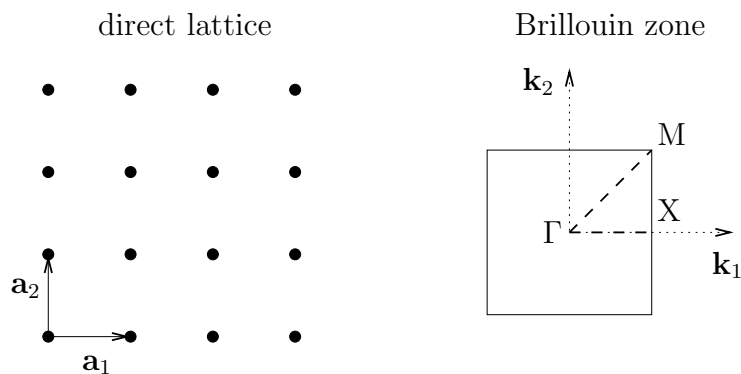


Figure 5.14: The two-dimensional square atomic lattice.

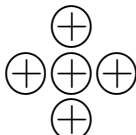
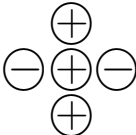
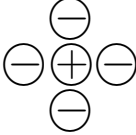
\mathbf{k} -point	$\varphi_s(\mathbf{k}, \mathbf{r})$	conclusion about the energy
Γ $\mathbf{k} = (0, 0)$		fully bonding \Rightarrow minimum of the energy
X $\mathbf{k} = (\frac{\pi}{a}, 0)$		half/ half \Rightarrow mid value energy
M $\mathbf{k} = (\frac{\pi}{a}, \frac{\pi}{a})$		fully antibonding \Rightarrow maximum of the energy

Table 5.1: Schematic picture of the Bloch states of an s -band of a square lattice. Compare with Eq. (5.60) for the basis function, with $\hat{\varphi}_\alpha = s$ -orbital. The Bloch state $\varphi_s(\mathbf{k}, \mathbf{r})$ is shown at one atom and its four nearest neighbors.

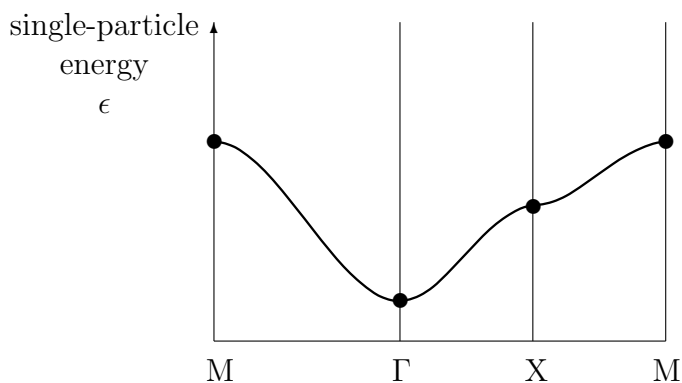


Figure 5.15: Band structure of s -orbitals of the square lattice (qualitative presentation). The dots mark the estimates obtained from Table 5.1.

For the band structure of p -states we discuss p_z (oriented perpendicular to the plane of the lattice) and p_x or p_y separately, because the two types of functions are for a two-dimensional system independent for symmetry reasons: p_z is antisymmetric with respect to the plane of the lattice, p_x and p_y are symmetric with respect to the plane of the lattice.

The illustrations of the wave functions of p_z look qualitatively the same as for s -states (at least when looking from the top on the lattice plane). The dispersion of p_z -orbitals is thus qualitatively the same as that of s -orbitals (cf. Fig. 5.15).

In Fig. 5.16 we summarize the results for these p_x , p_y -states, of the p_z -, and of the lower-lying s -states to the band structure shown in Fig. 5.16. We recognize that this band structure is similar to the result of nearly free electrons. The s - or p -band is similar to a

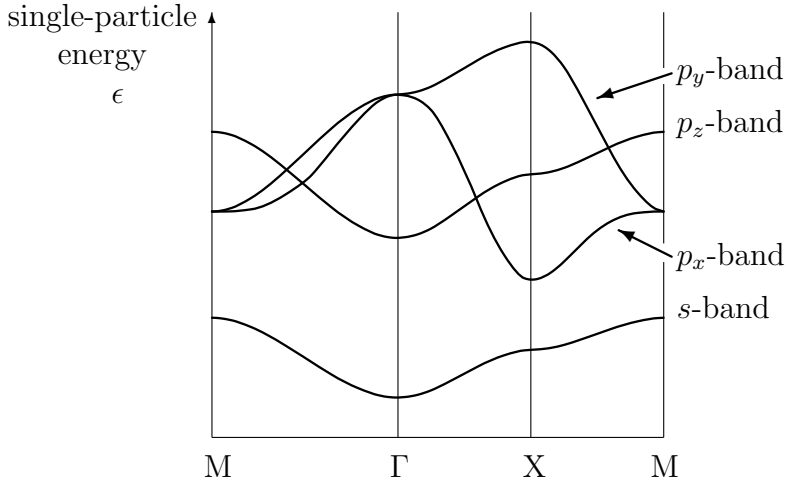


Figure 5.16: Band structure of s - and p - states in the square lattice (qualitative representation, the relative position of the p_z band with respect to the p_x -, p_y -band is chosen arbitrarily).

\mathbf{k} -point	$\varphi_{p_x}(\mathbf{k}, \mathbf{r})$	$\varphi_{p_y}(\mathbf{k}, \mathbf{r})$
Γ $\mathbf{k} = (0, 0)$		
	strongly antibonding	strongly antibonding
X $\mathbf{k} = (\frac{\pi}{a}, 0)$		
	fully bonding	fully antibonding
M $\mathbf{k} = (\frac{\pi}{a}, \frac{\pi}{a})$		
	strongly bonding	strongly bonding

Table 5.2: Schematic picture of the Bloch states of the p_x - and p_y -bands of a square lattice. Compare with Eq. (5.60) for the basis functions, with $\hat{\varphi}_\alpha = p_x$ - or p_y -orbital. The Bloch states $\varphi_{p_x}(\mathbf{k}, \mathbf{r})$ and $\varphi_{p_y}(\mathbf{k}, \mathbf{r})$ are shown at one atom and its four nearest neighbors.

parabola of free electrons, reduced to the 1st Brillouin zone and split at the points satisfying the Bragg-condition. This can also be shown mathematically, because a plane wave can be expanded in spherical harmonics:

$$e^{i\mathbf{k}\mathbf{r}} = 4\pi \sum_{l=0}^{\infty} \sum_{m=-l}^l i^l \sqrt{\frac{\pi}{2kr}} J_{l+1/2}(kr) Y_{lm}^*(\Omega_{\mathbf{k}}) Y_{lm}(\Omega_{\mathbf{r}}) \quad , \quad (5.72)$$

with $\Omega_{\mathbf{k}}$ and $\Omega_{\mathbf{r}}$ labelling the spatial angle and $J_{l+1/2}$ representing the Bessel function of index $l + \frac{1}{2}$.

The above discussion and explanation of the band structure clarifies the meaning of the quantum number \mathbf{k} . It describes the phase difference of orbitals that are centered at different atoms, and $\lambda = \frac{2\pi}{|\mathbf{k}|}$ is the wave length of the wave function. In a diatomic molecule there are only two phases: bonding and antibonding (or $+1$ and -1). In a crystalline solid there are an infinite number of phases covering the full range from “bonding” to “antibonding” with respect to the nearest neighbor interaction. The more bonding states are occupied (compared to antibonding states) the stronger bound (the more stable) is the material (e.g. Fe has a higher cohesive energy than Cu).

5.4 The Density of States, $N(\epsilon)$

The density of states is defined as the number of states per unit volume at the energy ϵ :

$$N(\epsilon) = \sum_n \frac{2}{(2\pi)^3} \int_{\text{1.BZ}} \delta(\epsilon - \epsilon_n(\mathbf{k})) d^3k \quad . \quad (5.73)$$

We want to write $N(\epsilon)$ differently to point out the characteristic structure, which enables a relatively direct comparison between band structure and density of states.

For this purpose we write the number of states per unit volume $[\epsilon, \epsilon + d\epsilon]$ as follows:

$$N(\epsilon)d\epsilon = \sum_n N_n(\epsilon)d\epsilon \quad , \quad (5.74)$$

where n is the band index and $N_n(\epsilon)$ the density of states of the band n . Then we have:

$$N_n(\epsilon)d\epsilon = \frac{2}{(2\pi)^3} \int_{\text{1.BZ}} d^3k \cdot \begin{cases} 1 & \text{if } \epsilon \leq \epsilon_n(\mathbf{k}) \leq \epsilon + d\epsilon \\ 0 & \text{otherwise} \end{cases} \quad . \quad (5.75)$$

This is a volume integral in \mathbf{k} -space, which is enclosed by the surfaces $\epsilon_n(\mathbf{k}) = \epsilon$ and $\epsilon_n(\mathbf{k}) = \epsilon + d\epsilon$. $\delta\tilde{k}(\mathbf{k})$ shall be the distance of these two surfaces perpendicular to the first surfaces. Then we have:

$$N_n(\epsilon)d\epsilon = \frac{2}{(2\pi)^3} \int_{\epsilon_n(\mathbf{k})-\epsilon=0} \delta\tilde{k}(\mathbf{k}) df \quad , \quad (5.76)$$

and we obtain

$$N_n(\epsilon)d\epsilon = \frac{2}{(2\pi)^3} \int_{\epsilon_n(\mathbf{k})-\epsilon=0} \frac{1}{|\nabla_{\mathbf{k}}\epsilon_n(\mathbf{k})|} df \quad , \quad (5.77)$$

because

$$\nabla_{\mathbf{k}} \epsilon_n(\mathbf{k}) = \frac{\partial \epsilon_n(\mathbf{k})}{\partial \tilde{k}(\mathbf{k})} \cdot \hat{\mathbf{n}}(\mathbf{k}) \quad , \quad (5.78)$$

where $\hat{\mathbf{n}}$ is the unit vector with a direction perpendicular to $\epsilon_n(\mathbf{k}) = \epsilon$.

Characteristic structures occur at energies where the gradient in the denominator of Eq. (5.77) becomes zero. These positions are also called *Van-Hove singularities*. Examples for such singularities are given in Fig. 5.17. For three-dimensional systems these divergences in the integrand can be integrated.

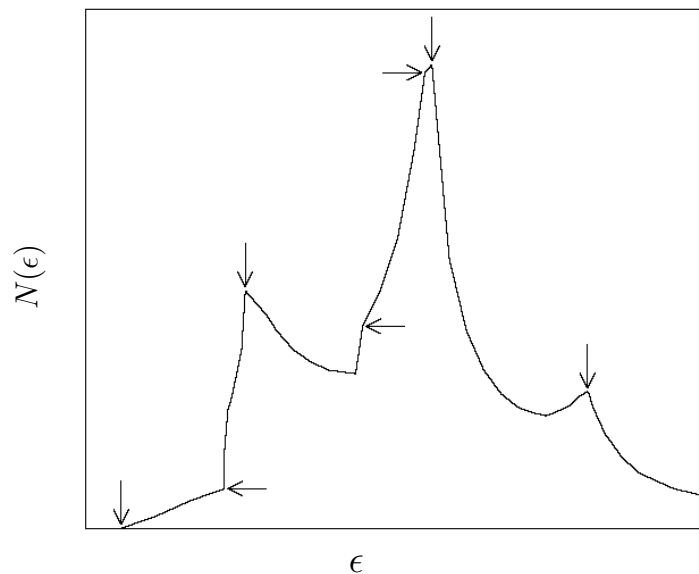


Figure 5.17: The density of states of a band. Singularities in the density of states can be identified (arrows).

5.5 Other Methods for Solving the Kohn-Sham Equations of Periodic Crystals

To be completed later. For now see:

http://wwwitp.physik.tu-berlin.de/ekreide/ss08/TFP/2008-05-27/pdf/lect_col.pdf

5.5.1 The Pseudopotential Method

To be completed later. For now see:

http://wwwitp.physik.tu-berlin.de/ekreide/ss08/TFP/2008-05-27/pdf/lect_col.pdf

5.5.2 APW and LAPW

To be completed later. For now see:

http://www.itp.physik.tu-berlin.de/ekreide/ss08/TFP/2008-05-27/pdf/lect_col.pdf

5.5.3 KKR, LMTO, and ASW

To be completed later. For now see:

http://www.itp.physik.tu-berlin.de/ekreide/ss08/TFP/2008-05-27/pdf/lect_col.pdf

5.6 Many-Body Perturbation Theory (beyond DFT)

To be completed later. For now see:

http://www.itp.physik.tu-berlin.de/ekreide/ss08/TFP/2008-05-27/pdf/lect_col.pdf

At first: a reminder of the basic theory and some additional plots

From the many-particle problem to the Kohn-Sham functional

Then two examples:
what is it good for?

“the *ab initio* line of computational sciences and engineering”

Modeling Materials and Bio-Molecular Properties and Functions: The Many-Body Schrödinger Equation

$$(\hat{T}^e + \hat{T}^{ion} + \hat{V}^{e-e} + \hat{V}^{e-ion} + \hat{V}^{ion-ion})\Psi = E\Psi$$

With: $\Psi(\mathbf{r}_1, \dots, \mathbf{r}_N; \mathbf{R}_1, \dots, \mathbf{R}_M)$

$$\hat{T}^e = \sum_{k=1}^N \frac{\mathbf{p}_k^2}{2m}$$

$$\hat{T}^{ion} = \sum_{I=1}^M \frac{\mathbf{p}_I^2}{2M_I}$$

$$\hat{V}^{e-e} = \frac{1}{2} \frac{1}{4\pi\epsilon_0} \sum_{k \neq k'}^{N,N} \frac{e^2}{|\mathbf{r}_k - \mathbf{r}_{k'}|}$$

$$\hat{V}^{ion-ion} = \frac{1}{2} \frac{1}{4\pi\epsilon_0} \sum_{I \neq I'}^{M,M} \frac{Z_I Z_{I'}}{|\mathbf{R}_I - \mathbf{R}_{I'}|}$$

$$\hat{V}^{e-ion}(\mathbf{r}_k, \mathbf{R}_I) = \sum_{k=1}^N \sum_{I=1}^M v_I^{ion}(|\mathbf{R}_I - \mathbf{r}_k|)$$

We know the operators and the interactions. We can write them down.

No open question here!

???

Born-Oppenheimer Approximation

$$\Psi(\mathbf{r}_1, \dots, \mathbf{r}_N; \mathbf{R}_1, \dots, \mathbf{R}_M) = \sum_{\nu} \Lambda_{\nu}(\{\mathbf{R}_I\}) \Phi_{\nu, \{\mathbf{R}_I\}}(\{\mathbf{r}_k\})$$

Where Φ_{ν} are solutions of the “electronic Hamiltonian”:

$$H_{\{\mathbf{R}_I\}}^e \Phi_{\nu, \{\mathbf{R}_I\}}(\{\mathbf{r}_k\}) = E_{\nu, \{\mathbf{R}_I\}}^e \Phi_{\nu, \{\mathbf{R}_I\}}(\{\mathbf{r}_k\})$$

$$H^e = T^e + V^{e-e} + V^{e-ion}$$

frequently (commonly) applied approximations:

- neglect non-adiabatic coupling (terms of order m/M_I)
- keep only Λ_0

➡ the dynamics of electrons and nuclei decouple

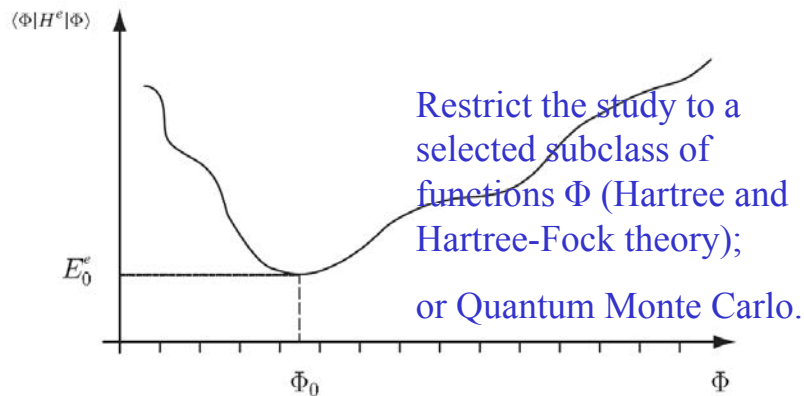
Some Limits of the Born-Oppenheimer Approximation

It does not account for correlated dynamics of ions and electrons. For example:

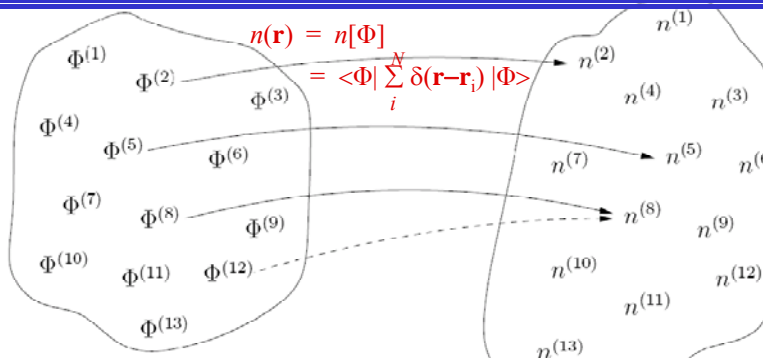
- polaron-induced superconductivity
- dynamical Jahn-Teller effect
- some phenomena of diffusion in solids
- non-adiabaticity in molecule-surface scattering
- etc.

Wave-Function Theories

$$H^e = \sum_{k=1}^N -\frac{\hbar^2}{2m} \nabla_{\mathbf{r}_k}^2 + \sum_{k=1}^N v(\mathbf{r}_k) + \frac{1}{2} \frac{1}{4\pi\epsilon_0} \sum_{\substack{k,k' \\ k \neq k'}}^{N,N} \frac{e^2}{|\mathbf{r}_k - \mathbf{r}_{k'}|}$$



The Hohenberg-Kohn Theorem (1964)

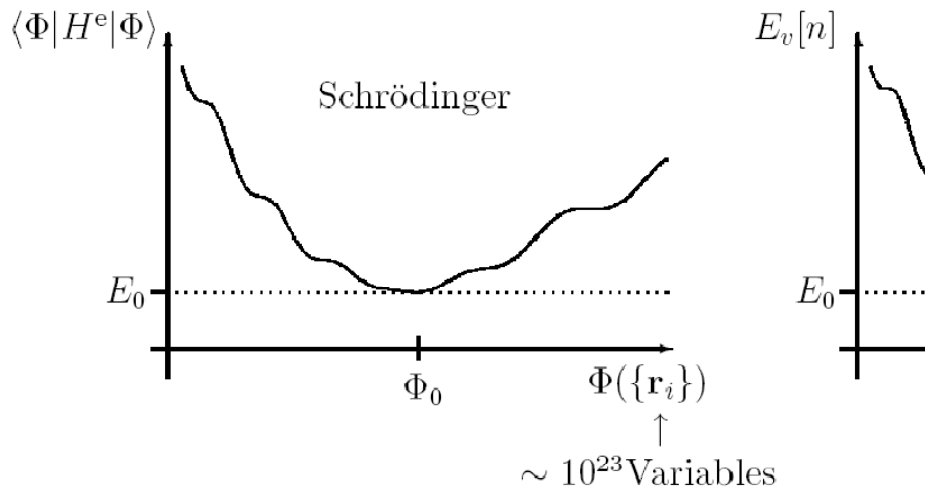


The set of non-degenerate ground state wave functions Φ of arbitrary N -electron Hamiltonians.

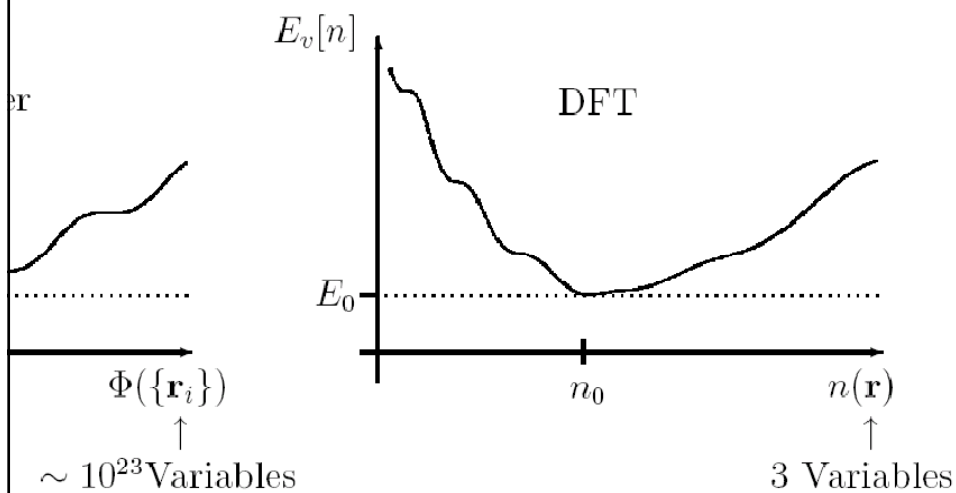
The set of particle densities $n(\mathbf{r})$ belonging to non-degenerate ground states of the N -electron problem.

The dashed arrow is not possible

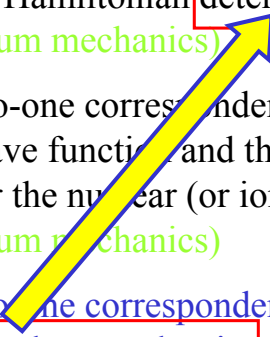
Comparison of Wave-Function and Density-Functional theory



Comparison of Wave-Function and Density-Functional theory



Summary of Hohenberg-Kohn Density-Functional Theory (DFT) -- 1964

- The many-body Hamiltonian determines everything. (standard quantum mechanics)
 - There is a one-to-one correspondence between the ground-state wave function and the many-body Hamiltonian [or the nuclear (or ionic) potential, $v(\mathbf{r})$]. (standard quantum mechanics)
 - There is a one-to-one correspondence between the ground-state electron-density and the ground-state wave function. (Hohenberg and Kohn)
- 

The Kohn-Sham Ansatz

- Kohn-Sham (1965) – Replace the original many-body problem with an independent electron problem that can be solved!
- Only the ground state density and the ground state energy are required to be the same as in the original many-body problem.

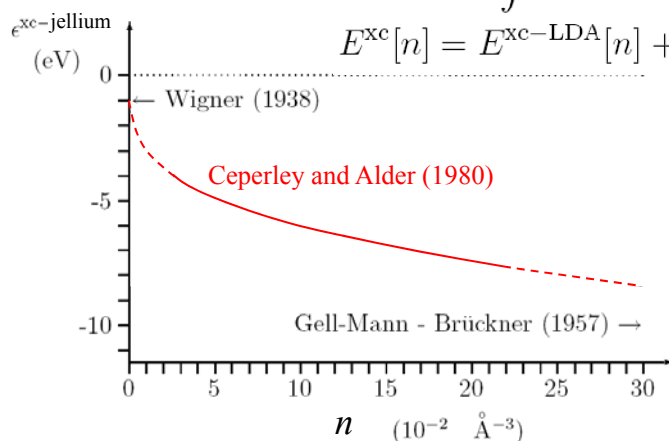
$$E_v[n] = T_s[n] + \int v(\mathbf{r})n(\mathbf{r})d^3\mathbf{r} + E^{\text{Hartree}}[n] + E^{\text{xc}}[n]$$

- Maybe the exact $E^{\text{xc}}[n]$ functional cannot be written as a closed mathematical expression. Maybe there is a detour similar to that taken for $T_s[n]$? The challenge is to find useful approximate xc functionals.

T_s , E^{Hartree} , and E^{xc} are all *universal* functionals in $n(\mathbf{r})$, i.e., they are independent of the special system studied. (general theory: see the work by Levy and Lieb)

$$E^{\text{xc}}[n] = \int \epsilon^{\text{xc}}[n] n(\mathbf{r}) d^3\mathbf{r}$$

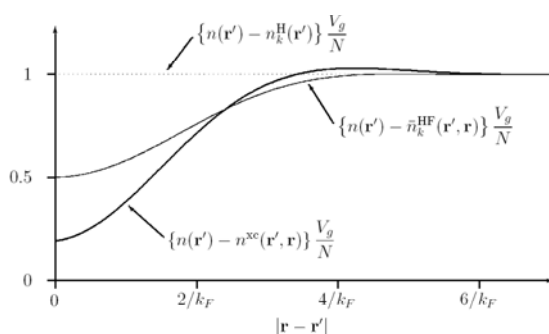
$$E^{\text{xc}}[n] = E^{\text{xc-LDA}}[n] + O(\nabla n)$$



neglecting $O(\nabla n)$ is the local-density approximation

The Exchange-Correlation Hole

$$v^{\text{Hartree}}(\mathbf{r}) + v^{\text{xc}}(\mathbf{r}) = \frac{e^2}{4\pi\epsilon_0} \int \frac{n(\mathbf{r}') - n^{\text{xc}}(\mathbf{r}, \mathbf{r}')}{|\mathbf{r} - \mathbf{r}'|} d^3\mathbf{r}'$$



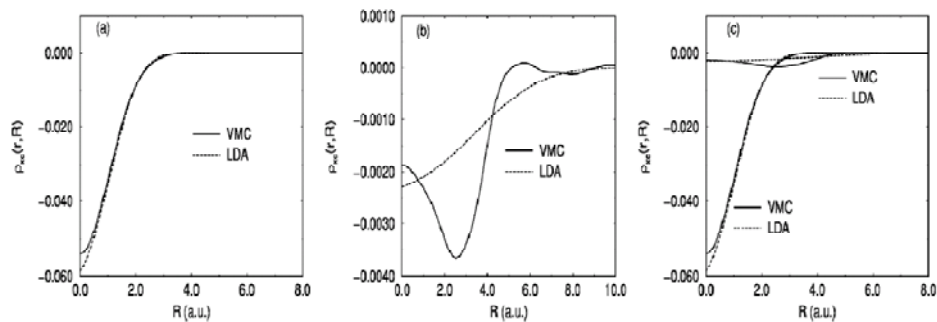
Comparison of Hartree, Hartree-Fock, and density-functional theories for jellium

For non-jellium systems and the LDA (or the GGA) the shape of $n^{\text{xc}}(\mathbf{r}, \mathbf{r}')$ is incorrect. However, only its spherical average enters:

$$E^{\text{xc}}[n] = \frac{e^2}{4\pi\epsilon_0} \int d^3\mathbf{r} n(\mathbf{r}) \int \frac{n^{\text{xc}}(\mathbf{r}, \mathbf{r}')}{|\mathbf{r} - \mathbf{r}'|} d^3\mathbf{r}'$$

Exchange-Correlation Hole in Silicon

R. Q. Hood, M. Y. Chou, A. J. Williamson, G. Rajagopal, and R. J. Needs, *PRB* 57, 8972 (1998)



The spherically averaged exchange-correlation hole in **variational Monte Carlo (VMC)** and DFT-LDA with (a) one electron fixed at the bond center, (b) one electron fixed at the tetrahedral interstitial site, and (c) plots (a) and (b) superimposed with the same scale.

Most-Cited Papers in APS Journals

11 papers published in APS journals since 1893 with >1000 citations in APS journals (~5 times as many references in all science journals)

Publication	# cites	Av. age	Title	Author(s)
PR 140, A1133 (1965)	3227	26.7	Self-Consistent Equations Including Exchange and Correlation Effects	W. Kohn, L. J. Sham
PR 136, B864 (1964)	2460	28.7	Inhomogeneous Electron Gas	P. Hohenberg, W. Kohn
PRB 23, 5048 (1981)	2079	14.4	Self-Interaction Correction to Density-Functional Approximations for Many-Electron Systems	J. P. Perdew, A. Zunger
PRL 45, 566 (1980)	1781	15.4	Ground State of the Electron Gas by a Stochastic Method	D. M. Ceperley, B. J. Alder
PR 108, 1175 (1957)	1364	20.2	Theory of Superconductivity	J. Bardeen, L. N. Cooper, J. R. Schrieffer
PR 19, 1264 (1967)	1306	15.5	A Model of Leptons	S. Weinberg
PRB 12, 3060 (1975)	1259	18.4	Linear Methods in Band Theory	O. K. Anderson
PR 124, 1866 (1961)	1178	28.0	Effects of Configuration Interaction of Intensities and Phase Shifts	U. Fano
RMP 57, 287 (1985)	1055	9.2	Disordered Electronic Systems	P. A. Lee, T. V. Ramakrishnan
RMP 54, 437 (1982)	1045	10.8	Electronic Properties of Two-Dimensional Systems	T. Ando, A. B. Fowler, F. Stern
PRB 13, 5188 (1976)	1023	20.8	Special Points for Brillouin-Zone Integrations	H. J. Monkhorst, J. D. Pack

PR, Physical Review; PRB, Physical Review B; PRL, Physical Review Letters; RMP, Reviews of Modern Physics.

From Physics Today, June, 2005

Certainties about Density Functional Theory

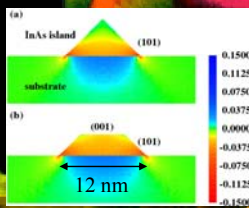
1. **DFT in principle:** It is exact; a universal $E^{\text{xc}}[n]$ functional exists.
2. **DFT in practice:** It is probably not possible to write down $E^{\text{xc}}[n]$ as a closed mathematical expression. We need approximations.

The success of DFT proves that “simple” approximations to the exchange correlation functional can provide good results – if you know what one is doing.

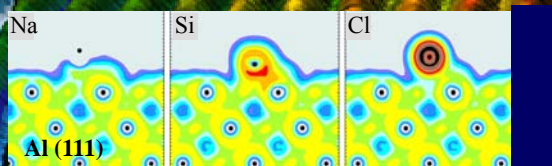
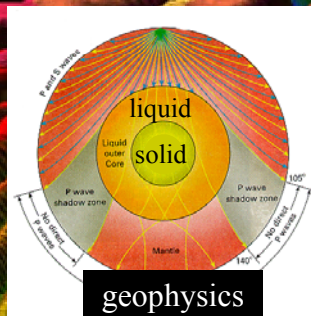
The search (research) for new xc functionals goes on.

Ab Initio Electronic Structure Calculations: Status and Challenges

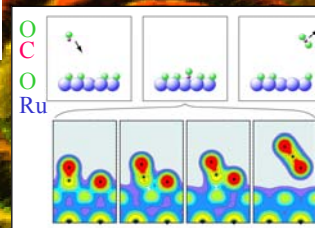
from the earth core to quantum dots to mad cow disease



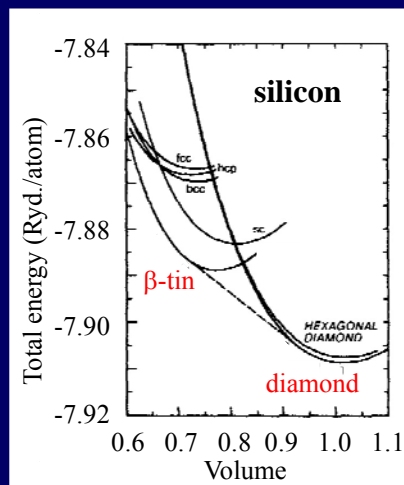
stress field at semiconductor nano structures



electron density of adsorbates



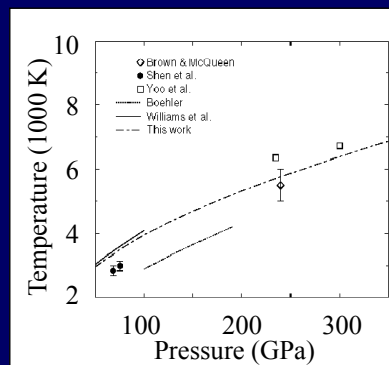
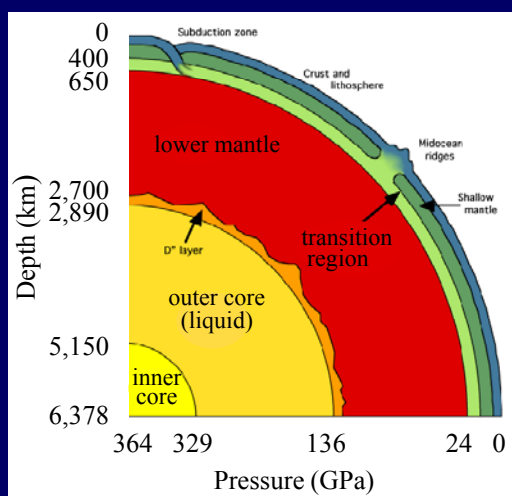
The first (convincing) DFT calculations: Stability of crystals and crystal phase transitions



*M. T. Yin and
M. L. Cohen
PRB 26 (1982)*

*see also:
V.L. Moruzzi, J.F. Janak,
and A. R. Williams
Calculated Electronic
Properties of Metals
Pergamon Press (1978)*

Ab initio melting curve of Fe as function of pressure



*D. Alfe, M. J. Gillan,
and G. D Price
NATURE 401 (1999)*

Summary

- Interacting electrons determine the properties and function of real materials and bio molecules.
- Approximate xc functionals have been very successful, but for highly correlated situations and for excited states there are problems.

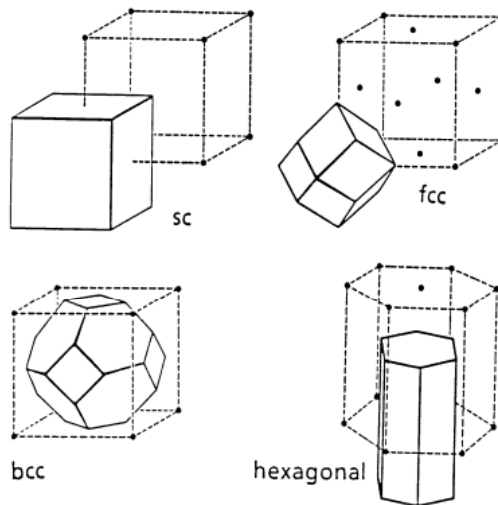
Important arenas for future theoretical work:

- Correlated systems, e.g. f-electron chemistry
- Thermodynamic phase transitions, e.g. melting
- Surfaces, interfaces, nanostructures – in realistic environments
- Modeling the kinetics, e.g. of catalysis or crystal growth (self-assembly and self-organization)
- Molecules and clusters in solvents, electrochemistry, fuel cells, external fields, transport
- Biological problems

The challenges:

- Find practical ways to correct the xc approximation.
- Develop methods for bridging the length and time scales.

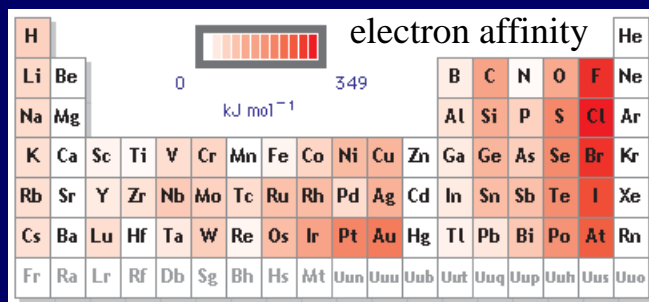
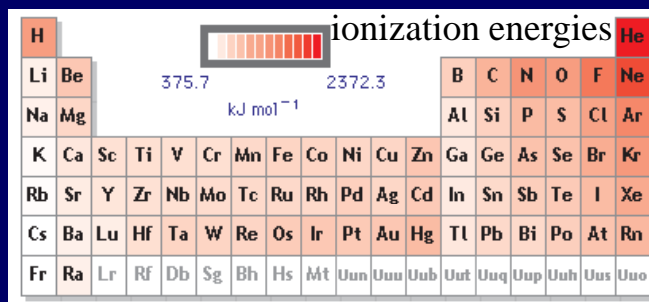
Some Bravais lattices and the corresponding Wigner-Seitz cells



June 3, 2008

	Ne	Ar	Kr	Xe
c_o (theory)	3.13 Å	3.75 Å	3.99 Å	4.33 Å
c_o (exp.)	2.99 Å	3.71 Å	3.98 Å	4.34 Å
E^{coh} (theory)	27 meV	89 meV	120 meV	172 meV
E^{coh} (exp.)	20 meV	80 meV	110 meV	170 meV

Table 6.3: Equilibrium nearest neighbor distance c_o and cohesive energy E^{coh} of the noble gases, as resulting from experiment and the pair potential approximation discussed in the text (theory). The larger deviation of c_o for the lightest element Ne is due to zero-point vibrations, which are neglected in the theory [from Ashcroft and Mermin].



(96 kJ/mole = 1 eV). [From Webelements].

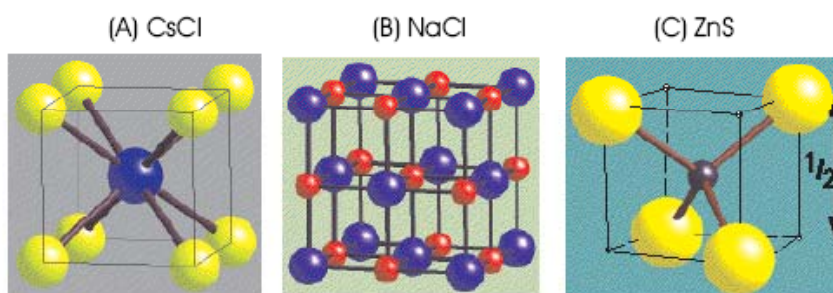
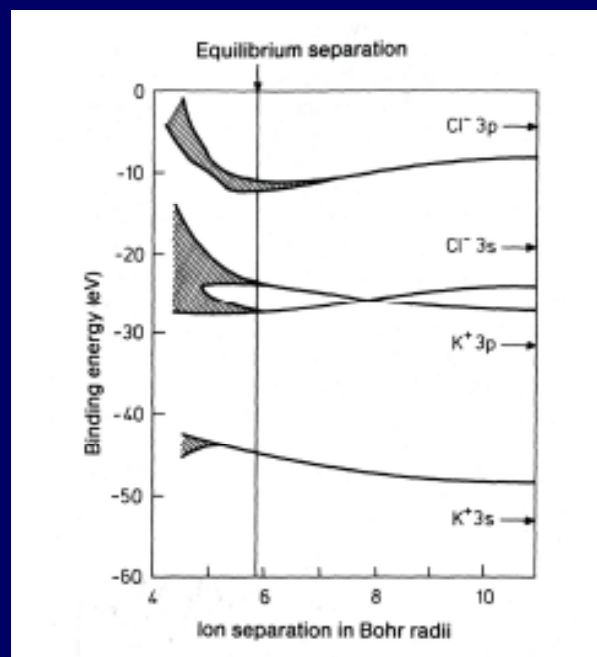
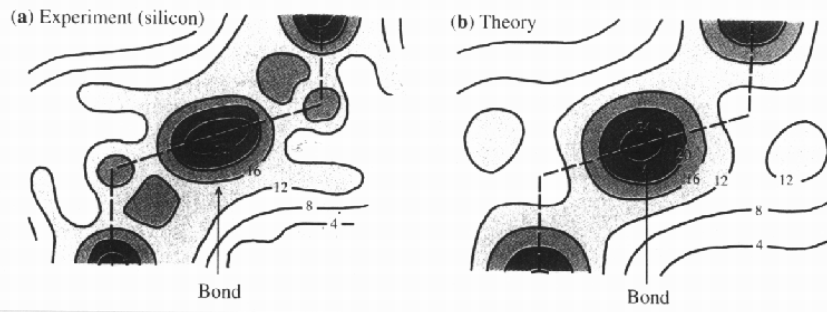


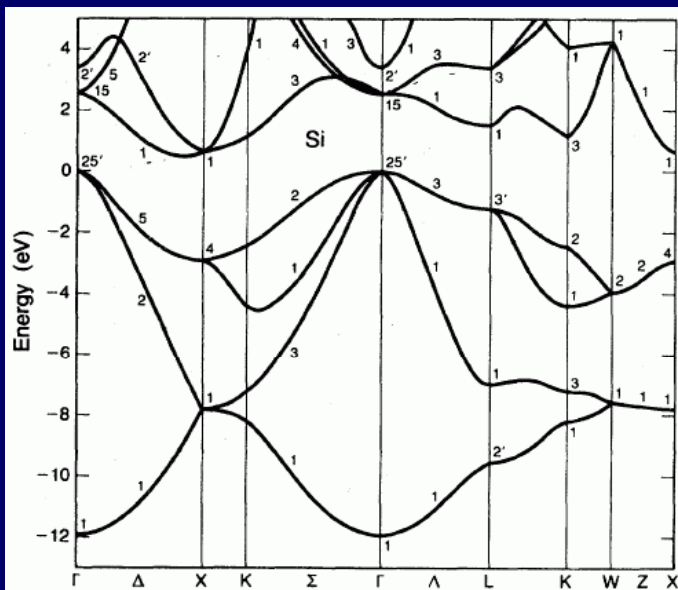
Figure 6.9: The two most common ionic crystal lattices: (A) Cesium chloride and (B) Sodium chloride; and (C) the less common zinc blende structure.



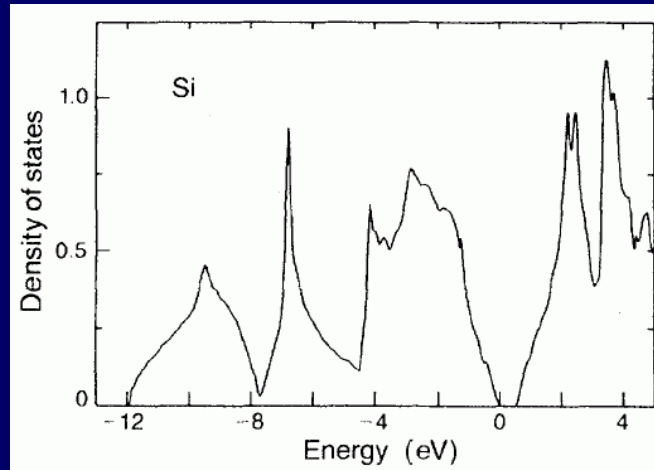
June 6, 2008



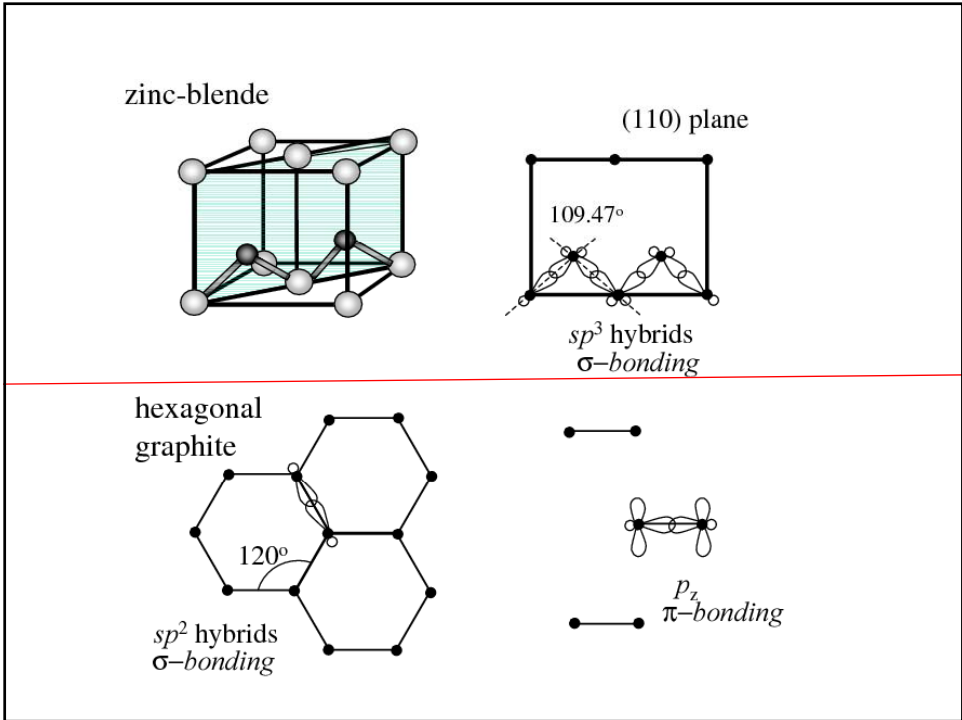
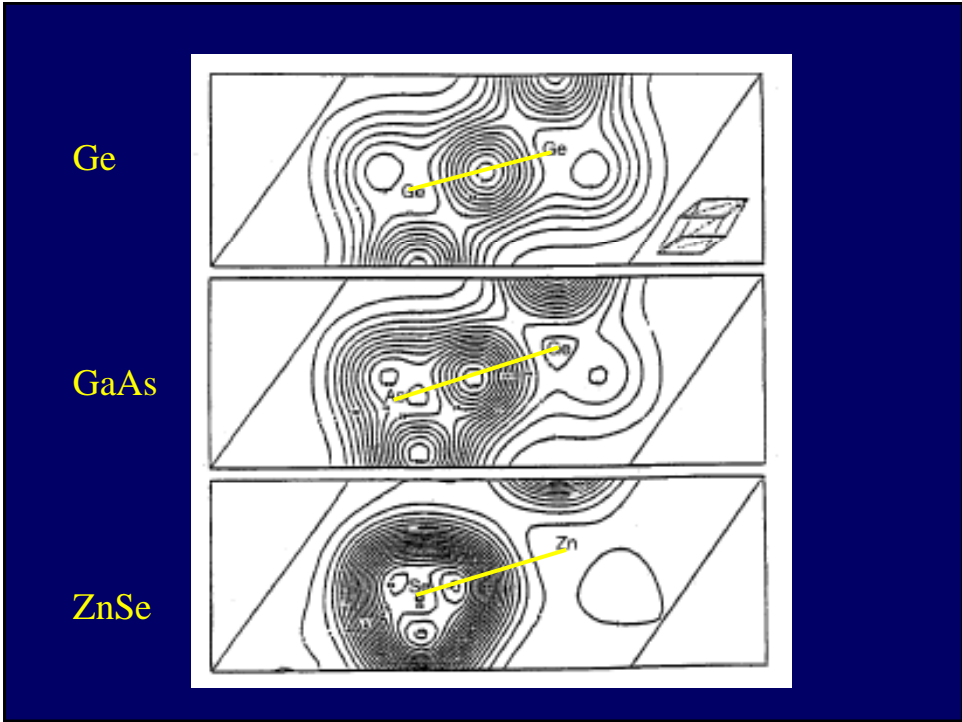
Si bandstructure



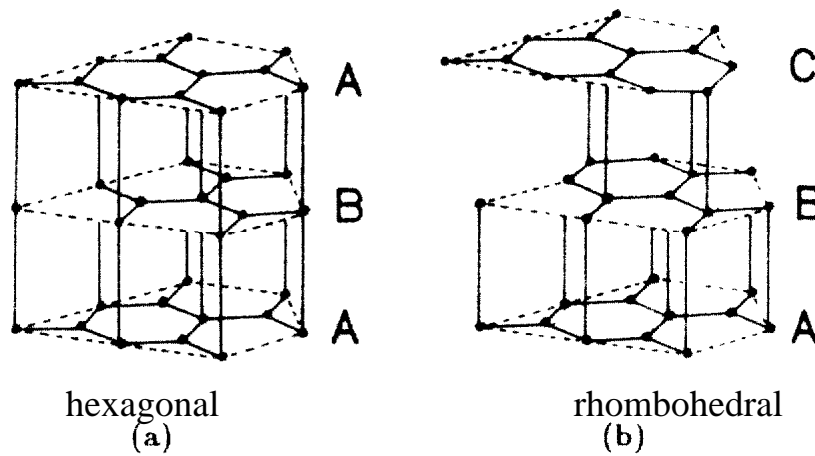
density of states



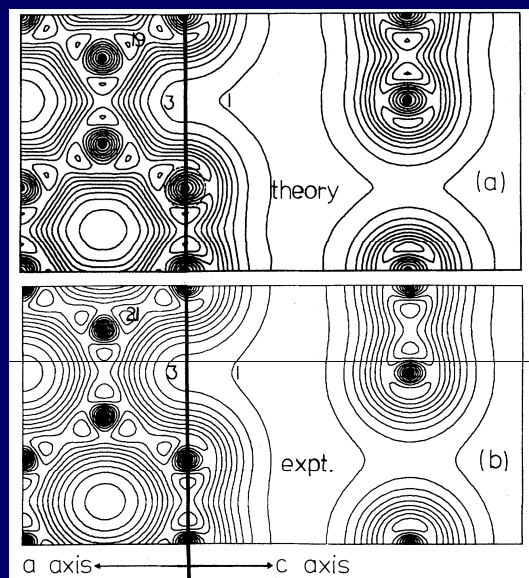
Element		a_o (Å)	E^{coh} (eV/atom)	B_o (Mbar)
C	theory	3,602	7,58	4,33
	exp.	3,567	7,37	4,43
	%diff.	<1%	3%	-2%
Si	theory	5,451	4,67	0,98
	exp.	5,429	4,63	0,99
	%diff.	<1%	1%	-1%
Ge	theory	5,655	4,02	0,73
	exp.	5,652	3,85	0,77
	%diff.	0,2%	4%	-5%



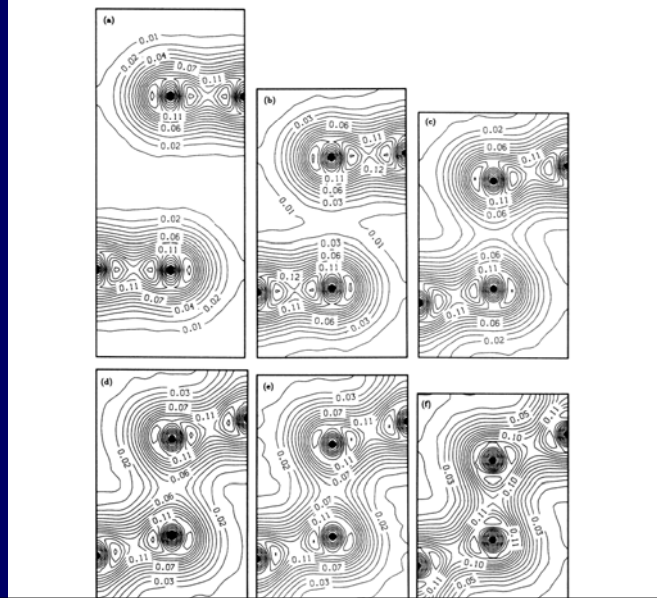
layered structures of graphite



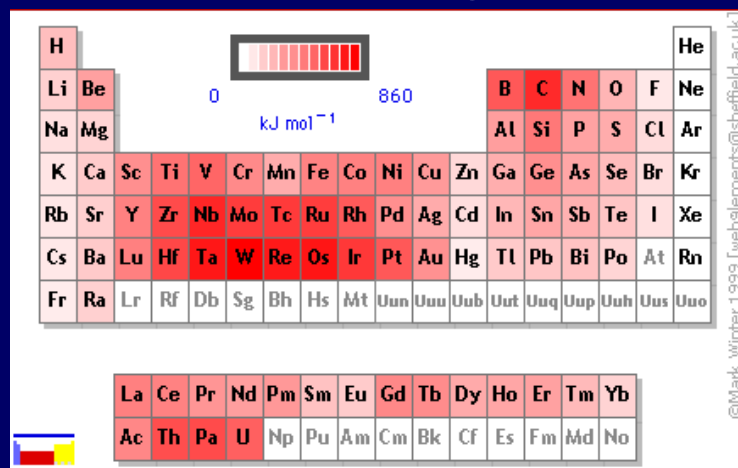
e-density graphite theory vs. experiment



e-density graphite -- diamond phase transition



Cohesive energies



(96 kJ/mole = 1 eV). [From Webelements].

